АКАДЕМИЯ НАУК СССР
AKADEMIIA NAUK SSSR

ОПТИКА И СПЕКТРОСКОПИЯ
OPTICS AND SPECTROSCOPY

MARCH 1959 - VOL. VI - No. 3
MART 1959 - TOM. VI - VYP. 3

Translated on the Initiative of
THE OPTICAL SOCIETY OF AMERICA, INC.
With a Grant-in-Aid from
THE NATIONAL SCIENCE FOUNDATION
by MORRIS D. FRIEDMAN, INC.

RUSSIAN EDITORIAL STAFF

Editor: S. E. FRISH

Assistant Editor: P. P. FEOFILOV

Corresponding Secretary: L. S. SAZONOV

Associate Editors:

M. M. GUREVICH M. A. EL'IASHEVICH A. A. LEBEDEV V. P. LINNIK
S. L. MANDEL'SHTAM I. V. OBREIMOV V. K. PROKOF'EV
N. N. SOBOLEV A. N. TERENIN A. I. TUDOROVSKII

Translation Editorial Staff

MORRIS D. FRIEDMAN

DR. JAMES R. ARONSON, *Arthur D. Little, Inc.*
FRED W. BEHNKE, *Perkin-Elmer Corp.*
DR. A. R. H. COLE, *Massachusetts Institute of Technology*
DR. RICHARD DALVEN, *Raytheon Co.*
DR. SUMNER P. DAVIS, *University of California*
CYRUS FELDMAN, *Oak Ridge National Laboratory*
DR. JOHN S. WAUGH, *Massachusetts Institute of Technology*
DR. ARTHUR W. WINSTON, *Allied Research Corp.*

Published semi-monthly by the Optical Society of America, Inc., 121 Lincoln Avenue, Rochester, New York. Business and Editorial office: 33 University Road, Cambridge 38, Mass. Subscriptions for one year to members of the Society: Associates $13.00; Regular members and Fellows $17.00. Subscriptions for non-members of the Society: One Year U. S. and Possessions, $25.00; Foreign $28.00. Back numbers: $3.00 per copy. Lithoprinted in the USA.

Application for 2nd Class mailing privileges pending at Post Office, Boston, Mass.

АКАДЕМИЯ НАУК СССР
AKADEMIIA NAUK SSSR

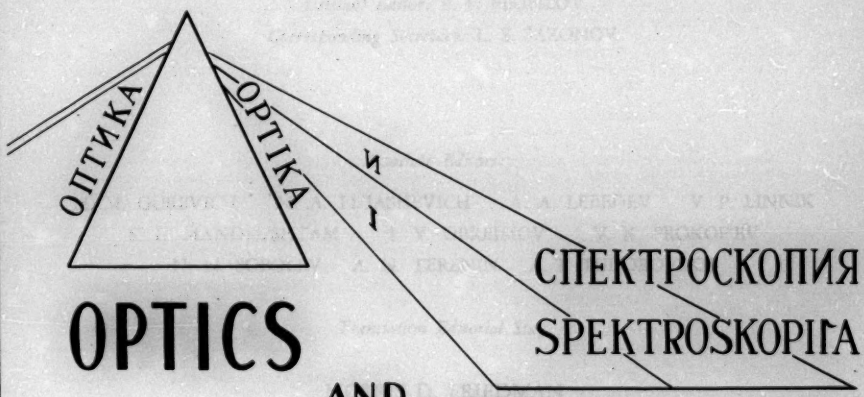

OPTICS AND SPECTROSCOPY

MARCH 1959 - VOL. VI - No. 3
MART 1959 - TOM. VI - VYP. 3

Translated on the Initiative of
THE OPTICAL SOCIETY OF AMERICA, INC.
With a Grant-in-Aid from
THE NATIONAL SCIENCE FOUNDATION
by MORRIS D. FRIEDMAN, INC.

OPTICS AND SPECTROSCOPY

RUSSIAN EDITORIAL STAFF

Editor: S. E. FRISH

Assistant Editor: P. P. FEOFILOV

Corresponding Secretary: L. S. SAZONOV

Associate Editors:

M. M. GUREVICH M. A. EL'IASHEVICH A. A. LEBEDEV V. P. LINNIK
S. L. MANDEL'SHTAM I. V. OBREIMOV V. K. PROKOF'EV
N. N. SOBOLEV A. N. TERENIN A. I. TUDOROVSKII

Translation Editorial Staff

MORRIS D. FRIEDMAN

DR. JAMES R. ARONSON, *Arthur D. Little, Inc.*
FRED W. BEHNKE, *Perkin-Elmer Corp.*
DR. A. R. H. COLE, *Massachusetts Institute of Technology*
DR. RICHARD DALVEN, *Raytheon Co.*
DR. SUMNER P. DAVIS, *University of California*
CYRUS FELDMAN, *Oak Ridge National Laboratory*
DR. JOHN S. WAUGH, *Massachusetts Institute of Technology*
DR. ARTHUR W. WINSTON, *Allied Research Corp.*

Published semi-monthly by the Optical Society of America, Inc., 121 Lincoln Avenue, Rochester, New York. Business and Editorial office: 33 University Road, Cambridge 38, Mass. Subscriptions for one year to members of the Society: Associates $13.00; Regular members and Fellows $17.00. Subscriptions for non-members of the Society: One Year U. S. and Possessions, $25.00; Foreign $28.00. Back numbers: $3.00 per copy. Lithoprinted in the USA.

Application for 2nd Class mailing privileges pending at Post Office, Boston, Mass.

RUSSIAN EDITORIAL STAFF

Editor: S. E. FRISH

Assistant Editor: P. P. SIDORIUK

Corresponding Secretary: L. S. SAZONOV

Associate Editors:

M. M. GUREVICH M. A. ELIASHEVICH A. A. LEBEDEV V. P. LINNIK
S. I. MANDELSHTAM I. V. OBREIMOV V. K. PROKOFEV
N. N. SOBOLEV A. N. TERENIN A. I. TUDOROVSKII

Translation Editorial Staff

MORRIS D. FRIEDMAN

DR. JAMES R. ARNOLD, Arthur D. Little, Inc.
FRED W. BUHNER, Perkin-Elmer Corp.
DR. A. S. H. COLE, Massachusetts Institute of Technology
DR. RICHARD DALVEN, Rawson Co.
DR. SUMNER P. DAVIS, University of California
CYRUS FELDMAN, Oak Ridge National Laboratory
DR. JOHN S. WAUGH, Massachusetts Institute of Technology
DR. ARTHUR W. WINSTON, Allied Research Corp.

Published semi-monthly by the Optical Society of America, Inc., 111 Lincoln Avenue, Rochester, New York. Business and editorial office: 33 University Road, Cambridge 38, Mass. Subscriptions for one year to members of the Society: Americas $15.00, Regular members and Fellows $7.00. Subscriptions for non-members of the Society: One Year U. S. and Possessions $15.00; Foreign $18.00. Back numbers, $1.00 per copy. Lithoprinted in the USA.

Application for bulk rates mailing privileges pending at Post Office, Boston, Mass.

TOM VI, Vyp. 3 OPTIKA I SPEKTROSKOPIIA Mart, 1959
VOL. VI, No. 3 OPTICS AND SPECTROSCOPY March, 1959

SODERZHANIE

L. M. VOLKOVA
Effektivnye secheniia vozbuzhdeniia spektral'nykh linii kaliia 273
E. IA. SHREIDER
Izmerenie intensivnostei v bal'merovskoi serii i opredelenie kontsentratsii vozbuzhdennykh atomov v razriade 279
N. N. SOBOLEV, A. V. POTAPOV, V. F. KITAEVA, F. S. FAIZULLOV, V. N. ALIAMOVSKII, E.T. ANTROPOV, I.L. ISAEV
Spektroskopicheskoe issledovanie sostoianiia gaza za udarnoi volnoi. I 284
S. P. ERKOVICH
O sile ostsilliatora dlia gamma-sistemy polos NO 297
V. A. LOGINOV
Opredelenie molekuliarnykh postoiannykh iz polosatykh spektrov metodom paraboloicheskogo interpolirovaniia 304
V. N. SOSHNIKOV
Temperaturnaia zavisimost' secheniia pogloshcheniia vidimogo sveta dvuokis'iu azota 315
I. G. FRISHMAN
Raspredelenie energii v spektrakh poliarnykh siianii v oblasti 3900 - 8700 Å 323
R. S. LEREDEV
Raschet kolebatel'nogo spektra molekuly metiltsiklopentana 329
L. M. SVERDLOV, E. P. KRAINOV
Kolebatel'nye spektry nepredel'nykh uglevodorodov. VII. Raschet i interpretatsiia kolebatel'nogo spektra 334
I. D. POLIAKOVA, SH. SH. RASKIN
O spektrakh kombinatsionnogo rasseianiia nekotorykh galoido-proizvodnykh uksusnoi kisloty v raznykh fazovykh sostoianiiakh 343
O. V. SVERDLOVA
O vliianii rastvoritelia na elektronnye spektry pogloshcheniia benzola i khlorbenzola 349
A. N. NIKITINA, M. D. GALANIN, G. S. TER-SARKISIAN, B. M. MIKHAILOV
Spektry pogloshcheniia i liuminestsentsiia rastvorov nekotorykh zameshchennykh polienov 354
IU. V. NABOIKIN, E. N. PAVLOVA, B. A. ZADOROZHNYI
Osobennosti liuminestsentsii ortodizameshchennykh aromaticheskikh uglevodorodov. I 366
V. L. LEVSHIN, V. B. GUTAN, E. N. KARZHAVINA
O vozmozhnosti rekombinatsionnykh protsessov svecheniia v vol'framatakh i uranilovykh soedineniiakh 372
F. I. FEDOROV
K teorii opticheskoi aktivnosti kristallov II 377
G. B. RAIS
Formuly Frenelia dliia sluchaia padeniia obyknovennoi volny na ploskost' dvoinikovaniia odnoosnogo prozrachnogo kristalla 384
P. G. KARD
Ob ustranenii dubletnoi struktury polosy propuskaniia svetofil'tra s polnym otrazheniem 389
A. O. SALL'
O poroge chuvstvitel'nosti infrakrasnogo absorbtsionnogo gazoanalizatora s gazovoi moduliatsiei 394

CONTENTS

Effective Excitation Cross-sections of the Spectral Lines of Potassium 179
Measurements of Intensities in the Balmer Series and Determination of the Concentration of Excited Atoms in the Discharge 182
Spectrographic Investigation of the State of a Gas Behind a Shockwave. I 185
On the Oscillator Strength of the γ-Band System of NO 193
Determination of Molecular Constants from Band Spectra by the Parabolic Interpolation Method 197
Temperature Dependence of the Absorption Cross Section of Nitrogen Dioxide for Visible Light 203
Energy Distribution in the Polar Aurorae in the Region 3900 - 8700 Å 208
Calculation of the Vibrational Spectrum of the Methylcyclopentane Molecule 211
Vibration Spectra of Unsaturated Hydrocarbons VII. Calculation and Interpretation of the Vibration Spectrum of Cyclopentene 214
On the Raman Spectra of Some Halogen Derivatives of Acetic Acid in Various Phases 220
Solvent Effects on the Electronic Absorption Spectra of Benzene and Chlorobenzene 223
The Absorption and Luminescence Spectra of Solutions of some Substituted Polyenes 226
The Luminescence of Ortho-disubstituted Aromatic Hydrocarbons 231
On The Possibility of Recombination Processes in the Luminescence of Tungstate and Uranyl Compounds 234
On the Theory of Optical Activity in Crystals II 237
Fresnel Formulas for an Ordinary Wave Incident on the Twinning Plane of a Transparent Uniaxial Crystal 241
On Elimination of the Doublet Structure of the Transmission Band in a Total-Reflection Light-Filter 244
On the Threshold of Sensitivity of an Infrared Absorption Gas Analyzer with Gas Modulation 247

TOM VI, Vyp. 3 OPTIKA I SPEKTROSKOPIIA Mart, 1959
VOL. VI, No. 3 OPTICS AND SPECTROSCOPY March, 1959

SODERZHANIE

L. M. VOLKOVA
Effektivnye secheniia vozbuzhdeniia spektral'nykh linii kaliia 273
E. IA. SHREIDER
Izmerenie intensivnostei v bal'merovskoi serii i opredelenie kontsentratsii vozbuzhdennykh atomov v razriade 279
N. N. SOBOLEV, A. V. POTAPOV, V. F. KITAEVA, F. S. FAIZULLOV, V. N. ALIAMOVSKII, E.T. ANTROPOV, I.L. ISAEV
Spektroskopicheskoe issledovanie sostoianiia gaza za udarnoi volnoi. I 284
S. P. ERKOVICH
O sile ostsilliatora dlia gamma-sistemy polos NO 297
V. A. LOGINOV
Opredelenie molekuliarnykh postoiannykh iz polosatykh spektrov metodom parabolicheskogo interpolirovaniia 304
V. N. SOSHNIKOV
Temperaturnaia zavisimost' secheniia pogloshcheniia vidimogo sveta dvuokis'iu azota 315
I. G. FRISHMAN
Raspredelenie energii v spektrakh poliarnykh siianii v oblasti 3900 - 8700 Å 323
R. S. LEBEDEV
Raschet kolebatel'nogo spektra molekuly metiltsiklopentana 329
L. M. SVERDLOV, E. P. KRAINOV
Kolebatel'nye spektry nepredel'nykh uglevodorodov. VII. Raschet i interpretatsiia kolebatel'nogo spektra 334
I. D. POLIAKOVA, SH. SH. RASKIN
O spektrakh kombinatsionnogo rasseianiia nekotorykh galoido-proizvodnykh uksusnoi kisloty v raznykh fazovykh sostoianiiakh 343
O. V. SVERDLOVA
O vliianii rastvoritelia na elektronnye spektry pogloshcheniia benzola i khlorbenzola 349
A. N. NIKITINA, M. D. GALANIN, G. S. TER-SARKISIAN, B. M. MIKHAILOV
Spektry pogloshcheniia i liuminestsentsiia rastvorov nekotorykh zameshchennykh polienov 354
IU. V. NABOIKIN, E. N. PAVLOVA, B. A. ZADOROZHNYI
Osobennosti liuminestsentsii ortodizameshchennykh aromaticheskikh uglevodorodov. I 366
V. L. LEVSHIN, V. B. GUTAN, E. N. KARZHAVINA
O vozmozhnosti rekombinatsionnykh protsessov svecheniia v vol'framatakh i uranilovykh soedineniiakh 372
F. I. FEDOROV
K teorii opticheskoi aktivnosti kristallov II 377
G. B. RAIS
Formuly Frenelia dliia sluchaia padeniia obyknovennoi volny na ploskost' dvoinikovaniia odnoosnogo prozrachnogo kristalla 384
P. G. KARD
Ob ustranenii dubletnoi struktury polosy propuskaniia svetofil'tra s polnym otrazheniem 389
A. O. SALL'
O poroge chuvstvitel'nosti infrakrasnogo absorbtsionnogo gazoanalizatora s gazovoi moduliatsiei 394

CONTENTS

Effective Excitation Cross-sections of the Spectral Lines of Potassium 179
Measurements of Intensities in the Balmer Series and Determination of the Concentration of Excited Atoms in the Discharge 182
Spectrographic Investigation of the State of a Gas Behind a Shockwave. I 185
On the Oscillator Strength of the γ-Band System of NO 193
Determination of Molecular Constants from Band Spectra by the Parabolic Interpolation Method 197
Temperature Dependence of the Absorption Cross Section of Nitrogen Dioxide for Visible Light 203
Energy Distribution in the Polar Aurorae in the Region 3900 - 8700 Å 208
Calculation of the Vibrational Spectrum of the Methylcyclopentane Molecule 211
Vibration Spectra of Unsaturated Hydrocarbons VII. Calculation and Interpretation of the Vibration Spectrum of Cyclopentene 214
On the Raman Spectra of Some Halogen Derivatives of Acetic Acid in Various Phases 220
Solvent Effects on the Electronic Absorption Spectra of Benzene and Chlorobenzene 223
The Absorption and Luminescence Spectra of Solutions of some Substituted Polyenes 226
The Luminescence of Ortho-disubstituted Aromatic Hydrocarbons 231
On The Possibility of Recombination Processes in the Luminescence of Tungstate and Uranyl Compounds 234
On the Theory of Optical Activity in Crystals II 237
Fresnel Formulas for an Ordinary Wave Incident on the Twinning Plane of a Transparent Uniaxial Crystal 241
On Elimination of the Doublet Structure of the Transmission Band in a Total-Reflection Light-Filter 244
On the Threshold of Sensitivity of an Infrared Absorption Gas Analyzer with Gas Modulation 247

A. I. ODINTSOV
Istochnik sveta s atomnym puchkom bol'shoi intensivnosti 398
M. L. SOSINSKII
Rtutnaia duga nizkogo davleniia dlia issledovaniia passeianiia sveta 405
KRATKIE SOOBSHCHENIIA
S. S. BATSANOV
Vzaimosviaz' refraktsii i potentsialov ionizatsii atomov 412
A. I. FINKEL'SHTEIN, F. L. MALACHEVSKAIA, A. M. FISHER, B. G. RABOVSKII
Prostoi sposob prigotovleniia plastinok iz bromistogo kaliia dlia infrakrasnoi spektroskopii tverdykh tel 415
V. V. ZELINSKII, V. P. KOLOBKOV, N. D. KRASNITSKAIA
K voprosu o temperaturnom tushenii fluorestsentsii 417
V. P. SYCHEV
K voprosu ob udarakh vtorogo roda v smesi gazov N_2+Ar 419
IU. A. TSIRLIN, S. N. KOMNIK, L. M. SOIFER
Zavisimosti vykhoda liuminestsentsii pri alfa i gamma bozbuzhdenii kristallov CsI(Tl) ot kontsentratsii Tl 422
A. A. KAPLIANSKII
Lineichataia liuminestsentsiia rentgenizovannykh kristallov ftoristogo litiia 424
P. P. FEOFILOV
Orientatsiia tsentrov lineichatoi liuminestsentsii v rentgenizovannykh kristallov LiF 426
E. V. KONDRAT'EVA
Opredelenie kvantovogo vykhoda liuminestsentsii trekhvalentnogo iona terbiia v rastvorakh 427

A High Intensity Atomic Beam Light Source 250
Low Pressure Mercury Arc for the Investigation of Light Scattering 254
BRIEF REPORTS
The Correlation Between Refraction and the Ionization Potentials of Atoms 258
A Simple Method of Producing Potassium Bromide Plates for the Infrared Spectroscopy of Solids 260
On The Question of The Thermal Quenching of Fluorescence
On Collisions of the Second Kind in a Mixture of N_2+Ar 263
Luminescence Yield of CsI(Tl) Crystals Under α and γ Excitation As A Function of Tl Concentration 265
Line Luminescence of X-rayed LiF Crystals 267
Orientation of Centers of Linear Luminescence in X-rayed LiF Crystals 268
Determination of the Luminescence Quantum Yield of the Trivalent Terbium Ion in Solution 269
Abbreviations Often Encountered and Used Herein 271
Affiliations of Authors from Issue 3 272
Symbols for Sources of Translations 272

RUSSIAN ALPHABET WITH TRANSLITERATION

А	а	a	Р	р	r
Б	б	b	С	с	s
В	в	v	Т	т	t
Г	г	g	У	у	u
Д	д	d	Ф	ф	f
Е	е	e	Х	х	kh
Ж	ж	zh	Ц	ц	ts
З	з	z	Ч	ч	ch
И	и	i	Ш	ш	sh
Й	й	I	Щ	щ	shch
К	к	k	Ъ	ъ	mute hard sign
Л	л	l	Ы	ы	y
М	м	m	Ь	ь	mute soft sign
Н	н	n	Э	э	e
О	о	o	Ю	ю	iu
П	п	p	Я	я	ia

Litho Printed by Blackburn Printing Company, West Concord, Mass.

TOM VI, Vyp. 3 OPTIKA I SPEKTROSKOPIIA Mart, 1959
VOL. VI, No. 3 OPTICS AND SPECTROSCOPY March, 1959

Effective Excitation Cross-sections of the Spectral Lines of Potassium.

L. M. VOLKOVA

Abstract: Effective electron excitation cross-sections have been determined for two arc and eleven spark lines of potassium as a function of the energy of the impinging electrons. The measurements were made by two methods - photographic photometry, using an ISP-51 spectrograph with a camera having $F_2 = 270$ mm, and the photoelectric method, with the same spectrograph and the collimating attachment PS-381.

THE SHAPE OF THE EXCITATION FUNCTIONS OF THE SPECTRAL LINES OF POTASSIUM

The measurements were made using a Hanle-type tube. The electrodes were made in the shape of truncated cones in order to decrease the length of the collision zone and to utilize the greatest fraction of the radiation produced. A pressed oxide cathode served as the source of electrons in the gun. The gun emitted a monochromatic beam of electrons with an energy spread no greater than 1 ev. In Fig. 1, the retardation curve (1) is given for V = 40 V. In the same figure, the differential curve (2) shows that 90% of all electrons in the beam had energies within a range of 1 ev.

The shape of the beam did not change as the speed of electrons was varied within the operating range.

The metallic potassium necessary for the production of the vapor was subjected to many (5-6) preliminary high-vacuum distillations. In the last stage of distillation, the pressure in the tube was of the order of 10^{-7} mm. The last ampoule of potassium was sealed under high vacuum and placed in a special side-arm of the tube. After conditioning of the tube (degassing of electrodes and walls, activation of the cathode) the ampoule of potassium was broken, and the potassium once more distilled into the side-arm in the lower portion of the tube. During the measurements, the system was continuously pumped out through a capillary 1.5 mm in diameter and approximately 3 cm long. In order to achieve the necessary vapor pressures of potassium, the tube was placed in an electric oven with two independent windings. This made it possible to maintain the potassium side-arm and the test tube at different temperatures (the temperature of the latter was 50 - 70° higher to prevent deposition of potassium on the walls of the discharge tube and on the electrodes).

At the operating temperature (127.5°) there was no noticeable spreading of potassium around the system, nor was any darkening of the walls of the tube observed. The temperature in the side-arm was measured with a mercury thermometer, whose bulb was in contact with the potassium side-arm. This thermometer was calibrated in tenths of a degree. The temperature of the side-arm was kept constant within ± 0.5°. The vapor pressure of potassium was computed from the formula [1]:

$$\log p = A - \frac{B}{T}$$

where T is the temperature of the side-arm, A = 10.36, B = 4503 and p is the pressure in mm Hg.

The measurements were made at 127.5°, which corresponds to a pressure of $p = 1.3 \cdot 10^{-10}$ mm. For 27 eV impinging electrons (the minimum energy in the work with spark lines) this pressure corresponds to the mean free path

$$\lambda = \frac{1}{Q_{sum}\, p} = \frac{1}{360 \cdot 1.3 \cdot 10^{-4}} = 21 \text{ см.}$$

The value of Q_{sum} for the potassium atom was taken from the work of Brode [2]. Since the length of the collision zone was 0.8 cm, λ was $\gg l$, and it may be assumed that there were no multiple collisions between electrons and potassium atoms in the collision zone. This is further proven by the linear dependence of line intensity on current.

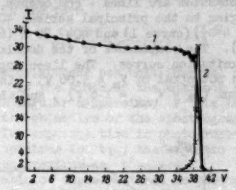

Fig. 1. Retardation curve for the electron velocity V = 40V.

Explanations are in the text.

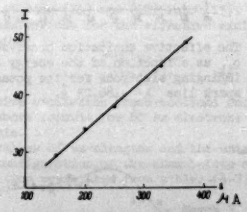

Fig. 2. Intensity of the line λ = 4263.48 Å as a function of the current of exciting electrons for the velocity V = 45V. The vapor pressure of potassium is $p = 1.3 \cdot 10^{-4}$ mm.

From Fig. 2 it is seen that at a potassium vapor pressure of $p = 1.3 \cdot 10^{-4}$ mm, the dependence of the intensity of the line λ = 4263 Å on the current remains linear up to 380 μa. The measurements of the excitation curves were made at i=300μa.

The fact that all excitation function curves of potassium lines begin at a potential equal to the sum of ionization and excitation potentials of the given spectral line is another indication that the excitation of a spectral line is produced by a single collision with an electron.

The data on the electron configuration of the atom before and after a transition for the lines under investigation, is given in the table.

The excitation function for the potassium spark line $\lambda = 4186.31$ Å, is shown in Fig. 3. As is seen from the figure, the curve begins at $V = V_i + V_a = 4.32 + 23.09 = 27.4$, slowly rises to a maximum at $V \sim 45$ V, and then drops off even more slowly.

In Fig. 4 the excitation function is given for the line $\lambda = 4263.48$ Å. Different symbols on the graph correspond to measurements made on different days. The intervals between measurements ran to several months. As seen from Fig. 4, the scatter of points near the maximum does not exceed 10% of the value of the corresponding ordinate. The other lines investigated have similarly behaving excitation functions. Fig. 5 gives the excitation function for the line $\lambda = 4115$ Å.

In Fig. 6 the excitation function is given for two potassium arc lines - components of a doublet belonging to the principal series: 4044.14 Å ($6^2P_{3/2} - 4^2S_{1/2}$) (curve 1) and 4047.20 Å ($6^2P_{1/2} - 4^2S_{1/2}$) (curve 2). The components of the doublet have similar excitation curves. The lines appear at an excitation potential of $V_a = 3.06$ V, rise rapidly to a maximum ($V_a - V_{max} = 1.6$ V), and slowly drop off.

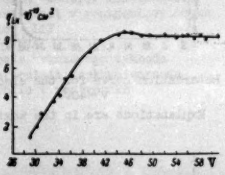

Fig. 3. The effective excitation cross-section q_{1k} as a function of the energy of the impinging electrons for the potassium spark line $\lambda = 4186.23$ Å.

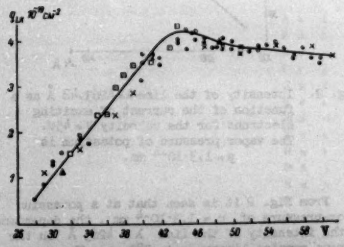

Fig. 4. The effective excitation cross-section q_{1k} as a function of the energy of the impinging electrons for the potassium spark line $\lambda = 4263.48$ Å.
Different symbols on the graph correspond to measurements made on different days.

λ Å	Configuration	q_{1k} 10^{-19} cm^2 for 60 V.
4044.14	$6^2P_{3/2} - 4^2S_{1/2}$	20.9
4047.20	$6^2P_{1/2} - 4^2S_{1/2}$	10.4
4115	$3p^6(^2P^\circ_{1/2})4p - 3p^6(^2P_{1/2})4s$ $j=1$ $j=1$	1.5
4134.72	$3p^6(^2P^\circ_{1/2})4p - 3p^6(^2P_{3/2})4s$ $j=2$ $j=2$	1.5
4149.17	$3p^6(^2P^\circ_{3/2})4p - 3p^6(^2P^\circ_{1/2})4s$ $j=1$ $j=0$	1.5
4186.23	$3p^6(^2P^\circ_{3/2})4p - 3p^6(^2P^\circ_{3/2})4s$ $j=2$ $j=2$	9.2
4222.98	$3p^6(^2P^\circ_{3/2})4p - 3p^6(^2P^\circ_{1/2})4s$ $j=1$ $j=1$	1.1
4225.61	$3p^6(^2P^\circ_{3/2})4p - 3p^6(^2P^\circ_{3/2})3d$ $j=2$ $j=1$	0.8
4263.31	$3p^6(^2P^\circ_{3/2})4p - 3p^6(^2P^\circ_{3/2})4s$ $j=2$ $j=2$	3.5
4305	$3p^6(^2P^\circ_{3/2})4p - 3p^6(^2P^\circ_{3/2})3d$ $j=2$ $j=2$	0.9
4309.08	$3p^6(^2P^\circ_{3/2})4p - 3p^6(^2P^\circ_{3/2})4s$ $j=2$ $j=1$	2.3

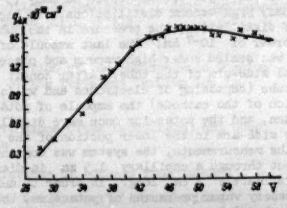

Fig. 5. The effective excitation cross-section q_{1k} as a function of the energy of the impinging electrons for the potassium spark line $\lambda = 4115$ Å.

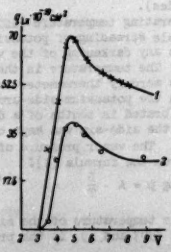

Fig. 6. The dependence of the effective cross-section q_{1k} on the energy of the impinging electrons, for the arc lines of potassium $\lambda = 4044.14$ Å (1) and 4047.20 Å. (2).

ABSOLUTE VALUES OF EFFECTIVE EXCITATION CROSS-SECTIONS OF SPECTRAL LINES OF POTASSIUM

Effective cross-sections were determined for the excitation of 11 potassium lines by 60 eV electrons. The measurements were made by photographically comparing the line investigated with a portion of the continuous spectrum of a ribbon filament tungsten lamp, having a known spectral energy distribution. The calibration of the lamp was performed at the Mendeleev All-Union Metrological Research Institute (VNIIM).

The effect on the photographic plate of the spectrograph is determined by the brightness within the boundaries of the slit image. At large slit widths (when diffraction may be neglected) and when the collimator is completely filled, the illumination caused by the line, is determined by expression [3]

$$A_l = \frac{\beta\pi}{4}\left(\frac{d}{F_2}\right)^2 K_\lambda, \qquad (1)$$

where $[A_l] = \text{erg/sec.} \times \text{cm}^2$; β is a coefficient which takes account of the light losses in the spectrograph; K_λ is the integral line brightness; d is the diameter of the collimator lens and F_2 is the focal length of the camera objective.

In the case of direct excitation of the line from the ground level, the number of events of photon emission may be set equal to the number of excitation events [3]

$$w_\nu d\nu = n_l K \nu_{ik}, \qquad (2)$$

where $([w_\nu\, d\nu] = \text{erg/cm}^2 \times \text{sec})$, $w_\nu\, d\nu$ is the radiant power and n_l is the number of excitation events to level i per unit time per unit volume ($[n_l] = 1/\text{cm}^3 \times \text{sec}$).

In the case of excitation by impact of an electron of a given speed

$$n_l = N_0 N_e q_{ik}, \qquad (3)$$

where N_0 is the concentration of atoms in the normal state ($[N_0] = 1/\text{cm}^3$), N_e is the number of electrons passing through a unit of cross-section of the beam in 1 sec. ($[N_e] = 1/\text{cm}^2 \times \text{sec.}$), q_{ik} is the effective cross-section for excitation by electron impact ($[q_{ik}] = \text{cm}^2$).

Substituting (3) in (2), we obtain

$$w_\nu d\nu = N_0 N_e q_{ik} h\nu_{ik}. \qquad (4)$$

The radiant power and brightness are related by the equation

$$k_\nu d\nu = \frac{1}{4\pi} w_\nu d\nu \frac{d\tau}{ds_n}, \qquad (5)$$

where $d\tau$ is the radiating volume and ds_n is the projection of the radiating volume in the direction of propagation. In our case, the light from the radiating cylinder having a radius $r = 1.3$ mm and height $h = 8$ mm is collected by a lens of 60 mm diameter at a distance of 180 mm. Since the dimensions of illuminating cylinder are considerably smaller than the dimensions of the lens and the distance to it, $ds_n = 2hr$; $d\tau = \pi r^2 h$;

$$k_\nu d\nu = \frac{1}{4\pi} w_\nu d\nu \frac{\pi r^2 h}{2hr} = \frac{r}{8} w_\nu d\nu. \qquad (6)$$

Substituting (4) and (6) into (1), we obtain

$$A_l = \frac{\beta\pi}{32}\left(\frac{d}{F_2}\right)^2 r N_0 N_e q_{ik} h\nu_{ik}, \qquad (7)$$

where

$$N_0 = \frac{p}{kT_2}. \qquad (8)$$

T_2 is the temperature of the collision zone and p is the vapor pressure of potassium in bars.

In an experiment. we measure i , the current to the receiver. This is related to N_e^* , the number of electrons, which pass through the cross-section of the beam in 1 sec., by the equation

$$N_e^* = \frac{i}{e_0}, \qquad (9)$$

where e_0 is the charge of an electron.

The electron concentration N_e of eq. (7) is related to N_e^* by the equation

$$N_e = N_e^* \frac{1}{\pi r^2}, \qquad (10)$$

where r is the radius of the electron beam.

Substituting (8), (9), and (10) into (7), we have

$$A_l = \frac{\beta}{32}\left(\frac{d}{F_2}\right)^2 \frac{p \cdot i}{kT_2 e_0} q_{ik} h\nu_{ik}. \qquad (11)$$

The illumination produced by a portion of the continuous spectrum of the tungsten lamp may be expressed in the form

$$A_{cont.} = \frac{\beta\pi}{4} k_\lambda \frac{s_1}{F_1 D_\lambda}\left(\frac{d}{F_2}\right)^2. \qquad (12)$$

k_λ is the brightness per unit interval of wavelength, s_1 is the width of the entrance slit, D_λ is the angular dispersion, F_1 is the focal length of the objective of the spectrograph's collimator. The exposure time in photographing the potassium spectrum is t_l ; the exposure time for the tungsten spectrum is t contin.

The ratio of exposure times in photographing the line and the continuous spectrum of the tungsten lamp is proportional to the intensities I_l and I contin.

$$\frac{A_l t_l}{A_{cont.} t_{cont.}} = \frac{I_l}{I_{cont.}}. \qquad (13)$$

Substituting (11) and (12) into (13), we obtain the expressions for the effective excitation cross-section

$$q_{ik} = \frac{I_l}{I_{cont.}} \cdot \frac{8\pi kT_2 r k_\lambda s_1 t_{cont.}}{\beta p h\nu_{ik} F_1 D_\lambda t_l}. \qquad (14)$$

The effective excitation cross-sections calculated with the above formula for 60 ev electrons are given in the table.

The values of wavelengths and the data on the electron configuration of the atom before and after the transition were taken from tables [4-7].

March 3, 1958

References

1. Smithsonian Physical Tables, Ed. 9, 1954
2. R. B. BRODE: Phys. Rev., 34, 673 (1929)
3. S. E. FRISH: UFN, 43, 512 (1951)
4. A. N. ZAIDEĬ, V. K. PROKOF'EV, S. M. RAISKII: Tablitsi Spektral'nikh Linii (Tables of Spectral Lines) GITTL, Leningrad (1952)
5. T. L. DE BRUIN: Phys., 38, 94 (1926)
6. CH. E. MOORE: Atomic energy levels as derived from analyses of optical spectra. Washington. USGPO, 1948
7. R. F. BACHER, S. GOUDSMIT: Atomic Energy States. N.Y., 1932

TOM VI, Vyp. 3 OPTIKA I SPEKTROSKOPIIA Mart, 1959
VOL. VI, No. 3 OPTICS AND SPECTROSCOPY March, 1959

Measurements of Intensities in the Balmer Series and Determination of the Concentration of Excited Atoms in the Discharge

E. IA. SHREIDER

Abstract: Measurements have been made of the relative intensities of the lines of the Balmer series, and of the reabsorption of radiation by the first members of this series. Concentrations of excited atoms have been calculated from the degree of reabsorption and from observed line intensities. On the basis of comparison of calculated and observed values, it has been concluded that an equilibrium distribution does not exist in the discharge.

In order to obtain the spectrum of atomic hydrogen, we used the long discharge tube proposed by Wood [1]; atomic hydrogen radiation is produced by the center section of this tube. The atomic hydrogen discharge has been investigated by several authors. They have determined the dependence of the line intensities of the Balmer series on current and pressure [2] and have also determined the concentration of excited atoms in the second quantum level [3].

The work of Ornstein and Lindeman did not take account of reabsorption. In the work of Ladenburg and Carst, there was no investigation of the dependence of the concentration of excited atoms on the parameters of the discharge.

In the present work we used the discharge tube shown in figure 1 to study the radiation emitted by the discharge. The electrodes were made of aluminum. The diameter of the tube was 13 mm. The effective length of the tube was 48 cm. The tube was divided into three symmetrical parts, each forming an independent discharge tube. The distance from each of the electrodes to the horizontal part of the tube was about 80 cm. The intensity of the discharge in each of the horizontal sections was compared with its intensity in the center sections. The radiation from the tube fell on the slit of a UM-2 monochromator, whose dispersion was 65 Å/mm. in the H_α region and 25 Å/mm. in the H_β region. After leaving the monochromator, the radiation fell on the cathode of a FEU-19 photomultiplier. After amplification, the current was registered by a galvanometer whose sensitivity was 10^{-7} amp. per division. The photoelectric apparatus has been described by Osherovich and coworkers [4]. All sections of the tube contributed equally to the illumination of the slit of the monochromator. This is confirmed by the fact that the recorded intensity was the same for all three discharge tubes. The hydrogen was obtained by electrolysis and passed through the tube under reduced pressure. It was impossible to carry out measurements in a sealed discharge tube because of the absorption and subsequent liberation of hydrogen by the electrodes. The pressure (in the absence of any discharge) was measured at the point where the gas enters the tube Power was supplied to the tube by a 5000 volt transformer. The pressure in the various experiments varied from 0.25 to 1.5 mm. Hg., and the current from 70 to 250 ma. The high voltage was turned on several minutes before the beginning of the measurements in order to obtain steady state conditions.

Measurements were made of the relative intensities of the lines in the Balmer series. The intensities of the lines H_α, H_β, H_γ, and H_δ, emitted by the center section of the tube, were compared with the radiation from an absolute blackbody. In view of the fact that the H_α and H_β lines are strongly reabsorbed, a calculation was made of the reabsorption effect.

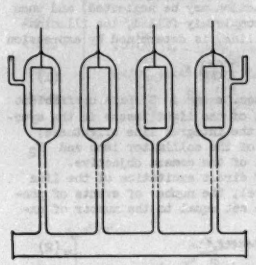

Figure 1. The Discharge Tube.

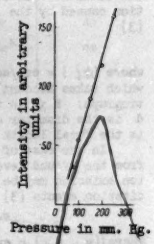

Figure 2. Intensity of H_α as a function of current.

As is well known [5,6] the intensity of radiation in the presence of reabsorption may be written

$$I = I_0 l S, \qquad (1)$$

where I_0 is the intensity of illumination in the absence of reabsorption, l is the length of the discharge tube and S the coefficient which takes account of the reabsorption of radiation. Values of S for various $k_0 \cdot l$ have been calculated by Ladenburg [5] (k_0 is the coefficient of absorption at the center of the line).[1] Hence in order to determine k_0 and S, it is sufficient to measure the intensity of radiation from a uniformly glowing column of the tube as a function of the length of column. In our case, we measured the intensity of radiation emitted by the entire length of the horizontal section of the tube and by its center section (the ratio of the lengths is 3:1).

The results obtained are presented in Table 1.

Table 1
Relative intensities of the lines of the Balmer series corrected for reabsorption[2]

Pressure in mm. Hg.	H_α	H_β	H_γ	H_δ
0.25	1000	180	22	2.8
0.30	1000	190	26	3.2
0.35	1000	170	29	4.1

[1] Ladenburg's calculations were made on the assumptions that the column was uniform along its entire length and that the line shape had the Doppler form.

[2] The intensity of the H_α line was not taken as 1000 at all pressures.

Measurements were also made of the current dependence of the intensity of the lines of the Balmer series. Figure 2 shows the intensity of the H_α line as a function of current at a pressure of 0.30 mm. The intensities of the lines have been corrected for reabsorption. Similar curves are plotted for H_β, H_γ, and H_δ for various pressures from 0.25 to 1.10 mm. At low currents, the line intensity does not increase linearly with increasing current (the straight line does not go through the origin). This may be explained by the fact that the excitation of atomic hydrogen occurs in two steps: dissociation and excitation.

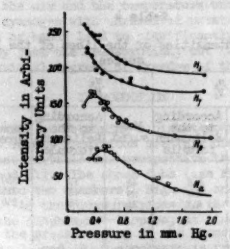

Figure 3. Pressure dependence of the intensities of H_α, H_β, H_γ, and H_δ.

In Figure 3 we give the curves describing the change in intensity of the lines of the Balmer series as a function of pressure. In complete agreement with the relationships which hold for monoatomic gases, the curve for H_α has a maximum; for H_β the maximum is reached at a lower pressure, and for H_γ and H_δ the maxima are absent. The excitation potentials for H_α, H_β H_γ, and H_δ are, respectively, 12.0, 12.7, 13.0, 13.2 ev. The higher the excitation potential the lower the pressure at which the maximum is obtained. The intensities of the lines H_α and H_β have been corrected for reabsorption. No corrections were made for H_γ and H_δ, in view of the very small degree of reabsorption.

It is very important to correct for reabsorption, since in the case of the H the coefficient S varies from 0.48 to 0.95. Thus in certain cases correcting for reabsorption can increase the intensity by a factor of 2.

Measurements of reabsorption allow one to determine the concentration of excited atoms in the second quantum level. As has already been pointed out, it is possible to find k_0 from the tables of Ladenburg [5]. Knowing k_0, it is possible to determine the concentration N_k of excited atoms from the well-known formula

$$N_k = \frac{1}{3}\,\frac{k_0 mc}{f_{km}\lambda_0 e^2}\sqrt{\frac{\pi\mu}{RT}} \qquad (2)$$

where n and e are the mass and charge of the electron, μ is the molecular weight of the gas, λ_0 is the wave length of the center of the line, c is the velocity of light, R is the gas constant, T is the temperature and f_{km} is the oscillator strength.[3]

Table 2.

Concentration of excited atoms $N_k \times 10^{-10} cm^{-3}$.

Current in ma.	Pressure in mm. Hg.						
	0.25	0.30	0.35	0.45	0.68	1.10	1.50
250	6.0	4.3	2.9	2.5	1.7	0.64	0.56
200	3.1	2.5	2.3	1.8	1.5	0.52	—
150	2.2	1.6	1.5	1.3	1.1	0.50	—
100	0.9	—	—	—	—	—	—

In Table 2 we give the concentrations of excited atoms in the second quantum level calculated from formula (2). The calculations were carried out using reabsorption measurements made with H_α.[4] The concentration of excited atoms decreases with increasing pressure but increased with increasing current.

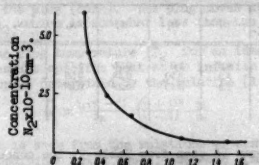

Figure 4. Pressure dependence of the concentration of excited atoms in the second quantum level.

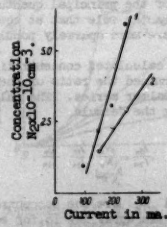

Figure 5. Dependence of the concentration of excited atoms in the second quantum level on current. Curve 1: p = 0.25 mm. Hg. Curve 2: p = 0.35 mm. Hg.

[3] The fine structure of the H_α and H_β lines was not taken into account. This might affect the absolute values of the concentrations of excited atoms but the shape of the curves would remain the same.

[4] The oscillator strengths here and below were derived from data taken from Landolt's tables. [7]

In figure 4, we show the concentration of excited atoms in the second quantum level as a function of pressure for a constant current of 250 ma. In figure 5, we give the concentration of excited atoms in the same excited level as a function of current for pressures of 0.25 and 0.35 mm. These curves show that the concentration of excited atoms in the second quantum level is a linear function of current. Saturation is not achieved because the current density is so low. The dependence is not linear for small currents since the current must first dissociate the hydrogen molecules and then excite the atoms.

It is possible to compute the temperature corresponding to a Boltzmann distribution over the first and second levels from the pressure of the gas in the discharge tube and the observed concentration of excited atoms in the second quantum level at three pressures and a current of 250 ma. Thus, one may calculate the concentration of excited atoms in quantum levels 3 through 6.[5] These data are given in Table 3.

Table 3

Concentration of excited atoms $N_k \times 10^{-10} cm^{-3}$ and excitation temperature.

Pressure in mm. Hg.	N_3	N_4	N_5	N_6	N_2	T° abs.
0.25	6.0	1.0	0.75	0.73	0.82	8450
0.30	4.3	0.70	0.48	0.50	0.50	8170
0.35	2.9	0.43	0.28	0.28	0.29	7870

As may be seen from Table 3, the concentration of excited atoms for transitions to higher levels falls at first and then slowly begins to increase. This may be explained by the close proximity of the levels and the rapid increase of their statistical weighting factors (which are proportional to the square of the principal quantum number). This contradicts the rule that at equilibrium, the higher levels are more sparsely populated than the lower levels.

Using the calculated concentrations of excited atoms, we determined the ratio of the line intensities of the Balmer series. The calculations were made using the formula

$$\frac{I_{kn}}{I_{2n}} = \frac{N_l}{N_k} \cdot \frac{f_{kn}}{f_{ln}} \cdot \frac{\nu_{kn}}{\nu_{ln}} \qquad (3)$$

where N_l and N_k are the concentrations of excited atoms in the upper levels for each of the two transitions, f_{kn} and f_{ln} are the oscillator strengths and ν_{kn} and ν_{ln} are the frequencies of the lines.

A comparison of the directly measured intensity ratios (see Table 1) with those calculated from formula (3) (assuming a Boltzmann distribution) is shown in Table 4. It is clear from the table that the agreement between the measurements and the values calculated from the Boltzmann formula for the H_α / H_β intensity ratio may be considered satisfactory. There is no such agreement, however, for H_γ and H_δ. That is to say, the H_α line is considerably more intense than would be expected if the intensity of the line were determined by the concentration of excited atoms as calculated from the Boltzmann distribution. This indicates that for the upper levels (5,6, etc.), the populations are considerably lower than those calculated from the Boltzmann formula, and hence the conditions of the discharge are very far from equilibrium.

Table 4

Relative intensities of the lines of the Balmer series.

p in mm. Hg.	$\frac{H_\alpha}{H_\beta}$		$\frac{H_\alpha}{H_\gamma}$		$\frac{H_\alpha}{H_\delta}$	
	Measured	According to the Boltzmann formula	Measured	According to the Boltzmann formula	Measured	According to the Boltzmann formula
0.25	6.3	5.4	46	13	350	23
0.30	5.3	5.8	39	13	310	26
0.35	5.2	6.0	35	15	240	28

In conclusion, I would like to express my gratitude to S. E. Frish for guidance in this work.

July 28, 1958

References

1. R. W. WOOD: Phil Mag., 44, 538 (1922)
2. L. S. ORNSTEIN, H. LINDEMAN: Z. Phys., 63, 8 (1930)
3. A. CARST, R. LADENBURG: Z. Phys., 48, 192 (1928)
4. A. L. OSHEROVICH, E. N. PAVLOVA, S. F. RODIONOV, L. M. FISHKOVA: ZTF, 19, 184 (1949)
5. R. LADENBURG, S. LEVY: Z. Phys., 65, 189 (1930)
6. S. E. FRISH, I. P. BOGDANOVA: Sbornik pamiati S. I. Vavilova (Collection in memory of S. I. Vavilov) Akad. Nauk Press, Moscow, 1952
7. LANDOLT-BÖRNSTEIN: Zahlenwerte und Funktionen aus Physik, Chemie, Astronomie, Geophysik und Technik. Bd. I, Teil I, 1950
8. E. WREDE: Z. Phys., 54, 53 (1929)
9. H. D. BECKEY, P. WARNECK: Z. Naturf., 10a, 62-67 (1955) (See translation 57-2079, 14 pp.)

[5] The calculation was made with the formula $p = n_0 kT$. It has been assumed that the gas is completely dissociated, [8,9] i.e. $N_0 = 2n_0$, where n_0 is the number of hydrogen molecules, and N_0 is the number of hydrogen atoms per unit volume.

TOM VI, Vyp. 3
VOL. VI, No. 3

OPTIKA I SPEKTROSKOPIIA
OPTICS AND SPECTROSCOPY

Mart, 1959
March, 1959

Spectrographic Investigation of the State of a Gas Behind a Shockwave. I

N. N. SOBOLEV, A. V. POTAPOV, V. F. KITAEVA, F. S. FAIZULLOV
V. N. ALIAMOVSKII, E. T. ANTROPOV, I. L. IBAEV

Abstract: A series of systematic experiments has been carried out to determine the air temperature behind a shockwave according to the relative intensity of non-resonance Na and Li lines for shockwave velocities of 3 - 4 km/sec. Sodium and lithium were introduced into a shock tube in the form of NaCl and LiCl. It has been established that the large scatter in the experimental results depended on reabsorption, whose degree varied from experiment to experiment. The considerable concentrations of dyestuffs in the air, which was required to produce measurable line intensities, lead to reduced values of the temperature in comparison with the theoretical values. An added reason is the inhomogeneous cross-sectional distribution of the coloring material. It appears to be concentrated near the cold wall of the shock-tube.

In order to eliminate this inhomogeneity effect in a subsequent series of experiments, dicyanogen was added to the air and the temperature was determined according to the relative intensity of the vibrational bands of cyanogen with unresolved rotational structure. A large series of experiments showed that different pairs of bands lead to significantly different temperatures. The scatter being observed cannot be explained by just the reabsorption, but is apparently also related to the lag in the equilibrium build-up in the vibrational degrees of freedom of the cyanogen.

INTRODUCTION

Methods of obtaining a high-temperature plasma under laboratory conditions are very diverse. One of the most suitable and prospective is the shock-tube method [1]. The shock-tube (see Fig. 1) is divided into two chambers: High (H) and low (L) pressure. As the pressure rises in the high-pressure chamber the diaphragm collapses, at time t_0. Because of the pressure jump at the boundary of the two gases 1 and 4, a shockwave is propagated in the gas 1 and a rarefaction wave in the gas 4.

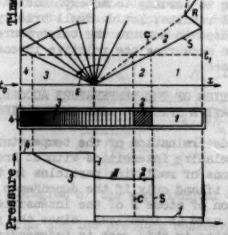

Figure 1. Diagram of shock tube operation

H - High pressure chamber; L - low pressure chamber; D - diaphragm; C - contact surface; R - reflected wave; S - shockwave; 1 - unperturbed low pressure gas; 2 - stopper; 3 - perturbation zone; 4 - unperturbed high pressure gas; E - expansion fan; I - pressure distribution at t_0 when the diaphragm bursts; II - pressure distribution at $t_1 > t_0$.

For an infinite pressure drop, the ratio of the shockwave propagation speed U_s to the speed of sound a_1 in the gas 1 will be [1]

$$\frac{U_s}{a_1} = M_1 = \frac{\gamma_1+1}{\gamma_1-1} \cdot a_4/a_1,$$

where M_1 is the Mach number, γ is the adiabatic index.

Hence, the shockwave speed will be greater the greater the speed of sound a_4 in the dissipating gas.

Between the shockwave front and the contact surface delimiting the gas, there is formed the section 2 of the gas 1 which is heated to a high temperature. We will subsequently call this section the plug (cork). The plug moves at the speed u_2 which is somewhat less than the shockwave speed U_s.

The plug temperature T_2 for an ideal gas with constant specific heat at an infinite pressure drop is determined by the relation [1]

$$\frac{T_2}{T_4} \simeq \frac{\gamma_4(\gamma_1-1)}{2\gamma_1} \cdot \left(\frac{\gamma_1+1}{\gamma_4-1}\right)^2 \cdot \frac{\mu_1}{\mu_4}.$$

It is seen from the relations presented that, other conditions being equal, the Mach number M_1 and the temperature T_2 of the gas behind the shockwave will be greater, the smaller the molecular weight of the dissipating gas and the larger the molecular weight of the gas to be dissipated.

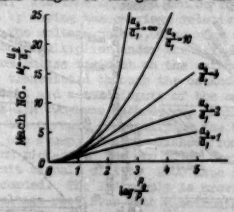

Figure 2. Dependence of M_1 on the logarithm of the pressure drop.

A similar conclusion is obtained for a finite pressure drop also. Shown in Figure 2 is a graph of the dependence of the Mach number on the logarithm of the pressure drop for various ratios of the speeds of sound a_4 and a_1. The curve for $\frac{a_4}{a_1} = 4$ corresponds approximately to the case when hydrogen is used as the accelerating gas and air or argon as the gas being accelerated.

Knowing the shockwave velocity U_s, we can, by using the laws of conservation of mass

(1) $$\rho_1 U_s = \rho_2 (U_s - u_2),$$

momentum

(2) $$p_1 + \rho_1 U_s^2 = p_2 + \rho_2 (U_s - u_2)^2,$$

energy

(3) $$H_1 + \frac{1}{2} U_s^2 = H_2 + \frac{1}{2} (U_s - u_2)^2$$

and relations defining the enthalpy

(4) $$H = \frac{5}{2} (1 + \alpha) R_0 T + \alpha \frac{q_0}{m_0},$$

and the degree of ionization

(5) $$\alpha = \left[\frac{n^3}{(2\pi m)^{3/2}} \cdot \frac{p}{(kT)^{5/2}} \cdot \frac{g_0}{g_1} \exp\left(-\frac{q_0}{kT}\right) + 1 \right]^{-\frac{1}{2}}$$

and the equation of state of the gas

(6) $$p/\rho = (1 + \alpha) R_0 T$$

find the six unknown quantities p_2, ρ_2, u_2, H_2, T_2 and α referring to the state of a monatomic gas with ionization potential q_0 found in the sample.*

Presented in Figure 3 are the results of computing the state of argon behind a shockwave by using the relations (1) - (6). The temperature, density and degree of ionization are represented graphically as a function of the Mach number M_1. As is seen from Figure 3, a temperature on the order of 9000° K is reached in the sample, the density increases 4 times in comparison to the initial density at a Mach number of 10, i.e., for a shockwave speed of the order of 3.2 km/sec. Ionization starts at higher value of M_1. Hence, the density, ionization and temperature depend not only on U_s but also on the density of the original gas. At $M_1 = 18$, the temperature reaches 15,000°, the ionization 0.20, and the density is increased 7 - 8 times.

Figure 3

State of argon behind a shockwave. p_1 (in mm Hg): 1-1; 2-5; 3-15. Dotted line is without taking ionization into account.

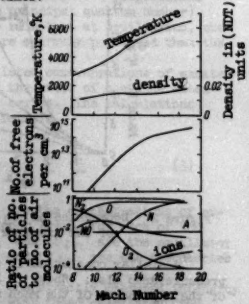

Figure 4

State of air behind a shockwave. p_1 = 1 mm Hg.

* g_0 and g_1 are the statistical weights of the ground level of a neutral atom and ion, m_0 is the mass of an atom.

A similar computation can be made for air also, but it is complicated because of the dissociation of oxygen at temperatures of 2500°. The results of a computation for a case corresponding to an initial 1 mm air pressure are presented in Figure 4 [2]. As is seen from a comparison of figures 3 and 4 for the same Mach number values M_1, the air temperature is less than the argon temperature, both because the specific heat of air is larger than the specific heat of argon, and because of dissociation. At $M_1 = 17$, the air temperature reaches only 6000°, and the density increases 12 times. The oxygen is almost completely dissociated, while N_2 starts to dissociate. Present in significant quantities are NO, N, O and charged particles. The electron concentration reaches 10^{14} cm^{-3}.

The data presented above on the states of air and argon behind a shockwave characterize the possibilities of operation with a shock tube. It is necessary to verify the correctness of these predictions since a number of assumptions are introduced, not always with sufficient foundation, in making gasdynamic computations. First of all, the assumption of thermodynamic equilibrium in the sample, i.e., in the gas behind the shockwave, needs verification.

The temperature is the fundamental parameter characterizing the state of the gas behind the shockwave. However, a comparison of theoretical data on the temperature with experimental results has not yet been made because of the lack of a method to measure the gas temperature behind the shockwave.

The present paper is devoted to the development of an optical method of measuring the air temperature behind a shockwave, to making systematic measurements, and to a comparison of the results of theory and experiment.

Prior to turning to an explanation of the experimental results, let us dwell briefly on the methods we used to measure the temperature, which are based on measuring the relative intensities of spectral lines.

DETERMINATION OF THE TEMPERATURE ACCORDING TO THE RELATIVE SPECTRAL LINE INTENSITIES

The determination of the temperature by the method of relative intensities without knowing the concentrations of radiating particles in the source is possible if and only if the dependence on the concentration of atoms N of the intensities of the lines being used is identical, since the ratio of the intensities in this case is independent of the concentration of radiating particles. This holds in two cases [3]:

1) In the absence of reabsorption, i.e., for a linear dependence of the intensities of both lines on the atom concentration N ;

2) For complete reabsorption of both lines, i.e., for proportionality of the line intensities $\sqrt{N}$.

In the first case, the ratio of the intensities of the two spectral lines for a Boltzmann distribution of the atom energies is

(7) $$\frac{I_1}{I_2} = \frac{A_1 g_1 \lambda_2}{A_2 g_2 \lambda_1} \cdot e^{-\frac{E_1 - E_2}{kT}},$$

where the subscripts 1 and 2 refer to the first and second lines, respectively, A is the probability of transition, g and E the statistical weight

and the energy of the top level, T the temperature, k the Boltzmann constant. In this case the temperature is determined by the expression

$$T = -\frac{E_1 - E_2}{k}\left[\ln\frac{J_1}{J_2} - \ln\frac{A_{1g1}\lambda_2}{A_{2g2}\lambda_1}\right]^{-1} \tag{8}$$

In the second case, i.e., when both lines are completely reabsorbed and have a common low level, the ratio of their intensities is given by [3]

$$\frac{J_1}{J_2} = \left(\frac{\lambda_2}{\lambda_1}\right)^3 \sqrt{\frac{A_{1g1}\gamma_1}{A_{2g2}\gamma_2}} \cdot e^{-\frac{E_1 - E_2}{kT}} \tag{9}$$

where γ is the line half-width. If the line half-width is determined just by the van der Waal interaction of a radiating atom with the neighboring particles (as is valid for low degrees of ionization), then according to [4]

$$\gamma = 17.0 \cdot C_6^{2/5} v^{3/5} N,$$

and (9) becomes

$$\frac{J_1}{J_2} = \left(\frac{\lambda_2}{\lambda_1}\right)^3 \sqrt{\frac{A_{1g1}}{A_{2g2}}} \cdot \left(\frac{C_{61}}{C_{62}}\right)^{1/5} e^{-\frac{E_1 - E_2}{kT}}. \tag{10}$$

where C_{61} and C_{62} are van der Waals constants for the first and second lines, v and N are the velocity and the number of perturbing particles per unit volume.

The formula to determine the temperature according to two completely reabsorbed lines follows from (10)

$$T = -\frac{E_1 - E_2}{k}\left[\ln\frac{J_1}{J_2} - 2\ln\frac{\lambda_2}{\lambda_1} - \frac{1}{2}\ln\frac{A_{1g1}}{A_{2g2}} - \frac{1}{5}\ln\frac{C_{61}}{C_{62}}\right]^{-1} \tag{11}$$

DESCRIPTION OF THE APPARATUS

The apparatus (fig. 5) on which the investigations were conducted was placed in a steel tube of 92 mm inner diameter. The inner surface of the tube is treated and chromed for purity. The apparatus consists of a high-pressure chamber (I) 0.5 m long and a low pressure chamber (II) 4 m long

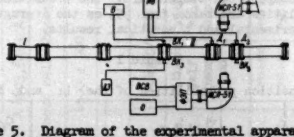

Figure 5. Diagram of the experimental apparatus

I and II - high and low pressure chambers; B- vacuum gauge; BK, BK_2, BK_3 - vacuum stopcocks; D_1 and D_2 - ionization pick-offs; C time measurer - (chronograph) ISP-51 - spectrograph; FEP - photoelectric cell; BCB - High voltage stabilized rectifier; O - oscilloscope

The high and low pressure chambers are separated by a diaphragm. Hydrogen was used as the propelling gas and it was supplied to the high pressure chamber from a cylinder in which the hydrogen pressure in the high-pressure chamber was set by the rupture of the aluminum diaphragm and was 110 - 130 atm. The air filling the low pressure chamber was evacuated by a vacum pump to the required vacuum. The fundamental part of our investigations was made at a vacum of 10 mm Hg. The shockwave velocity was measured by using ionization pick-offs and a chronograph. The spectrum of gas emission behind the shockwave was recorded photographically and photoelectrically. The ISP-51 spectrograph, used to photograph the spectrum, and the photoelectric instrument were placed opposite the inspection holes of the tube located opposite each other at about 3 - 4 m from the diaphragm.

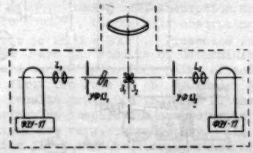

Figure 6. Optical diagram of the photoelectric attachment (FEU-17; $UF\text{-}13_1$, $UF\text{-}13_2$, M_1, M_2)

The photoelectric instrument consists of an ISP-51 spectrograph and an FEP photoelectric cell, which is connected to the middle camera (f = 270 mm) of the spectrograph in place of the cell. The optical diagram of the photoelectric adapter is shown on figure 6, the electrical diagram on Figure 7. The photoelectric adapter (Fig. 6) consists of two identical parts and permits two spectrum lines to be isolated. Each part contains a UF-13 output slit, a lens L and a photo-multiplier FEU-17 or FEU-22 on a carriage, which can be moved perpendicularly to the optical axis of the chamber. Two aluminized mirrors M_1 and M_2 move perpendicularly to the optical axis independently of the carriage and permit the required region of the spectrum to be developed on the output slits. The line selected can be focussed on the slit by moving the carriage relative to the mirror. The voltage pulses, occurring on the load of the photo-multiplier under the effect of the light flux pulses incident on the cathode of the FEU are transmitted through the cathode follower to the first and second inputs of the amplifier of the OK-17M two-beam cathode ray oscilloscope. Starting the circuit (intensifying the beam and starting the sweep) is accomplished from a special ionization pick-off. The amplifier characteristics permit signals of 3 to 2000 μsec duration to be recorded. The FEU supply is provided by a high voltage rectifier with electronic stabilization. The sensitivity of the circuit can be changed in steps by using calibrated dividers at the rectifier output and continuously by using potentiometers at the amplifier input. The OK-17M oscilloscope has a folding photographic attachment which permits the oscillograms to be photographed from the screen onto a film. Films of type RF-3 or Daylight type were used.

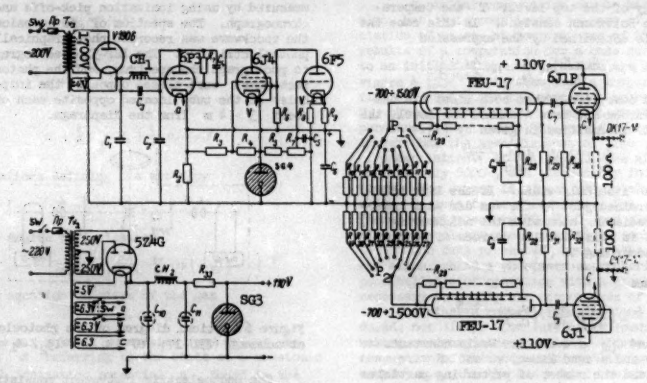

Figure 7. Electronic diagram of the photoelectric attachment.

DETERMINATION OF THE AIR TEMPERATURE BEHIND THE SHOCKWAVE ACCORDING TO THE LITHIUM AND SODIUM LINES

The investigation of the air glow behind a shockwave in a pure shock tube with a 3.7 km/sec shockwave velocity and an initial air pressure of 10 mm Hg has shown that the glow spectrum consists of Na and Ca resonance lines and AlO bands, i.e., of lines and bands of substances composing the compounds which contaminate the air and walls of the tube. In particular, the appearance of the AlO band results from contamination of the tube during destruction of the diaphragm. Hence, the air glow spectrum in a pure shocktube did not contain lines suitable for measuring the temperature by the method of relative intensities. In this connection, the necessity arose of introducing a material into the shocktube which would give lines in the emission spectrum of the gas behind the shockwave suitable to measure the temperature. Lithium and sodium were selected as such substances and they were introduced into the shocktube in the form of NaCl and LiCl powders.

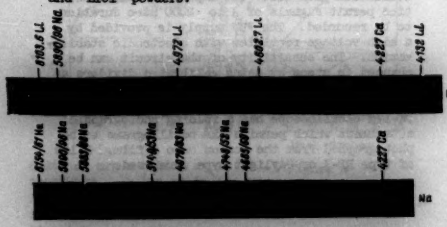

Figure 8. Spectrum of the air glow behind a shockwave upon the introduction of LiCl and NaCl in a shocktube.

Upon the introduction of 15 g of salt, it was distributed over the tube walls in a uniform layer after 3 - 4 experiments and the intensity of the series of Li and Na lines in the majority of the subsequent 20 - 30 experiments was sufficient for quantitative measurements and the determination of the temperature by the method of relative intensities.

Shown in Figure 8 is the spectrum of the airglow behind the shockwave when colored by LiCl and NaCl salts. Presented in Table 1 are the fundamental data on these lines which are necessary to compute the temperature. The transition probabilities are taken from [5] as the average of experimental and theoretical results.

Table 1

Transition probabilities of the Li and Na Lines

Element	λ (in Å)	A.g. (relative unit)	E (in eV)	$C_6 \cdot 10^{30}$ (in $cm^6 sec^{-1}$)
Li	6103	1.0	3.86	0.12
	4603	0.38	4.32	0.56
	4132	0.13	4.85	1.50
Na	8195—93	10.5	3.81	0.057
	6161—54	0.27	4.12	0.99
	5688—83	2.17	4.29	0.53
	5153—49	0.13	4.51	2.32
	4983—79	10	4.59	1.52
	4669—65	0.43	4.71	3.34

The first large series of experiments on determining the air temperature behind the shockwave was made according to the relative intensities of the lithium lines 6103 and 4603 Å. Since the degree of reabsorption of the lithium lines was not checked, the results were processed under two assumptions: 1) the line intensity is not distorted by reabsorption and the temperature can be

Table 2

Air temperature behind a shockwave determined by the relative intensities of the Li and Na lines (in °K)

v_{av} (in km/sec)	computed	λ 4603,6103 Å without self absorption	λ 4603/6103 Å with self absorption	Number of experiments
		a. Lithium		
3.7	3950	4500 ± 900	2800 ± 300	45

b. Sodium

v_{av} (in km/sec)	computed	λ 4980/6160 Å without self absorption	λ 4980/6160 Å with self absorption	No. of exp.	λ 4980/5688 Å without self absorption	λ 4980/5688 Å with self absorption	No. of exp.	λ 5153/6160 Å without self absorption	λ 5153/6160 Å with self absorption	No. of exp.	λ 4668/6160 Å without self absorption	λ 4668/6160 Å with self absorption	No. of exp.	Methods used
3.50±0.2	4300	2800±500	3500±700	11	3300±800	1900±300	13	—	—	—	2800±400	2600±300	2	Without cutting off the layer near the wall
3.7	3850	2500±300	2840±540	23	3000±500	1800±200	27	2900±200	2000±100	5	3300±400	2900±300	10	Without cutting off the layer near the wall
3.7±0.2	3850	2700±400	2400±600	15	2400±200	2300±400	17	6000±2400	3100±600	6	3100±400	2800±500	16	Cutting off the layer near the wall

determined by means of (8) without taking reabsorption into account; 2) the lines are completely reabsorbed, so that it is necessary to take reabsorption into account and the temperature should be determined by using (11).

The results of determining the air temperature behind the shockwave according to the lithium lines are presented in Table 2. As is seen from the results of Table 2, the experimental temperature determined without taking self-absorption, appears to equal $4500 \pm 900°$, taking self-absorption into account, it is $2800 \pm 300°$. Presented in this same Table 2 are the results of determining the temperature according to four pairs of sodium lines (see the first two rows of b Sodium). As is seen from the results presented in Table 2, the results of measuring the temperature according to the different lines are very contradictory. All the pairs in both the first and the second method of processing the results yield neither concordant results nor agreement with theoretical data.

Before turning to a further discussion of the results, let us note that the results presented in Table 2 have been obtained in measuring line intensities by a photographic method. Results differing from those presented in Table 2 have been obtained in measurements by a photoelectric method. Special experiments have shown that this depends on the existence of intense background, whose intensity varies from experiment to experiment exactly as does the absolute line intensity. It would be necessary to take the background into account in the same experiment in which the line intensity is measured. Taking the background into account was possible in the photographic method of recording. Only the intensities of two lines could be measured in one experiment without taking the background into account when a two-channel photoelectric attachment is used. In order that the background could also be measured simultaneously, it would be necessary to have at our disposal a four-channel photoelectric instrument, which we did not have.

The lack of agreement of the data presented in Table 2 could be explained by the non-equilibrium state of the gas behind the shockwave. But before making such a fundamental conclusion, it is necessary to consider other possible explanations. First of all, the question arises of which method of processing must be used, whether to take reabsorption into account or not. We could clarify this question by verifying the relative intensities of the sodium doublet components. In the absence of reabsorption, their relative intensities must equal 1:2, or for complete reabsorption 1:1.4.

The experiments conducted led to the following result. The sodium concentrations in the case for which recording of the lines is possible, are such that the line intensity is found to be on the transition part of the growth curve. The lines are partially reabsorbed but not so much so that their intensities would be proportional to N. The degree of reabsorption varies from experiment to experiment. Apparently, the very great scatter in the values of the temperatures determined in the various experiments is thus explained.

If this is so, then we can indicate only the limits within which the gas temperature lies. One of the limits will be the temperature obtained taking reabsorption into account, the other, without taking reabsorption into account.

The pair of lines 4668/6160 Å yields not very different temperature values when processed either by (8) or (11).

The average gas temperature behind the shockwave according to this pair of lines was also taken as the most reliable. It is 3000° K, i.e., lower than the computed value 3950° K corresponding to the velocity of shockwave propagation in air of 3.7 km/sec.

One of the possible reasons for this difference can be the nonuniformity of the temperature over the plug cross-section. The temperature of the gas layer near the wall would appear to be larger, from the self-reversal of the sodium D-lines observable in all the experiments. We arrived at this same conclusion on the basis of experiments on photographing the plug from the endplate of the shock tube by using a high-speed movie camera with a radially shuttered lens. It is seen from Figure 9, on which a photograph of the plug, thus obtained, is presented, that the fundamental part of the glow, specified by the sodium D -lines, is concentrated near the shock tube wall in the form of an annulus. Measurement and computation from the photographs showed that sodium moves from the walls 7 - 8 mm within the tube. The average temperature of the layer near the wall can be almost the temperature of the axial sections of the plug but it can also differ radically. In order to explain this question, we made a series of experiments in which the cut-off of the layer near the wall was guaranteed by using an opening of special form and the stream was colored by sodium chloride placed on a plate located in the diametral plane of the tube. Thus, intense coloring of the stream at which the sodium line could be considered reabsorbed, was achieved at the same time as the temperature should be taken as the temperature determined taking reabsorption into account. The effectiveness of the cut-off of the layer near the wall was verified by the absence of noticeable self-reversal of the sodium D -lines. The results of determining the temperature according to the sodium lines when cutting off the layer near the wall and coloring the core of the plug are presented in the last row of Table 2b. As is seen, even in these experiments, in our opinion the most accurate, the temperature determined by taking reabsorption into account is considerably lower than the computed value. The explanation of this difference is simple enough. An estimate of the sodium concentration in the air behind the shockwave according to the degree of reabsorption of the sodium line showed that it reaches 1 %. In order to melt, evaporate and dissociate such a quantity of sodium, an expenditure of energy is necessary. This leads to a reduction in the air temperature behind the shockwave. Computations verified the experimental result. The sodium concentrations required for a sufficiently intense glow change the thermodynamic properties of air behind the shockwave. Therefore, it is impossible to use the method of relative intensities of the sodium lines in order to investigate the state of air behind a shockwave.

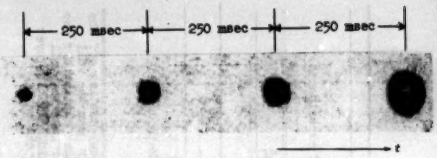

Figure 9. Photographs of the plug from the end of the tube, made by using a high-speed movie camera.

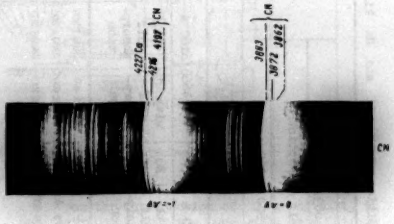

Figure 10. Spectrum of the CN glow behind a shockwave.

DETERMINATION OF THE AIR TEMPERATURE BEHIND A SHOCKWAVE ACCORDING TO CYANOGEN BANDS

One of the most prominent inadequacies of the determination of the air temperature behind a shockwave by means of the sodium and lithium lines was that these substances were introduced into the tube in the solid phase. We could not regulate their concentration. Sodium and lithium either were admitted from the tube walls or from a plate specially inserted into the tube, which could distort the gas dynamic properties of the flow.

It would be most correct to color the air by introducing the substance in the gaseous phase. This would guarantee the uniform mixing of the air and the coloring matter and such an acute question of the cold layer near the wall would not arise. However, it would not be easy to select such a gas. After various attempts, we hit upon dicyanogen, which decomposed into the CN radical at high temperatures and gave an intense band spectrum for concentrations on the order of 10 - 15 % in air (see Fig. 10). The method of measuring the temperature according to the CN bands with unresolved structure was carried out to a high degree of perfection by Brinkman [6] and Smit [7].

Table 3.

Gas temperature behind a shockwave determined by CN bands (°K)

Concentration $(CN)_2$ (in %)	v_{av}, km/sec	T (in °K) computed	λ 4197/4216 Å	No. of exp.	λ 3872 3883 Å	No. of exp.	Gas used	Method used
20	3.56±0.3	3760*	3700±500	42	~6700±1100	24	air	photographic
17	3.52±0.2	3700	4200±900	9	—	—	air	photoelectric
17	3.55±0.2	3780	4200±700	9	—	—	air	photographic
15	3.45±0.2	3580	2300±300	18	6200±400	4	nitrogen	photographic
0.2	3.4	4640	3700±500	3	7100±1500	2	nitrogen	photographic

Table 4.

Gas temperature behind a shockwave determined by the relative intensities of five CN 4216 A bands (v = - 1) in an N_2 + $(CN)_2$ mixture (°K)

Concentration $(CN)_2$ (%)	v_{av} km/sec	T (in °K) computed	2-1	3-1	4-1	5-1	3-2	4-2	5-2	4-3	5-3	5-4	No. of exp.
15	3.3±0.1	3400	2910±230	4180±120	4940±800	4610±290	8020±1420	8000±1560	5630±610	8500±2400	4720±1150	4090±1030	5
2.2±0.4	3.43±0.1	4400	3470±410	4810±150	4610±220	4360±200	6050±880	5700±840	4810±240	5530±840	4440±350	3880±660	5
2.2±0.3	3.14±0.1	4600	3460±510	4450±550	5130±400	4200±400	6330±270	6980±650	4450±510	7310±1330	3820±480	2690±390	7

* The temperature for air has been calculated without taking into account the influence of the $(CN)_2$. The influence of dicyanogen on the thermodynamic properties of the nitrogen has been taken into account in computing the temperature of the stopper for nitrogen and dicyanogen mixtures.

The first experiments on measuring the air temperature behind a shockwave using the CN bands 4197/4216 Å gave encouraging results (see Table 3); the temperature determined by this pair of bands appears to be close to the computed value. Experiments on measuring the air temperature for various shockwave speeds gave a systematic growth of the temperature with increasing shockwave speed. However, the second pair of CN bands 3872/3883 Å gave systematically high values of the temperature (~ 7000 - 8000° K).

Experiments to determine the nitrogen temperature behind the shockwave (Table 3) gave the same results. The temperature determined by the pair of CN bands 3872/3883 Å appears to be very much higher than the computed temperature and the temperature determined by the CN 4197/4216 Å bands. This could be explained by reabsorption since the 3872/3883 Å pair has a higher transition probability and ends up on the ground energy level in comparison with the 4197/4216 Å pair of bands. In order to clarify this question, the cyanogen concentration was reduced to 0.2 %, nevertheless the temperature determined according to the 3872/3883 Å band remained very much greater than the temperature determined according to the 4197/4216 Å band.

Two assumptions can be proposed to explain the difference observed. Either the pair of 3872/3883 Å CN bands is reabsorbed also at such low concentrations as 0.2 %, or a delay occurs in the establishment of equilibrium in the cyanogen vibrational levels. In order to verify the last assumption, a new series of experiments was formulated. The nitrogen temperature behind the shockwave was determined according to the relative intensity of the five vibrational CN bands ($\Delta v = -1$), whose transition probabilities were determined by Somers [8]. The results of these measurements are given in Table 4. As is seen from the results presented, the various pairs of bands yield a different temperature, where the differences reach very large values. From an analysis of the results of Table 4 it follows that the differences in the temperatures observed according to the various pairs could hardly be explained just by reabsorption. Apparently, there occurs a non-equilibrium distribution of the CN molecules over the vibrational levels.

CONCLUSION

The experimental results show the difficulties which beset attempts to use the method of relative intensities for a pyrometric investigation of air and nitrogen behind a shockwave. In that temperature range which can be obtained in shock tubes, nitrogen and air do not emit spectral lines. It is necessary to color the gas being investigated. The coloring of a nitrogen and air by metal salts appears to be hardly suitable since it does not guarantee a homogeneous distribution of the impurity atoms over the volume being investigated; the necessary impurity concentrations appear to be so large that the thermodynamic properties of the gas being investigated change substantially.

In order to guarantee homogeneous coloring over the volume, it is most expedient to color the nitrogen and air by gaseous impurities. However, gases do not exist which emit atomic lines at temperatures of 3000 - 4000° .

Homogeneous coloring of the nitrogen and air can be guaranteed by using dicyanogen and by using cyanogen vibrational bands for a pyrometric investigation. But, as the results presented above show, this is apparently hindered by the finite build-up time of the equilibrium of the molecules over the vibrational degrees of freedom.

It seems to us, and this confirms the research already conducted in our laboratory, that it is most correct to use the generalized method of spectral line reversal [9] to solve the problem of investigating the state of air and nitrogen behind a shockwave in the 1500 - 5000° K temperature range. As regards the method of relative intensities, it should only be used to investigate gases with temperatures above 5000° K. In particular, it is expedient to investigate the state of noble gases behind strong shockwaves by using hydrogen lines.

April 3, 1958

References

1. E. L. RESLER, SHAO-CHI LIN, A. KANTROWITZ: J. Appl Phys., 23, 1390 (1952)
2. L. LAND, SHAO-CHI LIN:J. Appl. Phys., 28, 754 (1957)
3. N. N. SOBOLEV: ZETF, 19, 25 (1949); Tr. FIAN USSR, 7, 754 (1957)
4. A. UNSOLD: Sb. - Modern problems of astro- and solar physics. IL, Moscow, 1951
5. A. P. DRONOV, A. G. SVIRIDOV, N. N. SOBOLEV: OiS, 5, 490 (1958)
6. H. BRINKMAN: Optische studie van de electrische lichtboog. Amsterdam, 1937
7. J. A. SMIT: Het verkrijgen en meten van constante hoge temperaturen. Jens-Utrecht, 1950
   J. L. SPIER, J. A. SMIT: Physica, 9, No. 7, 597 (1942)
   J. L. SPIER, M. M. SMIT-MIESSEN: Physica, 9, No. 4, 422 (1942)
   M. M. SMIT-MIESSEN, J. L. SPIER: Physica, 9, No. 2, 193 (1942)
8. P. J. SOMERS: Onderzoek van een boogontlading in stikstof bij verhoogde druk. Nijmegen, 1954
9. A. G. SVIRIDOV, N. N. SOBOLEV: ZETF, 24, 93 (1953); N. N. SOBOLEV, A. V. POTAPOV, V. F. KITAEVA, F. S. FAIZULLOV, V. N. ALIAMOVSKII, E. T. ANTROPOV, I. L. ISAEV: IAN USSR, Ser. fiz., 22, 730 (1958) (See CTT Bulletin)

TOM VI, Vyp. 3 OPTIKA I SPEKTROSKOPIIA Mart, 1959
VOL. VI, No. 3 OPTICS AND SPECTROSCOPY March, 1959

On the Oscillator Strength of the γ-Band System of NO

S. P. ERKOVICH

Abstract: Analysis of the experimental data of Marmo and Mayence gives a value for the oscillator strength of the γ band system of NO of 0.043 in contradiction to the value 0.0025 of Weber and Penner. It is shown that Weber and Penner obtained their result on the basis of assumptions which actually had not been fulfilled in the conditions of their experiment.

The problem of absolute intensities of the electronic transitions $X^2\Pi - A^2\Sigma$ (γ-band) and $X^2\Pi - B^2\Sigma$ (β-band) in NO molecules has gained more importance recently. Both these band systems correspond to transitions which would be forbidden for dissociated atoms. However, according to Mulliken [1], for molecules such transitions can in certain cases, as for example the N - V transition, be of high intensity with a total oscillator strength of the order of 0.1 and larger. Attributing the β-bands of NO to N - V transitions one can expect that $f_\beta \sim 0.1$ and a comparision of experimental data [2] on transitions in the β- and γ-band region shows that f_β and f_γ should have values of the same order. Weber and Penner [3] on the other hand obtained from their experiments $f_\gamma = 0.0025$.

In this publication we make an attempt to determine f_γ from the experiments of Marmo [2] and Mayence [4]. We show that Weber and Penner obtained f_γ by applying an incorrect method to process their experimental data.

BASIC RELATIONS

The transmission of the spectrograph can be defined by the expression [5]

$$T_i = \frac{I_i}{I_{bl}} = \frac{\int_0^\infty e^{-k_j l} \varphi(|\nu - \nu_i|)\, d\nu}{\int_0^\infty \varphi(|\nu - \nu_i|)\, d\nu}, \tag{1}$$

where $\varphi(|\nu - \nu_i|)$ is a function whose form is determined by the parameters of the spectrograph; ν_i is the wave number of the transmission band of the spectrograph; l is the thickness of the absorbing layer.. The absorption coefficient k_ν is defined by the sum of absorption coefficients of all rotational lines i.e.

$$k_\nu = \sum_j k_{j\nu}. \tag{2}$$

If the single lines of the band overlap slightly one can represent the transmission T_i in the form

$$T_i = \frac{1 - \sum_j \int_0^\infty (1 - e^{-k_{j\nu} l}) \varphi(|\nu - \nu_i|)\, d\nu}{\int_0^\infty \varphi(|\nu - \nu_i|)\, d\nu}. \tag{3}$$

Since in our case the width of the rotational lines δ is much smaller than the width of the transmission band of the spectrograph and since consequently $\varphi(|\nu - \nu_i|)$ changes little within the limits of δ we can write

$$T_i = \frac{1 - \sum_j \varphi(|\nu_j - \nu_i|) \int_0^\infty (1 - e^{-k_{j\nu} l})\, d\nu}{\int_0^\infty \varphi(|\nu - \nu_i|)\, d\nu}. \tag{4}$$

where ν_j is the wave number of the line center.

Taking according to [5] as the function $\varphi(|\nu - \nu_i|)$ an expression of the form

$$\varphi(|\nu - \nu_i|) = \begin{cases} 0 & \text{for } \nu \leqslant \nu_i - a, \\ (\nu - \nu_i + a)\frac{1}{a} & \text{for } \nu_i - a \leqslant \nu \leqslant \nu_i, \\ (\nu_i - \nu + a)\frac{1}{a} & \text{for } \nu_i \leqslant \nu \leqslant \nu_i + a, \\ 0 & \text{for } \nu \geqslant \nu_i + a, \end{cases} \tag{5}$$

where a is the width of the transmission band of the spectrograph we get

$$T = 1 - \frac{1}{a} \sum_j \varphi(|\nu_j - \nu_i|) \int_0^\infty (1 - e^{-k_{j\nu} l})\, d\nu. \tag{6}$$

We write the absorption coefficient $k_{j\nu}$ in the form

$$k_{j\nu} = \frac{S_j \delta}{\pi} \frac{1}{(\nu - \nu_j)^2 + \delta^2}. \tag{7}$$

Here

$$S_j = \int_0^\infty k_{j\nu}\, d\nu.$$

The integral in (6), equals $2\sqrt{S_j \delta l}$ when one substitutes the quantity $(\nu - \nu_j)^2$ for $(\nu - \nu_j)^2 + \delta^2$ in $k_{j\nu}$. This substitution does not affect the result of our calculations substantially if, under the conditions of the experiment, as was the case in [2,4], $e^{-k_j \nu l} \approx 0$ for $(\nu - \nu_j)^2 \approx \delta^2$. In this case we get:

$$T = 1 - \frac{1}{a} \sum_j \varphi(|\nu_j - \nu_i|) \cdot 2\sqrt{S_j \delta l}. \tag{8}$$

For one line of the band the integral S_j equals [1, 6]

$$S_j = \frac{8\pi^3 \nu_1^3}{3hc} \frac{n_{v'j''}}{2j''+1} i_{j''} G' q(v'v'') R_e^2. \tag{9}$$

Where j" is the rotational quantum number of the lower level; $n_{v'j''}$ is the concentration of molecules in the lower electronic vibrational-rotational state; $q(v'v'')$ is the Franck-Condon factor ($q(1,0)=0.330$; $q(2,0)=0.291$ [7]) R_e is the electronic moment of the transition, G' is Mulliken's multiple transition factor; $i_{j''}$ is the square of the matrix element of the rotational transition (intensity factor of Hönl-London).

Expressing R_e in (9) by the total oscillator strength for a given electronic transition from the relation

$$f = \frac{8\pi^3 c m R_e^2 \bar{\nu} G'}{3h}, \tag{10}$$

we obtain

$$S_j = \frac{\pi e^2 \nu_1}{c^2 m \nu (2j+1)} \; n_{\nu'' j''} \; i_{j''} q(\nu'\nu'') f, \tag{11}$$

where $\bar{\nu}$ is the average value of the wave number for a given electronic transition which we will identify with the wave number of the band $\gamma(0,0)$ equalling 4.43×10^4 cm^{-1}.

We determine the molecular concentrations $n_{\nu'' j''}$ for the states $X^2\Pi_{\frac{3}{2}}$ and $X^2\Pi_{\frac{1}{2}}$ correspondingly from the relations:

$$n_{\nu'' j''} = N(1-\exp[-\frac{hc\omega''}{kT}])\exp[-\frac{hc\omega''\nu''}{kT}](2j''+1)\exp[-\frac{B''j''(j''+1)hc}{kT}] \times \frac{B''hc}{kT} \; \frac{g_{3/2} \exp[-\frac{\Delta E}{kT}]}{g_{1/2} + g_{3/2} \exp[-\frac{\Delta E}{kT}]}, \tag{12}$$

$$n_{\nu'' j''} = N(1-\exp[-\frac{hc\omega''}{kT}])\exp[-\frac{hc\omega''\nu''}{kT}](2j''+1)\exp[-\frac{B''j''(j''+1)hc}{kT}] \times \frac{B''hc}{kT} \; \frac{g_{1/2}}{g_{1/2} + g_{3/2} \exp[-\frac{\Delta E}{kT}]}. \tag{13}$$

Where $g_{\frac{1}{2}} = 2$ and $g_{\frac{3}{2}} = 2$ are the electronic statistical weights of the states $X^2\Pi_{\frac{1}{2}}$ and $X^2\Pi_{\frac{3}{2}}$; $\Delta E = 121$ cm^{-1} is the energy interval between the levels $X^2\Pi_{\frac{1}{2}}$ and $X^2\Pi_{\frac{3}{2}}$; $B'' = 1.7046$ cm^{-1} is the rotational constant of the level $X^2\Pi$; $\omega'' = 1904$ cm^{-1}.

We define the Hönl-London intensity factors by the equation [6]

$$\left.\begin{aligned} j' = j'', \quad & i = \frac{(2j+1)\Omega^2}{j(j+1)}, \\ j' = j'' \pm 1, \quad & i = \frac{j^2 - \Omega^2}{j}, \end{aligned}\right\} \Omega' = \Omega'', \tag{14a}$$

$$\left.\begin{aligned} j' = j'', \quad & i = \frac{(2j+1)(j \pm \Omega)(j \pm \Omega + 1)}{2j(j+1)}, \\ j' = j'' \pm 1, \quad & i = \frac{(j+\Omega)(j+\Omega-1)}{2j}, \\ j' = j'' \pm 1, \quad & i = \frac{(j-\Omega)(j-\Omega+1)}{2j}, \end{aligned}\right\} \Omega' = \Omega'' \pm 1. \tag{14b}$$

The damping constant δ we can obtain from the relation

$$= \frac{1}{4\pi c} A_{\nu'\nu''} = \frac{2\pi e^2 \nu_1^3}{mc^2 \bar{\nu}} f. \tag{15}$$

Substituting the expressions (11) and (15) in (8) we get

$$T = 1 - \frac{2\pi e^2 \nu_1^3}{mc^2 \bar{\nu}} l \sum_j \varphi(|\nu_j - \nu_1|) \sqrt{2i_{j''} q(\nu'\nu'') l \frac{n_{\nu'' j''}}{2j''+1}}. \tag{16}$$

The absorption function $A = 1 - T$ will have the form

$$A_{calc.} = \frac{2\pi e^2 \nu_1^3}{mc^2 \bar{\nu}} l \sum_j \varphi(|\nu_j - \nu_1|) \sqrt{2i_{j''} q(\nu'\nu'') l \frac{n_{\nu'' j''}}{2j''+1}}. \tag{17}$$

ANALYSIS OF EXPERIMENTAL DATA OF MARMO AND MAYENCE

If we compare (17) with the experimental value of the absorption function for a given ν_1, i.e. with the quantity

$$A_{exp.} = 1 - T_{exp.} = 1 - \exp[-\frac{kpl}{760}] \tag{18}$$

where p is the pressure of NO in mm Hg ; k is the experimental value of the absorption coefficient determined by the equation $I = I_0 e^{-kl}$ normalized to standard pressure, we get

$$f = \frac{1 - e^{-\frac{kpl}{760}}}{\frac{2\pi e^2 \nu_1^3}{mc^2 \bar{\nu}} \sum_j \varphi(|\nu_j - \nu_1|) \sqrt{2i_{j''} q(\nu'\nu'') l \frac{n_{\nu'' j''}}{2j''+1}}} \tag{19}$$

Since the absolute value of ν_1 was not identified precisely we calculated the absorption function with the aid of (17) in units of f, i.e. $\frac{A_{calc.}}{f}$, for several values of ν_1 within a given band which allowed us to obtain a band contour similar to the experimental band contour. The oscillator strength was determined from the relation

$$f = \frac{1 - e^{[-\frac{k_{max} pl}{760}]}}{\frac{A_{calc.\,max.}}{f}}. \tag{20}$$

The calculation with the experimental data of Marmo [2] in the region of the long wave length band maximum of $\gamma(1,0)$ and $\gamma(2,0)$ is shown in Table 1.

TABLE 1

bands	p, mm Hg	k-Marmo's value	$T_{exp.}$	$\frac{A_{calc}}{f}$	f
(2,0)	4.0	7.9	0.824	4.12	0.043
	7.9	4.75	0.79	5.81	0.036
	14.8	4.4	0.67	7.93	0.0416
	50	4.1	0.282	14.8	0.049
(1,0)	14.8	4.7	0.651	7.57	0.046
				Average	0.043

For the calculation of the function $\varphi(|\nu_j - \nu_1|)$ we used data from the analysis of the rotational band structure by Schmid [8]. The transmission band-width of the spectrograph in Marmo's experiments was 0.85 A, the thickness of the absorbing layer was $l = 4.7$ cm. The temperature of the experiment we assumed to be 293°K.

The experimental data of Mayence [4] are expressed in k values determined by the equation $k = \frac{1}{l} \log_{10} \frac{I_0}{I}$ and normalized to standard pressure, the pressure at which the experiment was done not being indicated in her publication. The data of Mayence for the long wave maximum of the $\gamma(1,0)$-band are given in the column l and k of Table 2.

Taking into account that according to (17) $A_{calc.} \sim \sqrt{pl}$ we can write

$$\frac{1 - T_{exp.}}{\sqrt{l}} = \text{const.} \quad \text{for } p = \text{const}, \tag{21}$$

where

$$T_{exp.} = e[-\frac{k \cdot 2.303\, pl}{760}].$$

TABLE 2

l (in cm)	k (in cm^{-1})	$T_{exp.}$	$\frac{A_{calc.}}{f}$	f
0.1	9.5	0.971	0.908	0.032
1.0	3.6	0.897	2.88	0.036
5.0	1.6	0.784	6.41	0.034
50	0.65	0.347	20.3	0.032

The graphical solution of equation (21) gives $p \approx 10$ mm Hg.

Assuming that the transmission band width of the spectrograph in the experiment of Mayence was approximately the same as that of Marmo, which is indicated in [2], we find the oscillator strength from relation (20). The results of the calculation are shown in Table 2.

Since the exact parameters of Mayence's spectrograph are not known one should consider the data in Table 2 as less precise.

To check the uniqueness of the results obtained we also made a calculation for the short wave length maximum of the $\gamma(1,0)$ -band. The results of these calculations are shown in Table 3. Since in this case the line density is considerably higher than in the region of the long wave length maximum, the data in Table 3 are also less precise.

TABLE 3

l (in cm)	p (in mm Hg)	k (in cm^{-1})	$T_{exp.}$	$\frac{A_{calc.}}{f}$	f	Remarks
0.1	10	15 - 2.303	0.955	1.20	0.037	From data of Mayence
1.0	10	6.5 - 2.303	0.82	3.81	0.047	
5.0	10	2.7 - 2.303	0.664	8.47	0.040	
4.7	14.8	8.9	0.445	10	0.056	From data of Marmo

DISCUSSION OF RESULTS

In the calculation of f we did not consider collision broadening and Doppler broadening. Collision broadening may be neglected only at low pressures when $\delta_0 \gg \delta_{coll.}$. For the highest pressure used, p = 50 mm Hg, the ratio of $\frac{\delta_0 + \delta_{coll.}}{\delta_0}$ is ~ 3 i.e. neglecting the quantity $\delta_{coll.}$ leads to the overestimation of f by a factor of $\sqrt{3} \approx 1.7$. The data in Table 1 seem to confirm this effect although it is considerably weakened by the compensating influence of overlapping of lines at higher pressure.

The Doppler broadening however, does not influence the intensity distribution in the line wings and consequently does not affect noticeably the value of the integral in (6).

In order to check the results we made a numerical integration of the expression (1) with the coefficient k_ν, obtained considering the combined damping action (emission + collision broadening) and Doppler effect, assuming that f = 0.040. For the long wave length maximum of the $\gamma(1,0)$ band, for p = 14.8 mm Hg and for l = 4.7 cm we obtained T = 0.70 while the experimental value is 0.65, which confirms the correctness of our results. Simultaneously we checked numerically the degree of overlapping of lines, which confirms the possibility of using relation (4).

Since our results distinctly contradict the data of Weber and Penner [3] we made an analysis of their experiments in order to clarify the reasons for our disagreement.

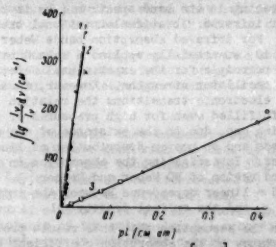

Figure 1. Dependence of $\int \lg \frac{1}{T} d\nu$ on the optical density pl. 1 - experimental line of Weber and Penner (dots: experimental data) 2 - theoretical dependence for f = 0.0025 values of l for the theoretical points: x – 0.005 cm, +–0.0025 cm, □ – 0.08 cm, Δ – 0.04 cm, O – 0.0042 cm.

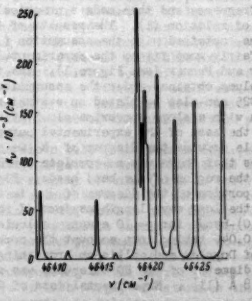

Figure 2. Absorption coefficient in the region of the long wave maximum of the $\gamma(1.0)$ -band.

It follows from (1) that in those cases where in the total transmission interval of the spectrograph

$$e^{-k_\nu l} \approx \text{const}, \tag{22}$$

then

$$T_i \approx e^{-(k_\nu l)_{av.}} \tag{23}$$

and consequently

$$\int \ln \frac{1}{T} d\nu \approx \int k_\nu d\nu = pl \int k'_\nu d\nu , \tag{24}$$

where k'_ν is the absorption coefficient normalized to unit pressure. The last integral is connected with f by the well known relation [9].

$$\int k'_\nu d\nu = \frac{n\pi e^2}{mc^2}\,\frac{\nu}{\bar{\nu}}\,q(v'v'')f.$$

For sufficiently wide rotational lines the relation (22) is fulfilled better the smaller the distance between the lines and the more uniform their spacing in the band spectrum (as is the case for infrared vibrational-rotational transitions.) For infrared absorption bands Weber and Penner [10] successfully applied a method based on this principle for the experimental determination of oscillator strengths. However, in the case of electronic transitions the relation (22) is not fulfilled even for high pressures of the broadening gas, due to the existence of one or more heads and an uneven distribution of line intensities. Investigating the absorption in the γ -band region of NO Weber and Penner [3] obtained a linear dependence between the integral $\int \lg \frac{1}{T}\, d\nu$ and the optical density pl. Proceeding from the assumption that this result proves the constancy of the absorption coefficient due to large broadening and strong line overlapping, they obtained $f_\gamma = 0.0025$.

To check their assumption we calculated for the $\gamma(1,0)$ -band the value of $\int \lg \frac{1}{T}\, d\nu$ for small pl by using relation (8), which is valid for small overlapping, and also for large pl. In the latter case, for calculating T, we first drew a graph of the dependence of $k_\nu = \sum k_{j\nu}$ on the frequency and then made a numerical integration of relation (1). The results of the calculations, obtained with the assumption $f = 0.040$, gave a fairly good fit to the experimental data of Weber and Penner (see Figure 1). The theoretical values obtained under the assumption $f = 0.0025$ can also be placed on a straight line although with a slope approximately 17 times less than in the case of the experimental curve.

While drawing the diagram of k_ν we convinced ourselves that there was no complete overlapping even in the region of the band heads. Figure 2 shows a portion of the diagram of k_ν in the region of the long wave length maximum of the γ (1,0)-band for $p = 10$ atmos. calculated for $f = 0.040$ taking into account the combined effect of Doppler and collision broadening. The optical diameter of the NO molecules was assumed to be 3.8 Å [11] . Experimental data of Geydon and Fairbairn [12] on measuring the collision line widths of γ -bands for NO at $p = 1$ atmos. also indicate the absence of sufficiently complete overlapping. Since in this case

$$T_1 = (e^{-k_\nu l})_{av.} > e^{-(k_\nu l)_{av.}}, \tag{25}$$

where

$$(e^{-k_\nu l})_{av.} = \frac{\int e^{-k_\nu l}\varphi(|\nu - \nu_1|)d\nu}{\int \varphi(|\nu - \nu_1|)d\nu}$$

and since

$$\int \lg \frac{1}{T}\, d\nu < pl \int k'_\nu\, d\nu, \tag{26}$$

one can represent the results of Weber and Penner [3] in the form of an inequality $f_\gamma > 0.0025$.

With the feeling of pleasant duty I express my deep gratitude to L. M. Biberman for his guidance in this work and also to V. A. Fabrikant for his continuous interest.

March 17, 1958

References

1. R. S. MULLIKEN: J. Chem. Phys., 7, 14, 20 (1939)
2. F. F. MARMO: JOSA, 1186 (1953)
3. D. WEBER, S. S. PENNER, J. Chem. Phys., 26, 860 (1957)
4. J. MAYENCE: Ann. de phys., Ser. 12, 7, 453 (1952)
5. J. R. NIELSEN, V. THORNTON, E. B. DALE: Rev. Mod. Phys., 16, 307 (1944)
6. R. S. MULLIKEN: Rev. Mod. Phys., 3, 89 (1931)
7. W. R. JARMAIN, P. A. FRASER, R. W. NICHOLLS: Astrophys. J., 118, 228 (1953)
8. R. SCHMID: Z. Phys., 49, 428 (1928); 64, 84 (1930)
9. A. UNSÖLD: Physik der Sternatmosphären. Berlin, Springer, 1938 (IL, Moscow, 1949)
10. S. S. PENNER, D. WEBER: J. Chem. Phys., 807, 817, 974, (1951)
11. W. R. THORSON, R. M. BADGER: J. Chem. Phys., 27, No. 3, 609 (1957)
12. A. G. GAYDON, A. R. FAIRBAIRN: Proc. Phys. Soc., A67, 474 (1954)

TOM VI, Vyp. 3 OPTIKA I SPEKTROSKOPIIA Mart, 1959
VOL. VI, No. 3 OPTICS AND SPECTROSCOPY March, 1959

Determination of Molecular Constants from Band Spectra by the Parabolic Interpolation Method

V. A. LOGINOV

Abstract: This paper is devoted to the exposition of a method of precise mathematical processing of the results of measurements of the fine structure of electronic-vibrational-rotational bands of diatomic molecules.

A scheme for the solution of this problem is expounded using the general method of parabolic interpolation according to the least squares method (the Chebyshev method) and it is shown that calculations by interpolating according to the Chebyshev method are easily included in the scheme of solution of the normal equations.

As an example the Q branches of a band are examined; in particular a sample calculation is made for the Q branch of the (11-2) band of the $^1\Pi \rightarrow {}^1\Sigma$ transition of the BeO molecule. Tables of powers and sums of powers of $x_J = J(J+1)\cdot 10^{-3}$ are given which considerably shorten the calculations connected with the formation of the normal equations.

INTRODUCTION

For the calculation of the thermodynamic functions of gases with the high degree of precision required for many practical purposes, the knowledge of sufficiently precise values of the molecular constants (electronic, vibrational, rotational, etc.) is very necessary. The determination of the molecular constants with the greatest possible degree of precision from the experimental data on the fine (or hyperfine) structure of molecular spectra is also necessary for the verification of the correctness of the theoretical formulas of the different branches of the bands observed in the electronic-vibrational-rotational spectra of molecules and also of the theoretical relations connecting the different molecular constants.

The problem connected with the determination of the molecular constants from band spectra with a high degree of precision requires, first of all, the use of instruments with the highest possible resolution and with the least reciprocal linear dispersion, of special sources of radiation and of corresponding experimental procedures which guarantee the best conditions for obtaining the most precise results, and secondly, this problem requires the use of the most precise method for mathematically processing the experimental data.

However, the mathematical processing of the experimental data on the rotational structure of molecular spectra by the method of least squares [1,2] according to the usual scheme turns out to be so time-consuming that up to the present time there have been no works in the literature on molecular spectroscopy where the degree of the interpolation polynomial was in turn determined with the aid of this method, which reflected the experimental data with a precision agreeing with the precision of measurement and where the most probable values of the molecular constants were found with estimates of their accuracies.

Even in those articles where the rotational structures of the bands were obtained with very high degrees of accuracy, the mathematical processing was carried out, as a rule, by rather crude methods (for example, graphically), with the result that the precision of the numerical values of the molecular constants obtained in these works turned out to be an order of magnitude lower than that which could have been obtained from the same experimental data by correctly processing them mathematically. An example of a similar kind with the data of Scheib [3] on the molecular constants of the $X^2\Sigma$ state of BO may be found in the literature [4].

As is well known, Birge and Shea [5] gave an account of a method for quickly determining the coefficients of the polynomial (1) according to the least squares method for equally spaced values of the independent variable, but the formulas and tables worked out by Birge and Shea cannot be used by us because in processing the experimental data on the rotational structure we have a more complex case when the variable x, corresponding to the known values of the interpolation functions, takes on unequally spaced values.

The purpose of the present work is the exposition of a scheme for using the parabolic interpolation method in the method of least squares (the Chebyshev method [6]) for the mathematical processing of the rotational structure branches of the bands of diatomic molecules in such a form as will be particularly convenient for computations and will, in particular, allow estimation at each stage of the quadratic error which corresponds to the degree of the interpolation polynomial taken.

As is shown below, the scheme employed not only greatly simplifies the computations and leads to a greater economy of time (both in carrying them out by calculators and in utilizing calculating machines) but, what is most important of all, it makes it possible to increase the degree of the interpolation polynomial without doing all the calculations anew, to estimate the quadratic error corresponding to the degree of the polynomial taken at each stage, to determine the degree of the polynomial in relation to the precision of the approximation obtained, and also to find the root mean square error in the determination of the molecular constants.

For clarity the scheme of application of the Chebyshev method is presented for the concrete example of the Q branch of the (11-2) band of the $^1\Pi \rightarrow {}^1\Sigma$ transition of the BeO molecule.

1. GENERAL EXPRESSION FOR THE INTERPOLATION FUNCTION

In smoothing computations, which we encounter in the determination of the molecular constants from experimental data on the rotational structure of electron bands, the peculiarity of the mathematical problem reduces to the fact that the precise analytical expression of the functions

interesting us is unknown, but the value of the interpolation function can be immediately found from measurements by spectral methods for a number of values of the rotational quantum number J, and represented in general form with sufficient precision in the form of a polynomial

$$y = C_0 + C_1 x + C_2 x^2 + \ldots, \tag{1}$$

where $x = \varphi(J)$; $C_0, C_1, C_2 \ldots$ are unknown coefficients, subject to determination; moreover the degree of the polynomial is unknown beforehand, and is determined in relation to the precision of the approximation obtained.

The problem which arises in the processing of experimental data is reduced, first of all, to the verification of the possibility of approximating the experimental data by a polynomial of the form (1) with a small number of terms, and secondly, to the determination of the most probable numerical values of the molecular constants x and to the estimation of their precision.

2. SOLUTION OF THE NORMAL EQUATIONS (THE METHOD OF GAUSS)

We may consider the unknown coefficients $C_0, C_1, C_2 \ldots$ in (1) as values determined by the functions $a = 1$; $b = x$; $c = x^2 \ldots$ Denoting these values by $X_1, X_2, X_3 \ldots$, respectively, we reduce equation (1) to the form

$$y = aX_1 + bX_2 + cX_3 + \ldots . \tag{2}$$

If the number of observed y_i is larger than the number of unknowns $X_1, X_2, X_3, \ldots$, then the problem connected with obtaining the most probable values $X_1, X_2, X_3 \ldots$, is solved according to the least squares method. From the n conditional linear equations

$$a_i X_1 + b_i X_2 + c_i X_3 + \ldots = y_i (i=1,2,\ldots,n), \tag{3}$$

where $a_i, b_i, c_i \ldots$ are unknown coefficients; y_i are measured quantities possessing random measurement errors, we form m normal equations

$$\begin{aligned} [aa]X_1 + [ab]X_2 + [ac]X_3 + \ldots &= [ay] \\ [ab]X_1 + [bb]X_2 + [bc]X_3 + \ldots &= [by] \\ \ldots\ldots\ldots\ldots\ldots\ldots \end{aligned} \tag{4}$$

Applying the method of Gauss [7] for the solution of the system (4), we arrive at the system of reduced equations

$$\begin{aligned} X_1 + \frac{ab}{aa} X_2 + \frac{[ac]}{[aa]} X_3 + \ldots &= \frac{[ay]}{[aa]} \quad (=K_0), \\ X_2 + \frac{[bc1]}{[bb1]} X_3 + \ldots &= \frac{[by1]}{[bb1]} \quad (=K_1), \\ X_3 + \ldots &= \frac{[cy2]}{[cc2]} \quad (=K_2), \\ \ldots\ldots\ldots\ldots \end{aligned} \tag{5}$$

from which we obtain unique values for $X_1, X_2, X_3, \ldots X_m$ according to a simplified scheme (see Table 1).

TABLE 1

Scheme of Solution of the Normal Equations (Doolittle Scheme)

	X_1	X_2	X_3	
N_1	$[aa]$	$[ab]$	$[ac]$	$[ay]$
E_1	1	$\frac{[ab]}{[aa]}$	$\frac{[ac]}{[aa]}$	$\frac{[ay]}{[aa]}$
N_2	—	$[bb]$	$[bc]$	$[by]$
(I)	—	$-\frac{[ab][ab]}{[aa]}$	$-\frac{[ab][ac]}{[aa]}$	$-\frac{[ab][ay]}{[aa]}$
I	—	$[bb1]$	$[bc1]$	$[by1]$
E_2	—	1	$\frac{[bc1]}{[bb1]}$	$\frac{[by1]}{[bb1]}$
N_3	—	—	$[cc]$	$[cy]$
(I)	—	—	$-\frac{[ac][ac]}{[aa]}$	$-\frac{[ac][ay]}{[aa]}$
(2)	—	—	$-\frac{[bc1][bc1]}{[bb1]}$	$-\frac{[bc1][by1]}{[bb1]}$
II	—	—	$[cc2]$	$[cy2]$
E_3	—	—	1	$\frac{[cy2]}{[cc2]}$

The weight of the quantity X_k $(k=1,2,3,\ldots,m)$ is $p_k = \frac{\Delta}{\Delta_{kk}}$, where Δ is the determinant of the system of normal equations (4), and Δ_{kk} is the minor corresponding to the diagonal element. The root mean square error for unit weight is obtained as

$$\sigma_0 = \pm \sqrt{\frac{[vv]}{n-m}} \tag{6}$$

The root mean square error of the quantity X_k will equal

$$\sigma_k = \frac{\sigma_0}{\sqrt{p_k}} \quad (k = 1, 2, 3, \ldots, m).$$

3. THE CHEBYSHEV METHOD AND ITS CONNECTION WITH THE FORMULAS AND SCHEMES OF GAUSS

The coefficients in the series (1) depend on the degree of the polynomial, therefore well-known difficulties arise in the computation of the coefficients in the case of a subsequent raising of the degree of the polynomial, since each time it is necessary to perform the computations anew.

These difficulties are removed if, in place of (2), we make use of polynomials of the orthogonal Chebyshev functions [6]

$$y = \sum_{i=0}^{i=m} K_i \psi_i(x) = K_0 \psi_0(x) + K_1 \psi_1(x) + \ldots + K_m \psi_m(x), \tag{7}$$

where the Chebyshev coefficients $K_0, K_1, \ldots, K_m$ are constant quantities and equal the right-hand terms of the reduced equations (5)

$$K_0 = \frac{[ay]}{[aa]}; \quad K_1 = \frac{[by1]}{[bb1]}; \quad K_2 = \frac{[cy2]}{[cc2]} \ldots, \tag{8}$$

and the polynomials are related to the functions of $x(a = 1; b = x; c = x^2 \ldots)$ by the following equations

$$
(9)\qquad
\begin{aligned}
&\psi_0(x) = 1;\\
&\psi_1(x) = -\frac{[ab]}{[aa]}\psi_0(x) + x;\\
&\psi_2(x) = -\frac{[ac]}{[aa]}\psi_0(x) - \frac{[bc1]}{[bb1]}\psi_1(x) + x^2;\\
&\ldots\ldots\ldots\ldots\ldots\ldots
\end{aligned}
$$

which are easily found by making use of the columns of the scheme of solution of the normal equations (see Table 1).

Each new approximation in the present method reduces to the calculation of a new term of the type $K_i\,\psi_i(x)$, where all coefficients K_i and functions $\psi_i(x)$ remain unchanged.

This is the practical advantage of the method of Chebyshev over the application of the usual scheme of the method of least squares with parabolic interpolation.

The sum of the squared errors remaining after each approximation is

$$
(10)\qquad [\varepsilon\varepsilon] = [yy] - [aa]\,K_0^2 - [bb1]\,K_1^2 - [cc2]\,K_2^2 - \ldots,
$$

where $[\varepsilon\varepsilon]$ is decreased with each approximation by a quantity proportional to the square of the corresponding Chebyshev coefficient.

Hence it appears to be possible at each step of the calculation to determine $[\varepsilon\varepsilon]$ and, hence, to determine the degree of the approximation.

In order to give the solution of a larger order system of normal equations and to facilitate the computational operations it is necessary to put these computations into a definite scheme.

We shall consider the scheme of Doolittle in the present work [8].

4. THE DOOLITTLE SCHEME

The Doolittle scheme contains characteristic features for the solution of the normal equations which are related to their symmetry.

We introduce the following notation (Table 1). N_1, N_2, N_3 . . . are the normal equations (4); E_1, E_2, E_3 . . . are the reduced equations (5).

(1), (2) . . . are the coefficients obtained by the respective multiplication of the coefficients of the equations E_1, E_2 . . . by the coefficients of the corresponding equations of the scheme (see Table 1).

In the first section of the scheme we have two lines - for copying the first equation in N_1 and E_1, which is obtained by dividing equation N_1 (i.e.,all the coefficients of line N_1) by its first coefficient $[aa]$. In the first line of the second section of the scheme we copy the second normal equation N_2, beginning with the coefficient $[bb]$. Then we multiply the coefficient $[ab/aa]$ of equation E_1 successively by the coefficients of equation N_1, beginning with $[ab]$, and copy the products with reversed sign in the second line of the second section of the scheme (this will be line (1)) and having taken the algebraic sum of the first and second lines of this section, we obtain the first transformed equation in the Gaussian scheme, which we denote by the Roman numeral I. We divide equation I by $[bb1]$ and obtain E_2. Having now marked off the completed second section, we copy down in the first line of the following third section the coefficients of the third normal equation N_3, beginning with $[cc]$. Returning to the first section of the scheme, we take the coefficient $[ac/aa]$ of equation E_1 and multiply it by the coefficients of equation N_1, i.e., of the first normal equation, beginning with $[ac]$. We then copy the result with reversed sign in the second line of the third section and obtain (1). Then, returning to the second section, we take the coefficient $[bc1/bb1]$ from equation E_2 and multiply it by the coefficients of equation I, beginning with $[bc1]$. The result is added with reversed sign to the third line of the third section and we obtain (2). Having taken the algebraic sum of the first, second and third lines of this section, we obtain in its fourth line the second transformed equation in the Gaussian scheme: $[cc2]\,X_3 = [cy2]$, which we denote by the Roman numeral II. We then divide equation II by its first coefficient $[cc2]$ and obtain E_3. Having completed this third section of the scheme, we mark it off by a horizontal line and begin the next (fourth) section, which we complete, of course, in a completely analogous manner. In our case we shall restrict ourselves to an unknown X_3, which we determine from equation E_3, consequently it is not necessary to complete the fourth section.

5. TRANSFORMATION OF THE EQUATIONS OF THE Q BRANCH

As is well known [9], theory gives the following approximate expression for the dependence of the wave number of a Q branch rotational structure line on J:

$$
(11)\qquad \nu = Q(J) = \nu_0 + (B_\nu' - B_\nu'')J(J+1) - (D_\nu' - D_\nu'')J^2(J+1)^2 + \ldots,
$$

where ν_0 is the zero line of the band according to (9); B_ν', D_ν' . . . and B_ν'', D_ν'' . . . are the rotational constants in the upper and lower electronic states of the molecules; J is the rotational quantum number ($J = J' = J''$).

Since equation (11), the coefficients of which we must determine in the order of the successive rise in the degree of the polynomial, is inconvenient for calculating because of large numbers, we may transform it to the form (1), by introducing the variable $x = J\,(J+1)\cdot 10^{-3}$ and for simplifying the calculations by putting

$$
(12)\qquad y = \nu - \tilde{\nu}_0 - (\tilde{B}_\nu' - B_\nu'')\,J\,(J+1);
$$

$$
(13)\qquad
\begin{aligned}
&C_0 = \nu_0 - \tilde{\nu}_0;\quad C_1 = [(B_\nu' - B_\nu'') - (\tilde{B}_\nu' - B_\nu'')]\cdot 10^3;\\
&C_2 = -(D_\nu' - D_\nu'')\cdot 10^6 \ldots .
\end{aligned}
$$

Here $\tilde{\nu}_0$ is an approximate value of ν_0; $(B_\nu' - B_\nu'')$ is a quantity determined from the condition that ν in (11) is a linear function of $J(J+1)$.

Taking into account that in the present case $a = 1$; $b = x$; $c = x^2 \ldots$, $[aa] = n$; $[ab] = [x]$; $[ac] = [x^2]$; . . ., we compiled a table of powers and sums of powers of x_J (Table 5), having in mind that in actual practice it is not necessary to go higher than x_J^6.

6. DETERMINATION OF ν_0, $B'_v - B''_v$ AND $D'_v - D''_v$ FOR THE (11-2) BAND OF THE $^1\Pi \rightarrow {}^1\Sigma$ SYSTEM OF THE BeO MOLECULE

As a numerical example we shall consider the determination of the wave number of the zero line ν_0, of the differences of rotational constants $B'_v - B''_v$ and $D'_v - D''_v$ for the (11-2) band of the $^1\Pi \rightarrow {}^1\Sigma$ system of the BeO molecule, according to our observations. An exposure of the spectrum of a beryllium arc in air was made in a DFS-3 spectrograph [10] in the first ordersof a plane grating with 1200 lines per mm (theoretical resolving power in first orders of the grating - 144,000, reciprocal linear dispersion - 2 Å/mm).

Table 2

No. N_0 p/p i	J	Q(J), cm^{-1}	J(J+1)	μ_J [15]	Q(J)-μ_J	y_J [12]	x_J	x_J^2	$y_J y_J \cdot 10^4$	ε_J cm^{-1} [14]
1	14	17771.03	210	− 86.94	17857.97	4.07	-0.210	0.0441	49	+0.01
2	15	58.63	240	− 99.36	99	09	240	0576	81	−02
3	16	45.36	272	−112.61	97	07	272	0740	49	−03
4	18	16.32	342	−141.59	91	01	342	1170	01	00
5	19	00.53	380	−157.33	86	−04	380	1444	16	04
6	20	17683.98	420	−173.89	87	−03	420	1764	09	01
7	21	66.61	462	−191.28	89	−01	462	2134	01	−02
8	22	48.32	506	−209.49	81	−09	506	2560	81	04
9	23	29.30	552	−228.54	84	−06	552	3047	36	00
10	24	09.41	600	−248.41	82	−08	600	3600	64	01
11	26	17567.20	702	−290.64	84	−06	702	4928	36	−02
12	27	44.81	756	−313.00	81	−09	756	5715	81	02
13	28	21.65	812	−336.18	83	−07	812	6593	49	00
14	29	17497.67	870	−360.20	87	−03	870	7569	09	−02
15	30	72.86	930	−385.04	90	00	930	8649	00	−04
16	31	47.17	992	−410.71	88	−02	992	9841	04	00
17	32	20.70	1056	−437.21	91	01	1.056	1.1151	01	00
18	33	17393.38	1122	−464.53	91	01	1.122	1.2589	01	03
19	34	65.29	1190	−492.68	97	07	1.190	1.4161	49	00

In Table 2 we give the wave numbers of the observed (unperturbed) lines of the Q branch of the (11-2) band, and also the sequence and results of the calculations for the determination of y_J according to (12). In Table 2 the values of x_J and x_J^2 necessary for the determination of $[xy]$, $[x^2y]$, are copied from Table 5, values of $y_J y_J \cdot 10^4$ are given, and

$$\epsilon_J = Q(J)_{calc.} - Q(J)_{obs.} \tag{14}$$

are given for the third approximation.

To decrease the writing in Table 2 the following notation was introduced:

$$\mu_J = (B_v - B_v)J(J+1). \tag{15}$$

Utilizing the data of Table 2 (for J = 34 and 14), we find by calculation

$$B'_v - B''_v = \frac{17365.29 - 17771.03}{1190 - 210} = -0.41402.$$

Table 3

J	n 1	2	3	4
34	14.280	10.4901	9.1703	8.7267
13	−0.910	−0.1067	−0.0148	−0.0022
17	−0.306	−0.0936	−0.0287	−0.0088
25	−0.650	−0.4225	−0.2746	−0.1785
Sums $[x^n]$.	12.414	9.8673	8.8522	8.5372

From these same tables we find the proper quantity $\tilde{\nu}_0$=17,857.9. Having determined the sums $[xy]$, $[x^2y]$, $[yy]$, we calculate the coefficients of the normal equations according to the scheme of Table 3, i.e., we copy from Table 5 the sums of powers ($[x]$, $[x^2]$, $[x^3]$, $[x^4]$) for the largest quantum number J = 34 and copy with reversed sign the corresponding sums of powers for the smallest quantum number minus one, i.e., for J = 14 - 1 = 13, and the powers x_J, x_J^2, x_J^3, x_J^4 for the missing lines, which in the case considered are for J = 17 and 25. Having taken the algebraic sum of the copied numbers by columns, we obtain $[x^n]$ (n=1,2,3,4) for the observed lines.

Thus we have 19 values of $Q(J)_{obs}$ (Table 2).

Having determined with the aid of a calculator $[xy]$, $[x^2y]$, $[yy]$ and having copied from Table 3 the values of the sum of the powers, we shall have: n=19; $[x]$=12.414; $[x^2]$=9.8673; $[x^3]$=8.8522; $[x^4]$=8.5372; $[yy]$=-0.25; $[xy]$=-0.20818; $[x^2y]$=-0.115379; $[yy]$=0.0617.

We shall process these data according to the normal equation scheme (see Tables 1 and 4).

Table 4

	1st approximation	2nd approximation	3rd approximation	Right hand terms	$[\varepsilon\varepsilon]$
N_1...	19	12.4140	9.8673	−0.25	$[yy]$ = 0.0617
E_1...	1	0.653368	0.519332	K_0 −0.0131579	0.0033
					$[\varepsilon\varepsilon]$ 0.0584
N_2...	—	9.8673	8.8522	−0.208180	—
(J)	—	−8.1109	−6.4470	0.163342	—
I	—	1.7564	2.4052	−0.044838	0.0011
E_2...	—	1	1.36930	K_1 −0.0255284	$[\varepsilon\varepsilon]$ 0.0573
N_3...	—		8.5372	−0.115379	—
(J)	—		−5.1344	0.129833	—
(I)	—		−3.2937	0.061401	—
II	—		0.1191	0.075855	0.0483
E_3...	—		1	K_2 0.6369	$[\varepsilon\varepsilon]$ 0.0090

Let us calculate successfully by columns, each of which, as we know, corresponds to a Chebyshev approximation; here with the present column the column of right-hand terms corresponding to it is also filled up, then the Chebyshev coefficients K_0, K_1, K_2, . . . appear in the reduced lines at the "I" level in this column. Squaring them, multiplying them respectively by $[aa]$, $[bbl]$, etc., i.e., by the number standing immediately above "I", or instead of that multiplying K by the number standing immediately above it and subtracting the product at first from $[yy]$, then from the first remainder, etc., we obtain $[\varepsilon\varepsilon]$, corresponding to each approximation.

At each stage we make up Chebyshev polynomials and their products with the K coefficients. Thus we find

$\varphi_0(x) = 1$; $K_0\varphi_0(x) = -0.013158$;

$\varphi_1(x) = -0.853368 + x$; $K_1\varphi_1(x) = 0.016679 - 0.025528x$;

$\varphi_2(x) = 0.375385 - 1.369392x + x^2$; $K_2\varphi_2(x) = 0.23908 - 0.87217x + 0.6369x^2$.

Table 5

Values of powers and sums of powers of $x_J = J(J+1)\cdot 10^{-3}$

$$[x^n] = x_1^n + x_2^n + \ldots + x_J^n \quad (n = 1,2,\ldots,6)$$

J	J(J+1)	x_J	[x]	x_J^2	$[x^2]$	x_J^3	$[x^3]$
1	2	0.002	0.002	—	—	—	—
2	6	.006	.008	—	—	—	—
3	12	.012	.020	0.0001	0.0002	—	—
4	20	.020	.040	.0004	.0006	—	—
5	30	.030	.070	.0009	.0015	—	—
6	42	.042	.112	.0018	.0032	0.0001	0.0001
7	56	.056	.168	.0031	.0064	.0002	.0003
8	72	.072	.240	.0052	.0116	.0004	.0007
9	90	.090	.330	.0081	.0197	.0007	.0014
10	110	.110	.440	.0121	.0318	.0013	.0027
11	132	.132	.572	.0174	.0492	.0023	.0050
12	156	.156	.728	.0243	.0735	.0038	.0088
13	182	.182	.910	.0331	.1067	.0060	.0148
14	210	.210	1.120	.0441	.1508	.0093	.0241
15	240	.240	1.360	.0576	.2084	.0138	.0379
16	272	.272	1.632	.0740	.2823	.0201	.0581
17	306	.306	1.938	.0936	.3760	.0287	.0867
18	342	.342	2.280	.1170	.4929	.0400	.1267
19	380	.380	2.660	.1444	.6373	.0549	.1816
20	420	.420	3.080	.1764	.8137	.0741	.2557
21	462	.462	3.542	.2134	1.0272	.0986	.3543
22	506	.506	4.048	.2560	1.2832	.1296	.4838
23	552	.552	4.600	.3047	1.5879	.1682	.6520
24	600	.600	5.200	.3600	1.9479	.2160	.8680
25	650	.650	5.850	.4225	2.3704	.2746	1.1427
26	702	.702	6.552	.4928	2.8632	.3459	1.4886
27	756	.756	7.308	.5715	3.4348	.4321	1.9207
28	812	.812	8.120	.6593	4.0941	.5354	2.4561
29	870	.870	8.990	.7569	4.8510	.6585	3.1146
30	930	.930	9.920	.8649	5.7159	.8044	3.9189
31	992	.992	10.912	.9841	6.7000	.9762	4.8951
32	1056	1.056	11.968	1.1151	7.8151	1.1776	6.0727
33	1122	1.122	13.090	1.2589	9.0740	1.4125	7.4852
34	1190	1.190	14.280	1.4161	10.4901	1.6852	9.1703
35	1260	1.260	15.540	1.5876	12.0777	2.0004	11.1707
36	1332	1.332	16.872	1.7742	13.8519	2.3633	13.5340
37	1406	1.406	18.278	1.9768	15.8287	2.7794	16.3134
38	1482	1.482	19.760	2.1963	18.0251	3.2550	19.5684
39	1560	1.560	21.320	2.4336	20.4587	3.7964	23.3648
40	1640	1.640	22.960	2.6896	23.1483	4.4109	27.7757
41	1722	1.722	24.682	2.9653	26.1136	5.1062	32.8819
42	1806	1.806	26.488	3.2616	29.3752	5.8905	38.7725
43	1892	1.892	28.380	3.5797	32.9549	6.7727	45.5452
44	1980	1.980	30.360	3.9204	36.8753	7.7624	53.3076
45	2070	2.070	32.430	4.2849	41.1602	8.8697	62.1773
46	2162	2.162	34.592	4.6742	45.8344	10.1057	72.2830
47	2256	2.256	36.848	5.0895	50.9239	11.4820	83.7650
48	2352	2.352	39.200	5.5319	56.4558	13.0110	96.7761
49	2450	2.450	41.650	6.0025	62.4583	14.7061	111.4822
50	2550	2.550	44.200	6.5025	68.9608	16.5814	128.0636

J	x_J^4	$[x^4]$	x_J^5	$[x^5]$	x_J^6	$[x^6]$
1	—	—	—	—	—	—
2	—	—	—	—	—	—
3	—	—	—	—	—	—
4	—	—	—	—	—	—
5	—	—	—	—	—	—
6	—	—	—	—	—	—
7	—	—	—	—	—	—
8	—	—	—	—	—	—
9	0.0001	0.0001	—	—	—	—
10	0.0001	0.0003	—	—	—	—
11	0.0003	.0006	—	—	—	—
12	0.0006	.0011	0.0001	0.0001	—	—
13	0.0011	.0022	.0002	.0003	—	—
14	0.0019	.0042	.0004	.0008	0.0001	0.0001
15	0.0033	.0075	.0008	.0016	.0002	0.0003
16	0.0055	.0130	.0014	.0031	.0004	.0007
17	0.0088	.0218	.0026	.0057	.0008	.0015
18	0.0137	.0354	.0047	.0104	.0016	.0032
19	0.0206	.0563	.0079	.0183	.0030	.0062
20	0.0311	.0874	.0131	.0314	.0054	.0117
21	0.0456	.1330	.0210	.0525	.0097	.0214
22	0.0656	.1985	.0332	.0856	.0168	.0382
23	0.0928	.2914	.0513	.1369	.0293	.0675
24	0.1296	.4210	.0778	.2146	.0487	.1131
25	0.1785	.5995	.1160	.3307	.0754	.1885
26	0.2429	.8423	.1705	.5011	.1197	.3082
27	0.3267	1.1690	.2470	.7481	.1867	.4949
28	0.4347	1.6037	.3530	1.1011	.2866	.7815
29	0.5729	2.1766	.4984	1.5995	.4336	1.2152
30	0.7481	2.9247	.6857	2.2952	.6470	1.8622
31	0.9664	3.8911	.9606	3.2558	.9529	2.8151
32	1.2435	5.1346	1.3132	4.5690	1.3867	4.2018
33	1.5848	6.7214	1.7781	6.3471	1.9851	6.1869
34	2.0053	8.7267	2.3664	8.7335	2.8348	9.0366
35	2.5205	11.2472	3.1758	11.9093	4.0015	13.0381
36	3.1479	14.3950	4.1930	16.1023	5.5859	18.6232
37	3.9079	18.3029	5.4945	21.5967	7.7252	26.3484
38	4.8238	23.1267	7.1489	28.7457	10.5947	36.9431
39	5.9224	29.0492	9.2390	37.9846	14.4128	51.3559
40	7.2339	36.2831	11.8637	49.8483	19.4564	70.8123
41	8.7929	45.0760	15.1414	64.9897	26.0735	96.8858
42	10.6382	55.7142	19.2127	84.2024	34.6962	131.5940
43	12.8140	68.5282	24.2441	108.4465	45.9608	177.5538
44	15.3696	83.8978	30.4317	138.8782	60.2547	237.7085
45	18.3604	102.2582	38.0059	176.8841	78.6723	316.3808
46	21.8485	124.1067	47.2366	224.1207	102.1255	418.5063
47	25.9034	150.0101	58.4380	282.5587	131.3362	550.3424
48	30.6020	180.6121	71.9758	354.5345	169.2671	719.6296
49	36.0300	216.6421	88.2735	442.8080	216.2701	935.8997
50	42.2825	258.9246	107.8204	550.6284	274.9420	1210.8417

Therefore the system of successive approximations for the function y will be

$$y^{(0)} = K_0\varphi_0(x) = -0.013; \qquad [\varepsilon\varepsilon] = 0.0584;$$

$$y^{(1)} = \sum_{i=0}^{i=1} K_i\varphi_i(x) = 0.004 - 0.025528x; \qquad 0.0573;$$

$$y^{(2)} = \sum_{i=0}^{i=2} K_i\varphi_i(x) = 0.242 - 0.8977x + 0.637x^2; \qquad 0.0090.$$

Each of these formulas gives the best expression for y in the form of a polynomial of zero, first and second degree in x, where each $[\varepsilon\varepsilon]$ written at the side corresponds to each one of them. Taking (13) into account, we determine the values of ν_0, $B'_v - B''_v$, and $D'_v - D''_v$ for the successive approximations

$$\nu_0^{(0)} = 17857.89; \quad (B'_v - B''_v)^{(0)} = -0.41402;$$

$$\nu_0^{(1)} = 17857.90; \quad (B'_v - B''_v)^{(1)} = -0.41405;$$

$$\nu_0^{(2)} = 17858.14; \quad (B'_v - B''_v)^{(2)} = -0.41492;$$

$$(D'_v - D''_v)^{(2)} = -0.637 \cdot 10^{-4}.$$

We have restricted ourselves here to the third approximation because our calculations showed (we do not reproduce them here) the unsuitability of a further increase in the degree of the polynomial.

We note that the numbers standing in Table 4 above "1" of the reduced line (19, 1.7564, 0.1191) are the weights of the coefficients K_0, K_1, K_2. We see that they decrease rapidly so that the determination of K_2 already is made here under very unfavorable conditions.

We calculate the weight with the help of the determinant and minors for the third approximation

$$\Delta = 3.97; \; \Delta_{11} = 5.88; \; \Delta_{22} = 84.8; \; \Delta_{33} = 33.37.$$

We obtain for the weights X_1, X_2, X_3 the following values:

$$p_1 = 0.68; \; p_2 = 0.06; \; p_3 = 0.119.$$

The weight p_3, found according to Table 4 for X_3, coincides with the value 0.119 to the limits of accuracy of the calculation. Having $[\varepsilon\varepsilon] = 0.0090$; $n = 19$; $m = 3$, and making use of (6), we find

$$\sigma_0 = \pm 0.024.$$

Knowing p_k and σ_0, we determine the root mean square error of the unknowns X_1, X_2, X_3

$$\sigma_1 = \pm 0.03; \; \sigma_2 = \pm 0.1; \; \sigma_3 = \pm 0.07.$$

After this we proceed to the determination of the root mean square errors in ν_0, $B'_v - B''_v$, and $D'_v - D''_v$. Taking (13) into account, we find

$$\sigma(\nu_0) = \pm 0.03 \text{ cm}^{-1}; \; \sigma(B'_v - B''_v) = \pm 0.1 \cdot 10^{-3} \text{ cm}^{-1}; \; \sigma(D'_v - D''_v) = \pm 0.07 \cdot 10^{-4} \text{ cm}^{-1}.$$

So, for the third approximation we obtain

$$\nu_0^{(3)} = 17858.14 \pm 0.03 \text{ cm}^{-1}; \; (B'_v - B''_v)^{(3)} = -0.4149 \pm 0.0001 \text{ cm}^{-1};$$

$$(D'_v - D''_v)^{(3)} = (-0.64 \pm 0.07) \cdot 10^{-4} \text{ cm}^{-1}.$$

CONCLUSIONS

1. A scheme is expounded for utilizing the method of parabolic interpolation according to the method of least squares for the mathematical treatment of experimental data on the rotational structure of the branches of bands of diatomic molecules in a form convenient for calculating the molecular constants and estimating their accuracy.

2. The applicability is demonstrated of applying the parabolic interpolation method according to the method of Chebyshev for the mathematical treatment of experimental data on the rotational structure of the electronic-vibrational-rotational bands of diatomic molecules.

3. The Doolittle scheme is utilized, which is very convenient for the solution of the normal equations in interpolation, according to the Chebyshev method, of the experimental data on the fine structure of molecular spectra with the aim of obtaining the most probable values of the molecular constants.

4. The value of the method is illustrated by an example of the determination of the numerical values of the zero line ν_0 and the differences of the rotational constants $B'_v - B''_v$, and $D'_v - D''_v$ for the Q branch of the (11-2) band of the $^1\Pi \rightarrow {}^1\Sigma$ system of the BeO molecule. For this case it is shown that the introduction of a constant D in the rotational term is necessary, while the introduction of the constant F is not necessary, since a polynomial of the second degree in $J(J+1)$ already reflects the experimental data with a precision coinciding with the precision of measurement.

5. In Table 5 are given values of powers and sums of powers of $x_J = J(J+1) \cdot 10^{-3}$, which makes the finding of the coefficients of the normal equations extraordinarily convenient and simple.

In conclusion the author considers it his pleasant duty to thank V. M. Tatevskii for his interest in the work and valuable remarks expressed in the discussion of this work.

April 11, 1958

References

1. K. P. IAKOVLEV: Matematicheskaia obrabotka rezul'tatov izmeranyi (Mathematical treatment of results of measurements). Moscow-Leningrad, 1950
2. E. T. WHITTAKER, G. ROBINSON: Calculus of Observations (Translated as: Mathematical treatment of results of measurements, IL, Moscow-Lening. 1933)
3. W. SCHEIN: Z.Phys., 60, 74 (1930)
4. A. A. MAL'TSEV, IU. A. KUZIAKOV, V. M. TATEVSKII: Materialy X Vsesoiuznogo soveshchaniia po spektroskopii. Molekuliarnaia spektroskopiia (Materials of the X All-Union Conference on Spectroscopy. Molecular Spectroscopy). L'vov, vol. I, 475, 1957
5. R. T. BIRGE, J. D. SHEA: Univ. Cal. Publ. Math., 2, No. 5, 67 (1927)
6. P. L. CHEBYSHEV: Polnoe sobranie sochinenii (Complete Works) Moscow-Leningrad, II, 1947
7. N. IDEL'SON: Sposob naimen'shikh kvadratov (Method of least squares), Leningrad, 1932
8. F. N. KRASOVSKII, V. V. DANILOV: Rukovodstvo po vysshei geodezii (Handbook of higher geodésy) Moscow, Part 1, 1939
9. G. HERZBERG: Introduction to the Spectra and Structure of Diatomic Molecules. Van Nostrand, N.Y. (IL, Moscow, 1949)
10. V. K. PROKOF'EV: IAN USSR, Fiz. ser., 18, No. 6, 643-661 (1954) (See CTT Bulletin)

TOM VI, Vyp. 3 OPTIKA I SPEKTROSKOPIIA Mart, 1959
VOL. VI, No. 3 OPTICS AND SPECTROSCOPY March, 1959

Temperature Dependence of the Absorption Cross Section of Nitrogen Dioxide for Visible Light

V. N. SOBHNIKOV

Abstract: A semi-empirical calculation is given of the absorption of light by NO_2 at temperatures of 2000-7000°K. using a choice of the unknown molecular parameters corresponding to transitions from the vibrational ground state, which are in agreement with the experimental absorption curves. In choosing the parameters use is made of the existence of a large change in the normal coordinate systems of the ground and excited electronic states. It is shown that with a suitable choice of the parameters, the absorption may be regarded with sufficient accuracy as due to a single oscillator.

INTRODUCTION

One is confronted by the problem of the absorption of light by NO_2 when considering absorption in hot air. The question is also of intrinsic theoretical interest. Since, however, the NO_2 molecule has been studied very little, it is necessary to go through very laborious calculations to obtain even preliminary results which give the absorption probability with an accuracy of about 30%. It is shown below that it is sufficient to know the absorption curve $\sigma_\nu = f(\nu)$ [1,2], valid for normal temperatures and corresponding to the fundamental transition from the zero vibrational level, and that from this curve one can deduce the temperature dependence of the differential cross section $\sigma(\nu,T)$, averaged over the upper vibrational levels, which appears in the relation:

$$\frac{I_\nu}{I_{\nu 0}} = e^{-\sigma(\nu,T)\rho},$$

(where ρ is the number of absorbing molecules per cm^3, ν is the wavenumber in cm^{-1}, and I_ν and $I_{\nu 0}$ are the intensities of the transmitted and incident illumination respectively).

As is well known, the system of vibrational normal coordinates rotates and is displaced (relative to the system in the ground state) as a single unit in an excited electronic state; moreover, for the symmetric tri-atomic molecule, two fully symmetric coordinates x_1 and x_2 transform into each other, whereas at first the third, antisymmetric coordinate x_3 transforms into itself, i. e.[3]

$$(1)\qquad \left.\begin{aligned} x_1' &= a_{11}x_1 + a_{12}x_2 + C_1,\\ x_2' &= a_{21}x_1 + a_{22}x_2 + C_2,\\ x_3' &= x_3. \end{aligned}\right\}$$

The point of our method consists in selecting the system of unknown parameters t in such a way that the calculated absorption cross section $\sigma_0(\nu,t) \equiv \sigma_0(\nu)$, corresponding to transitions from the vibrational ground state, would satisfy the requirements for the "best fit" to the experimental curve $\sigma_\nu = f(\nu)$ at each frequency ν, i.e.

$$(2)\qquad \sigma_\nu = \sigma_0[\nu,t(\nu)];\ \frac{d\sigma_\nu}{d\nu} = \frac{\partial}{\partial\nu}\sigma_0[\nu,t(\nu)];\ \frac{d^2\sigma_\nu}{d\nu^2} = \frac{\partial^2}{\partial\nu^2}\sigma_0[\nu,t(\nu)].$$

To require equality of higher order derivatives is senseless due to the uncertainty in determining σ_ν. We will concern ourselves only with the fundamental parameters; that is, with the displacements C_1 and C_2, with the separation between the minima of the electronic-potential surfaces ξ_e, and with the electronic transition probability

$$W_e = \left|\int \psi_e \mu^e \psi_e' \, d\tau_e\right|^2,$$

where μ^e is the electronic dipole moment operator. Here and henceforth a prime will designate quantities in excited electronic states. We are assuming also that the complete transition probability factors into an electronic and a vibrational part,

$$(3)\qquad W \sim W_e \cdot W_\nu, \text{where } W_\nu = \left|\int \psi_\nu \psi_\nu' d\tau_\nu\right|^2,$$

ψ_ν and ψ_ν are a set of initial and final oscillator functions. The influence of these assumptions on the quantity $\sigma(\nu,T)$ will be considered later. In addition we make the important assumption [supported to a certain extent by the shape of the experimental curve $\sigma_\nu = f(\nu)$] that the transition takes place in the usual way, i.e., from the electronic ground state to a definite excited state.

CALCULATION OF $\sigma(\nu,T)$

If in equation (2) we take logarithms and replace σ_ν by $\log_{10}\sigma_\nu$ and σ_0 by $\log_{10}\sigma_0$, we find that a change in ϵ_e results in a displacement of the curve $\log_{10}\sigma(\nu)$ along the abscissa, whereas a change in W_e displaces the curve along the ordinate.

Since, as will be demonstrated, the final result is independent both of a rotation of the normal coordinates and of the vibrational frequencies, we assume

$$(4)\qquad a_{11} = a_{22} = 1,\ a_{12} = a_{21} = 0,\ \nu_1 = \nu_1',\ \nu_2 = \nu_2',\ \nu_3 = \nu_3'.$$

It is not necessary to consider rotational transitions, since there enters into the cross section a sum over rotational probabilities which gives the value unity.[4]

For a transition from the vibration level (m, n, p), the absorption cross section in the spectral band of wavenumbers $\nu \pm \frac{\Delta\nu}{2}$ is equal to

$$\sigma_{mnp}(\nu) = \frac{\text{const}}{\Delta\nu}\sum_{\Delta\nu}\left|M_{mnp}^{klq}\right|^2 \cdot \nu,$$

according to [5]. Here M_{mnp}^{klq} is the vibrational matrix element (3), and the summation, corresponding to an average over the upper vibrational levels, extends over all k, l, q for which wavenumbers fall in the interval $\Delta\nu$. The size of the latter is not very important, since at every point ν the summation $\sum_{\Delta\nu}$ is proportional to $\Delta\nu$. We chose $\Delta\nu = 2100$ cm and correspondingly we replace the curve σ_ν taken on a small interval $\Delta\nu$, by the only slightly different curve

$$f(\nu)=\sigma_\nu^{av}=\frac{1}{\Delta\nu}\int_{\nu-\frac{\Delta\nu}{2}}^{\nu+\frac{\Delta\nu}{2}}\sigma_\nu d_\nu. \tag{5}$$

Taking equations (1) and (4) into account, the matrix elements were calculated directly up to and including fifth order, and the general expression was then obtained by induction. Thus we have $\left|M^{kl}_{mn}\right|^2=\left|M^{kl}_{mnp}\right|^2$ (in agreement with the evaluation of reference [3] for the case $\nu_3\neq\nu_3'$):

$$\left|M^{kl}_{mn}\right|^2=\left|M^{k}_{m}\right|^2\left|M^{l}_{n}\right|^2,\quad \left|M^{n}_{m}\right|^2=\left|M^{m}_{k}\right|^2,$$

$$\left|M^{n}_{m}\right|^2=\frac{m!}{n!}\xi^{n-m}e^{-\xi}\left[\frac{n\ldots(n-m+1)}{m!0!}+\ldots\right.$$

$$\left.\ldots(-1)^{k-1}\frac{n\ldots(n-m+k)}{(m-k+1)!(k-1)!}\xi^{k-1}+\ldots(-1)^m\frac{\xi^m}{0!m!}\right]^2$$

where $\xi\equiv\frac{c^2\omega_\nu}{2h}$ and ω_ν is the circular vibration frequency.* In accordance with reference [6] for the vibrational frequencies we chose *

$$\nu_1=1373,\quad \nu_2=648,\quad \nu_3=1616\ \text{cm}^{-1}.$$

From the experimental curve $\lg\sigma_\nu^{av.}$ one can calculate at every point $\log\frac{\nu}{14{,}000}$ (14,000 cm^{-1} was chosen arbitrarily from considerations of convenience - since this is the point at which the extrapolated curve $\log\sigma_\nu$ begins). Then displacing the calculated curve arbitrarily

$$\lg\frac{\text{const}\ \sigma_o(\nu)}{\nu}=\lg\sum_{\Delta\nu}e^{\xi_1+\xi_2}\left|M^{kl}_{oo}\right|^2\equiv\lg Z_{oo}(\nu),$$

along the axes (where ν is measured from the lowest excited electronic level) we found the position of the curve for which it fit the experimental curve at a certain point ν_0, thus determining the proper reading for ν. This fixed the position of all the curves $\log Z_{mn}(\nu)$, which were found by a similar method.

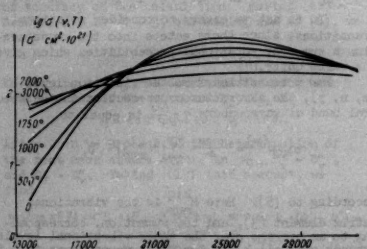

Figure 1

By this method it was possible to choose $W_e(\nu_0)$, $\xi_2(\nu_0)$, and $\epsilon_e(\nu_0)$ corresponding to a certain ξ_1, and satisfying the requirements of best fit at the point ν_0 of the curve $\log\sigma_\nu$. **

Since, strictly speaking, it is necessary to take not $\log\sigma_0(\nu)$ but rather

$$\lg\sigma(\nu,293^\circ)=\lg[\sigma_o(\nu)+\alpha(293^\circ)\sigma_{010}(\nu)],$$

it is necessary to add to $\log\sigma_0$ a negligible correction $\alpha(\nu)$ corresponding to the value of Z_{01} at $W_e=W_e(\nu)$, $\xi_2=\xi_2(\nu)$, $\epsilon_e=\epsilon_e(\nu)$, and a given ξ_1; (negligible since $\alpha(293^\circ)\sim0.042$). In this way it turned out to be possible to construct curves $\log\sigma(\nu,293)$ which was in good agreement with the whole experimental curve in the red region up to the maximum. The total cross section was calculated from the formula

$$\lg\sigma_k(\nu,T)=A_k(\nu)+\lg\left(Z^{(k)}_o+Z^{(k)}_1\exp\left[-\frac{\epsilon_k}{kT}\right]\right.$$

$$\left.+Z^{(k)}_2\exp\left[-\frac{2\epsilon_k}{kT}\right]+\ldots\right)-\lg Z^{(k)}(T)+\lg\frac{\nu}{14000},$$

where we have taken the extreme values of the two parameters (ξ_1,ξ_2), equal to:

1) $\xi_1=\xi_{10}=9.16$, $\xi_2=0$; 2) $\xi_1=0$, $\xi_2=\xi_{20}=31.9$.

In equation (6), $k=1.2$; $Z^{(k)}_1$ is the $Z^{(k)}_{mn}(\nu)$ introduced above taken for the case $n=0$ or $m=0$; $A_k(\nu)=B+\lg W^k_e(\nu)$, where B does not depend on ν and T; and $Z^{(k)}(T)$ is the vibrational partition function

$$Z^{(k)}(T)=\frac{1}{1-e^{-\frac{\epsilon_k}{kT}}},\quad \epsilon_k=2\pi hc\nu_k.$$

The value of ν in Z_1 and the magnitude of $A_k(\nu)$ are determined by fitting equation (6) to the experimental curve. The first choice of the parameters above corresponds to a one-dimensional oscillator with frequencies $\nu_1=\nu_1'=1373$ cm^{-1}; the second choice to $\nu_2=\nu_2'=648$ cm-1. Direct comparison of the two cases shows that for $T>2000^\circ$ the deviation of $\sigma(\nu,T)$ from the average curve (see figs. 1,2) is less than 15%, and for $T\sim1000^\circ$, less than 30-60%. Since if at any point ν we increase i, the value of $Z^{(k)}_i$ oscillates around a certain mean value, we have restricted $i\leq5$, and for the remaining Z_i we have inserted the averaged value just mentioned (in the two cases the terms $Z_i\geq6$

---

* It will become apparent later on that the insertion of more recent data (Ref.[7]) will not alter the final results.

** In the case of NO_2, at least for $1500\leq\nu_0\leq2500$ cm^{-1}, one may represent the curve for 'best fit' $\xi_2=\xi_2(\xi_1)$ by a semi-empirical formula

$$\left(\frac{\xi_1}{\xi_{10}}\right)^{\frac{1}{\sqrt{s}}}+\left(\frac{\xi_2}{\xi_{20}}\right)^{\sqrt{s}}=1,\ (*)$$

(where $\xi_{10}(\nu_0)$ and $\xi_{20}(\nu_0)$ are constants and $s=\frac{\nu_1}{\nu_2}$), which gives, as it must, the equation of a circle for $s=1$, $C_1^2+C_2^2=$ const. Furthermore, using (*) and by using a graphical representation of the Frank-Condon principle [3], one may write an expression for ϵ_e

$$\frac{\epsilon_e-\epsilon^e_{01}}{\xi_{10}\cdot\nu_1}=1-\frac{\xi_1}{\xi_{10}}-\frac{1}{s}\left(\frac{\xi_{20}}{\xi_{10}}\right)\left[1-\left(\frac{\xi_1}{\xi_{10}}\right)^{\frac{1}{\sqrt{s}}}\right]^{\frac{1}{\sqrt{s}}}$$

where ϵ_e is given in cm^{-1} and $\epsilon^e_{01}=$ const. For $\nu_1=1373$, $\nu_2=648$, $\nu_0=15\,400$ cm^{-1}, for example, $s=2.12$; $\xi_{10}=9.16$; $\xi_{20}=31.9$; $\epsilon^e_{01}=12\,000$ cm^{-1}; $C_{10}=8.65\cdot10^{-21}$; $C_{20}=23.5\cdot10^{-21}\left[g^{\frac{1}{2}}\ \text{cm}\right]$.

give contributions of 10 and 50% respectively.) In view of the small difference between the curves Z_1 for the two extreme cases (after having been fitted to the experimental curve) we see that a change of $\nu_1 = \nu_1$ or of $\nu_2 = \nu_2$ does not produce any influence on the end result, nor is there an effect due to either a change in $Z_1(\nu)$ or a change in the populations of the levels. In equation (6) by replacing $e^{-\frac{n\varepsilon_1}{kT}}$ and $Z^{(1)}(T)$ by $e^{-\frac{n\varepsilon_2}{kT}}$ and $Z^{(2)}(T)$ and vice versa, the curves for the two cases very nearly change places. Extrapolating to the case where the populations of the levels are computed for $\nu_2 \sim 700\ cm^{-1}$ and Z_1 for $\nu_2 \sim 350\ cm^{-1}$, we find that it is necessary (in taking account of the possibility of halving the frequencies $\nu_2 = \nu_2$) to raise the average curves obtained above at all frequencies ν by an amount corresponding to an increase in $\sigma(\nu,T)$ of 5% (the increase begins at $T \sim 4000^o$). This correction has been made in the curves of figures 1 and 2.

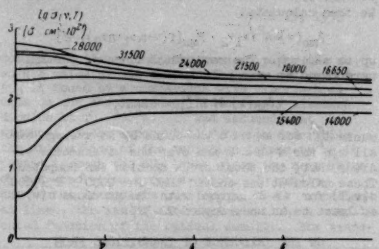

Figure 2

The influence of anharmonicity in the vibrations in the low state is also negligible since according to reference [7], the anharmonicity for levels 5-10 is small and will not make a contribution to $\sigma(\nu,T)$ of more than a few percent.

CERTAIN GENERAL CONSIDERATIONS AND ADDITIONAL BASIS FOR THE CORRECTNESS OF $\sigma(\nu,T)$

The form of the curves Z_1 introduced above reminds one of the square of the oscillator functions $\psi_1^2(\eta)$ where $\eta \equiv x\sqrt{\frac{\omega}{\hbar}}$, ω is the angular vibration frequency, and x is the oscillator coordinate. Since we are treating the case for large change in the potential curves (for example, for $\nu_1 = 1373$ the maximum of Z_0 corresponds to a transition to a level with n approximately 10), we are led to the idea that the oscillator functions of the excited electron states might be represented as δ-functions of the classical turning points.

$$\psi_n'(\eta) = A_n^2\delta(\eta - \eta_{TP}).$$

Due to the normalization of $\psi_n'(\eta)$, A_n^2 is decreased by a factor of approximately $(1+\frac{1}{n^2})$ when $n \to n+1$, i.e. the deviation from $(A_n^2)_{av}$ is about 15% in the region of interest to us where $n \sim 3$-16.

During the successive determinations of the matrix elements the limiting point on the upper parabola moves along η, and the curve which shows the dependence of the magnitude of the matrix element on η turns out (for proper choice of the signs of ψ_n) to be essentially a constant factor times the same curve $\psi_0(\eta)$, $\psi_1(\eta)$, ..., averaged however in the same fashion as in equation (5) over a certain interval $\Delta\eta^{avg}$. From this it is obvious that the curves $Z_i(\nu) \sim |\mu_i^{n_i}(\nu)|^2$ have the form of a series development in the squares of functions of the lower level $\psi_i(\eta)$ over energies corresponding to the numbers of the upper levels n. In order to make this series development fit the experimental curve $Z_0(\nu)$ it is possible to multiply all the low lying $\psi_i(\eta)$ by the same factor or else to expand the curves along the abscissa axis η without affecting the final results. However, the averaging over $(\Delta\eta)^{av}$ is not an operation which can be compensated simultaneously for all $\psi_i(\eta)$. For example, choosing $\Delta\eta^{avg} = 0.85\Delta\eta_0$ (where $\Delta\eta_0$ is the interval between the extrema for n = 0), taking the average for $\psi_0(\eta)$ and $\psi_1(\eta)$, and then multiplying $\psi_0^{avg}(\eta)$ and $\psi_1^{av}(\eta)$ by a certain number α so that they become equal to the maxima $\alpha\psi_0^{avg}$ and ψ_0, and displacing the points $\alpha\psi_0^{avg}$ and $\alpha\psi^{avg}$ simultaneously along so that the curves ψ_0 and $\alpha\psi_0^{avg}$ coincide, we find that $\alpha\psi_1^{avg}$ differs from ψ_1 by about 10% in a small interval around the extrema; i.e., the difference between $(\alpha\psi_1^{avg})^2$ and ψ_1 is 20%. The error in the cross section $\sigma(\nu,T)$ also will not be larger than this order of magnitude.

From the foregoing there follows a simple method of constructing $Z_i(\nu)$ when $Z_0(\nu)$ is known; one constructs the curves $\log \psi_0^2(\eta)$ and $\log Z_0(\nu)$; then by matching them at their maxima we find the constant factor A^2 (for all $\psi_i^2(\eta)$) and the function $\eta = f(\nu)$. Hence we find

$$\lg Z_i(\nu) = \lg A^2\nu_k^2\,[f(\nu+\nu_k)],$$

where ν_k is the eigen frequency of the vibration. Calculations by both methods, for example of $Z_{10}(\nu)$ for $i < 5$, differ by a sufficiently small amount to demonstrate the applicability of the δ- function approximation, despite its rather crude character.* We note, however, a certain greater generality in the first method due to the fact that it does not require that $A_n^2 \simeq$ const. in the interval n under consideration.

It is now clear that the anharmonicity of the vibrations in excited states, as well as changes in the upper frequency ν_k are taken care of by fitting to the experimental curve for all $Z_i(\nu)$.

* The difference between the corresponding curves is included by making a certain relative displacement along the ν axis by $\Delta\nu \leq \nu_1$, according to the increase in i. This displacement has almost no effect on the magnitude of $\sigma(\nu,T)$.

In the general case we use a graphical representation of the normal coordinates [3] (fig. 3).

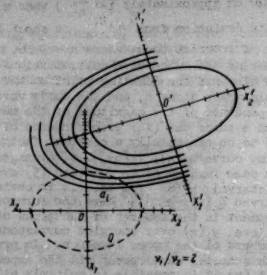

Figure 3

The points, calculated from the formula

$$x^2 = \sqrt{\frac{h\left(n+\frac{1}{2}\right)}{\pi c \nu_i}},$$

correspond to projection of the boundary points of the parabolas onto the plane. The curves (which are either circles or ellipses) correspond to vibrations with definite energies, in accordance with the equation

$$\nu_1\left(n_1+\frac{1}{2}\right)+\nu_2\left(n_2+\frac{1}{2}\right)=\text{const}.$$

Analogously, we replace the ψ-functions of the upper levels by δ-functions of the turning points. In determining $Z_{mn}(\nu)$ for every ν one must perform a summation over the squares of the matrix elements corresponding to points in a narrow band along the given energy curve $\epsilon(\nu)$. Thus if the axes $O'X_1'$ and $O'X_2'$ pass far from the point O, then due to the small extent of the initial oscillator functions, $Z_{mn}(\nu)$ is a series expansion (in the wavenumber ν) of plane cross sections in the region Q. Variations in the frequencies ν_1' or ν_2' can obviously be taken care of by a displacement of the normal coordinates of the higher state in such a way that the position of the segments a_i, relative to OX_1 and OX_2, and the energy gradient $\epsilon(\nu)$ in Q remain unchanged.

If one of the axes, for example $O'X_1'$, passes near the point O for large displacement OO', then by analogous method one may change the frequency ν_1', by setting $\nu_1' = \nu_2'$ and carrying out a corresponding displacement of the normal coordinates of the higher state. In the case of degenerate vibrations the total transition probability in a state with a given energy does not depend on the angle of rotation of these coordinates. Hence it is sufficient to consider the effect of a rotation of the normal coordinates of the lower state only. We introduce the transformation

$$x_1 = x_1\sqrt{\frac{\nu_1}{h}} \text{ and } x_2 = x_2\sqrt{\frac{\nu_2}{h}},$$

where ω_1 and ω_2 are the angular frequencies of the eigen vibrations. Let c be the separation in the plane $(\eta_1\eta_2)$ of the corresponding segments a_i from the origin. Integrating the product of the squares of the initial oscillator functions $\psi_m^2(\eta_1)\ \psi_n^2(\eta_2)$ along the lines $\eta_2 = a\eta_1 + c$, we find apart from a common factor $A^2\sqrt{\nu_1\nu_2}$ (where A^2 is independent of the frequencies) the following expressions:

$$F_{00} = e^{-\gamma},$$
$$F_{10} = \frac{e^{-\gamma}}{x}\,[1+2\gamma(x-1)],$$
$$F_{20} = \frac{e^{-\gamma}}{2x^2}\,[(3-2x+x^2)+4\gamma(x-1)(3-x)+4\gamma^2(x-1)^2],$$
$$F_{11} = \frac{e^{-\gamma}}{x^2}\,[3(x-1)+2\gamma(6-6x+x^2)+4\gamma^2(x-1)] \equiv \text{т. д.},$$

where

$$\gamma \equiv c^2, \quad x \equiv 1+a^2 \equiv F_{Q}(\gamma, x) = F_{\nu}\left(\gamma, \frac{x}{x-1}\right).$$

We made the calculation for one point, $\varkappa = 2$, corresponding to $a = \frac{\partial\eta_2}{\partial\eta_1} = \tan 45°$. From a comparison of $F_{00}(\nu)$, we determined A^2 and the relation $\gamma = f(\nu)$. We then calculated

$$Z_{mn}(\nu) = A^2\sqrt{\nu_1\nu_2}\cdot F_{mn}[f(\nu+m\nu_1+n\nu_2),\ 2]$$

up to $m+n=6$. The remaining values of the Z_{mn} were found by extrapolation

$$Z_{mn}(\nu) \simeq Z^{av}_{m+n} = \text{const},$$

where Z_k^{av} for $m+n<6$ was found by an average over all m,n for $m+n=k$ and over the wavenumbers ν. After that, the total cross section was computed. These calculations showed that for $2000° \leq T \leq 7000°$, $\sigma(\nu,T)$ for $\varkappa = 2$ agreed with the previous $\sigma(\nu,T)$ at least to an accuracy of 20-30%.

ON THE INFLUENCE OF TRANSITIONS FROM HIGH LYING ELECTRONIC LEVELS

Tentative data on the electron levels are presented in references [8] and [9]. They are too indefinite however to permit one to draw any conclusions about the contribution to the absorption of light by transitions from excited electronic states at high temperatures. This contribution may be included by suitable additions to the Z(T) computed earlier and to the transition probability $W_{trans}(\nu,T)$. Thus the final absorption probability may be written

$$W(\nu,T) = \frac{W_{trans}(\nu,T) + \alpha\exp\left[-\frac{\epsilon_e}{kT}\right]\cdot W_{trans}(\nu,T)}{Z(T)+\exp\left[-\frac{\epsilon_e}{kT}\right]\cdot Z'(T)},$$

where ϵ_e is the height of the lowest excited electronic state above the ground state, and $Z'(T) \simeq Z(T)$. It is natural to take $\alpha \sim 1$; and in this case there is no change in the $\sigma(\nu,T)$ found previously.

We consider also the case $W = 2\frac{W_{trans}}{Z(T)}$. Putting $T = 7000°$ and $\epsilon_e = 3500\ \text{cm}^{-1}$, we find $e\left[-\frac{\epsilon e}{kT}\right] \sim 0.5$ and $\alpha = 4$. It is natural to assume in this case that the electronic part of the probability W_e for transitions from excited states can only decrease, and hence to relate the 4-fold increase in the probability to the vibrational part W_ν.

We now consider an equivalent oscillator with $\nu_2=\nu_2=648\ cm^{-1}$, $\xi_1=0$, $\xi_{20}=\xi_o=32$, which has an absorption curve at T=293°K that coincides with the experimental curve.* These estimates of $\sigma_{\xi o}(\nu,T)$ allow one to conclude that the maximum in $\sigma_{\xi o}(\nu,T)$ for T=7000° and $\xi_o=0$ is some 20 times greater than the magnitude of $\sigma_{\xi o}(\nu,T)$ for $\xi_o=32$ (for the same temperature, wavenumber, and electronic transition probability.) However, already when $\xi_o \sim 4$ the maximum of $\sigma_{\xi o}(\nu,T)$ is only some 4 times larger than $\sigma_{\xi o}(\nu,T)$ for $\xi_o=32$ (and the same ν and T). Thus we see that the contribution of the excited electronic levels is important only in the event of small relative displacements of the normal coordinates of both excited levels, and in the limiting case of $\epsilon_e=350\ cm^{-1}$ this event seems improbable. An increase in ϵ_e leads to a rapid increase in α.

In conclusion I extend my thanks to my scientific director M. A. El'iashevich.

April 15, 1958

Comments in Proof: In the present paper the absolute value of the absorption cross section of NO_2 is found by a comparison with experimental data on the absorption of radiation by nitrogen dioxide at T 300°K. It was assumed that the exponent of the exponential function describing the attenuation of the radiation intensity as it passes through the NO_2 layer gives the mean value of the absorption cross section. In reality, due to the incomplete overlapping of the rotational lines, the law of attenuation will be a complicated function of the optical density. For transmission of radiation through a dense layer a law that is nearly exponential sometimes holds. However, this is connected with the fact that in the intervals corresponding to the largest values of the absorption coefficient there is practically no transmission; emission occurs only in spectral intervals with small absorption coefficients. The cross section estimated under these conditions by means of the exponent of the exponential function may be considerably reduced. This is in agreement with data obtained from an analysis of the experimental data by Raizer (ZETF 34, 483, 1958) ** in which the cross section for λ= 6500 A° was about three times larger than ours. The author's attention was drawn to the above facts by L. M. Biberman during a discussion of this paper.

* According to the Frank-Condon principle, ξ_o is the number of the vibrational level to which transitions from the ground state take place with maximum probability.

References

1. H. H. HOLMES, F. DANIELS: J. Am. Chem. Soc., 56, 630 (1934)
2. J. K. DIXON: J. Chem. Phys. 8, 157 (1940); T. C. HALL, Jr., F. E. BLACET: J. Chem. Phys., 20, 1745 (1952)
3. F. DUSHINSKII: Acta Physicochim. USSR, 7, 551 (1937)
4. G. HERZBERG, E. TELLER: Z. Phys. Chem., 21, 410 (1933)
5. D. I. BLOKHINTSEV: Osnovy kvantovoi mekhaniki (Principles of quantum mechanics) GITTL, Moscow-Leningrad, 1949
6. G. HERZBERG: Molecular structure and molecular spectra. vol. II. Spectra of polyatomic molecules. Van Nostrand, 1951 (IL, 1949)
7. G. E. MOORE: JOSA, 43, 1045 (1953)
8. R. S. MULLIKEN: Rev. Mod. Phys., 14, 204 (1942)
9. A. D. WALSH: J. Chem. Soc., 2260 (1953)

** see Sov. Phys. JETP, 34 (1958)

TOM VI, Vyp.3 OPTIKA I SPEKTROSKOPIIA Mart, 1959
VOL VI, No. 3 OPTICS AND SPECTROSCOPY March, 1959

Energy Distribution in the Polar Aurorae in the Region 3900-8700 Å

I. G. FRISHMAN

Abstract: This article contains basic electrophotometric results of absolute brightness measurements of the strongest spectral emissions of the polar aurorae in the 3900-8700 Å region obtained at Murmansk during 1954-1957. The spectral energy distribution in that region for different auroral forms is derived from these measurements. The absolute brightnesses measured were corrected for absorption in the earth's atmosphere.

INTRODUCTION

The study of polar aurorae spectra plays an important role in the investigation of the structures of high layers in the atmosphere and of the physical processes at these altitudes. The basic difficulty in these studies is the faintness of emission and their large fluctuations. Exposures ranging from tens of minutes in the visible region to many hours in the infrared region are necessary in order to obtain a satisfactory spectrum. The spectrographic method made it possible to detect and to identify almost all strong lines of the spectrum. It is, however, inapplicable when such spectral characteristics as the absolute magnitude of the emission (emitted power density), redistribution of the spectral energy due to fast changes from one auroral form to another are to be studied; the structure of the energy distribution within this wide spectrum is also often difficult to obtain.

Electrophotometric methods of measurements are quite effective in such investigations because of their high accuracy, small time constant, and comparative simplicity of absolute calibration, although they are inferior to spectrographic methods in distinguishing the monochromatic parts of the spectrum.

In the USSR, the electrophotometric measurements of absolute brightness of aurora polaris were first used by Rodionov and Fishkova in 1949 [1]. The electrophotometer they used had a wide aperture angle (0.9 steradian) and the light filters in the infrared region transmitted very wide spectral intervals ($\sim$ 1000Å).

Since 1954 the author regularly has been making photoelectric measurements of absolute brightness of the polar aurorae in this wide region of the spectrum. The 1954 measurements were made with an electrophotometer whose electronic parts were designed by the photometric laboratory NIFI LGU [2]. (photometer 1). The instrument's aperture angle was 56 sq. dexrees. Six narrow-band light filters ($\Delta\lambda$ = 150Å)* covered the region 5500-8700Å, so that the transmission maxima corresponded to the positions of the strongest lines in this part of the spectrum: 5577 and 6300Å, and bands 7200, 7700, 7900 and 8680 Å [3-4] One measurement lasted 1.5 minutes.

Since 1956 measurements have been made with an electrophotometer of our own design [5]. (Photometer 2). The aperture angle of the photometer is 3.6 sq. degrees. Three interference filters ($\Delta\lambda$ = 120) transmitted the bands 3914 and 4278 and the line 5577 Å. One measurement lasted 1 second. Both photometers were calibrated in absolute units. Figure 1 illustrates the use of these filters.

Photometer 2 contained collimating optics with a lens diameter of 250 mm. This was lacking in photometer 1. In photometer 2, an FEU-19 was used as a light receiver which is more sensitive than the FEU-22 used in photometer 1. Thus the

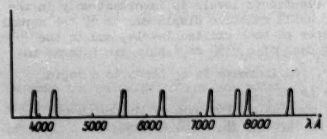

Fig. 1. The transmission regions of light filters.

sensitivity of photometer 2 for the line 5577Å was 40 times greater than that of the photometer 1. Therefore we could measure the faintest glows with photometer 2 while with photometer 1 only glows of medium intensity could be recorded although with the same accuracy as with photometer 2.

ANALYSIS OF LIGHT ABSORPTION IN THE ATMOSPHERE

The estimation of light absorption in the atmosphere for the spectral analysis of polar aurorae is very important because the range of zenith angles within which the glow is observed extends from zero to 75-80°. While comparing the violet and the green regions of the spectrum, the error in determining their relative intensities can reach 100% for large zenith angles if the light absorption in the atmosphere is not taken into account.

For a particular wave length λ the brightness B_λ of a luminous source seen on earth is related to its brightness $B_{0\lambda}$ outside the atmosphere by the expression

$$\lg B_\lambda = \lg B_{0\lambda} + M(z) \lg p_\lambda$$

(without special consideration of the aerosol component of the atmosphere). Here, p_λ is the coefficient of atmospheric transparency; M(z) - the amount of air mass along the ray path for the angle z (Bemporad function). If, during the observation, the luminous source is seen at varying values of z while B_λ is measured and p_λ remains constant, a graph with coordinates log B_λ and M(z) will show a series of points lying on a straight (Buger) line. The slope of this line yields p_λ, and where it crosses the ordinate log B_λ, the value log $B_{0\lambda}$. Once $B_{0\lambda}$ is determined for constant transparency, it is always possible to determine p_λ with the above formula by measuring B_λ. This method has become well known [6] and we used it to determine the cofficients of transparency. We selected for observation the Moon (measured by photometer 1) and Jupiter (measured by photometer 2).

* $\Delta\lambda$ - spectral half-width of the light filter.

The transparency coefficients measured by photometer 1 were determined once a night at constant transparency, and all the data obtained with photometer 1 were corrected for it, thus accounting for atmospheric absorption. The results include only those data for which good visual transparency was observed. This approximation of the transparency coefficients obtained for one particular night contains negligible errors if used for other nights, because the transparency coefficients for the near infrared region of the spectrum change very little.

We obtained the following transparency coefficients:

λ(Å)	5577	6300	7200	7700	7900	8680
P_λ	0.79	0.87	0.90	0.89	0.92	0.90

Using photometer 2, the brightnesses of Jupiter outside the atmosphere $B_{0\lambda}$ were determined with different filters during a night of stable atmospheric transparency and were then utilized for determining transparency coefficients during any other night of observation because the brightness of Jupiter was measured right after each brightness measurement of the polar aurora.

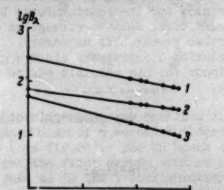

Fig. 2. Buger lines derived from Jupiter observations on three wavelengths.
wavelengths: (inÅ) 1-4278 2-5577 3-3914

Figure 2 shows Buger lines for each wave length. They were derived from Jupiter observations during the night from February 13 to 14, 1956. As is seen from the Figure, the points lie on a straight line, which indicates the stability of atmospheric transparency during the measurements.

Table 1 contains observed transparency coefficients for different nights. It can be seen that the spectral atmospheric transparency, especially in the violet region, is quite unstable and changes significantly from night to night. We know from literature that the data about spectral transparency differ considerably for different observation sites.

Table 1

Date	Time	λ (in Å)		
		3914	4278	5577
10.02.56	22 hrs. 42 min.	0.62	0.68	0.78
11.02.56	22 hrs. 49 min.	0.62	0.65	0.75
13.02.56	21 hrs. 24 min.	0.55	0.62	0.76
28.02.56	22 hrs. 57 min.	0.57	0.62	0.76
7.03.56	23 hrs. 34 min.	0.37	0.49	0.81
14.03.56	01 hrs. 08 min.	0.49	0.54	0.70

ABSOLUTE INTENSITIES OF EMISSION AND ENERGY DISTRIBUTION OVER THE SPECTRUM

Many authors made photoelectric measurements of absolute brightnesses of the polar aurora. All, except [1], measured the intensity of only one or two lines in the visible region of the spectrum [7-9] for short periods. As a result of our systematic studies, we were able to measure the absolute brightnesses over a wide range of the spectrum, where for comparatively narrow spectral intervals in the region 7200-8700 Å their magnitudes were measured for the first time.

The range of brightnesses of polar aurorae is very great. There are indications that the amplitude** of brightness can reach 1000 [10].

The minimum magnitude of brightness of the green line 5577 Å that we observed was 3×10^{-4} erg/sec. cm^2 steradian, the maximum 11×10^{-2} erg/sec. cm.^{2} steradian, which corresponds to an amplitude ratio 367. The absolute intensities of all other measured components have the same order of magnitude.

Table 2

Type of Glow	Photometer 2			Photometer 1					
	J_{3914}	J_{4278}	J_{5577}	J_{5577}	J_{6300}	J_{7200}	J_{7700}	J_{7900}	J_{8680}
Diffuse arc	66.2 388	35.2 210	27.4 186	89.6 185	24.6 18.3	16.9 18.2	47.7 70.6	60.5 96.5	42.8 140
Ray arc	236 2650	131 1300	123 1110	119 826	15.7 34.2	48.7 17.4	30.4 99.0	39.2 176	82.4 88.5
Drapery	264 550	150 328	137 280	124 280	34.2 15.9	17.4 16.4	33.3 79.5	45.1 95.3	43.7 54.2
Diffuse Glow	43.2 306	32.2 179	21.0 159	23.5 229	15.6 40.1	48.5 85.5	60.0 124	19.4 197	123 83.0

Table 2 contains some typical cases of absolute intensities.

Based on the large number of absolute brightness measurements, we obtained relative intensities of lines and bands (Table 3) for different types of glow. These types are listed in the table in order of their appearance at the Murmansk latitude.

Table 3

	λ (in Å)								
	3914 (0,0)N_2^+1N	4278 (0,1)N_2^+1N	5577 OI	6300 OI	7200 (4,2)N_2^+	7700 (3,0)N,1P	7900 (1,0)N_2^+	8680 NI
Diffuse arc	244 175 370	131 97 200	100	15 10 36	19 10 33	44 31 110	56 31 106	50 21 100
Ray arc	200 154 256	111 97 140	100	10 4 185	8 4 42	20 7 115	33 10 193	26 11 70
Drapery	196 169 244	112 100 135	100	15 9 30	9 5 28	23 10 77	34 20 77	25 19 105
Diffuse glow	196 156 238	109 97 130	100	33 7 68	33 6 200	39 10 280	80 29 154	78 18 480

**Ratio of maximum to minimum brightness

Designating the intensity of the green line as 100, we can combine the results of different years and calculate the relative intensities of other lines and bands relative to the green lines, which is the basic content of this paper. The left column under each wave length gives the average magnitude of relative intensity, the right column - minimum and maximum intensities obtained from all data.

An identification of the transitions is given below each value of λ : The region 7200-8700 Å is identified according to Meinel [3-4]. 1 N is the first negative, 1 P the first positive system of bands.

Let us analyze the average magnitudes of relative intensities. The difference between the energy distribution in spectra of diffuse and ray forms is apparent. The relative intensities of the infrared bands are higher for diffuse displays than for those with ray structure. Vegard discovered this for the 6300 Å line and for the first positive system of N_2 bands [11-12]. According to our measurements Vegard's results can also be extended to bands N_2^+ and NI. Vegard [11-12] showed that the relative intensities of the bands 3914 Å and 4278 Å are higher for diffuse arcs than for ray arcs. Our measurements confirm it. We think that these differences of relative intensities show that diffuse and ray forms of the glow belong to different spectral types.

On the basis of our measurements, the energy distribution in the green-violet region of the spectrum can be corrected. Vegard showed in [13] and in later papers that the ratios I_{5577}/I_{3914} and I_{5577}/I_{4278} are always greater than one, i. e. the absolute magnitudes of intensities in the bands 0--0 and 0--1 N_2 are less than the intensity of the green line. Vegard's measurements were not corrected for light absorption in the atmosphere, although the measurements were made at large zenith angles. Our results were the same when we did not allow for absorption. Taking absorption into account greatly changed the intensity ratios: The intensities of the bands at 3914 and 4278 Å proved to be higher than the intensity of the green line. The correctness of our taking absorption into account is confirmed by the fact that the ratio of intensities of the bands does not change with zenith distance as one would expect, since it is the emission of one system of bands.

Zhuravlev [14], who used a slitless spectrograph in his survey of polar aurorae spectra, found the same results when they were corrected for absorption.

Vegard [15] found a height effect, i. e., that the intensity of the negative system of N_2^+ bands increases with height of the glow faster than the intensity of the green line. The ratio (I_{4278}/I_{5577}) upper to I_{4278}/I_{5577} lower according to Vegard, lies within 1.4 - 1.9. Usually this is considered important because it gives evidence of the rapid increase of ionization of nitrogen molecules with height.

We think that this effect does not exist. Vegard did not allow for absorption. A simple analysis shows that even for an angular difference of 3-5° within which the bottom and the top of the glow are observed at $z = 75°$ absorption gives the same results as the Vegard effect because the atmosphere becomes more transparent for the violet portion of the spectrum during upward motion.

This makes us doubt the existence of the Vegard height effect.

The analysis of minimum and maximum values of relative intensities (Table 4) shows that the change of intensities of the violet bands is not greater than 2.5, while the relative intensities of the red and the infrared region of the spectrum change very strongly. This shows evidence of stronger fluctuations in the energy distribution in the red and infrared regions of the spectrum.

The variations are particularly strong in the spectra of diffuse glows which are observed after intense displays. From all our data we can conclude that the relative intensities of infrared bands increase while the overall intensity diminishes and that the energy distribution in the infrared end of the spectrum becomes similar to the energy distribution in the spectrum of the night sky which is relatively richer in radiation in the infrared region than the polar aurora. This was generally outlined in [1].

This factor can be of great importance for the theory of excitation of the infrared bands in the night air glow and the polar aurorae but we do not have sufficient data to strengthen our conclusion. Further research is necessary.

In conclusion I express my sincere gratitude to S. F. Rodionov for his valuable advice throughout this work.

September 22, 1958

References

1. S. F. RODIONOV, L. M. FISHKOVA: DAN USSR, 70, 6 1001 1003 (1950) (See RT-920, 6 pp.)
2. A. L. OSHEROVICH, E. N. PAVLOVA, S. F. RODIONOV, L. M. FISHKOVA: ZTF, 19, 2, 184 (1949)
3. A. B. MEINEL: Astrophys. J., 112, 562 (1950)
4. A. B. MEINEL: Trans. Amer. Geophys. Union, 31, 21 (1950)
5. I. G. FRISHMAN: PiTE, No. 1, 128 (1958)
6. V. B. NIKONOV: DAN USSR, 45, 143 (1944) (In (English)
7. A. OMHOLT: J. Atm. Terr. Phys., 5, No. 4, 243 (1954)
8. E. V. ASHBURN: J. Atm. Terr. Phys., 6, No. 1, 57 (1955)
9. E. V. ASHBURN: J. Geophys. Res., 60, No. 2, 205 (1955)
10. M. A. DAUVILLIER: J. de Phys. et le Rad., 5, 398 (1934)
11. L. VEGARD, L. HARANG: Geofys. publ. (Norske videnskaps-akademi i Oslo)10, No. 5 (1933)
12. L. VEGARD: E. TØNSBERG: Geofys. publ. (Norske videnskaps-akademi i Oslo) 11, No. 16 (1937)
13. L. VEGARD: Erg. der exakt. Naturwiss., 17, 229 (1938)
14. S. S. ZHURAVLEV: Tr. NIZMIR, Leningrad, No. 11, 174 (1955)
15. L. VEGARD: Geofys. publ. (Norske videnskaps_ akademi i Oslo), 16, No. 1 (1945)

TOM VI, Vyp. 3 OPTIKA I SPEKTROSKOPIIA Mart, 1959
VOL. VI, NO. 3 OPTICS AND SPECTROSCOPY March, 1959

Calculation of the Vibrational Spectrum of the Methylcyclopentane Molecule

R. S. LEBEDEV

Abstract: In accordance with a mechanical model a calculation of the normal frequencies of vibration of methylcyclopentane was carried out, and the form of some of them was determined. A theory is advanced concerning the nature of the characteristic frequencies in a series of cyclopentane and its derivatives.

Methylcyclopentane is the first substitution product in the series of cyclopentane hydrocarbons. It is possible to judge the interest in this naphthene by the large number of experimental investigations: The Raman spectrum of $C_5H_9CH_3$ was presented in references [1-10], data concerning the IR spectrum are given in the work of the authors [11-16]; however, interpretation of the spectra is absent. For detailed analysis of the $C_5H_9CH_3$ spectrum a calculation of the normal frequencies of vibration of the molecule is necessary, which is carried out in the present work.

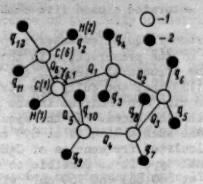

1 — atom C, 2 — atom H.

Methylcyclopentane was obtained from cyclopentane by substituent of a second hydrogen atom by the CH_3 group (see figure). The CH bonds of the substituent and the first carbon atom of the ring are arranged just as in the t-configuration of ethane.*

The complication of the original cyclopentane structure was reduced to C_5 by the symmetry of the molecule. For calculation of methylcyclopentane we introduced the normal vibrational coordinates (corresponding to the figure). They were reported in the following way: For changes 1) of the length of the CC bonds: Q_i(i=1-6); 2) the length of the CH bonds: q_i(i=1-12); 3) of the angles between corresponding CC bonds: $\gamma_{1.5}, \gamma_{1.2}, \gamma_{2.3}, \gamma_{3.4}, \gamma_{4.5}, \gamma_{5.6}, \gamma_{6.1}$; 4) of the angles between CH bonds: $\alpha_{3.4}, \alpha_{5.6}, \alpha_{7.8}, \alpha_{9.10}, \alpha_{12.11}, \alpha_{12.2}, \alpha_{11.2}$; 5) for changes of the HCC angles there was introduced the sum total of 22 equivalent coordinates β_{ij}.**

Coordinates for non-planar vibrations of the ring and possible rotation of the CH_3 group were not introduced because of the absence of force constants. Potential and kinetic energy interactions between equivalent normal coordinates were determined.*** The latter were presented in reference [17]. In addition to the constants used for the calculation of the cyclopentane molecule [17], there was adopted $K_q(CH_3) = 8.08 \times 10^5$ cm^{-2}.

* It was assumed that the methyl group has no influence on the geometry of the rest of the cyclopentane molecule.

** The first subscripts correspond to the number of CC bonds (Q), the second subscript to the number of CH bonds (q).

*** The matrices of potential and kinetic energy coefficients have 54 elements, and so are not cited in detailed form.

The complication of the geometry of the cyclopentane molecule determined supplementary relationships between the dependent coordinates. The total number of supplementary relationships for methylcyclopentane turn out to be equal to 8. The correctness of the composition of the matrices of potential and kinetic energy coefficients was verified by them.

The calculated model of methylcyclopentane had only one element of symmetry-planarity C_s. The latter determined two possible types of vibration by relation to it: symmetrical (A') and antisymmetrical (A'').

Vibrations of the type A' arise from the following relationships bewteen equivalent normal coordinates: $Q_1 = Q_5$, $Q_2 = Q_4$, $Q_3 = Q_3$, $Q_6 = Q_6$, $q_1 = q_7$, $q_2 = q_5$, $q_3 = q_9$, $q_4 = q_{10}$, $q_8 = q_6$, $q_3 = q_7$, $q_{12} = q_{11}$, $\alpha_{3.4} = \alpha_{9.10}$, $\alpha_{5.6} = \alpha_{7.8}$, $\alpha_{12.2} = \alpha_{11.2}$, $\alpha_{12.11} = \alpha_{12.11}$, $\gamma_{1.5} = \gamma_{1.5}$, $\gamma_{1.2} = \gamma_{1.5}$, $\gamma_{2.3} = \gamma_{3.4}$, $\gamma_{4.5} = \gamma_{4.5}$, $\beta_{1.6} = \beta_{1.6}$, $\beta_{6.12} = \beta_{6.11}$, $\beta_{1.6} = \beta_{1.6}$, $\beta_{1.2} = \beta_{1.1}$, $\beta_{2.3} = \beta_{3.1}$, $\beta_{10.3} = \beta_{4.1}$, $\beta_{3.4} = \beta_{4.3}$, $\beta_{10.4} = \beta_{4.3}$, $\beta_{7.4} = \beta_{5.3}$, $\beta_{4.4} = \beta_{4.3}$, $\beta_{7.2} = \beta_{5.3}$, $\beta_{4.3} = \beta_{4.3}$.

The obtained matrices of potential and kinetic energy coefficient have 31 elements.

Vibrations antisymmetrical to planarity C_s, are possible in the case where $-Q_1 = Q_5$, $-Q_2 = Q_4$, $Q_3 = 0$, $q_1 = q_2 = 0$, $-q_3 = q_9$, $-q_4 = q_{10}$, $-q_6 = q_8$, $-q_5 = q_7$, $-q_{12} = q_{11}$, $-\alpha_{3.4} = \alpha_{9.10}$, $-\alpha_{5.6} = \alpha_{7.8}$, $-\alpha_{12.2} = \alpha_{11.2}$, $\alpha_{12.11} = 0$, $\gamma_{1.5} = 0$, $-\gamma_{1.2} = \gamma_{4.3}$, $-\gamma_{2.3} = \gamma_{3.4}$, $-\gamma_{4.1} = \gamma_{4.5}$, $\beta_{1.2} = \beta_{1.6} = 0$, $-\beta_{6.12} = \beta_{6.11}$, $-\beta_{1.1} = \beta_{1.3}$, $-\beta_{3.1} = \beta_{4.3}$, $-\beta_{4.1} = \beta_{10.3}$, $-\beta_{3.4} = \beta_{4.4}$, $-\beta_{4.3} = \beta_{10.4}$, $-\beta_{4.3} = \beta_{7.4}$, $-\beta_{4.3} = \beta_{4.4}$, $-\beta_{4.3} = \beta_{7.2}$, $-\beta_{4.3} = \beta_{4.3}$.

Matrices of the A'' vibration type have 23 elements. In the matrix of symmetrical vibrations, the approximate symmetry for the ring, CH_3 group, and CH_2 group, was taken into consideration. For this purpose we composed matrices of transformation C-1 and C. Part of the matrix of transformation C of symmetrical vibrations for coordinates Q and γ takes the form

$$C = \begin{array}{c} \\ \\ \\ \\ \\ \\ \end{array} \begin{array}{cccccc|c} Q_1 & Q_2 & Q_3 & \gamma_{1.2} & \gamma_{1.3} & \gamma_{2.3} & \\ \hline 1 & 1 & 1 & 0 & 0 & 0 & Q_1 \\ 1 & -0.382 & -2.618 & 0 & 0 & 0 & Q_2 \\ 1 & -1.236 & 3.236 & 0 & 0 & 0 & Q_3 \\ 0 & 0 & 0 & 3.236 & -1.236 & 1 & \gamma_{1.2} \\ 0 & 0 & 0 & -2.618 & -0.382 & 1 & \gamma_{1.3} \\ 0 & 0 & 0 & 1 & 1 & 1 & \gamma_{2.3} \end{array}$$

and, correspondingly, part of the matrix C^{-1} of the symmetrical vibrations Q and γ takes the form

$$C^{-1} = \begin{array}{c} \\ \\ \\ \\ \\ \\ \end{array} \begin{array}{cccccc|c} Q_1 & Q_2 & Q_3 & \gamma_{1.2} & \gamma_{1.3} & \gamma_{2.3} & \\ \hline 0.4 & 0.4 & 0.2 & 0 & 0 & 0 & Q_1 \\ 0.524 & -0.2 & -0.324 & 0 & 0 & 0 & Q_2 \\ 0.076 & -0.2 & 0.124 & 0 & 0 & 0 & Q_3 \\ 0 & 0 & 0 & 0.124 & -0.2 & 0.076 & \gamma_{1.2} \\ 0 & 0 & 0 & -0.324 & -0.2 & 0.524 & \gamma_{1.3} \\ 0 & 0 & 0 & 0.2 & 0.4 & 0.4 & \gamma_{2.3} \end{array}$$

For coordinates β, γ, a the approximate symmetry was taken into account by relation to the planarity of the molecule in types of vibrations A' and A'' [18].

With the help of matrices of transformation there were obtained matrices of potential and kinetic energy coefficients in coordinates of approximate symmetry. The dependent coordinates were eliminated

by the method of Maiants [19]. The secular equations were solved by the method of diagonalization. Symmetrical vibrations determined 25 frequencies, for antisymmetrical 21 frequencies were obtained.

The results of the calculation of vibrational frequencies for methylcyclopentane and the interpretation suggested by us are given in the table.

Frequencies of the vibration types A′ and A″ can become apparent in the Raman and infrared spectra. The majority of spectral lines of $C_5H_9CH_3$ are diffuse bands which were resolved in some cases according to data of the later work [6].

Interpretation	Symmetry	Experimental frequencies (in cm-1) Raman spectrum (liquid) [4]	Infrared Spectrum [14]	Calculated Frequencies (in cm-1)
ν_1 (C—H)	A′	2912 (2)	2915	2977
ν_2 (C—H)	A′			2972
ν_3 (C—H)	A′			2941
ν_4 (C—H)	A′			2938
ν_5 (C—H)	A″	2961 (9)		2977
ν_6 (C—H)	A″	2928 (9)		2946
ν_7 (C—H)	A″	2871 (10)		2928
ν_8 (C—H)	A′			2907
ν_9 (C—H)	A′	2859 (7)		2881
ν_{10} (C—H)	A′			2880
ν_{11} (C—H)	A″			2891
ν_{12} (C—H)	A″			2881
—	—	—	2755	—
—	—	—	2880	—
—	—	2728 (1)	2832	—
—	—	—	2469	—
—	—	—	2278	—
—	—	—	2179	—
ν_{13} (H—C—H)	A′	1480 (1)[1]		1493
ν_{14} (H—C—H)	A′			1471
ν_{15} (H—C—H)	A′		1458	1473
ν_{16} (H—C—H)	A″	1458 (6)		1476
ν_{17} (H—C—H)	A″			1487
ν_{18} (H—C—H)	A′	1427 (2)		1434
ν_{19} (H—C—C)	A″	1352 (3)	1377	1381
ν_{20} (H—C—C)	A″			1316
ν_{21} (H—C—C)	A′	1318 (1)[1]	1351	1313
ν_{22} (H—C—C)	A′			1307
ν_{23} (H—C—C)	A′			1292
ν_{24} (H—C—C)	A″	1277 (1)[2]	1295	1291
ν_{25} (H—C—C)	A″			1252
ν_{26} (H—C—C)	A′			1249
ν_{27} (H—C—C)	A′	1192 (0)		1211
ν_{28} (H—C—C)	A′			1185
ν_{29} (C—C)	A″			1155
ν_{30} (C—C)	A″	1131 (0)[1]	1139	1169
ν_{31} (H—C—C)	A″			1147
ν_{32} (C—C)	A′	1021 (1)		1083
ν_{33} (C—C)	A″			1039
ν_{34} (H—C—C)	A′	999 (0)	979	1023
ν_{35} (H—C—C)	A″	980 (1)[3]		952
ν_{36} (H—C—C)	A″			947
ν_{37} (C—C)	A′	894 (6)[4]	889	863
ν_{38} (C—C)	A′	845 (1)	842	769
ν_{39} (H—C—C)	A′		—	880
ν_{40} (H—C—C)	A′	799 (0)[1]	—	790
ν_{41} (H—C—C)	A″		—	777
ν_{42} (C—C—C)	A″	534 (4)[3]	—	544
ν_{43} (C—C—C)	A′		—	528
ν_{44} (C—C—C)	A′	430 (1)	—	434
ν_{45} (C—C—C)	A″	344 (2)	—	335
ν_{46} (C—C—C)	A″	314 (1)	—	~250
—	—	227 (2)	—	—

Note: In parentheses are cited values of relative intensity of the lines.

1 Possible triplet [6].
2 Possible quartet [6].
3 Possible doublet [6].
4 Polarized

From analysis of data of the table it is evident that calculation gives significantly higher frequencies than experiment. In the infrared spectrum of methylcyclopentane there are bands in the 2800-2100 cm^{-1} region, while calculated frequencies in this region are absent. Not shown by calculation is the very low frequency at 227 cm^{-1} found in the Raman spectrum. Broad bands are present in the 3000-2800 cm^{-1} and 1500-1400 cm^{-1} region. Attributing the C-H frequency to the first region, corresponding changes of the HCH angle to the second, does not raise doubt. They agree with polarization of the C-H lines, with the order in the spectrum of N-methylpyrrolidine [20] and the spectral transition from the D_{5h} symmetry of cyclopentane to the C_s symmetry of methylcyclopentane.

Changes of the external angles HCC of the CH_2 groups are shown in the 1400-1700 cm^{-1} region. Frequencies corresponding to them have values analogous to the values in the spectra of pentane, isopentane and saturated closed five-membered ring systems.

The carbon frequencies deserve special attention because of the preservation in the cyclopentane series of the structural element, the ring. It is well known [21] that the fully symmetrical vibrations of the ring are manifest in the form of intense polarization lines. In the spectrum of methylcyclopentane such a line is at 890 cm^{-1} [21]. From the calculated frequencies of $C_5H_9CH_3$ of the A′ vibrational type it is possible to compare the frequencies at 880, 863 and 769 cm^{-1} with it.

Correct comparison of frequencies is possible only after detailed analysis. Hence, matrices of lesser order were chosen form the A′ matrix (not taken into account were coordinates q and coordinates corresponding to very close frequencies).

By the method of iteration roots were defined more precisely and the form of each normal vibration was determined. Change of the HCC angle corresponds to the 880 cm^{-1} frequency, which also confirms the form of this normal vibration in the coordinates of approximate symmetry.

$$\begin{array}{cccccccccc} & \beta'_{3.2} & Q'_1 & Q_2 & \beta'_{4.2} & \beta'_{12.6} & \beta_{11} & \gamma_{4.1} & \gamma'_{1.3} & \beta'_{5.1} \\ \nu_{29} = (4. & -1, & 0.04, & 0.16, & 2.78, & -0.94, & 1.54, & 0.02, & -0.04, & \end{array}$$

$$\begin{array}{cccccccc} \beta'_{6.1} & \gamma'_{1.3} & \beta'_{6.3} & \beta'_{1.2} & \beta'_{6.2} & \beta'_{6.3} & Q'_2 & \\ -0.09, & -0.33, & 0.05, & 0.01, & -0.07, & -0.05, & -0.05). & \end{array}$$

A direct change in the bonds between carbon atoms of the wing is described by the coordinate Q'_1. The frequency corresponding to it was shown to be too low by computation, 769 cm^{-1}. The lowering of the frequency was caused, primarily, by interaction of the ring with the C-C bond of the substituent. The form of the vibration indicates the same thing:

$$\begin{array}{cccccccccc} & Q'_1 & Q_2 & \beta'_{2.2} & \beta'_{12.2} & \alpha'_{2.12} & \beta_{1.1} & \gamma_{4.1} & \gamma'_{1.3} & \beta'_{5.1} \\ \nu_{28} = (1. & 1.43, & 0.07, & -1.70, & 0.55, & 0.08, & -0.52, & -0.27, & 0.24 & \end{array}$$

$$\begin{array}{cccccccc} \beta'_{6.1} & \gamma'_{1.3} & \beta'_{3.3} & \beta'_{6.3} & \beta'_{1.2} & \beta'_{6.2} & \beta'_{6.3} & \beta'_{6.3} & Q'_2 \\ 0.16, & 0.48, & 0.79, & 0.02, & -0.09, & 0.07, & -1.49, & -0.09, & 0.08). \end{array}$$

Potential energy coefficients are determined by the configuration used and in this sense it is impossible to alter them. Only by a more precise definition of the force constants is it possible to raise the frequency of interest to us by approximately 110 cm^{-1}, which we did not succeed in performing.

The frequency at 863 cm^{-1} corresponds to the coordinate $\gamma'_{1,2}$. The latter through an additional correlation was connected with the change of the length of C-C. Consequently, in normal vibration the whole ring participates, which its form indicates.

$$Q'_1 \quad Q_2 \quad \beta'_{2,3} \quad \beta'_{1,2,5} \quad \alpha'_{2,12} \quad \beta'_{1,1} \quad \gamma_{6,1} \quad \gamma'_{1,5} \quad \beta'_{2,1}$$
$$e_{37} = (1,\ 2.58,\ 0.16,\ 1.06,\ -0.42,\ 1.07,\ 1.17,\ -1.60,\ 1.10,$$
$$\beta'_{4,1} \quad \gamma'_{1,3} \quad \beta'_{4,3} \quad \beta'_{4,2} \quad \beta'_{4,5} \quad \beta'_{4,3} \quad \beta'_{4,3} \quad Q'_3$$
$$-0.73,\ -1.30,\ -0.37,\ 0.68,\ -0.78,\ -1.65,\ -1.32,\ 0.68)$$

We consider it possible to compare the given frequency with the 890 cm^{-1} frequency of the spectrum. The transition from cyclopentane (according to the calculation on reference [17] 859 cm^{-1}) to methylcyclopentane also does not change the value of the indicated frequency, but the principal coordinate corresponding to it is altered. If such a comparison is adopted, then only the 845 cm^{-1} frequency of the spectrum can be compared with the 769 cm^{-1} frequency.

The presence of two fully symmetrical carbon frequencies in the 900-800 cm^{-1} region corresponds to the experimental results of reference [20].

For a more detailed theoretical examination of the question of the presence of characteristic frequencies a more precise determination of the force constants of cyclopentane is necessary, as is calculation of the entire series of cyclopentane hydrocarbons.

The results we obtained are ground for doubt as to the presence of characteristic lines for the five-membered ring [21].

Continuing the analysis of the table, it is necessary to note that the very low spectral frequency at 227 cm^{-1} can not be compared to a calculation frequency. It is evidently necessary to assign it to nonplanar vibration of the ring analogous to N-methylpyrrolidine, pyrrolidine, tetrahydrothiophene [20]. The supposed order of frequencies of the nonplanar vibrations agrees with the similar order in toluene, equal to 216 cm^{-1} [22].

The remaining group of frequencies in the IR spectrum which were not examined, at 2755, 2660, 2632, 2469, 2278, 2179 cm^{-1}, cannot be explained theoretically. It seems possible to us to assume they are either the result of intramolecular interaction [23], or the result of a combination of fundamental frequencies, or by overtones.

In conclusion gratitude is due L. S. Maiants for valuable consultations.

References

1. E. CANALS, M. GODCHOT, G. CAUQUIL: C.R., 194 1574 (1932)
2. K. W. F. KOHLRAUSCH, A. W. REITZ, W. STOCKMAIR: Z. phys. Chem., 32, 229 (1936)
3. A. W. REITZ: Z. phys. Chem., B38, 381 (1937-38)
4. E. J. ROSENBAUM, H. F. JACOBSON: J. Am. Chem. Soc., 63, 2841 (1941)
5. K. W. F. KOHLRAUSCH: Ramanspektren. Hand. und Jahrbuch der chemischen Physik, vol. 9. Michigan, 1943
6. P. A. BAZHULIN, KH. E. STERIN, T. F. BULANOVA, O. P. SOLOVOVA, M. B. TUROVA-POLIAK, B. A. KAZANSKII: IAN USSR, OKhN, No. 1, 7 (1946)
7. D. R. DAUSLIN, H. M. HUFFMAN: J. Am. Chem. Soc., 68, 173 (1946)
8. M. R. FENSKE, W. G. BRAUN, R. V. WIEGAND, D. QUIGGLE, R. H. MC CORMICK, D. H. RANK: Anal. Chem., 19, 700 (1947)
9. W. G. BRAUN, D. F. SPOONER, M. R. FENSKE: Anal. Chem., 22, 1074 (1950)
10. G. S. IANDSBERG, P. A. BAZHULIN, M. M. SUSHCH. NSKII: Osnovnye parametry spektrov kombinatsionnogo rasseianiia uglevodorodov (Fundamental parameters of Raman spectra of hydrocarbons) Akad. Nauk Press Moscow, 1956
11. J. LECOMTE: C. R., 183, 27 (1926)
12. F. TRENKLER: Proc. Ind. Acad. Sci., 8A, 383 (1938)
13. H. M. TRIMBLE: Ind. Eng. Chem. Anal. Ed., 12, 52 (1940)
14. E. K. PLYLER, R. STAIR, C. J. HUMPHREYS: J. Res. Nat. Bur. Stand., 38, 211 (1947)
15. R. B. BARNES, R. C. GORE, U. LIDDEL, VAN ZANDT WILLIAMS: Infrared Spectroscopy Industrial Applications and Bibliography. N. Y. Reinhold, 1944
16. G. GAUTHIER: J. Phys. Rad., 14, 19 (1953)
17. R. S. LEBEDEV: Tr. Kemerovsk. Ped. Inst., 3 (1958)
18. M. V. VOL'KENSHTEIN, M. A. EL'IASHEVICH, B. I. STEPANOV: Kolebaniia molekul (Vibrations of Molecules), 1, GITTL, Moscow, 1949
19. L. S. MAIANTS: DAN USSR, 89, 423 (1953)
20. H. TSCHAMLER, H. VOETTER: Monatshefte fuer Chemie, 83, 302 (1953)
21. M. M. SUSHCHINSKII: IAN USSR, Ser. fiz., 17, 5,608 (1953)
22. A.V. SECHKAREV: Cand. Dissertation, NIFI LU, 1952
23. SH. SH. RASKIN, A. V. SECHKAREV: DAN USSR, 86, 509 (1952)

TOM VI, Vyp. 3 OPTIKA I SPEKTROSKOPIIA Mart, 1959
VOL. VI, No. 3 OPTICS AND SPECTROSCOPY March, 1959

Vibration Spectra of Unsaturated Hydrocarbons VII. Calculation and Interpretation of the Vibration Spectrum of Cyclopentene

L. M. SVERDLOV AND E. N. KRAINOV

Abstract: On the basis of experimental material accumulated to the present time by the study of vibrational spectra of cycloolefins, a calculation was made of the vibrational frequencies of one of the representatives of this class of molecules, cyclopentene. The calculation was based on the assumption of planarity of the carbon ring of the molecule. Agreement of calculated and observed frequencies confirm the choice of system of force constants and the geometrical model of the molecule. Some difficulties with the agreement of the question about polarization of some lines were noted. On the basis of the frequencies of vibration of cyclopentene which were obtained, the spectra of its simple alkyl derivatives were interpreted and their characteristic frequencies determined.

INTRODUCTION

Recently we have undertaken a systematic study of the vibration spectra of acyclic unsaturated hydrocarbons of various types [1-3]. It offers interest, using the results obtained from the study of more simple molecules, to pass on to the examination of more complicated unsaturated compounds, cycloolefins, for the purpose of investigating the influence on the vibration spectra of inclusion of a double bond in the ring system.

With respect to the vibrational spectrum of cycloolefins at the present time rather considerable experimental material has been accumulated (particularly with respect to the spectra of alkylcyclopentenes), however, to the present time articles are almost completely absent in the literature in which attempts were made to interpret the spectra even of the simple cycloolefins. In connection with this the actual problem arises of making a theoretical calculation of the frequencies of normal vibrations of simple representative cycloolefins for the purpose of ascertaining characteristic features of the vibrational spectra of cycloolefins of different types.

In this paper a calculation is made of the vibrational frequencies of an important representative of the cycloolefins, the cyclopentene molecule.

REVIEW OF EXPERIMENTAL MATERIAL AND CALCULATION OF VIBRATIONAL FREQUENCIES OF THE CYCLOPENTENE MOLECULE

The Raman spectra of cyclopentene have been investigated repeatedly [4-9]. In early articles [4-7] the data of vibration frequencies was taken with visual qualitative estimation of band intensity. In the papers of Akishin and coworkers [8] and Markova and co-workers [9] the data of intensity of lines were expressed in a single objective scale (however it must be noted that in some cases of intensity of a group of lines, found in these articles, they differ noticeably among themselves.) Polarization measurements were done by Reitz [5] and Gerding [7]. Infrared spectra of cyclopentene were investigated only in the 2500-4500 cm^{-1} region [10].

Theoretical calculation of the vibrational frequencies of cyclopentene have not been carried out by anyone yet, which is evidently explainable by their great complexity.

Before going over to the calculation we will examine the question of the geometry of the cyclopentene molecule, since electron diffraction investigations of the structure of cyclopentene have not been made. The basic assumption which we make consists of our belief that the important carbon ring of the molecule is planar. The correctness of this assumption can be verified by measurement of the vibrational frequencies of the molecule. If the calculated frequencies were to differ very much from the found, then, evidently, the model chosen differs significantly from the real configuration of the molecule. If, on the other hand, the difference between calculated and observed frequencies were to be found within the limits of the usual precision of similar calculations, then the conclusion follows from this that the model chosen differs comparatively little from the actual structure of the molecule.

In this case, if the carbon ring of the molecule is planar, then from consideration of the symmetry it follows directly that cyclopentene belongs to the C_{2v} group. We shall further examine the question of choice of geometrical parameters of the molecule. The Carbon-carbon double and single bond distances we assumed to be equal to the corresponding distances in acyclic unsaturated hydrocarbons which we used in previous calculations; r(C=C)=1.353 Å, r(C-C)=1.54 Å. While from the cyclic condition we get the following values for the angles between bonds: $\angle$(C-C-C)=105°58'; $\angle$ (C=C-C)=111°03'. Further we assume (see sketch) r(=C-H)=1.07 Å, r(C-H)=1.09 Å, $\angle \alpha_{a2} = \angle \alpha_{b2}$ = 124°28'; $\angle$HCH=109°28'. While for the angles $\angle$ C-C-H we get 111°21.

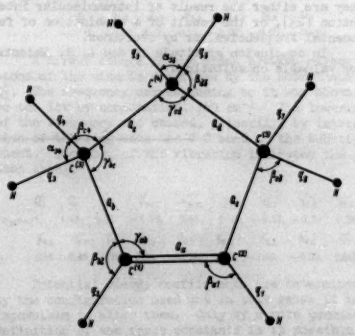

Figure 1. Vibrational coordinates of cyclopentene.

The calculation of frequencies of vibration was carried out by the method of El'iashevich and Stepanov [11].

In the case of cyclopentene there are 33 normal vibrations belonging to the following type of symmetry: $G = 11A_1 + 9B_1 + 6A_2 + 7B_2$.

For calculation we introduce 42 natural vibrational coordinates (changes of length of the bonds and of the size of the angles): (see figure 1) $q_i (i=1-8)$, Q_a, Q_b, Q_c, Q_d, Q_e, α_{34}, α_{56}, α_{78}, β_{ai} $(i=1-2)$, $\beta_{bj} (j=2,3,4)$, $\beta_{ck} (k=3,4,5,6)$, $\beta_{dl} (l=5,6,7,8)$, $\beta_{em} (m=1,7,8)$, γ_{ab}, γ_{bc}, γ_{cd}, γ_{de}, γ_{ae} (see figure 1), $\rho_a^{b_2}$, $\rho_a^{e_1}$, $\chi_{b_2}^{e_1}$, χ_c^{ab}, χ_d^{ae}. Here ρ_a^{b2} and χ_d^{ae} are angles, which determine respectively the departure of the CC bond from planarity of two bonds b2, and the departure of the (CC)d bond from planarity of the two bonds ae. χ_{b2}^{e1} is the angle of bending of the two = CCH groups one relative to the other.

Between coordinates there are 9 additional conditions:

1) $\gamma_{ab}+\beta_{a2}+\beta_{b2}=0$; 2) $\gamma_{ae}+\beta_{a1}+\beta_{e1}=0$;

3) $$2\gamma_{bc}\cot\phi_1\tan\frac{O_2}{2}-(\beta_{b3}+\beta_{b4}+\beta_{c3}+\beta_{c4}) + 2\alpha_{34}\cot\phi_1\tan\frac{O_2}{2}=0;$$

4) $$2\gamma_{de}\cot\phi_1\tan\frac{O_2}{2}-(\beta_{d7}+\beta_{d8}+\beta_{e7}+\beta_{e8}) + 2\alpha_{78}\cot\phi_1\tan\frac{O_2}{2}=0;$$

5) $$2\gamma_{cd}\cot\phi_2\tan\frac{O_3}{2}-(\beta_{c5}+\beta_{c6}+\beta_{d5}+\beta_{d6}) + 2\alpha_{56}\cot\phi_2\tan\frac{O_6}{2}=0;$$

6) $\gamma_{ab}+\gamma_{bc}+\gamma_{cd}+\gamma_{de}+\gamma_{ae}=0$;

7) $$Q_a-(Q_b+Q_e)\cos O_1+(Q_c+Q_d)\cos(O_1+O_2)+(\gamma_{ab}-\gamma_{ae})\frac{\sin O_1}{\sigma_b}+\gamma_{cd}\frac{\sin(O_1+O_2)}{\sigma_c}=0;$$

8) $$(Q_b-Q_e)\sin O_1-(Q_c-Q_d)\sin(O_1+O_2)+(\gamma_{ab}-\gamma_{ae})\left[\frac{\cos O_1}{\sigma_b}-\frac{\cos(O_1+O_2)}{\sigma_c}\right]-(\gamma_{bc}-\gamma_{de})\frac{\cos(O_1+O_2)}{\sigma_c}=0;$$

9) $$\frac{\sin(O_1+O_4)}{2\sin O_1\cdot\sin O_4}(\rho_a^{b2}-\rho_a^{e1}) + \frac{\sigma_b\sin O_2}{\sigma_b\sin(O_1+O_2)-\sigma_c\sin O_1}(\chi_c^{ab}-\chi_d^{ae})+\chi_{b2}^{e1}=0.$$

Here $O_1=\angle(C{=}C{-}C)$; $O_2=O_{bc}=\angle(C{-}C{-}C)$; $O_3=O_{cd}=\angle(C{-}C{-}C)$; $\phi_1=O_{b3}=\angle CCH$; $\phi_2=O_{c5}=\angle CCH$;

$$\sigma_b=\frac{r(C-H)}{r(C^{(1)}-C^{(5)})};\quad \sigma_c=\frac{r(C-H)}{r(C'^{3}-C^{(4)})}.$$

$O_4=O_{a2}=\angle C{=}C{-}H$.

Further, we will introduce coordinates of exact symmetry and coordinates of approximate symmetry for the groups $C^{(3)}H_2$ and $C^{(4)}H_2$. We shall cite some of these coordinates:

$$\varphi_1^{B1}=\frac{1}{2\sqrt{2}}[(\beta_{b3}+\beta_{b4}-\beta_{c3}-\beta_{c4})-(\beta_{e7}+\beta_{e8}-\beta_{d7}-\beta_{d8})];$$

$$\varphi_2^{B1}=\frac{1}{2}(\beta_{c5}+\beta_{c6}-\beta_{d5}-\beta_{d6});$$

$$\chi_1^{A2}=\frac{1}{2\sqrt{2}}[(\beta_{b3}-\beta_{b4}+\beta_{c3}-\beta_{c4})+(\beta_{e7}-\beta_{e8}+\beta_{d7}-\beta_{d8})];$$

$$\chi_2^{A2}=\frac{1}{2}(\beta_{c5}-\beta_{c6}-\beta_{d5}+\beta_{d6});$$

$$\psi_1^{B2}=\frac{1}{2\sqrt{2}}[(\beta_{b3}-\beta_{b4}-\beta_{c3}+\beta_{c4})-(\beta_{e7}-\beta_{e8}-\beta_{d7}+\beta_{d8})];$$

$$\psi_2^{B2}=\frac{1}{2}(\beta_{c5}-\beta_{c6}+\beta_{d5}-\beta_{d6}).$$

The force constants necessary for the calculation of matrices of potential energy were taken from calculations of acyclic olefins [1,2]

$K_a(C{=}C)=14.2$; $H_{ab}=H_{a1}=0.1$; $A_{a1}^a=0.45$; $A_{ab}^a=0.45$; $A_{ab}^a=1$;

$K_b(C{-}C)=7.02$; $H_{bc}=0.1$; $H_{b3}=H_{b3}=0$; $A_{b2}^b=A_{b3}^b=0.43$;

$A_{ab}^b=0.8$; $A_{bc}^b=0.5$; $a_{a1}^1=0.66$; $a_{b2}^2=0.35$; $h_{34}=0.05$;

$a_{34}^3=a_{b3}^3=0.35$; $K_\alpha=0.71$; $l_{34}^{b3}=-0.035$; $K_{a2}=0.77$;

$n_{a2}^{a1}=-0.025$; $m_{a2}^{ae}=0.095$; $K_{b2}=0.7$; $m_{b2}^{bc}=0.12$; $K_{b3}=0.92$;

$l_{b3}^{bc}=l_{b3}^{b4}=l_{b3}^{c3}=-0.035$; $m_{b3}^{ab}=0.12$; $m_{c3}^{c6}=0.12$; $n_{c3}^{c5}=-0.02$;

$m_{c3}^{cd}=0.12$; $K_{ab}=1.1$; $n_{ab}^{ae}=-0.025$; $n_{ab}^{bc}=-0.02$; $K_{bc}=1.1$;

$n^{cd}_{bc}=-0.02$; $K_{\chi_{b2}}{}^{el}=0.755$; $K_{\rho_a}{}^{b2}=0.317$; $U_{\rho_a 2\rho_a}{}^{b}{}_{el}=0.047$;

$U_{\rho_a}{}^{b2}{}_{\chi_{b2}}{}^{el}=0$.

Several of the force constants were calculated by the method of variation of constants:

$K_q(=C\text{-}H)=8.58$; $K_q(C\text{-}H)_{56}=7.69$; $K_q(C\text{-}H)_{34}=8.02$;

$K_{\chi_c}{}^{ab}=0.4$; $U_{\chi_c}{}^{ab}{}_{\chi_d}{}^{ae}=0.25$; $U_{\chi_c}{}^{ab}{}_{\rho_a}{}^{el}=0.06$;

$U_{\chi_c}{}^{ab}{}_{\beta_{c5}}=-0.05$; $U_{b2}{}^{b3}=0.044$ (in units 10^{-6} cm^2).

Having multiplied the symmetrical matrices of potential kinetic energy coefficients in numerical form, we obtain the secular equations of 11, 9, 7, and 6th orders, which were solved by the method of successive diagonalizations. Some roots of the 11th order equation were computed by the method of Maiants. Secular equations of the 11th and 9th order were solved also by an electronic computing machine.* The calculated and observed frequencies are presented in Table 1, where is also given a full interpretation of the Raman spectrum of cyclopentene. As is evident from the data of Table 1, there is sufficiently good agreement between calculated and observed frequencies - maximum error is 41 cm^{-1}, average error is 13.6 cm^{-1}, i.e. discrepancy between calculated and observed frequencies does not exceed the size of the discrepancies commonly obtained in carrying out analogous calculations for other molecules (paraffins, olefins.)

Table 1
Calculation and Interpretation of the Vibrational Spectrum of Cyclopentene

Coordinates	Symmetry	Calculated Frequencies	Raman Spectrum (liquid) ν	J	ρ	Coordinates	Symmetry	Calculated Frequencies	Raman Spectrum (liquid) ν	J	ρ	Infrared Spectrum (liquid)
Q(C=C) . .	A_1	1624	1614	150	0.12[2]	φ(=C—H)	A_1	3068	3060	270	0.31	3068(s.)
Q(C—C) . .	B_1	1118	1109	130	0.49	φ(=C—H)	B_1	3039				
Q(C—C) . .	A_1	965	965	70	0.19	φ*(C—H_{ax})	A_1	2857	2849	250	0.25	2852 (v.s.)
Q(C—C) . .	B_1	907	937	9								2902
Q(C—C) . .	A_1	906	900	140	0.13 dep.	φ⁻(C—H_{ax})	B_2	2904	2898	210	0.44	(v.s.)
γ(CCC) . .	B_1	708	702	5								
γ(CCC) . .	A_1	631	603	0	p.	φ*(C—H) .	A_1	2919	2916	210		
β(C=C—H)	B_1	1423				φ*(C—H) .	B_1	2917				2927 (v.s.)
β(C—C—H)	A_1	1214	1207	18	0.85							
C=C												2958
ρCH . . .	A_2	1102	1082	25[3]		φ⁻(C—H).	B_2	2967				(v.s.)
C=C												
ρCH . . .	B_2	786	772	2		φ⁻(C—H).	A_2	2967				
CCH						φ_1(CCH) .	A_1	1338				
ωCH . . .	A_2	417	387	31	0.87	φ_2(CCH) .	B_1	1322				
C—C						φ_3(CCH) .	B_1	1305	1297	17	0.5	
τC=C . . .	B_2	200				χ_1(CCH) .	B_2	1300				
s_{ab}(HCH) .	A_1	1496	1468	20	w.	χ_2(CCH) .	A_2	1290				
s(HCH) . .	B_1	1476			p.	χ_3(CCH) .	A_2	1222	1207	18	0.85	
s(HCH) . .	A_1	1441	1441	55	0.74	ψ_1(CCH) .	B_2	1040	1027	15	0.77*	
						ψ_2(CCH) .	A_2	824	800	vw.	dep.	
						ψ_3(CCH) .	B_2	720	702	5	dep.	

1 According to reference [9].
2 According to reference [7].
3 According to reference [8].
4 According to reference [5], depolarized.

* We take this opportunity to express our thanks to scientific workers at FIAN, M.M.Sushchinskii and R.I.Podlovchenko for solving these equations on the electronic computing machine.

DISCUSSION OF RESULTS

We shall examine the characteristic features of the vibrational spectrum of cyclopentene. For this we shall compare its spectrum with the spectra of molecules having the same structural elements that are in cyclopentene, namely the spectra of cis-butene-2. [2] (element and pentane ($CCH_2CH_2CH_2C$) [11] (see Table 2).

Table 2

Comparison of the Raman Spectrum of Cyclopentene with the Spectra of Cis-Butene-2 and Pentane

Coordinates	Cyclopentene	Cis-butene-2	Pentane
q (=C-H) . .	3060	3034	-
Q (C=C). . .	1614	1669	-
β (C=C-H). .	1207;1423calc.	1267;1422infrared	-
α (HCH). . .	1441;1468	-	1442;1462
φ (CCH). . .	1297[3]*	-	1268;1303[2]
χ (CCH). . .	1207;1297[2]	-	1170;1303[2]
ψ (CCH). . .	702;800;1027	-	739;766;993
Q (CeC). . .	900;937	-	840;993
	965;1108	-	1024;1144

* In square brackets is shown number of corresponding frequencies.

As is evident from the data of Table 2, inclusion of a double bond in the ring is most strongly reflected in size of the frequencies of the carbon chain: by comparison with pentane the frequencies of the carbon chain are displaced 40-60 cm^{-1}; the C-C frequency is lowered 55 cm^{-1} by comparison with cis-butene-2. An appreciable displacement is experienced also by the frequency of symmetrical vibration, β(C=C-H). As to the frequencies of deformational vibrations of the three CH_2 groups, they experience less change, part of the frequencies almost don't change, the others change 37 cm^{-1}. Consequently, the general character of the spectrum of the CH_2 groups in the transition from pentane to cyclopentene, is retained.

The good agreement between calculated and observed frequencies of cyclopentene can be considered, first of all, as evidence of the fact that the system of force constants used in the calculation give sufficiently well the features of the force field of cyclopentene, and consequently, the force constants taken from calculations of acyclic olefins can be used for calculation of frequencies of vibration of cycloolefins, for example, alkylcyclopentenes, cyclohexene, and alkylcyclohexenes.

Secondly, the results of the calculation show that the geometrical model assumed by us for the calculation is close to the real structure of cyclopentene.

However, it must be noted that the polarization of some of the lines does not agree with predictions of theory. In the first place this applies to the intense line at 1108, which, according to calculation, ought to be assigned to the antisymmetrical valence vibration of the carbon ring, and consequently, this line ought to be depolarized. Nevertheless, experiment shows that the 1108 line is polarized, although not very strongly (the degree of depolarization of this line is several times greater than the degree of depolarization of the fully symmetrical lines at 900 and 965 cm^{-1}). These difficulties with polarizations can be explained if it is assumed that the carbon ring does not have strict planarity, but is slightly bent. In this case the symmetry of the molecule will deviate a little from C_{2v}, the molecule will belong to group C_1, and all the lines ought to be polarized. But since the break of the ring is not too big, the values of the frequencies arising from the planar model which were calculated are close to experimental values.

Moreover, the degree of depolarization of lines which we assign to representations B_1, B_2, and A_2 ought to be greater than the degree of depolarization of the lines assigned to representation A_1.

We shall examine further the question concerning the interpretation of frequencies in the 2800-3000 cm^{-1} region. As is well known, the interpretation of this part of the spectrum is generally quite difficult, since the number of frequencies found is always greater than the number of frequencies which can be anticipated on the basis of theoretical calculations. We came across this difficulty, and in the case of cyclopentene in the Raman and infrared spectra found seven different frequencies, while calculation (using the usual assumption that all CH_2 groups are equal) only gives two different frequencies, corresponding to the symmetrical and asymmetrical CH vibrations of the CH_2 groups. This difficulty could be solved if it is assumed that the electron cloud distribution in two CH_2 groups which occupies different positions with respect to the double bond, are unequal. In this case the force constants K_1(C-H) (and CH frequencies) corresponding to these two groups ought to differ somewhat, one from the other. Adopting the indicated assumption it is possible to interpret the five most intense lines in the 2800-3000 cm^{-1} region as frequencies of fundamental vibrations (see Table 1). The two remaining lines at 2872 and 2951 cm^{-1} are assigned to overtones (see Table 4). The very large intensity of the 2951 cm^{-1} line in the Raman spectrum can be explained by Fermi resonance between the overtone of the 1468 cm^{-1} frequency (2936 cm^{-1}) and the frequency of symmetrical CH vibration of the CH_2 groups (positioned closer to the double bond) having a value of about 2931 cm^{-1}. As a result of the interaction, a separation of frequencies takes place - the overtone is displaced to 2951 cm^{-1}, but the frequency ν(C-H) to 2916 cm^{-1}, which are indeed found in the experiment.

The correctness of assignment of the remaining frequencies of cyclopentene is confirmed by the fact that, using these frequencies, all the remaining frequencies found in the Raman and infrared spectra of cyclopentene can be interpreted as combination frequencies or overtones (see Table 3).

The calculating of the vibrational frequencies of cyclopentene, and also of the molecule

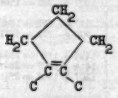

permitted interpretation of the spectra of simple alkylsubstituted cyclopentenes,

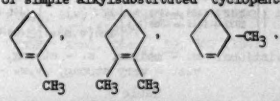

which gave the possibility of establishing characteristic frequencies of alkyl substituents of cyclopentene of different types. The results obtained are presented in Tables 4-6.

It is interesting to note that in this case, if the alkyl substituent occurs far from the double bond (in Table 3-6), then the C=C frequency has the same value that it has in cyclopentene. This may be explained by the fact that, as the calculation of the form of vibration corresponding to the C=C frequency shows, the vibrational coordinates connected with the CH_2 groups barely participate in this vibration. Therefore, substitution of hydrogen by alkyl radicals (in the CH_2 groups) does not affect the C=C frequency.

In this same case if we make substitution in positions 1 and 2, then the frequency of the C=C is increased, and under the condition of substitution of the type

attains the normal value characteristic for tetraalkyl substituted ethylenes

. Calculation of the molecule

shows this, and experiment confirms it.

Further we must note that the frequency of the fully symmetrical valence vibration of the carbon-carbon bond lying in the 900 cm^{-1} region (900 ± 25 cm^{-1}) is especially characteristic for the cyclopentene ring. This intensive polarized line is encountered in all the alkylcyclopentenes which is evident from the data of Tables 4-6 and from the following data [9]:

876,

888,

891,

921,

892 cm^{-1}.

Table 3

Interpretation of the Combination Frequencies and Overtones

Infrared Spectrum	Assignment	Raman Spectrum	Assignment
2586 (w.)	1468 + 1108 = 2576 (B_1)	1588 (w.)	1207 + 387 = 1594 (A_1)
	2958 − 387 = 2571 (B_1)		
2634 (w.)	1614 + 1027 = 2641 (B_2)	1645 (v.w.)	937 + 702 = 1639 (A_2)
2727 (w.)	1441 + 1297 = 2738 (B_1)	1673 (v.w.)	900 + 772 = 1672 (B_2)
	1614 + 1108 = 2722 (B_1)		
2765 (w.)	1468 + 1297 = 2765 (B_1)	2555 (v.w.)	1441 + 1108 = 2549 (B_1)
3228 (w.)	1614 + 1614 = 3228 (A_1)	2641 (v.w.)	1614 + 1027 = 2641 (B_2)
3298 (w.)	2927 + 387 = 3314 (B_2)	2675 (v.w.)	1207 + 1468 = 2675 (A_1)
	2902 + 387 = 3289 (B_1)		
4305 (m.)	2852 + 1441 = 4293 (A_1)	2726 (v.w.)	1614 + 1108 = 2722 (B_1)
	2852 + 1468 = 4320 (A_1)		
4379 (m.)	2916 + 1468 = 4384 (A_1)	2872 (w.)	1441 + 1441 = 2882 (A_1)
	2927 + 1441 = 4368 (B_1)		
		2951 (v.s.)	1468 + 1468 = 2936 (A_1)

Abbreviations: m. - medium, s. - strong, w. - weak, v.s. - very strong, v.w. - very weak.

Table 4

Characteristic Frequencies of Alkyl Substituents of Cyclopentene of the Type

Coordinates	C_6H_{10}	C_7H_{12}	C_8H_{14}	C_9H_{16}
φ(=C—H)	3044 **	—	—	—
φ_{CH_2}(C—H)	2961	2961	2961	2961
$\varphi^{+}_{CH_2}$(C—H)	2912 **	2904	2910	2916
$\varphi^{-}_{CH_2}$(C—H)	2857	2854	2854	2852
Q(C=C)	1657	1653	1653	1650
α_{CH_2}(HCH)	1465	1474	1468	1470
α_{CH_3}(HCH)	1445	1443	1443	1440
β(C=C—H)	1334	1325	1332	1337
Ψ_{CH_2}(CCH), χ_{CH_2}(CCH)	1298	1298	1298	1299
χ_{CH_2}(CCH)	1204	1204	1202	1200
Q(C—C)	1152 **	1152	1154	1152
Q(C—C)	1133	1133	1134	1133
Ψ_{CH_2}(CCH)	1028	1027	1028	1028
Q(C—C)	967	956	951	953
Q(C—C)	880	898	893	898
Q(=C—C_R)	822	822	—	825
γ(CCC)	579 **	582	583	585
$\rho_{\substack{C=C \\ CCC}}$	432	435	440	432

* Raman spectrum from reference [8].
** Reference [9].

Table 5

Characteristic Frequencies of Alkyl Substituents of Cyclopentene of the Type

Coordinates			
Q(C=C)	1686	1671	1679
α_{CH_2}(HCH)	1469	1468	1469
α_{CH_3}(HCH)	1441	1438	1441
Ψ_{CH_2}(CCH), χ_{CH_2}(CCH), Q⁻(=C—C_R)	1299	—	1298
Q(C—C), χ_{CH_2}(CCH)	1208	1208	1208
Ψ_{CH_2}(CCH)	1029	1040	1033
Q(C—C)	1007	1009	1009
Q(C—C)	909	916	912
Q⁺(=C—C_R)	702	702	694
γ(CCC)	580	614	580

* Raman spectra from reference [12].

Table 6

Characteristic Frequencies of Alkyl Substituents of Cyclopentene of the Type

Coordinates		
φ(=C—H)	3055	
Q(=C=C)	1614	1617
α(HCH)	1459	1460
α(HCH)	1441	1445
χ_{CH_2}(CCH)	1214	1204
Q(C—C_R)	1176	1170
Q(C—C)	1121	1120
Q(C—C)	967	985
Q(C—C)	937	935
Q(C—C)	898	912
γ(CCC)	582	595
$\chi_{\substack{CCH \\ CCH}}$	391	397

* Reference [9].
** Reference [8].

The small change of frequency of this vibration upon alkyl substitution of different types is explained in the following way. As was shown by the calculation of the form of the vibration corresponding to the indicated frequency of cyclopentene, in this vibration coordinates participate which are assigned both to the hydrocarbon ring and to the deformation vibration of the CH_2 and CH groups. Since upon alkyl substitution part of these coordinates change, then the frequency itself ought to change somewhat.

April 7, 1958

Note added to the proof: Recently P. A. Bazhulin investigated the infrared spectra of cyclopentene, and obligingly gave us the obtained data, which confirms our interpretation: 1616 (mod.)[Q(C-C)A_1]; 1467(s)[α(HCH)B_1]; 1449(s)[α(HCH)A_1]; 1432(m)[β(C=C-H)B_1]; 1356(s)[Ψ_1(CCH)A_1]; 1302(s)[Ψ_2(CCH)B_1]; 1284(m)[χ_1(CCH)B_2]; 1213(m)[β(C=C-H)A_1]; 1113(w)[Q(C-C)B_1]; 1048(v.s.)[Ψ_1(CCH) B_2]; 964(m)[Q(C-C)A_1]; 904(v.s.)[Q(C-C)$_{A_1}$; 762(w)[$\Psi_{\substack{CCH \\ CCH}}$ B_2]; 692(v.s.)[γ(CCC)B_1].

The remaining lines can be interpreted as component frequencies.

We take the opportunity to express thanks to P. A. Bazhulin for giving us this data prior to publication.

References

1. L. M. SVERDLOV, N. L. PAKHOMOVA: ZETF, 26, 64 (1954)
L. M. SVERDLOV, O. N. VINOKHODOVA: DAN USSR, 100, 45 (1955)
L. M. SVERDLOV: DAN USSR, 106, 80 (1956)
2. L. M. SVERDLOV: OiS, 1, 752 (1956)
3. L. M. SVERDLOV: Materialy X Soveshchaniia po spektroskopii (Materials X Conference on Spectroscopy), 1, 278, 1957, L'vov Univ. Press; DAN USSR, 112, 706 (1957)
4. M. GODCHOT, E. CANALS, G. CAUQUIL: C. R., 196, 780 (1933)
L. PIAUX: C.R., 198, 1496 (1934)
5. A. W. REITZ: Z. phys. Chem., 33, 179, 368 (1936); 38, 381 (1938)
6. K. KOHLRAUSCH: Raman Spektren, Leipzig, 1943 (IL, Moscow, 1952)
7. H. GERDING, A. P. VAN DER VET: Rec. trav. chim., 64, No. 5, 257 (1945)
8. P. A. AKISHIN, V. M. TATEVSKII, N. G. RAMBIDI, N. N. MEZENTSOVA, R. IA. LEVINA: ZFKh, 30, 660 (1956)
9. S. V. MARKOVA, P. A. BAZHULIN, M. M. SUSHCHINSKII: OiS, 1, 41 (1956)
G. S. LANDSBERG, P. A. BAZHULIN, M. M. SUSHCHINSKII: Osnovnye parametry spektrov kombinatsionnogo rasseianiia uglevodorodov) (Fundamental parameters of Raman Spectra of Hydrocarbons) Akad. Nauk Press, Moscow, 1956
10. Fiziko khimicheskie svoistva individual'nykh uglevodorodov (Physical chemical properties of individual hydrocarbons), vol. 6. Gostop tekhizdat, Moscow, 1957
11. M. V. VOL'KENSHTEIN, M. A. EL'IASHEVICH, B. I. STEPANOV: Kolebaniia molekul (Vibrations of molecules) vol. 1, GITTL, Moscow 1949
12. W. G. BRAUN, D. F. SPOONER, M. R. FENSKE: Anal. Chem., 22, 1074 (1950)
M. R. FENSKE: Anal. Chem., 19, 700 (1947)

TOM VI, Vyp. 3 OPTIKA I SPEKTROSKOPIIA Mart , 1959
VOL.VI, No. 3 OPTICS AND SPECTROSCOPY March , 1959

On the Raman Spectra of Some Halogen Derivatives of Acetic Acid in Various Phases

I. D. POLIAKOVA AND SH. SH. RASKIN

Abstract: The Raman spectra of $CH_2BrCOOH$, CCl_3COOH and $CH_2ClCOOH$ in different phases were obtained. For $CH_2ClCOOH$ the spectra of all three polymorphic crystalline modifications were investigated.

Upon changing the phase, characteristic changes were found in the spectra, most clearly expressed in $CH_2BrCOOH$ and CCl_3COOH. These changes, on the whole, are evidently connected with changes in the association of the molecules under the phase conditions, and appear most distinctly in the carbonyl frequency region.

Earlier we studied Raman spectra of compounds with hydrogen bonding [1,2]. In this paper are set down data obtained at the same time on the Raman spectra of trichloroacetic, chloroacetic and bromoacetic acids in different phases. The results we obtained are presented in Table 1. The interpretation of these spectra and their changes upon phase transitions present some difficulties at the present time, although in recent years papers have appeared on the infrared spectra of these or analogous compounds in various phases and investigations have been carried out on the structure of the crystal lattices of like compounds. These investigations, to a certain extent, facilitate the problem of interpretation of the spectra we obtained and permit the possibility of making some suggestions concerning the nature of the peculiarities noticed.

Before passing to an analysis of the frequencies of intramolecular vibrations, we shall dwell for a very short time on the spectral frequencies

Table 1

Frequencies (in cm^{-1}) and Intensities (in brackets) of Raman Spectra.

CH_2 BrCOOH		CCl_3COOH				CH_2 ClCOOH			
			liquid			crystal			
				intensity at		melting point			
crystal	liquid	crystal	frequency	60 °C	160 °C	51 °C	56 °C	61 °C	liquid
30 (3)		16 (1)					18 (1/2)	17 (1/2)	
		30 (1 1/2)							
80 (2)		44 (1 1/2)				30 (7)	31 (2)	30 (1 1/2)	
		62 (2)				40 (2)	41 (1 1/2)	41 (1/2)	
142 (1/2)	193 (1)	81 (1/2)					52 (1/2)		
245 (1)	249 (1/2)	95 (1/2)				57 (1/2)	56 (1/2)		
369 (7)	368 (4)	110 (1 1/2)	105	(1)			63 (1/2)		
393 (1/2)		156 (1/2)				68 (1/2)	69 (2)	68 (1/2)	
	543 (5)	180 (1/2)				78 (1/2)	75 (1/2)	75 (1 1/2)	
558 (7)		199 (7)	193	(3)	(3)		81 (1/2)		
595 (1/2)		207 (1)	203	(3)	(2 1/2)	86 (1/2)	89 (3)		
	624 (4)	217 (1 1/2)	214	(1)	(1)	99 (7)		95 (1/2)	
	639 (2)								
651 (1/2)		284 (5)	280	(4)	(3 1/2)	106 (7)	101 (1/2)	117 (2)	
732 (5)	732 (5)		293	(1)	(1)	115 (1)	114 (1/2)	124 (1/2)	
	780 (2)	324 (4)	319	(3)	(3)		123 (1/2)		
900 (1/2)	893 (1)	429 (4)	435	(2)	(5)	130 (1/2)			
905 (1)	903 (3)	453 (6)	448	(5)	(3)	139 (1/2)			
						144 (3)	148—164 (?)		
	1106 (1/2)		665	(2)	(1)	170 (1)	186 (7)		
1153 (1/2)	1153 (1/2)	685 (6)	685	(3)	(1 1/2)	233 (1/2)	239 (1)	239 (1 1/2)	236 (1)
1196 (1/2)						260 (1/2)	265 (1)	267 (1)	269 (1/2)
	1219 (1)	834 (1 1/2)	832	(2)	(1)	273 (1)	286 (7)		
	1277 (1/2)	881 (1/2)	856	(1)	(1/2)	293 (1)	300 (7)		
1314 (1/2)		956 (1/2)	952	(1)	(1/2)		369 (7)	410 (2)	
1390 (1)	1390 (1)	1266 (1/2)				418 (5)	425 (3)	423 (2 1/2)	418 (3)
1443 (1/2)	1427 (1/2)		1408	(1/2)		434 (2)	436 (3)		
1648 (1/2)		1430 (1/2)	1427	(1/2)		558 (1/2)	558 (1/2)	558 (7)	588 (1/2)
	1668 (1/2)	1687 (1/2)	1688	(1)			628 (1/2)		
1698 (0)	1743 (1/2)		1762	(1)		652 (1/2)	658 (1)	662 (1/2)	644 (1)
	1778 (1/2)							684 (7)	680 (1)
						789 (7)	781 (7)	789 (5)	792 (5)
						912 (2)	907 (4)	914 (2)	908 (2)
						933 (1/2)	930 (1)	933 (1 1/2)	932 (1/2)
							1170 (2)	1170 (2 1/2)	
						1183 (7)	1191 (1)	1183 (2)	1185 (1 1/2)
						1205 (7)	1204 (1)	1208 (2)	
									1273 (1/2)
									1316 (1/2)
						1408 (2 1/2)	1395 (3)	1400 (2)	1404 (3)
							1415 (1)	1421 (2)	
						1435 (2 1/2)			1436 (1/2)
						1450 (1/2)			
						1870 (1/2)			1669 (1)
							1700 (1 1/2)	1690 (1/2)	
							1746 (2)	1736 (2)	1725 (1/2)

The sign } means that the given frequency (or frequencies) appeared in the spectrum in the form of bands.

of the crystal lattice.* In Table 1 are presented frequencies of the Raman spectra of crystalline CCl_3COOH, $CH_2BrCOOH$, and three polymorphic crystalline modifications of $CH_2ClCOOH$ with melting points of 51, 56, and 61°, and also the Raman spectra of these compounds in the liquid phase. Single crystals of these materials were grown by the method of the drawn off capillary.

From comparison of the Raman spectra of the compounds in crystal and liquid phases it is possible to determine approximately the region of the frequencies of the crystal lattice, the greater part of which region in the liquid phase spectra is occupied by the wings of the Rayleigh lines.

It is easy to see that the richest spectrum with respect to the number of lines is the 56° m. pt. modification, which contains more frequencies in the Raman spectrum in the low frequency region than the two other polymorphic modifications of chloroacetic acid with melting points of 61 and 51°. We shall note that some of the lines of small displacement in the crystals of bromoacetic and trichloroacetic acids are very close in value to frequencies of monochloroacetic acid. The small number of lines in this region of the spectrum of the crystal of bromoacetic acid may be explained by the high symmetry of the lattice of this crystal, which, according to the data in the literature, belongs to the hexagonal class.

It should be mentioned further, that, in the transition from the solid to the liquid phase in the spectra of trichloroacetic and bromoacetic acids, characteristic changes take place in the frequency region of intramolecular vibrations. The sharp lines of the crystals are broadened and diffused into bands, and in some of them background (often unsymmetrical) and satellites appear. Moreover, some lines vanish, frequency shifts appear, and, what is particularly important, in certain areas of these spectra the number of lines is increased. These characteristics are clearly and distinctly noticeable in the spectra of trichloroacetic and bromoacetic acids, and to a lesser extent are apparent in the spectrum of chloroacetic acid. Evidently, these phenomena are connected with those changes in the association of the molecules of these compounds which take place on melting. This is clearly obvious both from the change of values and from the change of number of carbonyl frequencies.

Before passing on to an analysis of the changes in the carbonyl frequency region in the spectra of these compounds, it is advisable to dwell on phenomena of a similar kind found by one of us and Sechkarev in the spectrum of benzoic acid [2], since for this compound both crystal structure [3] and infrared spectrum [4] are known.

The crystal lattice of C_6H_5COOH is constructed of centro-symmetric dimers, in which the molecules are united by hydrogen bonds (Space group C_{2h}^5; Z = 4). In Table 2 are presented the frequencies in the 1700 cm^{-1} region of the Raman spectra and infrared spectra of these compounds in different phases.

Table 2

C_6H_5COOH	Raman spectrum ($\Delta\nu$ cm^{-1})	Infrared spectrum (ν cm^{-1})
crystal	1637	1689; 1792
	t = 130 (in °C)	
liquid	1650(3); 1692(0); 1725(1)	1700
	t = 250 (in °C)	
	1656 (2); 1695(0); 1730(2)	—

In the Raman spectrum of the crystal is found one carbonyl frequency, as was expected for a centro-symmetric dimer. In the infrared spectrum two frequencies are found, but the authors never speak about the origin of the 1792 cm^{-1} frequency. Its origin is all the more mysterious, since it is not found in the infrared spectrum of the liquid. Another thing is important to us from this data Instead of the one carbonyl line in the Raman spectrum of the crystal, in the spectrum of the liquid are found three lines, of which the 1650 cm^{-1} [3] frequency, evidently, should be assigned to the dimer, since in the spectrum of the crystal where only the dimers are present, a line is found at 1637 cm^{-1}. As to the weak line at 1692 cm^{-1}(0), this is evidently the 1700 cm^{-1} frequency which is weak in the infrared spectrum, and forbidden in the Raman spectrum, but appears in the latter due to an infringement of the selection rules. The 1725 cm^{-1} line ought to be assigned to the monomer, since upon heating it becomes stronger, while at the same time the 1650 cm^{-1} frequency weakens. Furthermore, in the infrared spectrum in a dilute solution C_6H_5COOH in CCl_4, two frequencies are found, at 1698 and 1741 cm^{-1}, of which the first was assigned by the authors to the dimer, and the second to the monomer, which is in full agreement with our results and interpretation.

We shall pass on now to an analysis of the carbonyl frequencies in the spectra we investigated of the halogen derivatives of acetic acid. In the Raman spectrum of a crystal of CCl_3COOH, as is shown in Table 1, one frequency is found, at 1687 cm^{-1}, while in the spectrum of the liquid a band is found with two maxima, at 1688 and 1762 cm^{-1}. It seems to us that these data show, in accordance with the statements above, that the CCl_3COOH lattice is made up of centro-symmetrical dimers.

In that case it is obvious that the existence of one of the carbonyl band maxima with frequency at 1688 cm^{-1} in liquid CCl_3COOH is testimony to the fact that dimers are, at least partly, retained in the liquid state, since we assigned the 1687 cm^{-1} frequency in the Raman spectrum of the crystal to the dimer. For interpretation of the second maximum it is necessary to enlist the data of the infrared spectrum. In the spectra of CCl_3COOH in solid and liquid phases one frequency, at 1745 cm^{-1}, was observed [4], but in CCl_4 solution there are found two frequencies for CCl_3COOH, at 1745 and 1789 cm^{-1}. In this case the frequency of the second maximum of the carbonyl band at 1762 cm^{-1} in the Raman spectrum of liquid CCl_3COOH can be interpreted either as the 1745 cm^{-1} frequency of the infrared spectrum, forbidden in the Raman

* Spectra of the low frequencies (to 120 cm^{-1}) of chloro- and trichloroacetic acids were first obtained in 1940. At this stage in the work V.I. Val'kov took part.

spectrum and appearing as a result of infringement of the selection rules or as the frequency of the monomer. Resolution of the question might be found by study of the temperature dependence behaviour of the Raman spectrum. But, unfortunately, upon raising the temperature from 60 to 160° the entire background was strongly increased, and we were unsuccessful in finding the weak carbonyl band at 160° ± 1

Examination of the frequencies in the 1700 cm^{-1} region of the spectra we obtained for bromo- and chloroacetic acids shows characteristic peculiarities of these spectra. Thus, in the spectrum of crystalline bromoacetic acid there are two frequencies: a band at 1648 cm^{-1} (20 cm^{-1} wide) and a weak line at 1696 cm^{-1}.

In the spectra of polymorphic modifications of crystalline chloroacetic acid were found the following frequencies in this region: in the modification with melting point at 51°, a band at 1670 cm^{-1}; in the 56° m.p. modification, a band at 1700 cm^{-1}(1½) and a line at 1746 cm^{-1}(2); in the 61° modification a band at 1690 cm^{-1}(½), and a line at 1736 cm^{-1} (2). Consequently, for most of these cases, with the exception of the 51° melting point modification of crystalline chloroacetic acid, two frequencies are found in the spectra. These facts lead at once to the inference that if, in the case of the 51° melting modification it is possible to assume the presence in the crystal of dimeric association, then in the remaining cases it is not possible to assume this. It is natural to ask the cause of the two frequencies in the spectra of the crystals. The answer to this question, as offered to us, is prompted by data concerning the structure of crystalline formic acid [5]. In spite of the original suggestion, in the crystal lattice of this molecule, dimers do not form, but rather it is constructed of infinitely long chains. Each molecule is connected with two neighbors by hydrogen bonds. The space group is C_{2v}^{2} and Z=4.

In view of the demonstrated interaction of the carbonyl groups belonging to different molecules, and, the splitting of the frequencies (connected with this interaction), it is completely natural to suppose that in the same or a similar structure it is not possible for a single frequency to be displayed in the Raman spectrum.

Thus, judging from the spectra, only in the case of the 51° melting modification of chloroacetic acid can it be supposed that the lattice is built of dimers. Since in this spectrum the carbonyl frequency is found at 1670 cm^{-1}, while in the spectrum of liquid chloroacetic acid bands with maxima at 1669 cm^{-1}(1) and 1725 cm^{-1} (½), the dimers are retained in the liquid phase. As regards the origin of the second maximum, it most probably is due to the carbonyl group, active in the infrared spectrum, but appearing in the Raman spectrum by an infringement of the selection rules.

With respect to changes in other regions of the spectra of these compounds we shall mention that in the Raman spectrum of bromoacetic acid in the liquid phase new intense frequencies appear at 543 cm^{-1} (5) and a band with maxima at 624 (4) and 639 cm^{-1}(2). This leads to the thought that in some cases there take place in these compounds upon changes of phase not only changes in the association of the molecules, but also, possibly, changes of rotational isomers.

While examining the behaviour of the spectra under conditions of phase transitions we noted that in the Raman spectra, evidently, some carbonyl frequencies appear, which are forbidden in the Raman, but permitted in the infrared. Comparison of these frequencies allows the possibility of judging concerning the magnitude of splitting, which, in the case of benzoic acid, is 40-50 cm^{-1}. This splitting, as is well known, is the result of interaction of the carbonyl groups belonging to different molecules, connected by hydrogen bridges. In view of the comparatively weak bond it was considered that this splitting ought to be small [6,7].

In the calculation of the vibrational spectrum of the dimer of formic acid [7] the value of the splitting was obtained as 1-2 cm^{-1}. The author of the indicated work saw the explanation of the divergence between found and calculated values of the splitting in the fact that, at that time, the infrared spectrum had been taken on gaseous formic acid and the Raman spectrum on the liquid, which, in the opinion of the author, might be the cause of such a discrepancy. However our data were obtained for a single phase, and comparison of them with the results of a study of the infrared spectrum for the same phase, clearly shows the inadequacy of this explanation. As to the other explanations suggested in the same paper, the author himself considers them of little likelihood.

It is possible to surmise that similar splitting and appearance of forbidden frequencies in the Raman spectra might take place also for the OH frequencies. In this case this phenomenon, probably, might call attention to itself by the wide band of the hydrogen bond.

April 7, 1958

References

1. I. D. POLIAKOVA, SH. SH. RASKIN, A. V. SECHKAREV, F. I. SKRIPOV: IAN USSR, Fiz. ser., 14, No. 4, 419 (1950)
SH. SH. RASKIN, R. I. SKRIPOV: ZETF, 26, No. 4, 479 (1954)
2. SH. SH. RASKIN, A. V. SECHKAREV: DAN USSR, 86, No. 2, 277 (1952); 86, No. 3, 509-512, (1952) (See RT-3861, 9pp.)
3. G. SIM, J. ROBERTSON, T. GOODWIN: Acta. Cryst., 8, 157 (1955)
4. S. BRATOR, D. AADZI, N. SHEPPARD: Spectrochim. Acta, 8, 249 (1956)
5. F. HOLTZBERG, B. POST, I. FRANKUCHEN: Acta Cryst., 6, 127 (1953)
6. K. W. F. KOHLRAUSCH: Ramanspektren, Leipzig, 1943 (IL, Moscow, 1952, p. 227)
7. L. M. SVERDLOV: IAN USSR, Fiz. ser., 17, 567 (1953)

TOM VI, Vyp. 3 OPTIKA I SPEKTROSKOPIIA Mart, 1959
VOL. VI, No. 3 OPTICS AND SPECTROSCOPY March, 1959

Solvent Effects on the Electronic Absorption Spectra of Benzene and Chlorobenzene

O. V. SVERDLOVA

Abstract: We investigated the displacements of the absorption bands of benzene and chlorobenzene in the region from 2500-2700 Å in a great number of solvents of different character and made an attempt to systematize and explain qualitatively the influence of the solvent in various cases.

For the present work benzene was chosen for investigation because its molecule is neutral and nonpolar, it is easily soluble in the majority of organic solvents and it has absorption bands in the near ultraviolet which are sufficiently narrow so that their shifts can be observed without interference by other changes in the spectrum. The work with chlorobenzene allows us to learn about the role of a substituent and the resulting dipole moment in the interaction between the absorbing substance and the solvent.

DESCRIPTION OF THE EXPERIMENT

The spectra were obtained with an ISP-22 quartz spectograph. A GSVD-120 Krypton lamp served as a light source. The spectra were measured in the usual manner with a MF - 2 microphotometer. The location of the absorption bands was determined in relation to the mercury lines at 2537 and 2480 Å, emitted by the lamp.

No.	Solvent	Dielectric constant	Refractive index at λ = 2500Å
1	N-hexane	1.85	1.433
2	Cyclopentane		1.484
3	Freon 113	1.84	
4	Methanol	35.7	1.371
5	Ethanol	26.8	1.410
6	Acetone	21.5	1.414
7	Water	81	1.379
8	CCl_4	2.12	1.55
9	Chloroform	5.14	1.522
10	Benzene	2.27	1.665
11	Chlorobenzene	10.35	1.675
12	Butanol	19.2	1.446
13	Ethylene glycol	41.2	1.487
14	Glycerin	56.2	1.526
15	Perfluoroheptane		1.270
16	N-heptane		1.45
17	Furan		1.25
18	Carbon disulfide		2.06
19	Acrylonitrile		1.555
20	Trichlorethylene	3.42	1.605
21	Caproic acid		1.475
22	Butyric acid		1.43
23	Acetic acid		1.475
24	PCl_3	3.72	1.64
25	Cyclohexene		1.5388
26	Butyl chloride		1.44
27	Cyclohexyl chloride		1.52

We investigated solutions of constant volume concentration (1% in the absorbing material). It has been shown previously that further dilution does not affect the spectrum of benzene [1].

Characteristic properties of the used solvents are given in the table. The values for the refractive indices at the wavelength of the absorbed light were taken basically from the literature [2].

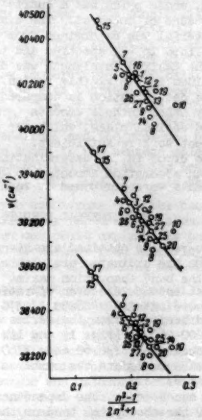

Figure 1. Dependence of the positions of the absorption bands of benzene on $\frac{n^2-1}{2n^2+1}$ for the solvent.

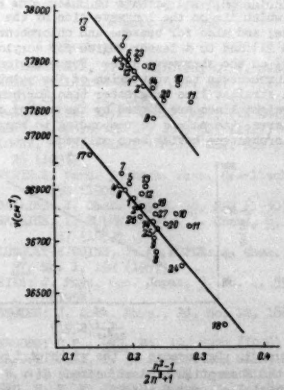

Figure 2. Dependence of the positions of the absorption bands of chlorobenzene on $\frac{n^2-1}{2n^2+1}$ for the solvent.

For substances for which such constants were not available (trichlorethylene, butyl chloride, cyclohexyl chloride, acrylonitrile, acetic, butyric, caproic acid) the refractive index in the region of 2500-2700 Å was determined by means of a liquid prism. For this purpose the spectrum of an iron arc or a mercury lamp was photographed using a spectrograph, whose prism was a quartz cell filled with the substance of interest. The dispersion of the prism material was determined from the separation between lines in the spectrum and the refractive index at the desired wavelength was determined using known values in the visible region. The accuracy of such a determination as compared with values obtained by other methods amounts to a few units of the third decimal place, which for the purpose of the present work is sufficient.

The error in the determination of the position of an absorption amounted to 10-15 cm^{-1}. The measurements were performed at room temperature.

EXPERIMENTAL RESULTS

The results obtained are given in Figures 1 and 2. On the ordinates are plotted the wave numbers of the band absorption maxima ν (cm^{-1}). The three most intense electron vibrational bands of benzene were examined (38250, 39170 and 40115 cm^{-1} in liquid benzene) from the series of bands in the region 2200-2600 Å (Fig. 1) and likewise the bands of chlorobenzene at 36760 and 37760 cm^{-1} (Fig. 2). The numerals designate the number of the solvent in the table.

As can be seen, the dependence of the wave number of the absorption band on the value of $\frac{n^2-1}{2n^2+1}$ for the solvent can be expressed by a straight line, the deviations from which are apparently random and within experimental error, except for points corresponding to carbon tetrachloride [8]* and perhaps to chloroform [9], both of which lie on the longwave side of the straight line; and also for benzene and chlorobenzene [10 and 11] and to a lesser degree for acrylonitrile [19] on the shortwave side. For solutions of chlorobenzene the scattering of the points around the straight line is greater than for benzene. The straight lines are fitted by the method of least squares, the points corresponding to benzene and chlorobenzene having been omitted.

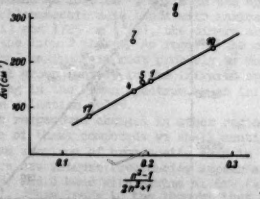

Figure 3. Dependence of the width at $D = \frac{3}{4} D_{max}$ of the absorption band of benzene at $\nu = 38250$ cm^{-1} on $\frac{n^2+1}{2n^2+1}$ for the solvent.

* The numbers in italics in the brackets correspond to the number of the solvent in the table.

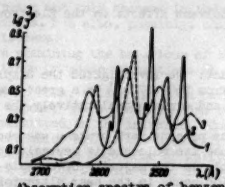

Figure 4. Absorption spectra of benzene solutions. 1 - in furan, 2 - in n-hexane, 3 - in carbon tetrachloride.

Together with the displacement there is observed a change of the width of absorption bands with increase of the refractive index of the solvent. For a series of solvents Figure 3 shows the dependence of the width $\Delta\nu$ of a band of benzene at $D = \frac{3}{4} D_{max}$. (D - the optical density of the solution) on $\frac{n^2-1}{2n^2+1}$ of the solvent: with the increase of the refractive index of the solvent there is an increase in the width of the bands.

Figure 4 shows the absorption of solutions of benzene in furan, hexane and carbon tetrachloride. One should note that in furan the band width becomes smaller so that each is resolved into two components corresponding to two most intense lines in the spectrum of benzene vapor.

DISCUSSION

The action of the solvent on the absorbing molecule can manifest itself in two ways: either a small number of molecules of the solvent forms with it a more or less stable complex of a definite structure, or a larger number of molecules of the solvent is influenced so that one can speak of the action of a continuous surrounding medium. An effect of the second type seems more probable for solutions of benzene because of its relative chemical inertness and nonpolarity.

The displacement of the electron absorption bands in solution relative to their location in vapor state, as a function of the polarizability of the solvent, is considered differently by various authors [3-5]. Thus Bayliss [3] assumed the solvent to be a continuous medium and considered the influence of this medium on the processes of light absorption and obtained a linear dependence of the displacement on the value of $f\left(\frac{n^2-1}{2n^2+1}\right)$, for the solvent, where n denotes the refractive index, and f the oscillator strength of the electronic transition. In later papers, e.g., that of Ooshika [5], more complex formulas are given, connecting the band displacement with the magnitude of the refractive index and the dielectric constant of the solvent, with the magnitude of the dipole moment of the molecule in the ground and excited states, and with the absorption coefficient.

Since in the case of benzene - a nonpolar molecule - the formula of Ooshika nearly reduces to the formula of Bayliss, we limit ourselves to an investigation of the dependence of the displacement on $\frac{n^2-1}{2n^2+1}$ i.e., we shall not consider f, considering that there is a smooth dependence of f on n.

The linearity of this dependence for benzene and chlorobenzene solutions confirms that here the role of the solvent is predominantly that of a continuous polarizing medium. The departures from linearity could be caused by some additional interaction between the molecules of the solvent and the solute.

The fact that for chlorobenzene fewer points lie on a straight line than for benzene can be explained by the interaction of the chlorobenzene dipole with individual molecules of the solvent. The frequency change occurs because the strength of this interaction is not the same in the ground and in the excited states. The deviation from linearity is not large (20 - 50 $cm.^{-1}$); it follows that the change of the dipole moment of the chlorobenzene molecule with its excitation is small and that the magnitude of dipole - dipole or dipole - polarization interaction changes little.

In figure 1 the largest deviation is seen for benzene itself (150 $cm.^{-1}$). Although it is impossible to determine a precise value of the index of refraction for benzene in the region of the absorption band (it was figured out by a graphical extrapolation from λ = 2700 Å), it can be assumed that there is no anomalous decrease within the band by which such a deviation could be explained; since, first, the dispersion curve for benzene is determined mainly by a more intense band - around 2000 Å, and secondly, the same effect is observed, as can be seen in Figure 2, not only for the pure chlorobenzene, but also for the solutions of chlorobenzene in benzene; and the index of refraction of benzene has been measured in the vicinity of the chlorobenzene absorption.

Benzene is characterized by special mobility of the π-electrons caused by the presence of three conjugated double bonds. One can apparently assume from the abnormal shift of absorption bands of the pure benzene that there is an interaction between the π-electrons of different molecules. The existence of complexes of benzene molecules, bonded by π-electrons of neighboring molecules, has been assumed by a number of authors to explain various experimental results [6, 7, 10]. No theory exists which could quantitatively explore such an assumption. Qualitatively, one can verify it with various solvents containing π-electrons. Among such solvents we used acetone, benzene, chlorobenzene, trichloroethylene, carbon disulfide, cyclohexene and acrylonitrile. Figures 1 and 2 show that only acrylonitrile gives a deviation from the straight line to the same side as pure benzene and chlorobenzene, but to a lesser degree. Like benzene and chlorobenzene, acrylonitrile has conjugated double bonds. It is possible that for the formation of π-electron complexes such conjugation is necessary.

The deviation from linearity to the longwave side, observed for solutions of benzene and chlorobenzene in CCl_4, can also be explained by the presence of specific interactions with CCl_4 molecules. This is confirmed by the change of band contour of benzene and chlorobenzene in CCl_4 solution. In Figure 4, along with the shift and broadening of the bands on going to carbontetrachloride solution is observed a redistribution of intensity. A shoulder appears in the region of 2650 Å, approximately corresponding to the position of the 0 - 0 band (taking account of the polarization shift) which is forbidden in benzene vapor. The possibility of existence of complexes of benzene with CCl_4 is mentioned in literature. Thus Kapustinskii and Drakin [8] investigated phase diagrams of binary mixtures and showed that at low temperatures there exist stable compounds of benzene with tetrahalogenomethanes especially with CCl_4. The cause for their formation is assumed to be the unsaturated character of halides in the tetrahalides and the presence of three resonating double bonds in the benzene molecule.

Rao and Jatkar [9] consider the benzene complexes with CCl_4, $CHCl_3$ and CH_2Cl_2 to be of the donor-acceptor type and assume that the benzene molecule is polarized by the chlorine atom. From this point of view one could explain the phenomenon. The fact that the deviations from linearity for solutions in CCl_4 appear on the long wave side can be explained by the fact that the probability for a complex formation is greater for excited benzene molecules because of their greater polarizability with respect to the ground state.

Thus one can assume that the influence of the solvent on the location of electronic absorption bands of benzene and chlorobenzene is mainly a polarization shift i.e. each molecule of the absorbing substance is acted upon at the same time by a large number of solvent molecules. The formation of localized bonds between the molecules of the solvent and the absorbing substance appears as a larger or smaller deviation from the general behavior.

I am deeply grateful to V. M. Chulanovskii under whose guidance this work was performed.

August 23, 1958

References

1. V. M. CHULANOVSKII, T. G. MEISTER, O. V. SVERDLOVA: Vestnik, Leningrad Univ., Ser. mat., fiz., khim., vol. 10, No. 8, 123 (1955)
2. LANDOLT-BORNSTEIN: Phys. Chem. Tab., 5th Ed., 1923; H. VOELLMY: Z. phys. Chem., 127, 305 (1927) T. M. LOWRY, C. B. ALLSOPP: Proc. Roy. Soc., A133, 26 (1931) F. F. MARTENS: Verh. Deutsch. Phys. Gesellsch., 3, 150 (1902)
3. N. S. BAYLISS: J. Chem. Phys., 18, 292 (1950) N. S. BAYLISS, L. HULME: Austr. J. Chem., 6, No. 3, 257 (1953)
4. H. C. LONGUET-HIGGINS, J. A. POPLE: J. Chem. Phys., 27, No. 1, 192 (1957)
5. Y. OOSHIKA: J. Phys. Soc. Japan, 9, No. 4, 594 (1954)
6. K. E. SHULER: J. Chem. Phys., 20, No. 12, 1865 (1952)
7. B. OKSENGORN: C.R., 242, No. 19, 2324 (1956)
8. A. F. KAPUSTINSKII, S. I. DRAKIN: IAN USSR, OKhN, No. 5, 435 (1947) (See R-563 from RIS)
9. N. S. RAO, S. K. K. JATKAR: Quart. J. Ind. Inst. Sci., 5, 65 (1942); 6, 1 (1943)
10. F. F. CHESHKO: ZFKh., 31, No. 10, 2260 (1957)

TOM VI, Vyp. 3 OPTIKA I SPEKTROSKOPIIA Mart, 1959
VOL. VI, No. 3 OPTICS AND SPECTROSCOPY March, 1959

The Absorption and Luminescence Spectra of Solutions of some Substituted Polyenes.

by

A.N. NIKITIN, M.D. GALANIN, G.S. TER-SARKISIAN and B.M. MIKHAĬLOV.

Abstract. The electronic absorption spectra of solutions of 18 substituted butadienes and hexatrienes in heptane, and also the luminescence spectra of these substances in heptane and in benzene, have been studied. The oscillator strengths for the long-wave length electronic transitions have been evaluated and the quantum yields for luminescence determined. It has been shown that the change in the spectra and in the intensity of absorption depends on the extent to which the system of conjugated double bonds is distorted out of plane. It has been found that the luminescence quantum yield of some compounds is higher in benzene solutions than in hexane, and that the reverse is true of others. The change in lifetime τ of the excited state has been measured, and used to show that the drop in quantum yield from 1,1.4,4 tetraphenyl-butadiene-1.3 in benzene solution occurs for the most part because of quenching by collisions of the second kind. But the change in τ of 1,6-diphenylhexatriene-1,3,5, cannot be explained in this way.

Some of the substituted polyenes, notably aryl butadienes and hexatrienes, are widely used as scintillators (in liquid solutions, solid plastics etc.). However a sufficiently full and detailed examination of the spectra has been carried out only for polyenes of the type $C_6H_5-(CH=CH)_n-C_6H_5$, where n = 1,..,7 [1,2]. There are few data on the absorption and emission spectra of other substituted polyenes [3-6]. We have investigated the absorption and luminescence spectra of the following substituted butadienes and hexatrienes: 1,4-diphenylbutadiene-1,3 (trans-trans) (I) ; 1,4-diphenyl-1-methylbutadiene-1,3 (2,5-diphenylpentadiene-2,4) (II) ; 1-phenyl-4-n-tolylbutadiene-1,3 (III); 1,1,4-triphenylbutadiene-1,3 (IV); 1,1,4-triphenyl-3-methylbutadiene-1,3 (V); 1,1,2 triphenylbutadiene-1,3 (VI) ; 1,1,4,4-tetraphenylbutadiene-1,3 (VII); 1,1,4,4-tetraphenyl-2,3-dimethylbutadiene-1,3 (VIII); 1-phenyl-4-(2-pyridyl) butadiene-1,3(IX); 1-phenyl-4-(2-quinolyl)butadiene-1,3 (X); 1,6-diphenylhexatriene-1,3,5 (all trans) (XI); 1-phenyl-6-n-tolylhexatriene-1,3,5 (XII); 1,6-diphenyl-5-methylhexatriene-1,3,5 (XIII); 1,6-diphenyl-4,5-dimethylhexatriene-1,3,5 (XIV); 1,5-diphenyl-4-methylhexatriene-1,3,5 (XV); 1,5-diphenyl-6-(2-pyridyl) hexatriene-1,3,5 (XVI); 1-phenyl-4,5-dimethyl-6-(2-pyridyl)hexatriene-1,3,5 (XVII); 1-phenyl-4,5-dimethyl-6-(2-quinolyl)hexatriene-1,3,5 (XVIII).

Compounds II, III, V, VIII and XII-XVII were obtained for the first time [7]* There are data in the literature on the absorption spectra of solutions of compounds I [1,3-6,8], IV [9], VII [3], IX [3], X [6], XI [1,6], and on the luminescence spectra of solutions of I, XI[1] and VII [5].

We have measured the absorption spectra of all the listed compounds in heptane, and also the luminescence spectra in the visible region. We have also determined the relative intensities in heptane and benzene of the total integrated (visible and ultra violet) luminescence. Also absorption spectra of compounds VII and XI were obtained in benzene and the luminescence of these substances was studied in a mixture of heptane and benzene (50-50). The lifetimes of the excited states of these two compounds were also studied in benzene, heptane, and in a mixture of the two. From the absorption spectra the oscillator strengths f of the long wavelength electronic transitions were calculated. From the luminescence data the quantum yields of emission were determined. Models were constructed to aid the structural study of the molecules.

*Compounds II and XII were synthesized by L.S. Povarov, and VIII by A.N. Hlokhina.

EXPERIMENTAL

The absorption spectra were measured with a SF-4 spectrometer. The luminescence spectra in the visible region were measured using a set-up consisting of a UM-2 monochromator and FEU-19 photomultiplier of calibrated spectral sensitivity. For the solutions emitting in the visible region, the quantum yield was obtained by comparison with a solution of fluorescein. The relative quantum yields of solutions whose luminescence extends into the near ultraviolet were estimated by numerically integrating the curves recorded using the FEU-19 photomultiplier. The absolute quantum yields of these solutions were obtained by comparison of the data with those obtained by spectrophotometric determinations on fluorescein in the visible region. The measurements of τ were obtained using a phase fluorometer [10].

Oscillator strengths were calculated using the expression

$$f = 1.29 \times 10^{-8} \int \epsilon(\nu) d\nu,$$

where ϵ is the molar extinction coefficient and ν is wave number.

The models were made from Stuart-Briegleb models. The compounds were all purified by chromatography on Al_2O_3 columns.

RESULTS

The results obtained are summarized in tables 1 and 2, and the absorption spectra of the substituted butadienes and hexatrienes are given in Figures 1-8.

Absorption. Almost all the substances investigated show two electronic transitions in the region 2200-4000 A, that at the longer wavelength being the more intense of the two. The long wavelength transition is the more sensitive to structural changes in the molecule. In both the butadiene and the hexatriene series the highest absorption intensity is found in molecules with the greatest extent of planarity in the double bonded system. The introduction of substituents along the polyene chain hinders planarity sterically. The result is a corresponding decrease in absorption intensity, and a shift in the spectrum to shorter wavelengths.

In compound II the CH_3 group interferes with the phenyl group (in the geometrical model the overlap between the two groups is about 0.5 A), which results in the twisting of the phenyl group out of the plane of the conjugated system. In the

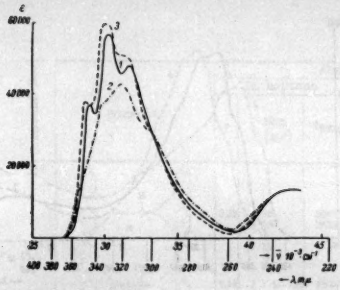

Figure 1 In heptane

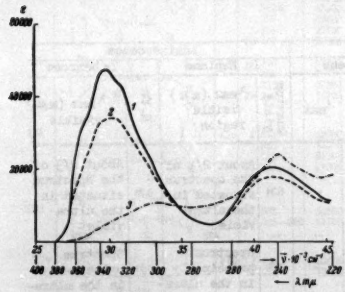

Figure 2 In heptane

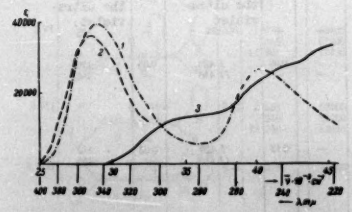

Figure 3 1-In heptane VII; 2-VII In Benzene; 3-VIII In heptane

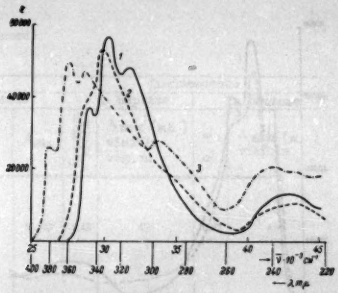

Figure 4 In heptane

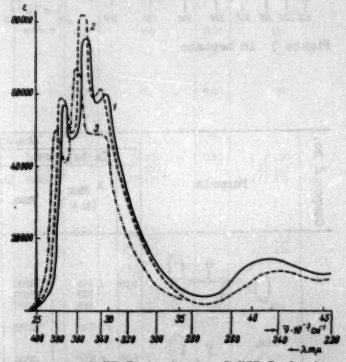

Figure 5 1-XI In heptane; 2-XII In heptane; 3-XI In benzene

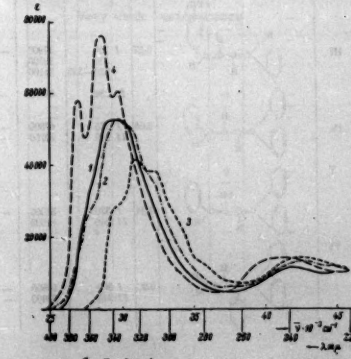

Figure 6 In heptane

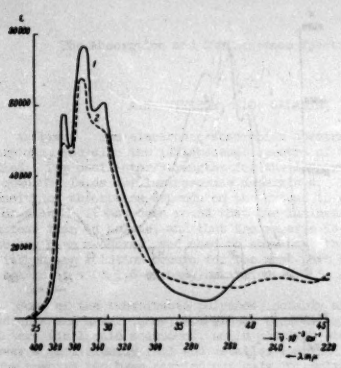

Figure 7 In heptane

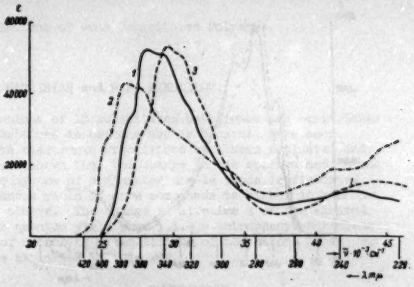

Figure 8 In heptane

Table 1

Compound No.	Formula	Absorption						Luminescence			
		In heptane			In benzene			In heptane		In benzene	
		f	λ Max (mμ)	ε max	f	λ Max (mμ)	ε max	Quantum yield	λ max (mμ) visible region	Q.Y.	λ max (mμ) visible
I	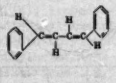	3.39	I 345 330 315	36900 56800 48300	—	—	—	0.31	About 2/3 of the spectrum situated in the ultra-violet	0.28	About 2/3 of the spectrum situated in the ultra-violet
			II 240	12000	—	—	—	—	425	—	425
II	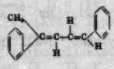	3.00	I 320 II 235	43000 13340	—	—	—	0.03	Spectrum principally in the ultra-violet	0.02	Spectrum principally in the ultra-violet
III	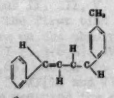	3.57	I 350 330 320—325	37900 59700 51100	—	—	—	0.38	About 2/3 of the spectrum situated in the ultra-violet	0.29	About 2/3 of the spectrum situated in the ultra-violet
			II 230	13100	—	—	—	—	425	—	425
IV	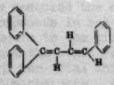	3.06	I 335 II 240	47800 20200	— —	— —	— —	0.06 —	I 420 II 440	0.05 —	420 440
V	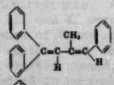	2.34	I 330 II 240	34000 17600	—	—	—	0.13	I 420 II 440	0.06	420 440
VI	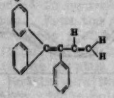	0.90	I 300 II 240	10900 23900	— —	— —	— —	0 —	— —	0 —	— —

Table 1 (continued)

Compound No.	Formula	Absorption: In heptane: f	Absorption: In heptane: λ_{Max} (mμ)	Absorption: In heptane: ε_{max}	Absorption: In benzene: f	Absorption: In benzene: λ_{Max} (mμ)	Absorption: In benzene: ε_{max}	Luminescence: In heptane: Quantum yield	Luminescence: In heptane: λ_{max} (mμ) visible region	Luminescence: In benzene: Q. Y.	Luminescence: In benzene: λ_{max} (mμ) visible
VII	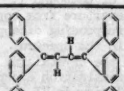	2.58	*I* 345 *II* 250	39100 26300	2.35 —	*I* 1.350 —	36200 —	0.43 —	450 —	0.07 —	450 —
VIII	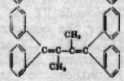	1.14	*I* 275—285 *II* 240	16000 26500	— —	— —	— —	0 —	— —	0 —	— —
IX	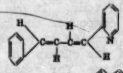	3.6	*I* 332.5 350 *II* 235	53200 37300 10200	— —	— —	— —	0.01 —	450 —	0.01 —	450 —
X	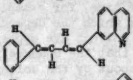	4.11	*I* 380 362.5 350 295 *II* 240	26000 49500 46800 27700 20400	— —	— —	— —	0.01 —	430 —	0.02 —	430 —
XI	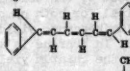	3.96	*I* 370 350 335 *II* 240	57600 76200 60200 14700	3.60 —	*I* 380 360 340—345	50000 67500 49500	0.32	*I* 425 *II* 450 *III* 475	0.62	*I* 430 *II* 455 *III* 475
XII	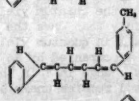	4.29	*I* 375 355 340 *II* 240	59000 82500 61200 11000	— —	— —	— —	0.36 —	*I* 430 *II* 455 *III* 475 —	0.65 —	*I* 430 *II* 455 *III* 475 —
XIII	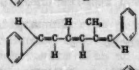	3.57	*I* 335 *II* 235—240	52500 11700	— —	— —	— —	0.06 —	450 —	0.02 —	450 —
XIV	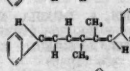	3.60	*I* 335 *II* 235	52800 13100	— —	— —	— —	0.01 —	— —	— —	— —
XV	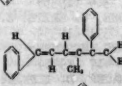	2.88	*I* 320—325 310—315 *II* 235	41500 38200 14300	— — —	— — —	— — —	Very weak luminescence —	— —	— —	— —
XVI	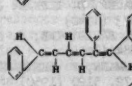	3.81	*I* 370 355 *II* 235	49400 67200 11200	— — —	— — —	— — —	0 — —	— — —	0 — —	— — —
XVII	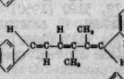	3.78	*I* 355 340 *II* 240	52400 51200 12450	— — —	— — —	— — —	0 — —	— — —	0 — —	— — —
XVIII	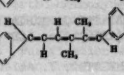	4.29	*I* 375	42900	—	—	—	0	—	—	—

Table 2

Quantum yields and lifetimes of the excited state for solutions of compounds VII and XI in heptane, in benzene, and in a 50% mixture of the two.

Compound No.	Formula	Quantum yield			10^{-9} sec.		
		In heptane	In heptane benzene mixture	In benzene	In heptane	In heptane benzene mixture	In benzene
VII	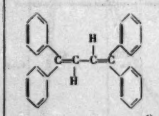	0.43	0.13	0.07	2.5	1.0	0.7
IX	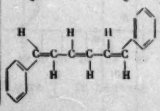	0.32	0.34	0.65	7.1	6.6	5.6

spectrum of this substance as compared with the spectrum of compound I there is observed a decrease in f and a small shift of the absorption maximum to shorter wavelengths. In compound VII, as is well known [11], the phenyl groups are inclined to each other at an angle of about 30°. For this reason, in spite of the increase in the size of the conjugated system, which results in a small shift of the spectrum to long wavelengths, the intensity is nevertheless significantly diminished. There is a similar situation in compounds IV, V and VI, which also have a phenyl group in position 1, and in VIII, where the phenyl group in position 4 is similarly situated. In compound V, the CH_3 group provides an additional steric factor when compared with IV. Because of the interference between this group and the phenyl group in position 4 (the overlap between the two groups is about 1.4 A), the phenyl group is forced out of the plane of the conjugated system. Furthermore, as a result of the overlap of the CH_3 group with the phenyl group in position 1, there is the possibility of rotation of one of the double bonds in the butadiene chain with respect to the other. In the spectrum of this substance, when compared with IV we see a decrease in the f value and a shift in the absorption maximum to shorter wavelengths. In compound V as compared with IV there is an additional steric factor. The phenyl group in position 2 overlaps the hydrogen atom in position 4 (overlap about 1.7 Å). As a result of this, the group in position 2 is significantly rotated with respect to the plane of the butadiene chain. The absorption intensity in this compound is very low and the maximum is shifted to short wavelengths. In compound VIII the CH_3 group distorts the butadiene chain so much that the double bonds are almost at right angles to each other. In this compound too, the f value is very low, and the spectrum is shifted markedly toward the u.v. In the hexatriene XIII, as in V, the methyl group produces steric hindrance, this time with the phenyl group in position 6, and its spectrum, when compared with XI shows corresponding changes. But the second CH_3 group in compound XIV cannot produce an additional distortion when compared with XIII. As may be seen from Fig. 1 and Table 1, the spectra of these two substances are almost identical. In compound XV, as in V, the phenyl group in position 5 interferes with the hydrogen in position 6. The introduction of a tolyl group instead of a phenyl in compounds III and XII leads to an intensity increase in absorption and a shift to long wavelengths. The quinonyl group (Compound X) results in a greater shift than does the pyridyl group in IX when the absorption spectra are compared with that of compound I. It should be noted that as the departure from coplanarity increases there is a corresponding disappearance of vibrational structure in the spectra.

Luminescence. In the crystalline state all the compounds under investigation except VIII and XVI are luminescent. Compounds VI, XI, and XII luminesce very weakly. For the compounds with the lowest f values (VI, VIII, XIII, XIV and XV) and those with a pyridyl or quinonyl substituent (IX, X, XVI, XVII and XVIII) luminescence is absent or negligibly small in solutions. It has also been observed that for some compounds the quantum yield of the luminescence is greater in benzene solution than in heptane, whilst for others the reverse is the case. At the same time, for example in compounds VII and XI, for which the dependence of quantum yields on the solvent are opposite to each other, it may be seen that the changes in absorption spectra brought about by the solvents (heptane and benzene) are identical for both compounds.

The decrease in luminescence yield for the solution of compound VII in benzene is accompanied by a decrease in τ, but the quantum yield obviously falls off more rapidly than does the lifetime. For compound XI the fall in quantum yield in heptane, on the other hand, is accompanied by an increase in τ. The reason for the change in τ in this case cannot be quenching, and remains unexplained.

January 16, 1958

References

1. K. W. HAUSSER, R. KUHN, A. SMAKULA, K. H. KREUCHEN: Z. f. phys. Chem., B 29, 363 (1935)
   K. W. HAUSSER, R. KUHN, A. SMAKULA: Z. f. phys. Chem., B 29, 384 (1935)
   K. W. HAUSSER, R. KUHN, G. SEITZ: Z. f. phys. Chem., B 29, 391 (1935)
   K. W. HAUSSER, R. KUHN, E. KUHN: Z. f. phys. Chem., B 29, 417 (1935)
2. G. N. LEWIS, T. T. MAGER, D. LIPKIN: J. Am. Chem. Soc., 62, 2973 (1940)
3. K. B. ALBERMAN, R. N. HASZELDINE, F. B. KIPPING: J. Chem. Soc., 3284 (1952)
4. Y. HIRSHBERG, E. BERGMANN, F. BERGMANN: J. Am. Chem. Soc., 72, 5120 (1950)
5. Y. HIRSHBERG, E. BERGMANN, F. BERGMANN: J. Am. Chem. Soc., 72, 5117 (1950)
6. C. COMPTON, W. BERGMANN: J. Org. Chem., 12, 363 (1947)
7. B. M. MIKHAILOV, G. S. TER-SARKISIAN: IAN USSR, OKhN, 1079, 1448 (1956) (See CB translation Bulletin)
8. A. SANDOVAL, Z. ZECHMEISTER: J. Am. Chem. Soc., 69, 553 (1947)
9. S. ISRAELASHVILI, F. BERGMANN: J. Chem. Soc., 1070 (1953)
10. M. D. GALANIN: DAN USSR, 73, 925-927 (1950) (See RT-488, 5 pp.)
11. G. E. COATES, L. E. SUTTON: J. Chem. Soc., 567 (1942)

TOM VI, Vyp. 3 OPTIKA I SPEKTROSKOPIIA Mart, 1959
VOL. VI, No. 3 OPTICS AND SPECTROSCOPY March, 1959

The Luminescence of Ortho-disubstituted Aromatic Hydrocarbons

1. The Absorption and Fluorescence Spectra of the Anilides of Salicylic and O-Methoxybenzoic Acids.

by

IU. V. NABOIKIN, E. N. PAVLOVA AND B. A. ZABOROZHNYI

Abstract: By means of a comparative study of the u.v. and i. r. absorption spectra, and the fluorescence spectra of the anilides of salicylaldehyde and o-methoxybenzoic acids, it has been shown that the large shift to longer wavelengths of the fluorescence spectrum of the former is a result of the formation of an intramolecular hydrogen bond.

It is well known that ortho-disubstituted aromatic hydrocarbons show a number of peculiarities which result from the interaction of the two closely placed funtional groups. There have been a great many publications devoted to the study of the absorption spectra of substances with ortho-substituents. The effect of orthosubstitution on fluorescence spectra remains almost uninvestigated. Only recently there have appeared a few papers by Weller on the fluorescence spectrum of salicylic acid and some of its derivatives [1,2]. It was shown that a hydroxyl group in the ortho position to carboxyl results in an anomalously large shift in the fluorescence spectrum to long wavelengths. This was explained as due to a shift of the hydroxyl proton to the carbonyl group in the excited state.

In the present work the absorption and fluorescence spectra of the anilides of salicylic and o-methoxybenzoic acid have been studied.

The u.v. absorption spectra were obtained using a SF-4 spectrophotometer. For the infrared absorption an IKS-11 spectrometer with a lithium fluoride prism was used. The fluorescence spectra were obtained on a UM-2 monochromator with an FEU-17 photomultiplier.

To excite the fluorescence a PRK-4 lamp fed from a stabilized source was used. The U.V. part of the spectrum was isolated by means of a UFS-3 filter, and also by using a combination of liquid filters. The optical system and sample arrangement were such that photometric measurements could be made. The reproducibility of some of the fluorescence spectra was checked on the ISP-51 spectrograph. The pH was determined using a glass electrode instrument, without taking account of activity coefficients.

The compounds investigated were synthesized by condensing salicylaldehyde and o-methoxybenzoic acid with aniline. The anilide of ortho-methoxybenzoic acid was also obtained by methylating the anilide of salicylic acid. The two preparations were identical. Purification was by repeated crystallization from various solvents. The melting points were in agreement with those of other authors, and purification was continued until the absorption and luminescence spectra ceased to change.

The structural formulae of these substances given below show that for the anilide of salicylic acid (I) an intramolecular hydrogen bond is possible, while for that of methoxybenzoic acid it is not (II).

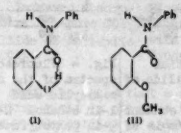

(I) (II)

The absorption spectra in various solvents are shown in Figures 1 and 2, and in Figure 3 are given the changes in the absorption spectrum of the anilide of salicylic acid as the concentration of alkali in the solution is varied. The latter shows that there is an increase in the intensity of the peak at 340 mμ as the concentration of alkali is increased. The spectrum of the anilide of O-methoxybenzoic acid, however, is almost unchanged by the addition of alcoholic NaOH.

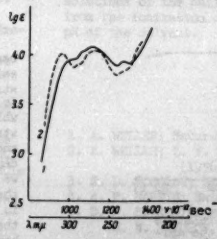

Fig. 1 The absorption spectrum of the anilide of salicylic acid.
1-in ethanol 2-in heptane

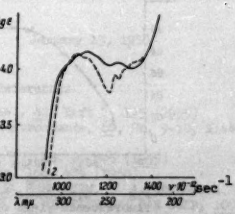

Fig. 2 The absorption spectrum of the anilide of salicylic acid.

In Figure 4 are shown fluorescence spectra of the anilide of salicylic acid in various solvents. The peculiarity of the luminescence of this substance is that it is strongly dependent on the nature of the solvent. In non-hydroxylic solvents there is an anomalously large Stokes (long-wave) shift, and the fluorescence maximum is at 470 mμ. In methyl, ethyl and butyl alcohols, the long wavelength band disappears and is replaced by one with maximum about 420 mμ. In methanol the intensity of this band is several times greater

than in ethanol and butanol. On increasing the pH of an alcoholic NaOH solution of the anilide of salicylic acid the intensity of the 420 mμ band increases.

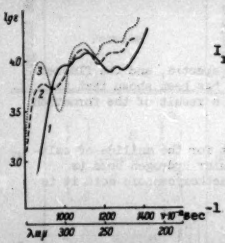

Fig. 3 The absorption spectrum of the anilide of salicylic acid.
1-in ethanol 2-in ethanol containing 5 moles/mole of NaOH, 3-in ethanol with 10 moles/mole of NaOH

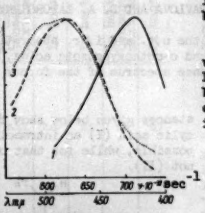

Fig. 4 Fluorescence spectra of the anilide of salicylic acid
1-in ethanol 2-in heptane 3-in polystyrene

In Figure 5 is shown the dependence on pH of the relative fluorescence yield of ethanolic NaOH solutions of the anilide of salicylic acid. If a drop of dilute H_2SO_4 is added to a solution of the anilide in ethanol, a blue green fluorescence is observed. From Figure 5 it may be seen that the fluorescence yield in the 420 mμ band is lowest at pH around 7.65.

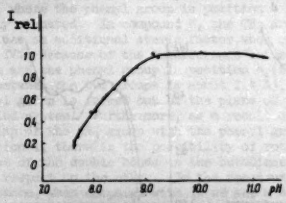

Fig. 5 Dependence of relative fluorescence yield of the anilide of salicylic acid in ethanol on pH.

If we add ethanol gradually to a benzene solution of the anilide of salicylic acid, the blue-green luminescence is quenched, and a band with maximum at 420 mμ appears. It is difficult to judge how far this process can go because of the solubility limit of ethanol in benzene. The picture is similar if we add ethanol to a dioxane solution of the anilide. At low ethanol concentrations the long wavelength band shows quenching, and at high concentrations the short wave emission appears with increasing brightness.

The anilide of o-methoxybenzoic acid shows a very weak emission in the u.v. region. It was impossible to record this spectrum, even by photographic methods.

It is possible to explain the appearance of a band with maximum at 314 mμ in the absorption spectrum of a heptane solution of the anilide of salicylic acid on the basis of a strong intramolecular hydrogen bond. In ethanol, because of interaction with the solvent and ionization this band diminishes.

It is well known that the formation of an internal hydrogen bond always lead to a long-wave shift in the electronic absorption bands [3]. For the anilide of O-methoxybenzoic acid such a bond is impossible, and in the absorption spectrum of this substance the long-wave is absent. This is well shown by comparison of Figures 1 and 2.

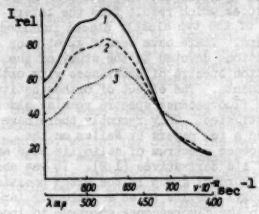

Fig. 6 Change in the fluorescence spectrum of the anilide of salicylic acid in benzene on addition of varying amounts of ethanol. (from 1 to 3 the ethanol concentration increases by 0.05 M.)

We may also infer the presence of a hydrogen bond from the infrared spectrum of the anilide of salicylic acid. As Figure 7 shows, the free OH stretching frequency at 3600 cm^{-1} is absent and is replaced by a weak but broad band at 3100-2700 cm^{-1} which at its lower wavelength limit overlaps the CH stretching band. According to Martin [4], the appearance of such a band in hydroxyl compounds is evidence for strong intramolecular forces. In fact, if we use the data of Shigorin and Shemiakin [5] for the frequency of the free OH stretching vibration in related compounds we may compute the energy of the hydrogen bond from the shift of the infrared band. It turns out to be approximately 8 kcal/mol. In the infrared spectrum of the anilide of salicylic acid a very sharp band appears at 3470 cm^{-1} which may be attributed to the NH stretching vibration. As expected this band is also present in the spectrum of the anilide of o-methoxybenzoic acid. In this case it is shifted to low frequencies by 70 cm^{-1}. In the region 3100-2700 cm^{-1}, however, only the C-H and $-CH_3$ stretching vibrations appear. In alcoholic solution, the intramolecular hydrogen bond is broken as a result of the interaction between the anilide and the solvent. It is now possible for the molecule to ionize as follows

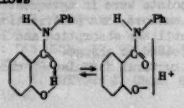

It is possible that the ionization of the molecule is followed by enolization of the amide group, as is considered probable by a number of authors for the anilide of 2-hydroxy--3-naphthoic acid.

In ethanol an absorption band with a maximum at 340 mμ is also observed. As shown in Figure 3, the intensity of this band increases markedly with increasing concentrations of alkali in the solution. All curves cross at a single point, indicating an equilibrium between two species-the ionic and the non-ionic. Here we have the typical bathochromic shift which is observed when organic anions are formed in solution.

In the case of the anilide of the methoxy acid, addition of alkali to the ethanol solution leads to no change in the absorption spectrum, since this substance has only very weak acidic properties.

The changes in the absorption spectrum of the anilide of salicylic acid parallel those in the luminescence spectrum. The characteristics of the emission of this substance may be explained either by using Weller's proposals [2], or in the following manner. According to Stepanov's predissociation theory [5] when molecules with hydrogen bonds have their -OH stretching vibrations excited, the hydrogen bond is broken. It seems probable that electronic excitation of molecules with intramolecular hydrogen bonds must also lead to rupture of the H- bond. During the lifetime of the excited state there is a redistribution of the excess vibrational energy in the various vibrational and rotational modes. It seems natural to suppose that the H-bond is reformed during this process. Thus emission is from molecules having a hydrogen bond in the excited state. In this case the energy levels may be represented as in Figure 8. Excited molecules have two upper states differing from each other by the presence (E_H^*) or absence (E^*) of the hydrogen bond. Each level has its own set of vibrational and rotational levels and gives a separate fluorescence band. These bands correspond to the transitions $h\nu_{f1}$ and $h\nu_{f2}$. The ratio of the intensities of the two bands is determined by the probability of the transition $h\omega_{H1}$, i.e., by the probability of forming a hydrogen bond in the excited state. In the case of salicylic acid and methyl salicylate two bands are observed [2], while in the anilide of salicylic acid only the band corresponding to the transition $h\nu_{f2}$ is observed, suggesting a strong excited-state hydrogen bond. Because of the transition $h\omega_{H1}$ there is an additional Stokes shift in the fluorescence spectrum. To decide whether the transitions $h\omega_{H1}$ and $h\omega_H$ are radiative or non-radiative additional infrared data are necessary.

In hydroxylic solvents, emission is observed only from ionic form; intermolecular effects are stronger than intramolecular. Thus the long wavelength emission is quenched on addition of alcohol to the benzene or dioxane solutions and the fluorescence with maximum at 420 mμ results. So in alcohol we see the luminescence of the ionic form only. The constancy of the position of the luminescence maximum if we pass over to butanol confirms this fact. The luminescence yield, however, depends on the pH of the alcohol.

For the anilide of methoxybenzoic acid the intramolecular hydrogen bond is impossible, and this substance therefore shows only the short wavelength emission, with very low quantum yield because of a high probability of radiationless transitions.

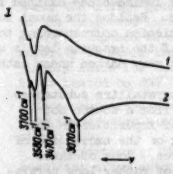

Figure 7 Infrared absorption spectra. 1-pure CCl_4, 2-the anilide of salicylic acid in CCl_4.

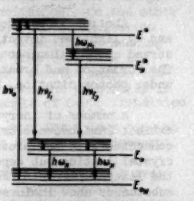

Figure 8. Energy level diagram for molecules with intramolecular hydrogen bonds.

It should be noted that a satisfactorily high scintillation yield is observed in solid polystyrene solutions of the anilide of salicylic acid. In Figure 4 is shown the fluorescence spectrum of the anilide in a polystyrene block. As may be seen, this emission belongs to the species possessing the intramolecular hydrogen bond.

CONCLUSIONS

1. The long wavelength emission of the anilide of salicylic acid results from the presence of an intramolecular hydrogen bond in that substance.

2. The short wavelength emission from alcoholic solutions of the anilide of salicylic acid results from the ionization of the molecule and depends on the pH of the solvent.

January 13, 1958

References

1. A. WELLER: Naturwiss., 42, Heft 7, 175 (1955)
2. A. WELLER: Z. f. Elektrochemie, 60, No. 9-10, 1144 (1956)
3. N. D. SOKOLOV: UFN, 57, No. 2, 205 (1955)
4. A. E. MARTIN: Nature, 166, 474 (1950)
5. D. N. SHIGORIN, M. M. SHEMIAKIN, L. A. SHCHUKINA, M. N. KOLOSOV, F. A. MENDELEVICH: DAN USSR, 108, No. 4, 672 (1956)
6. M. V. VOL'KENSHTEIN, M. A. EL'IASHEVICH, B. I. STEPANOV: Kolebaniia molekul (Vibrations of molecules), II. GITTL, Moscow-Leningrad, 1949

TOM VI, Vyp. 3 OPTIKA I SPEKTROSKOPIIA Mart, 1959
VOL. VI, No. 3 OPTICS AND SPECTROSCOPY March, 1959

On The Possibility of Recombination Processes in the Luminescence of Tungstate and Uranyl Compounds

V. L. LEVSHIN, V. B. GUMAN, AND E. N. KARZHAVINA

Abstract: The decay of luminescence excited in uranyl silicate and calcium tungstate by cathode rays and by light was investigated. Besides the usual luminescence, which decays exponentially, there was observed a thermoluminescent emission corresponding to the liberation of electrons from the trapping levels. The formation and breakdown of the trapping levels was investigated. The process observed is insignificant under photoexcitation, but is very marked under cathode excitation.

A number of inorganic crystalline substances exhibit luminescence arising from a source not connected with the presence of impurities in the crystal lattice but depending on the excitation of the lattice elements themselves. Some of these substances show luminescence of rather long persistence; among these are tungstate and uranyl compounds.

The luminescence of uranyl compounds has been very fully investigated. Under photoexcitation the decay is in most cases strictly exponential [1]. Various cases of more complicated decay laws mentioned in the literature can be explained as the result of two superposed exponential decay laws.[1] The persistence of luminescence in most uranyl salts is of the order of 10^{-4} sec, and decreases in the presence of quenching. The frequency of the electron transitions combines with the frequency of oscillation of the uranyl group UO_2. We are therefore dealing with luminescence of a molecular type. Under cathode excitation and under excitation by short-wave ultraviolet light (at low temperatures) a highly persistent luminescence has been observed, the duration being several seconds [2,3].

Tungstates belong to the group of substances in which luminescence can also arise from excitation of the crystal lattice itself. The luminescence is attributed to the anion WO_4^{2-}. The lattice of tungstates does not readily allow the introduction of impurities. Attempts to introduce the usual activators have led to negative results: most activators either do not enter the lattice at all, or change the intensity of emission without changing its character (e.g. activation by Mn and Bi). There are indications of activation of tungstates by rare earth metals. The decay of luminescence is basically exponential. These circumstances, and also the low output of these phosphors, point to the molecular nature of the luminescence of these substances. Under cathode excitation, a departure of the decay from a strictly exponential law was observed [4] in the late stages; this, however, does not prove the existence of recombination processes, and can be explained by the superposition of two or more exponential processes.

The aim of the present work was to examine the possibility of recombination processes in the luminescence in crystals of uranyl compounds and tungstates. We made use of curves of thermal luminescence, which allowed us to observe the localized levels of electrons liberated from the lattice structure under excitation, and to study the decay curves.

The observation of the localized levels of electrons, together with the hyperbolic law of the decay of the luminescence characteristic of these crystallophosphors, provides a very strong argument in favor of the existence of recombination processes in the luminescence of the substances mentioned.

The experiments were carried out with an apparatus developed at the P. N. Lebedev Physics Institute of the Academy of Sciences of the USSR (FIAN USSR) by an engineering group under the direction of A. G. Zavrazhin with the collaboration of E. N. Karzhavina. This apparatus permitted excitation of the phosphor samples by cathode rays and by light at temperatures from -185 to +300°, and permitted observation of the intensity of emission both under excitation and under thermal emission conditions.

Investigations were carried out on uranyl silicate (UO_2SiO_3) and on calcium tungstate ($CaWO_4$).

Uranyl silicate. The phosphor was excited by cathode rays with a current density of 1×10^{-7} A/cm², at a voltage of 14 kV, and at a temperature of -185°, the excitation lasting for 30 min. This duration was determined from prior experiments.

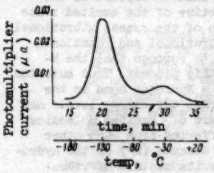

Fig. 1 Thermoluminescence curve for UO_2SiO_3 after cathode ray excitation.

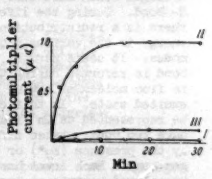

Fig. 2. Growth of intensity of separate maxima of the thermoluminescence curve of $CaWO_4$, as a function of duration of excitation by cathode rays.

It corresponds to the time when the intensity of the principal maximum of thermoluminescence first reaches a constant value; that is, it corresponds to the time when the localized levels are filled.

After an interval of the order of 15 minutes following the cessation of excitation, during which the natural decay of luminescence was completed, the samples were heated uniformly at the rate of 10 deg/min. The characteristic curve of thermoluminescence (Fig. 1) was obtained.

Under photoexcitation by the mercury lines at 366 and 313 mμ, carried out under similar conditions, no storage of light sums occurred.

For qualitative comparison of the intensity of recombination processes with the usual processes of luminescence under excitation, we note that the maximum intensity of emission of the phosphor during thermoluminescence at a heating rate of 10 deg/min amounted to only 0.07% of the intensity of luminescence of the phosphor under the electron beam used for excitation.

It is natural to ask whether the emission observed in thermoluminescence is due to some alteration in the crystal lattice caused by the action of the cathode rays. In this case the localized levels resulting from cathode ray excitation should still exist after the end of the irradiation, and their presence should result in the conservation of significant light sums on photoexcitation as well. To test this hypothesis, an experiment was carried out on uranyl silicate. Samples of uranyl compounds which had not been exposed to cathode rays, and samples which had been, both failed to yield thermoluminescence curves after photoexcitation. Thus, although the luminescence arises from the capture of electrons released under cathode ray action by ionization of separate areas in the crystal lattice, the charges later return to the ionized regions and reconstitute the lattice.

Calcium tungstate. A similar picture of the development of thermoluminescence can be observed when calcium tungstate is excited.

We used in our experiments a specimen of high purity, especially prepared by IU. S. Leonov (FIAN). The absence of rare earth impurities was certain.*

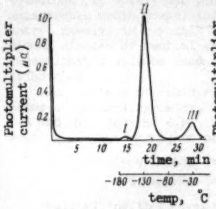

Fig. 3 Thermoluminescence curve of $CaWO_4$ after cathode ray excitation.

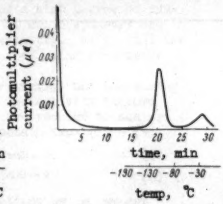

Fig. 4 Thermoluminescence curve of $CaWO_4$, after excitation by the mercury line at 366 mμ.

Excitation by the cathode beam was carried out as before. Figure 2 shows the increase in intensity of luminescence at three separate maxima (I, II, and III) of the thermoluminescence curve as a function of duration of cathode excitation. The increase is approximately exponential, and saturation is reached almost simultaneously in the three curves.

The final intensities of the maxima of the thermoluminescence are in the ratio of 1:50:6.

As opposed to uranyl silicate, calcium tungstate can show thermoluminescence after photoexcitation (λ=366 and 312 mμ), but preliminary exposure of the tungstate to cathode rays is required. A fresh sample of calcium tungstate, never exposed to cathode rays, shows no thermoluminescence after photoexcitation.

The maxima of thermoluminescence occur at the same points under cathode- and photoexcitation. Apparently cathode excitation produces a rather stable change in the crystal lattice; the localized levels occuring under cathode excitation are maintained for some time after the cessation of luminescence; their presence provides for the storage of light sums under photoexcitation. On the other hand, the change produced by cathode excitation in the tungstate lattice is reversible: heating a sample exposed to cathode rays decreases its capacity to store light sums, and the sample completely loses its thermoluminescent properties if it is heated to 200°. A sample of $CaWO_4$ irradiated with cathode rays and then kept for a long time at room temperature also loses its thermoluminescent properties.

Comparison of the thermoluminescence curves resulting after cathode and photoexcitation (Fig. 3 and 4) shows that, for the same intensity of luminescence of the phosphors under excitation, the magnitude of the highest peak (corresponding to a temperature of -120°) after photoexcitation by the mercury line at 366 mμ has a value only 0.02 of the corresponding magnitude after excitation by cathode rays.

The maximum intensity of emission during thermoluminescence of the tungstate, after preparatory excitation by cathode rays, was 0.02 of the intensity under direct excitation by cathode rays.

INVESTIGATION OF THE DECAY LAW FOR PERSISTENT LUMINESCENCE

Cathode irradiation of uranyl silicate and calcium tungstate at -185° yields a visible afterglow, corresponding to release from the lowest localized levels.

In Figure 5 the decay of the persistent luminescence of uranyl silicate is plotted on a log-log scale; Figure 6 shows the corresponding plot for calcium tungstate. It follows from Figures 5 and 6 that the decay in both cases follows a hyperbolic law $I = A\,t^{-\alpha}$: The decay index α has the value 0.8 for uranyl silicate, and 0.7 for calcium tungstate.

Because of the low emission intensity, a visible afterglow was observed for only 15 sec. Emission was observed with the aid of a photomultiplier for 10 minutes and longer.

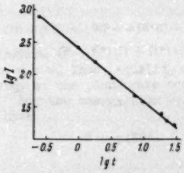

Fig. 5. Decay of persistent luminescence of UO_2SiO_3 excited by cathode rays.

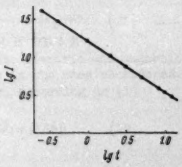

Fig. 6. Decay of persistent luminescence of $CaWO_4$ excited by cathode rays.

* Papers presented at the VIIth Congress on Luminescence, July 1, 1958.

The hyperbolic decay curve, characteristic of recombination processes occurring in typical crystallophosphors, and the existence of peak values of thermoluminescence, also characteristic of crystallophosphors, yield a highly plausible hypothesis as to the dislocation of the crystal lattice of calcium tungstate and uranyl silicate under the action of cathode rays and as to the formation of regions of electron localization, leading to the development of recombination processes in luminescence which are supplementary to the usual luminescence of the compounds mentioned above.

The hyperbolic decay curve, characteristic of recombination processes occurring in typical crystallophosphors, and the existence of peak values of thermoluminescence, also characteristic of crystallophosphors, yield a highly plausible hypothesis as to the dislocation of the crystal lattice of calcium tungstate and uranyl silicate under the action of cathode rays and as to the formation of regions of electron localization, leading to the development of recombination processes in luminescence which are supplementary to the usual luminescence of the compounds mentioned above.

As to the hypothesis that there are various centers arising from the presence of impurities in our sample and giving rise collectively to a hyperbolic decay law, we find it implausible both because of the purity of the calcium tungstate sample and because of the coincidence of the thermoluminescence spectra and of the basic luminescence of the tungstate.

March 27, 1958

References

1. S. I. VAVILOV, V. L. LEVSHIN: Z. Phys., 48, 397 (1928)
2. Z. M. SVERDLOV, A. N. SEVCHENKO: DAN USSR, 61, 821 (1948)
3. E. L. NICHOLS, H. L. HOWES in collaboration with E. MERRITT, D. T. WILBER, F. G. WICK: Fluorescence of the uranyl salts. Washington, 1919
4. A. V. MOSKVIN: Katodoliuminestsentsiia (Cathode Luminescence) GTTL, Moscow, 1948

TOM VI, Vyp. 3 OPTIKA I SPEKTROSKOPIIA Mart, 1959
VOL. VI, No. 3 OPTICS AND SPECTROSCOPY March, 1959

On the Theory of Optical Activity in Crystals

II. Crystals of Cubic Symmetry and Planar Classes of Central Symmetry

F. I. FEDOROV

Abstract: The optical properties (including energy relations) of optically active crystals of the cubic system are examined, taking into account magnetic terms. It appears that in planar classes of central symmetry, rotation of the plane of polarization is absent for propagation of light along the optical axes. These crystals differ radically from nonactive crystals, in that reflected light exhibits elliptical polarization. In conclusion we consider the question of defining the concept of an optically active medium.

As shown in [1]; Maxwell's equations together with the constitutive relations for plane waves in optically active media give the following

$$\mathbf{D} = -[\mathbf{mH}], \tag{1}$$

$$\mathbf{B} = [\mathbf{mE}], \tag{2}$$

$$\mathbf{D} = \alpha\mathbf{E} + ik[\alpha\mathbf{m}, \mathbf{E}], \tag{3}$$

$$\mathbf{B} = \mu\mathbf{H} + ik[\beta\mathbf{m}, \mathbf{H}], \tag{4}$$

where $\mathbf{m} = n\mathbf{n}$ is the vector refraction; $k = \frac{\omega}{c}$ is the wave number in vacuum; α, β are respectively the electric and magnetic activity tensors.

Here we investigate, with the aid of the basic equations (1) - (4), the propagation of light in anisotropic media possessing a high degree of symmetry, namely, in crystals of cubic symmetry and in planar classes of central symmetry. As in [1], the investigation will be conducted using invariance techniques.

In crystals of cubic symmetry, not possessing plane or central symmetry, the activity tensors α and β, just as ε, μ, are reduced to scalars. Writing $p = \chi\alpha$, $q = \chi\beta$, we obtain from (1) - (4)

$$\varepsilon\mathbf{E} + ip[\mathbf{mE}] + [\mathbf{mH}] = 0, \tag{5}$$

$$\mu\mathbf{H} + iq[\mathbf{mH}] - [\mathbf{mE}] = 0. \tag{6}$$

Multiplying these equations by $\mathbf{m}$ we get

$$\mathbf{mE} = \mathbf{mH} = 0. \tag{7}$$

To eliminate $\mathbf{E}$ and $\mathbf{H}$ we take the vector product of (5) and (6) with $\mathbf{m}$; taking account of (7) we obtain

$$\mathbf{H} = \frac{\varepsilon}{m^2}[\mathbf{mE}] - ip\mathbf{E}, \qquad \mathbf{E} = -\frac{\mu}{m^2}[\mathbf{mH}] + iq\mathbf{H}. \tag{8}$$

Substituting (8) into (5) and (6) gives

$$\mathbf{E} = i\frac{\chi}{n^2}[\mathbf{mE}], \qquad \mathbf{H} = i\frac{\chi}{n^2}[\mathbf{mH}], \tag{9}$$

where

$$\chi = \frac{n^2(1 - pq) - \varepsilon\mu}{\mu p + \varepsilon q}. \tag{10}$$

Substituting into the right hand part of (9) the expression for $\mathbf{E}$ from the same relation, we get $\frac{\chi^2}{n^2} = 1$, i.e. $\chi = \pm n$, which together with (10) yields the following equation for the index of refraction

$$n^2(1 - pq) \mp (\mu p + \varepsilon q) - \varepsilon\mu = 0. \tag{11}$$

Here (9) takes the form

$$\mathbf{E} = \pm i[\mathbf{nE}], \qquad \mathbf{H} = \pm i[\mathbf{nH}], \tag{12}$$

which denotes circularly polarized $\mathbf{E}$ and $\mathbf{H}$, +, to the right or −, to the left (see [6]). The positive and negative roots of expression (11) may be expressed respectively as follows:

$$n_\pm = \frac{\sqrt{\varepsilon\mu + \frac{1}{4}(\mu p - \varepsilon q)^2} \pm \frac{1}{2}(\mu p + \varepsilon q)}{1 - pq}. \tag{13}$$

Hence, the right and left hand waves are propagated with different speeds, which leads to rotation of the plane of polarization of light passing through the given medium. Neglecting in (13) terms of the second order with respect to p, q in view of their small magnitude, we obtain

$$n_\pm = n_0 \pm \frac{1}{2}(\mu p + \varepsilon q), \tag{14}$$

where $n_0 = \sqrt{\varepsilon\mu}$. The magnitude of the circular double refraction is equal to

$$\Delta n = n_+ - n_- = \mu p + \varepsilon q. \tag{15}$$

This corresponds to a specific rotation of the plane of polarization

$$\chi = \frac{1}{2}k\Delta n = \frac{1}{2}k(\mu p + \varepsilon q). \tag{16}$$

To investigate the energy relations it is necessary to convert to the real parts of the fields $\hat{\mathbf{E}} = \frac{1}{2}(\mathbf{E} + \mathbf{E}^*)$, $\hat{\mathbf{H}} = \frac{1}{2}(\mathbf{H} + \mathbf{H}^*)$.[1] Hence, we obtain for the electric energy (see [1])

$$w_e = \frac{1}{32\pi}(\mathbf{E} + \mathbf{E}^*)(\mathbf{D} + \mathbf{D}^*). \tag{17}$$

Utilizing (3) and taking into account that, in the given case, (see [12]) $\mathbf{E}^2 = \mathbf{E}^{*2} = 0$ and

$$[\mathbf{EE}^*] = [\mathbf{E}, \mp i[\mathbf{nE}^*]] = \mp i|\mathbf{E}|^2\mathbf{n}, \tag{18}$$

we obtain

$$w_e = \frac{1}{16\pi}(\varepsilon \pm p n_\pm)|\mathbf{E}|^2. \tag{19}$$

Hence, for the same $|\mathbf{E}|^2$ the energies of the right hand and left hand waves are different and depend upon the corresponding index of refraction. Analogously, we find for the magnetic field

$$w_m = \frac{1}{16\pi}(\mu \pm q n_\pm)|\mathbf{H}|^2. \tag{20}$$

From (1) to (4) it follows that

$$\mathbf{ED} = \mathbf{m}[\mathbf{EH}] = \mathbf{HB} = 0,$$

and

$$\mathbf{E}^*\mathbf{D} = (\varepsilon \pm p n_\pm)|\mathbf{E}|^2 = \mathbf{m}[\mathbf{E}^*\mathbf{H}] = \mathbf{HB}^* = (\mu \pm q n_\pm)|\mathbf{H}|^2, \tag{21}$$

therefore $(\mathbf{E} + \mathbf{E}^*)(\mathbf{D} + \mathbf{D}^*) = (\mathbf{H} + \mathbf{H}^*)(\mathbf{B} + \mathbf{B}^*)$, i.e. $w_e = w_m$. Thus, equality of the electric and magnetic energy of the plane wave occurs in the case considered.

For the energy flux vector, according to [1] we have

$$\mathbf{P} = \frac{c}{4\pi}[\hat{\mathbf{E}}\hat{\mathbf{H}}] - \frac{1}{8\pi}(\alpha[\hat{\mathbf{E}}\hat{\dot{\mathbf{E}}}] + \beta[\hat{\mathbf{H}}\hat{\dot{\mathbf{H}}}]) \tag{22}$$

or

$$\mathbf{P} = \frac{c}{16\pi}[\mathbf{E} + \mathbf{E}^*, \mathbf{H} + \mathbf{H}^*] - \frac{ic}{16\pi}(p[\mathbf{EE}^*] + q[\mathbf{HH}^*]). \tag{23}$$

From, (8), (9) it follows that

$$\mathbf{H} = -i\left(p + \frac{\varepsilon}{\chi}\right)\mathbf{E}, \qquad \mathbf{E} = i\left(q + \frac{\mu}{\chi}\right)\mathbf{H}. \tag{24}$$

Therefore $[\mathbf{EH}] = \mathbf{EH} = 0$. In addition, from (24) and (18) we have

$$[\mathbf{E}^*\mathbf{H}] = \frac{1}{n_\pm}(\varepsilon \pm p n_\pm)|\mathbf{E}|^2\mathbf{n} = 8\pi\frac{w_\pm}{n_\pm}\mathbf{n} = [\mathbf{EH}^*].$$

---

1 $\hat{\mathbf{E}}$ and $\hat{\mathbf{H}}$ designate the real parts of complex vectors $\mathbf{E}$ and $\mathbf{H}$.

With the help of these expressions and (21) we find

$$\mathbf{P}_{\pm} = \frac{c}{16\pi}\left\{8\pi\frac{v_{\pm}}{n_{\pm}} \mp (p|\mathbf{E}|^2 + q|\mathbf{H}|^2)\right\}\mathbf{n} = \frac{v_{\pm}}{16\pi}(\varepsilon|\mathbf{E}|^2 + \mu|\mathbf{H}|^2)\mathbf{n}. \quad (25)$$

Thus, the energy flux of plane waves in a isotropic optically active medium[2] is expressed in terms of phase velocity and field strength in exactly the same way as in nonactive media. The only difference is that $v_{\pm}$ is expressed through the parameters of the medium (13),(14), while the phase velocity in nonactive media is $v = \frac{c}{\sqrt{\varepsilon\mu}}$. In addition, $\varepsilon|\mathbf{E}|^2 \neq \mu|\mathbf{H}|^2$, and for isotropic nonactive media the relation

$$\mathbf{P} = v\mathbf{n}\mathbf{n} \quad (26)$$

usually does not hold under the given conditions.

Let us turn now to the planar classes of crystals with central symmetry. According to [1], for such crystals the activity tensors are clearly antisymmetric and take the form

$$\alpha = a\mathbf{e}\times, \quad \beta = b\mathbf{e}\times, \quad (27)$$

where $\mathbf{e}$ - is a unit vector along the axis of symmetry. At the same time the tensors ε and μ have the form common to all crystals with central symmetry [5],

$$\varepsilon = \varepsilon_0 + \varepsilon'\mathbf{e}\cdot\mathbf{e}, \quad \mu = \mu_0 + \mu'\mathbf{e}\cdot\mathbf{e}, \quad \varepsilon' = \varepsilon_e - \varepsilon_0, \quad \mu' = \mu_e - \mu_0. \quad (28)$$

Equations (3), (4) here take the following form

$$\mathbf{D} = \varepsilon_0\mathbf{E} + \varepsilon'\mathbf{e}\cdot\mathbf{e}\mathbf{E} + ip[[\mathbf{e}\mathbf{m}]\mathbf{E}], \quad (29)$$

$$\mathbf{B} = \mu_0\mathbf{H} + \mu'\mathbf{e}\cdot\mathbf{e}\mathbf{H} + iq[[\mathbf{e}\mathbf{m}]\mathbf{H}], \quad (30)$$

where $p = ka$, $q = kb$. It is at once apparent, that if the wave normal $\mathbf{n}$ is in the direction of the axis $\mathbf{e}$, then there will be no rotation of the plane of polarization, because here equations (29), (30) take the form $\mathbf{D} = \varepsilon\mathbf{E}$, $\mathbf{B} = \mu\mathbf{H}$, characteristic of nonactive crystals. Hence it is clear that the direction $\mathbf{e}$ will not differ from the optical axis in uniaxial nonactive transparent crystals. However, for all other directions the optical properties in the given crystals will differ from those of nonactive crystals. In order to demonstrate this, let us consider the simplified case $\mu = 1$, $q = 0$; we will not take into account the magnetic properties of the crystal, including the magnetic part of the optical activity. It should be noted that, in the literature, the magnetic terms in the optical activity have not been taken into account until now because of the resulting complications (see [3]). Thus, we have the equations:

$$\varepsilon\mathbf{E} + ip[[\mathbf{e}\mathbf{m}]\mathbf{E}] + [\mathbf{m}\mathbf{H}] = 0, \quad (31)$$

$$\mathbf{H} = [\mathbf{m}\mathbf{E}]. \quad (32)$$

Eliminating $\mathbf{H}$, we obtain

$$(\varepsilon + \mathbf{m}\times^2 + ip[\mathbf{e}\mathbf{m}]\times)\mathbf{E} = 0, \quad (33)$$

and consequently

$$(\varepsilon + \mathbf{m}\times^2 + ip[\mathbf{e}\mathbf{m}]\times) = 0. \quad (34)$$

Evaluating this determinant by means of an invariance technique [4] and taking into account (28), we see that equation (34) is resolved into two parts

$$\mathbf{m}^2 - \varepsilon_0 = 0, \quad (35)$$

$$\mathbf{m}\cdot\mathbf{m} - \varepsilon_0\varepsilon_e + p^2[\mathbf{e}\mathbf{m}]^2 = 0. \quad (36)$$

[2] All interpretations of the results above apply identically to optically active crystals with cubic symmetry and to optically active isotropic media.

Hence, in the given crystals there exist ordinary waves, whose index of refraction, according to (35) is equal to $n_0 = \sqrt{\varepsilon_0}$, and extraordinary waves with index of refraction

$$n_e^2 = \frac{\varepsilon_0\varepsilon_e}{(\varepsilon_0 + p^2)[\mathbf{e}\mathbf{m}]^2 + \varepsilon_e(\mathbf{e}\mathbf{m})^2}. \quad (37)$$

If we regard $\mathbf{m}$ as a radius vector, then (36) appears as an equation for the surface of normals of the extraordinary wave. Superposing the z axis upon the $\mathbf{e}$ axis, we get $\mathbf{m}\mathbf{e} = z$, $[\mathbf{m}\mathbf{e}]^2 = x^2 + y^2$, and (36) takes the form

$$\frac{x^2 + y^2}{\frac{\varepsilon_e}{1 + \frac{p^2}{\varepsilon_0}}} + \frac{z^2}{\varepsilon_0} = 1. \quad (38)$$

This is the equation of an ellipsoid of revolution. Thus, the result here, which differs from that for nonactive crystals of central symmetry, is just that the radius of the circular section of the ellipsoid becomes smaller by the ratio $\sqrt{1 + \frac{p^2}{\varepsilon_0}}$. In other words, the situation is as if ε_e were replaced by $\varepsilon_e' = \frac{\varepsilon_e}{1 + \frac{p^2}{\varepsilon_0}}$. For n/e the indices of refraction of both waves (36), (38) coincide. Hence, with respect to the behavior of the index of refraction, there are no essential differences in this case from nonactive crystals with central symmetry.

Let us now examine the polarization of the waves propagated in the crystals under consideration. For ordinary waves equation (33) takes the form

$$(\varepsilon'\mathbf{e}\mathbf{E} - ip\mathbf{m}\mathbf{E})\mathbf{e} + (\mathbf{m}\mathbf{E} + ip\mathbf{e}\mathbf{E})\mathbf{m} = 0. \quad (39)$$

Because $\mathbf{e}$ and $\mathbf{m}$ are independent vectors, then $\mathbf{e}\mathbf{E} = \mathbf{m}\mathbf{E} = 0$, hence

$$\mathbf{E}_0 \parallel [\mathbf{e}\mathbf{m}], \quad (40)$$

from which we obtain, according to (29), (32),

$$\mathbf{D}_0 = \varepsilon_0\mathbf{E}_0 \parallel [\mathbf{e}\mathbf{m}], \quad \mathbf{H}_0 \parallel [\mathbf{m}[\mathbf{e}\mathbf{m}]]. \quad (41)$$

Thus, with respect to polarization the ordinary waves differ from the same wave in uniaxial crystals [5].

For extraordinary waves the situation is somewhat different. Multiplying (37) by $[\mathbf{e}\mathbf{m}]$ and $\mathbf{m}$, we obtain

$$[\mathbf{e}\mathbf{m}]\mathbf{E} = 0, \quad (\mathbf{m}\mathbf{E} + ip[\mathbf{m}[\mathbf{e}\mathbf{m}]])\mathbf{E} = 0,$$

from which

$$\mathbf{E}_e \parallel [[\mathbf{e}\mathbf{m}], \ \mathbf{m} + ip[\mathbf{m}[\mathbf{e}\mathbf{m}]]]. \quad (42)$$

Since $\mathbf{E}_0^*\mathbf{E}_e \neq 0$, $[\mathbf{E}_0\mathbf{E}_e^*] \neq 0$, the vector $\mathbf{E}$ is elliptically polarized in the principal plane (plane of $\mathbf{e}$, $\mathbf{m}$). For $\mathbf{H}_e$ and $\mathbf{D}_e$, we obtain from (32) and (1)

$$\mathbf{H}_e = [\mathbf{m}\mathbf{E}_e] \parallel [\mathbf{e}\mathbf{m}], \quad \mathbf{D}_e = -[\mathbf{m}\mathbf{H}_e] \parallel [\mathbf{m}[\mathbf{e}\mathbf{m}]]. \quad (43)$$

Formulas (43) define the directions of $\mathbf{H}$ and $\mathbf{D}$ as for the case of extraordinary waves in nonactive uniaxial crystals [5].

Thus, the single difference in optical properties between the crystals under consideration and uniaxial nonactive crystals is that, in the former, the electric field of the extraordinary wave is polarized elliptically while in the latter, it is polarized linearly.

At first glance it might appear that this difference is impossible to demonstrate, since the transverse vectors, and in particular the light vector $\mathbf{D}$, behave identically in both cases. However, the indicated differences lend themselves to experimental investigation in principle. For this it is necessary to investigate the reflection of light from the crystals under consideration. The boundary conditions have the form (see [6])

$$\mathbf{H}+\mathbf{H}'-A_0\mathbf{H}_0-A_e\mathbf{H}_e=0, \quad [\mathbf{E}+\mathbf{E}'-A_0\mathbf{E}_0-A_e\mathbf{E}_e, \mathbf{h}]=0. \quad (44)$$

Here $\mathbf{H}$, $\mathbf{E}$, $\mathbf{H}'$, $\mathbf{E}'$ are respectively the magnetic and electric fields of the incident and reflected waves, $\mathbf{H}_0$, $\mathbf{H}_e$, $\mathbf{E}_0$, $\mathbf{E}_e$ are defined by expressions (41) - (43), A_0, A_e are unknown amplitude factors and $\mathbf{h}$ is the unit vector normal to the reflecting surface.

If the incident wave is linearly polarized and reflection takes place as usual (incomplete reflection), then for real $\mathbf{H}_0$, $\mathbf{H}_e$, $\mathbf{E}_0$, $\mathbf{E}_e$ the solutions of the linear equations (44) for $\mathbf{E}$, $\mathbf{H}$, A_0, A_e would be real; in particular the reflected wave would be linearly polarized. However, since, according to (42), $\mathbf{E}_e$ is an elliptical vector defined by a complex expression, this implies complex expressions for $\mathbf{E}'$ and $\mathbf{H}'$, i.e. elliptical polarization of the reflected wave.

Thus, planar classes of crystals with central symmetry and with $\alpha \neq 0$ must exhibit elliptical polarization of the reflected light, being completely transparent. It is true that the ellipticity will be very small, because it is proportional to the square of the activity parameter ρ; nevertheless in principle it can be detected. Hence, in spite of the absence of rotation of the plane of polarization, the fact that the tensors α, β, are different from zero implies definite differences in the optical properties of the crystals, which in principle can be detected by experiment. Consequently, the definition of the concept of optical activity should be dwelt upon somewhat.

Until now, in the technical literature, the property of optical activity has nearly always been identified with the phenomenon of rotation of the plane of polarization of linearly polarized light passing through an active medium. Sometimes it is even possible to find passages in which it is proposed that the term "optical activity", since it is considered to be not fully satisfactory or somewhat indefinite, should be replaced by the term "optical rotatory capability". However, as is well known, the ability to rotate the plane of polarization for all directions of propagation is present only in certain isotropic media and in cubic crystals. In all remaining crystalline optically active media, the rotation of the plane of polarization cannot take place in more than one or two fixed directions of propagation (along the optical axes). In other directions in active crystals of all symmetries, except cubic ones, there is no rotation of the plane of polarization, but elliptical double refraction does take place. Thus, rotation of the plane of polarization is a special property of crystals to be defined as optically active, exactly as for instance, the existence of a unique velocity of light is a property only of certain distinct and exceptional directions in crystals, namely the optical axes. This, of course, does not lessen the significance of the fact that rotation of the plane of polarization is unquestionably the most important and the most easily observable property of optically active media. However, as has just been made clear, in some types of crystalline media characterized by finding equations (3) and (4), rotation of the plane of polarization does not take place at all. Moreover, since the binding equations of such media differ from $\mathbf{D} = \epsilon\mathbf{E}$ and $\mathbf{B} = \mu\mathbf{H}$, the properties of light propagating in them also differ from the well-known properties of light in ordinary transparent crystals.

The question arises as what should be the classification of the crystals considered above of planar classes with central symmetry ? It is evident that it is impossible to classify them as ordinary transparent crystals characterized by tensors ϵ and μ. They also do not form some kind of isolated group, because other kinds of crystals, which admit to classification as optically active, do not possess the property of rotation of the plane of polarization in only one direction.

From the point of view of the theory of the electromagnetic field, the most accurate and consistent procedure will be to classify various media according to the characteristics of their electromagnetic constitutive equations. This follows directly from the fundamental nature of Maxwell's theory, with respect to which, for example, isotropic nonmagnetic media may be defined as those in which $\mathbf{D} = \epsilon\mathbf{E}$, where ϵ is a scalar and $\mu = 1$. Transparent crystals are characterized by the fact that ϵ is a tensor, and the electrical conductivity $\sigma = 0$. For absorbing crystals, we have $\mathbf{i} = \sigma\mathbf{E}$, where σ, like ϵ, is a tensor, etc.. However, optically active media have been made exceptions to this general rule, and it had been understood that these were media possessing the ability to rotate the plane of polarization of light passing through them. As shown above, such an approach leads to the situation that some kinds of crystals with specific optical properties are neglected and are left outside the frame of any classification. Similarly, certain other classes of crystals with central symmetry (inversions) also deprived of the property of rotating the plane of polarization, according to an existing classification [7] are referred to optically active crystals.

Therefore, it is appropriate to designate optically active media as those for which the constitutive equations take the form (see [1])

$$\mathbf{D} = \epsilon\mathbf{E} + [\alpha\nabla, \mathbf{E}], \quad \mathbf{B} = \mu\mathbf{H} + [\beta\nabla, \mathbf{H}] \quad (45)$$

or, correspondingly for plane waves, the form (3), (4), with α or β different from zero.[3] According to this, every medium which rotates the plane of polarization for one or more directions of propagation is an optically active medium, but not the converse.

---

[3] Such a definition is found also in [2], although there it is used inconsistently, because in addition to the condition $\alpha \neq 0$, the requirement that the tensor α be symmetric is also imposed.

It is easy to see why planar classes of central symmetry are not counted among those symmetry types admitting the property of optical activity. The fact is, that in the existing theory based on approximate [2,3], or formal [7,8], reasoning, concept of optical activity is defined through the expression $G = n \alpha n$, where n is the wave normal. For planar classes of central symmetry, as a consequence of the antisymmetry of α, the magnitude of G becomes zero.

February 15, 1958

References

1. F. I. FEDOROV: OiS, 6, 85 (1959) (See translation p. 49)
2. L. D. LANDAU, E. M. LIFSHITZ: Elektrodinamika sploshnykh sred (Macroscopic Electrodynamics) GITTL, 1957 (To be translated by Addison-Wesley, Reading, Mass.)
3. M. BORN: Optik, Berlin. J. Springer, 1933 (GNTIU, 1937)
4. F. I. FEDOROV: OiS, 1, 926 (1956) (Translation exists)
5. F. I. FEDOROV: Kristallografiia, 3, 49 (1958) (See Soviet Phys.-Crystallography 3, 46 (1958))
6. F. I. FEDOROV: DAN USSR, 84, 1171 (1952)
7. F. POCKELS: Lehrbuch der Kristalloptik, Leipzig, 1906
8. A. B. SHUBNIKOV: Opticheskaia kristallografiia (Optical crystallography) Akad. Nauk Press, 1950

TOM VI, Vyp. 3 OPTIKA I SPEKTROSKOPIIA Mart, 1959
VOL. VI, No. 3 OPTICS AND SPECTROSCOPY March, 1959

Fresnel Formulas for an Ordinary Wave Incident on the Twinning Plane of a Transparent Uniaxial Crystal

G. B. RAIS

Abstract: The purpose of this work was to obtain formulas for the reflection and refraction coefficients of ordinary and extraordinary rays (intensity), at the interface between the initial and twinning portions of a transparent uniaxial crystal for the case of incident ordinary rays.

The difficulty of examining the reflection and refraction at the interface between two crystals consists of the fact that the coordinate system of the interface does not coincide with the system of the principal dielectric axes. The reflection and refraction of light at the boundary between an isotropic medium and a transparent uniaxial crystal, was examined by Dashevskii [1] for the simplest cases and by Fedorov [2] in the most general form, using the invariant method.

Let us consider an incident plane light wave

$$E_k = E_0 e^{i(k_i x_i - \omega t)}, \tag{1}$$

then from Maxwell's equations for a transparent dielectric, the following equation is obtained for the components of the electric field vector:

$$\left\{\left(\frac{\omega}{c}\right)^2 \varepsilon_{ik} + k_i k_k - k^2 \delta_{ik}\right\} E_k = 0, \tag{2}$$

where ε_{ik} is the tensor of the dielectric permittivity; δ_{ik} is the unit tensor; $\vec{k} = \frac{2\pi}{\lambda}\vec{n}$ is the wave vector and $\omega = 2\pi\nu$ is the angular frequency. As is known, in order for E_k to have values other than zero, it is necessary that the determinant of the system (2) be equal to zero. From this condition, an equation relating ν and λ is found:

$$\left\|\left(\frac{\nu}{c}\right)^2 \varepsilon_{ik} + \frac{n_i n_k - \delta_{ik}}{\lambda^2}\right\| = 0 \tag{3}$$

In optics, the frequency ν is usually considered prescribed. The wavelength λ will be a root of (3). As is known from crystal optics for a given frequency ν and direction $\vec{n}$ in an anisotropic medium, there correspond two wavelengths λ_1 and λ_2. Substituting the obtained values of λ_α in the system (2), we obtain relations between corresponding E_k

$$E_k^{(\alpha)} = E_r^{(\alpha)} \Delta_{km}^{(\alpha)} \quad (\alpha = 1, 2), \tag{4}$$

where $\Delta_{km}^{(\alpha)}$ is the minor of the determinant $\Delta^{(\alpha)}$ (3).

The calculations will be made first in the system of principal axes: the OX_3 axis will be directed along the optic axis C_3, while the OX_1 and OX_2 axes will be directed anywhere in the plane perpendicular to C_3 (since the rank of ε_{ik} is equal to two and the axis C_3 is equivalent to C_∞ with respect to optic properties - German's theorem [3]).

It is obvious that $\varepsilon_{ik} = \varepsilon^{(1)}\delta_{ik}$, $\varepsilon^{(1)} = \varepsilon^{(2)} \neq \varepsilon^{(3)}$.

Then solving the determinant of the system (3), we will obtain:

$$\lambda_1 = \frac{1}{\sqrt{\varepsilon^{(1)}}} \cdot \frac{c}{\nu} \quad \text{(ordinary wave)} \tag{5}$$

$$\lambda_2 = \frac{1}{\sqrt{\varepsilon^{(1)} \cdot \varepsilon^{(3)}}} \sqrt{(n_1^2 + n_2^2)\varepsilon^{(1)} + n_3^2 \varepsilon^{(3)}} \cdot \frac{c}{\nu} \text{(extraordinary wave)}. \tag{6}$$

Solving equations (2), we get the components of the electric field vector for the ordinary and the extraordinary waves, respectively

$$E_1^{(1)} = E_0^{(1)} \cdot k_{20}, \quad E_2^{(1)} = -E_0^{(1)} k_{10}, \quad E_3^{(1)} = 0; \tag{7}$$

$$E_1^{(2)} = -E_0^{(2)} \cdot k_{10} k_{30}, \quad E_2^{(2)} = -E_0^{(2)} k_{20} k_{30}, \quad E_3^{(2)} = E_0^{(2)} (k_{10}^2 + k_{20}^2) \frac{\varepsilon^{(1)}}{\varepsilon^{(3)}}. \tag{8}$$

REFLECTION OF PLANE WAVES FROM THE TWINNING PLANE

The formulas for reflection of plane waves were previously derived for one particular position of the plane of incidence of the light [4]. However, in crystals, an experimental measurement of the intensity is not equal to the square of the electric field strength. Let us examine this problem in a general case. Let us transform to a new coordinate system (fig. 1) where the OX_3 axis is perpendicular to the twinning plane and the OX_2 axis lies at the intersection of the twinning plane and the plane of the principal section of the twinning crystal. Let φ_0 be the angle between the optic axis and the twinning plane, and $\sin\varphi_0 = r$, $\cos\varphi_0 = s$, then the relation between the direction cosines of the axes of the chosen and principal systems will be given by

$$\begin{array}{c} \\ {}^{3}a_0 = \end{array} \begin{array}{c} \quad i \quad k_0 \rightarrow \\ \downarrow \\ \left\{\begin{array}{ccc} 1 & 0 & 0 \\ 0 & r & -s \\ 0 & s & r \end{array}\right. \end{array} \quad \text{(in the initial portion of the crystal)} \tag{9}$$

$$\begin{array}{c} \\ {}^{3}a_0' = \end{array} \begin{array}{c} \quad i \quad k_0' \rightarrow \\ \downarrow \\ \left\{\begin{array}{ccc} 1 & 0 & 0 \\ 0 & -r & -s \\ 0 & s & -r \end{array}\right. \end{array} \quad \text{(in the twinned portion of the crystal)} \tag{10}$$

Accordingly, we obtain the values of the components of the dielectric permittivity tensor in the twinned and initial portions of the crystal, expressed through the principal values of dielectric permittivity. It turns out that ε_{23} (in the initial portion of the crystal) is equal to $-\varepsilon_{23}$ (in the twinned portion of the crystal). This is the reason for their optical dissimilarity.

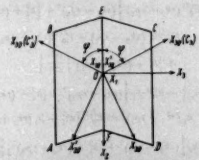

Figure 1. Principal section of a twinned crystal (shear plane)
EF - interface; OC_3 and OC_3' - directions of optical axes in the initial and twinned portions of the crystal

Let us examine the incidence of an ordinary wave on the twinning plane. In the most general case, there are two reflected and two refracted waves. The arguments $k_i x_i - \omega t$ of the wave

functions of those five waves must coincide due to the boundary conditions. From these conditions, geometric laws of reflection and refraction of ordinary and extraordinary waves are easily derived. In order to obtain the coefficients of reflection and refraction of plane waves at the interface, boundary conditions must be employed which consist of the continuity of tangential components of the electric and magnetic field strength vectors. As far as normal components of the electric and magnetic induction vectors are concerned, as is shown in [5] using the laws of reflection and refraction, they come as a consequence of the boundary conditions for the tangential components of the electric and magnetic field strengths and of Maxwell's equations. Thus, four boundary conditions remain

$$
\begin{aligned}
&E_1^{(1)} + E_1^{(2)} + E_1^{(3)} = E_1^{(1)} + E_1^{(2)},\\
&E_2^{(1)} + E_2^{(2)} + E_2^{(3)} = E_2^{(1)} + E_2^{(2)},\\
&H_1^{(1)} + H_1^{(2)} + H_1^{(3)} = H_1^{(1)} + H_1^{(2)},\\
&H_2^{(1)} + H_2^{(2)} + H_2^{(3)} = H_2^{(1)} + H_2^{(2)}.
\end{aligned}
\tag{11}
$$

Using the formula for transformation of vector components according to (9) and (10), let us express the wave vector components in the system of the principal axes by means of the wave vector components in the chosen system and the components of the electric field strength vector in the chosen system by means of the components in the system of the principal axes. Then let us express the components of the magnetic field strength vector $\vec{H}$ by means of the vector components of $\vec{E}$, according to one of Maxwell's equations

$$
\mathbf{H} = \frac{c}{\omega}\,[\mathbf{kE}]. \tag{12}
$$

Then the system of equations (11), expressed by the amplitudes of the vectors of the electric field strength of the incident, reflected and refracted ordinary and extraordinary waves becomes the following:

$$
\begin{aligned}
&E_0^{(1)}(rk_2 - sp_1) + E_0^{(2)} k_1 (sk_2 - rp_2) + E_0^{(3)}(rk_2 + sp_1) =\\
&\quad = -E_0'^{(1)}(rk_2 + sp_1) + E_0'^{(2)} k_1 (sk_2 - rp_2),\\
&-E_0^{(1)} rk_1 + E_0^{(2)}\left\{r(rk_2 + sp_2)(sk_2 - rp_2) - s\left[k_1^2 + (rk_2 + sp_2)^2\right]\frac{\varepsilon^{(1)}}{\varepsilon^{(3)}}\right\} - E_0^{(3)} rk_1 =\\
&\quad = E_0'^{(1)} rk_1 + E_0'^{(2)}\left\{r(rk_2 + sp_2)(sk_2 - rp_2) - s\left[k_1^2 + (rk_2 + sp_2)^2\right]\frac{\varepsilon^{(1)}}{\varepsilon^{(3)}}\right\}\\
&-E_0^{(1)} k_1 (sk_2 + rp_1) + E_0^{(2)}(rk_2 + sp_2)\left\{(sk_2 - rp_2)^2 + \left[k_1^2 + (rk_2 + sp_2)^2\right]\frac{\varepsilon^{(1)}}{\varepsilon^{(3)}}\right\} +\\
&\quad + E_0^{(3)} k_1 (sk_2 - rp_1) = -E_0'^{(1)} k_1 (sk_2 - rp_1) - E_0'^{(2)}(rk_2 + sp_2)\left\{(sk_2 - rp_2)^2 + \right.\\
&\quad \left. + \left[k_1^2 + (rk_2 + sp_2)^2\right]\frac{\varepsilon^{(1)}}{\varepsilon^{(3)}}\right\}\\
&E_0^{(1)}\left[sk_1^2 - p_1(rk_2 - sp_1)\right] - E_0^{(2)} rk_1\left\{(sk_2 - rp_2)^2 + \left[k_1^2 + (rk_2 + sp_2)^2\right]\frac{\varepsilon^{(1)}}{\varepsilon^{(3)}}\right\} -\\
&\quad - E_0^{(3)}\left[sk_1^2 + p_1(rk_2 + sp_1)\right] = E_0'^{(1)}\left[sk_1^2 + p_1(rk_2 + sp_1)\right] +\\
&\quad + E_0'^{(2)} rk_1\left\{(sk_2 - rp_2)^2 + \left[k_1^2 + (rk_2 + sp_2)^2\right]\frac{\varepsilon^{(1)}}{\varepsilon^{(3)}}\right\},
\end{aligned}
$$

where p_1 and p_2 are the normal components of the ordinary and extraordinary wave vectors, respectively.

This system of equations renders the solution of the problem of light reflection from the twinning plane for any orientation of the incidence plane. However, it is sufficient to consider the two most important cases:

1) the plane of incidence of light coincides with the plane of a principal section of the twinning crystal, and

2) the plane of incidence of light is perpendicular to the plane of a principal section of the twinning crystal.

The solution of the system of equations (11) for the first case when $k_1 = 0$, gives

$$
\mathbf{E}^{(1)} = \mathbf{E}'^{(1)}.
$$

Thus, in the case of coincidence of the plane of incidence of an ordinary ray with the plane of a principal section of a twinning crystal, the incident ordinary ray passes through the interface without changing direction and intensity.

The solution of the system of equations (11) for the second case ($k_2 = 0$) gives the values of amplitudes of oscillations of the electric vector of the ordinary and extraordinary (reflected and refracted) waves in terms of the amplitude of the incident ordinary wave $E_0^{(1)}$

$$
\begin{aligned}
E_0^{(2)} &= \frac{r^2 n_1^2 s^2 (p_1^2 - p_2^2)\, E_0^{(1)}}{p_1 p_2 (r^4 n_1^4 + s^4) + r^2 n_1^2 s^2 (p_1^2 + p_2^2)},\\
E_0'^{(1)} &= -\frac{p_1 p_2 (r^4 n_1^4 - s^4)\, E_0^{(1)}}{p_1 p_2 (r^4 n_1^4 + s^4) + r^2 n_1^2 s^2 (p_1^2 + p_2^2)},\\
E_0^{(3)} &= -\frac{rsk_1 p_1 (r^2 n_1^2 - s^2)(p_1 - p_2)\, E_0^{(1)}}{p_1 p_2 (r^4 n_1^4 + s^4) + r^2 n_1^2 s^2 (p_1^2 + p_2^2)},\\
E_0'^{(2)} &= \frac{rsk_1 p_1 (r^2 n_1^2 + s^2)(p_1 + p_2)\, E_0^{(1)}}{p_1 p_2 (r^4 n_1^4 + s^4) + r^2 n_1^2 s^2 (p_1^2 + p_2^2)}.
\end{aligned}
\tag{13}
$$

COEFFICIENTS OF REFLECTION AND REFRACTION OF LIGHT

In order to get the coefficients of light reflection (intensity), let us use the Umov-Poynting vector, which coincides in magnitude and direction with the energy flux

$$
\mathbf{S} = \frac{c}{4\pi}\,[\mathbf{EH}].
$$

Substituting the expression for $\vec{H}$ from (12) in the formula for $\vec{S}$, we will obtain

$$
\mathbf{S} = \frac{c^2}{4\pi\omega}\,[\mathbf{kE}^2 - \mathbf{E}(\mathbf{kE})]. \tag{14}
$$

At oblique incidence of light, the cross-section of the beam changes due to refraction. To comply with the law of conservation of energy, the normal component of the Umov-Poynting vector must be analyzed. Taking into account that in our case $k_2 = 0$, we obtain

$$
S_3 = \frac{c^2}{4\pi\omega}\left[k_3(E_1^2 + E_2^2) - k_1 E_1 E_3\right]. \tag{15}
$$

Calculating the normal components of the Umov-Poynting vector for the incident, reflected and refracted waves by using (15) and making the following substitutions $r^2 n_1^2 = u$ and $s^2 = v$, we obtain final expressions for the coefficients of reflection and refraction of light on the boundary of a twinned uniaxial transparent crystal, which are Fresnel formulas for the case of an interface between two **mirror-image symmetrical orientations of a uniaxial** transparent crystal, in a simple and symmetrical form

$$
\begin{aligned}
R_{\text{oo}} &= \frac{u^2 v^2 (p_1^2 - p_2^2)^2}{\left[p_1 p_2 (u^2 + v^2) + uv(p_1^2 + p_2^2)\right]^2},\\
D_{\text{oo}} &= \frac{p_1^2 p_2^2 (u^2 - v^2)^2}{\left[p_1 p_2 (u^2 + v^2) + uv(p_1^2 + p_2^2)\right]^2},\\
R_{\text{eo}} &= \frac{p_1 p_2 uv\,(p_1 - p_2)^2 (u - v)^2}{\left[p_1 p_2 (u^2 + v^2) + uv(p_1^2 + p_2^2)\right]^2},\\
D_{\text{eo}} &= \frac{p_1 p_2 uv\,(p_1 + p_2)^2 (u + v)^2}{\left[p_1 p_2 (u^2 + v^2) + uv(p_1^2 + p_2^2)\right]^2}.
\end{aligned}
\tag{16}
$$

The curves for coefficients of reflection of ordinary and extraordinary rays from the twinning plane, as a function of the angle of incidence of ordinary rays, are shown in figure 2. From (16), it is seen that when $p_2 = 0$, only reflected ordinary rays remain, i.e., there is a complete reflection of ordinary rays $R_{oo} = 1$. From (6) when $k_2 = 0$, we get an expression for the square of the normal component of the wave vector of the extraordinary wave

$$p_2^2 = \frac{\varepsilon^{(1)}\left[\varepsilon^{(3)}\left(\frac{\omega}{c}\right)^2 - k_1^2\right]}{\varepsilon^{(1)} p^2 + \varepsilon^{(3)} p^2}, \tag{17}$$

from which a simple formula follows for the angle, corresponding to complete reflection of an ordinary ray

$$\sin \alpha_0 = \frac{n_e}{n_0}. \tag{18}$$

Formula (18) can be used to determine the principal refractive index n_e of extraordinary waves in uniaxial transparent negative crystals [6] if n_0 is known from other measurements. When ordinary rays fall on the twinning plane at angles greater than the angle corresponding to complete reflection, p_2 becomes imaginary, which means that extraordinary rays have disappeared and that only rays of a single polarization are left, the reflected and refracted ordinary rays.

The derived formulas (16) and the curves of figure 2 indicate the absence of an analogy with the known Fresnel formulas for the case of an interface between two isotropic media.

The obtained formulas may be used in the study of phenomena taking place at the boundaries of elastic and residual twinning of uniaxial transparent crystals.

An investigation of the existence of a transition layer at the interfaces of mechanically twinned calcite crystals [7] was conducted by comparing the measured coefficients of reflection of ordinary rays from the twinning plane with those calculated from (16).

In conclusion, I express my gratitude to R. I. Garber for his suggestion of the topic of this work and for his constant attention to its progress.

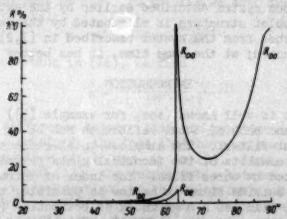

Angle of incidence

Figure 2. Curves of reflection coefficients of ordinary and extraordinary rays from the interface of a twinned uniaxial transparent crystal as a function of the angle of incidence of ordinary rays
R_{oo} - for ordinary rays; R_{oe} - for extraordinary rays

January 6, 1958

References

1. IA. V. DASHEVSKII: ZETF, 8, No. 8-9, 1007 (1938)
2. F. I. FEDOROV: DAN USSR, 84, 1171 (1952)
3. V. L. GERMAN: DAN USSR, 48, 95 (1945)
4. LORD RAYLEIGH: Phil. Mag., Ser. 5, 26, 241 (1888)
5. F. I. FEDOROV: Uch. Zap. BGU, 32, 169 (1957)
6. G. B. RAIS: Kristallografiia, 3, 101 (1958) (See Soviet Phys.-Crystallography, 3, 98 (1958))
7. G. B. RAIS: DAN USSR, 106, 841 (1956)

TOM VI, Vyp. 3 OPTIKA I SPEKTROSKOPIIA Mart, 1959
VOL. VI, No. 3 OPTICS AND SPECTROSCOPY March, 1959

On Elimination of the Doublet Structure of the Transmission Band in a Total-Reflection Light-Filter

P. G. KARD

Abstract: This paper develops the theory of a total-reflection light-filter of a new type, in which the doublet structure of the transmission band is eliminated. The new filter differs from those of the analogous system described earlier by the author [1,2], in that it has only two totally-reflecting layers. The doublet structure is eliminated by the use of auxiliary correcting layers. The new system is distinguished from the system described in [1,2] in the extreme simplicity of the principles on which it is constructed; at the same time, it has better characteristics.

INTRODUCTION

It is well known (see, for example [3]) that the phenomenon of total reflection can be applied to light-filters. The simplest total-reflection filter consists of two identical glass prisms separated by three films. The index of refraction of the outside films is as low as possible; the central film has a high index of refraction (equal to or higher than the index of refraction of the prisms, or at least only a little lower). The angle of incidence on the triple film should be large enough so that total reflection occurs at the outside films. For convenience, we call such a film totally reflecting, although in fact total reflection does not occur since the films are very thin. An apparatus of this type functions as a light filter; and the thicker the totally reflecting films, the narrower the transmission band (although it should be noted that there is an upper limit to the thickness of such films; this point is discussed in detail at the end of the present paper). Totally-reflecting filters have a number of advantages over filters of other types, but they have also one outstanding defect, arising from the doublet structure of the transmission band. Theory shows (see eq. (1) below) that in such a filter the position of the transmission band in the spectrum is determined by the phase shift occurring upon total reflection. Since the phase shift depends on the polarization of the incident light, there are two transmission bands instead of one, each linearly polarized and each possessing half the total intensity. This is the effect referred to as the doublet structure of the transmission band.

In two earlier papers [1,2] the author showed that this defect could be overcome by using more than two totally reflecting films in the multiple film layer between the prisms. With a suitable choice of the indices of refraction, thickness of film, and angle of incidence, both transmission bands can be made to coincide. In these systems, however, the angle of incidence must be very large, and the sharpness of the transmission band is too low. It is therefore desirable to find some other method. In the present paper it is shown that the doublet structure of the transmission band can be eliminated without increasing the number of totally reflecting films. The new process turns out to be simpler and more effective, since it allows the use of smaller angles of incidence and gives better contrast. Moreover, it has other advantages.

We first write down a number of equations relating to filters employing three films. For simplicity, we suppose that the index of refraction of the central layer is equal to the index of refraction of the prisms. Then, if we neglect absorption, which we assume to be sufficiently small, we may write

$$\frac{R}{D} = \frac{4R_1}{D_1^2}\sin^2(\beta-\mu) = \frac{4\cos^2\psi\,\mathrm{sh}^2\gamma\sin^2(\beta-\mu)}{\cos^2\mu\,\sin^2\psi} \tag{1}$$

Here R and D are the energy coefficients of the filter for reflection and transmission; R_1 and D_1 are the corresponding coefficients for the half-filter, i.e. in this case for one of the totally reflecting films, bounded on both sides by a medium with index of refraction equal to that of the prism. Also

$$\beta = knh\cos\vartheta, \tag{2}$$

$$\mathrm{tg}\,\mu = \mathrm{cth}\,\gamma\,\mathrm{tg}\,\psi, \tag{3}$$

$$\gamma = kh_1\sqrt{n^2\sin^2\vartheta - n_1^2}. \tag{4}$$

ψ is the phase shift occurring on total reflection; k is the wave number in vacuo, ϑ is the angle of incidence; n, h are the index of refraction and the thickness of the central film; and n_1, h_1 are the index of refraction and the thickness of the totally reflecting layers. Finally, we note that μ in (1) and (3) is the phase of the complex quantity $\frac{r_1}{d_1^2}$, where r_1 and d_1 are the amplitude coefficients of reflection and transmission for the half-filter.

Since equation (1) differs very little from the corresponding formula in reference [1] we do not repeat the derivation here.

The spectral position of the triple-film filter is, according to (1), given by the equation

$$\beta - \mu = l\pi, \tag{5}$$

where l is a non-negative integer. The doublet structure of the transmission band arises from the dependence of μ on the polarization, as indicated by (3).

1. A NEW TYPE OF TOTALLY-REFLECTING LIGHT-FILTER

To eliminate the doublet structure of the transmission band in a triple-film filter we try introducing four auxiliary correcting films (not totally-reflecting), one on either side of each of the two totally-reflecting films. If we denote the index of refraction of these correcting films by n_k, the filter can be described schematically by the product $(n\ n_k\ n_1\ n_k\ n\ n_k\ n_1\ n_k\ n)$. It differs from the triple-film in that the simple totally-reflecting film is replaced by the combination $n_k\ n_1\ n_k$; in other words, the half-filter in the new form is a triple layer in place of the previous single layer.

We write

$$kn_2h_2\cos\vartheta_2 = \pi, \tag{6}$$

where ϑ_K is the angle of incidence on the correcting films, and h_K the thickness of the films.

We now write an equation completely analogous to the first part of equation (1)

$$\frac{R}{D} = \frac{4R_3}{D_3^2}\sin^2(\beta - \nu), \tag{7}$$

where R, D, R_3, and D_3 are the energy coefficients of reflection and transmission of the new seven-layered filter and of the corresponding half-filter, and ν is the phase angle of the quantity $\frac{r_3}{d_3^2}$, where r_3 and d_3 are the amplitude coefficients for reflection and transmission of the half-filter. We must now calculate the quantities $\frac{r_3}{d_3^2}$ and $\frac{1}{d_3}$. These will yield the values of $\frac{R_3}{D_3^2}$ and ν. The calculation is conveniently carried out by the use of Vlasov's recurrence equations [4]. The amplitude coefficients for reflection and transmission at the boundaries of the layers $n\,n_c$, $n_c\,n_1\,n_c$, and $n_c\,n$ will be denoted by $\exp(-i\psi_K)$, $-\exp(-i\psi_K)$ and $-\rho$ (where ψ_K is the phase shift on total reflection at the boundary of the layers $n_K n_1$); the amplitude coefficients for transmission are therefore $\sqrt{1-\rho^2}$ and $\sqrt{2i}\sin\psi_K\exp(-i\psi_K/2)$. From this, taking account of equations (4) and (6), we find

$$\frac{r_3}{d_3} = \frac{e^{-\frac{i\varphi}{2}}\{[1+\rho^2+2\rho\cos(2\delta-\psi_K)]e^{i}-[1+\rho^2+2\rho\cos(2\delta+\psi_K)]e^{-i}\}}{2(1-\rho^2)\sin\psi_K}; \tag{8}$$

$$\frac{1}{d_3} = \frac{-e^{-\frac{i\varphi}{2}}\left[\left(e^{-i\left(i-\frac{\psi_K}{2}\right)}+\rho e^{i\left(i-\frac{\psi_K}{2}\right)}\right)^2 e^{i}-\left(e^{-i\left(i+\frac{\psi_K}{2}\right)}+\rho e^{i\left(i+\frac{\psi_K}{2}\right)}\right)^2 e^{-i}\right]}{2(1-\rho^2)\sin\psi_K} \tag{9}$$

Moreover, to simplify the whole theory we choose the thickness of the correcting layers so that $\delta = \frac{\pi}{2}$, i.e.

$$h n_K h_K \cos\vartheta_K = \frac{\pi}{2} \tag{10}$$

Under these conditions, multiplying (8) and (9) together, we find for the phase angle of $\frac{r_3}{d_3^2}$

$$\operatorname{tg}\nu = \operatorname{cth}\gamma\cdot\frac{(1-\rho^2)\sin\psi_K}{(1+\rho^2)\cos\psi_K - 2\rho},\quad 0<\nu<\pi. \tag{11}$$

This equation can be simplified. We write

$$\operatorname{tg}\frac{\varphi}{2} = \frac{1+\rho}{1-\rho}\operatorname{tg}\frac{\psi_K}{2} \tag{12}$$

and it follows from (11) that

$$\operatorname{tg}\nu = \operatorname{cth}\gamma\operatorname{tg}\varphi. \tag{13}$$

We must also calculate $\frac{R_3}{D_3^2}$. We find first from (8), taking account of (10) and (12),

$$\frac{R_3}{D_3} = \frac{\operatorname{sh}^2\gamma}{\sin^2\varphi} \tag{14}$$

from this follows

$$\frac{R_3}{D_3^2} = \frac{\operatorname{sh}^2\gamma(\operatorname{sh}^2\gamma+\sin^2\varphi)}{\sin^2\varphi} \tag{15}$$

Substituting this expression in (7), we have

$$\frac{R}{D} = \frac{4\operatorname{sh}^2\gamma(\operatorname{sh}^2\gamma+\sin^2\varphi)\sin^2(\beta-\nu)}{\sin^2\varphi} \tag{16}$$

It is worth noting that this equation can be rewritten so as to be completely analogous to the second part of (1). To do this we note that according to (13)

$$\operatorname{sh}^2\gamma + \sin^2\varphi = \frac{\cos^2\varphi\operatorname{sh}^2\gamma}{\cos^2\nu} \tag{17}$$

Substituting in (16), we find

$$\frac{R}{D} = \frac{4\cos^2\varphi\operatorname{sh}^2\gamma\sin^2(\beta-\nu)}{\cos^2\nu\sin^2\varphi} \tag{18}$$

The difference between this and equation (1) consists solely in the fact that here we have φ and ν in place of ψ and μ in (1). Also, according to (3) and (13), the relationship between φ and ν is identical to the relationship between ψ and μ. Therefore, our new filter acts exactly like the old three-layer filter, with one exception--that instead of a phase shift of magnitude ψ on total reflection, we have the phase shift φ defined by (12). The effect of the correction layers is confined, therefore, to changing the magnitude of the phase shift from ψ to φ.

By using this effect we can eliminate the doublet structure of the transmission band, since φ can be made the same for both polarizations. It is necessary only to make a suitable choice of the index of refraction n_K. No constraints are placed on the angle of incidence or on the thickness of the totally-reflecting films.

2. ELIMINATION OF THE DOUBLET STRUCTURE OF THE TRANSMISSION BAND

Denoting parallel and perpendicular polarization by subscripts $\parallel$ and $\perp$, we write the conditions for absence of doublet structure according to equation (12) as

$$\frac{1+\rho^{\parallel}}{1-\rho^{\parallel}}\operatorname{tg}\frac{\psi_K^{\parallel}}{2} = \frac{1+\rho^{\perp}}{1-\rho^{\perp}}\operatorname{tg}\frac{\psi_K^{\perp}}{2}$$

Substituting the expressions $\rho^{\parallel}$, $\rho^{\perp}$, $\operatorname{tg}\frac{\psi_K^{\parallel}}{2}$, and $\operatorname{tg}\frac{\psi_K^{\perp}}{2}$, we find

$$n_K = (n n_1)^{\frac{1}{2}} \tag{19}$$

This [together with equation (10), which determines the thickness of the correction layer] is the condition for the absence of the doublet structure. In principle, it is relatively easy to realize this condition. It is to be noted that in our new filter the doublet structure is eliminated by the choice of parameters relating only to the auxiliary layers. All other parameters may remain as they were in the three layer filter (it is only necessary that the angle of refraction φ_K in the correction layers should be real).

When equation (19) is satisfied, (12) yields the relationship

$$\cos\frac{\varphi}{2} = \frac{n_1 - n\sin^2\vartheta}{(n-n_1)\sin\vartheta} \tag{20}$$

This equation defines φ directly as a function of n, n_1, and φ. The fact that φ does not depend

on the polarization is not the only property that distinguishes it from ψ. Another property is that it may be chosen to be close to 180°. Although ψ may be chosen near to 180°, it is then necessary that the angle of incidence be close to 90°. When φ is chosen to be close to 180°, on the other hand, it is only necessary that ϑ_K be close to 90°. This follows from the fact that the numerator of the right hand side of (20) is equal to $n_1 \cos \vartheta_K$

3. WIDTH OF THE TRANSMISSION BAND OF THE FILTER

Let us return to equation (18). As in equation (5), the position of the transmission band in the spectrum is defined by the equation

$$\beta - \nu = l\pi \tag{21}$$

where l is a non-negative integer. We determine the half-width of the transmission band by putting $\beta = l\pi + \nu + \Delta\beta$ and $\frac{R}{\beta} = 1$. Since $\frac{\Delta\lambda}{\lambda} = \frac{\Delta\beta}{\beta}$,

$$\frac{\Delta\lambda}{\lambda} = \frac{D}{2[(l\pi + \nu)\cos\gamma \operatorname{sh}^2\gamma]} \tag{22}$$

It follows that the transmission band narrows as γ increases; that is, in accordance with (4), as the thickness of the totally-reflecting film is increased. This is understandable, since the same thing occurs in the three-layer filter. An important characteristic of the new filter, however, consists in an additional method for narrowing the transmission band. This method lies in choosing the angle of incidence so that φ is close to 180°. As we observed at the end of paragraph 2, this means that the angle of refraction ϑ_K should be close to 90°. It seems probable that this additional possibility will allow narrower transmission bands in the new filter than have ever been achieved with three-layer filters. Although the transmission band of a totally-reflecting three-layer filter can theoretically be made as narrow as we please, it turns out in practice (see [5]) that as the thickness of the totally-reflecting layer is increased, the width of the transmission band decreases only down to a certain limit. Attempts to decrease the width still further result in no decrease in band width but a sharp decrease in intensity. The filter therefore becomes practically opaque.

The cause of this discrepancy between theory and experiment lies apparently in variations in the thickness of the layers (see [3]), which are relatively more significant in thick layers than in thin. Since the filter described in this paper allows us to arrive at a given band width with thinner films, the influence of inhomogeneities should be smaller. Thus one might hope that the limit on the band width imposed by inhomogeities in thickness of the films would be smaller for the present filter than for the previous three-layer type.

One further remark is in order. A third method for narrowing the transmission band consists in using the highest possible order of interference l. The higher the order, however, the harder it is to exclude secondary maxima from the transmission band, since they lie closer to the principal transmission band. The new filter, which makes use of two independent methods for narrowing the transmission band, does not require the use of high-order interference. The secondary maxima are therefore far from the principal band, and there is no particular difficulty in suppressing them (if they do not eliminate themselves--- see below).

To illustrate these remarks, we present a numerical example. Let $\vartheta = 60^\circ$, $n = 1.7$, $n_1 = 1.3$. Then, according to (19), $n_K = 1.487$. We choose the thickness of the totally reflecting layer to be $\frac{\lambda}{2n_1}$; then $\gamma = 1.670$. We find from (20) and (13): $\varphi = 171^\circ 43'$, $\nu = 171^\circ 7'$. Setting $\beta = \nu$, (that is, $l = 0$), we find from (22)

$$\frac{\Delta\lambda}{\lambda} = \frac{1}{1900}$$

For variations in wave length, the quantities β, γ, and δ vary proportionately to the wave number (if we neglect dispersion). Making use of this fact, we can determine the secondary transmission maxima from (7) [these do not coincide for different polarizations, since (10) is far from being satisfied]. In this example it turns out that the nearest maximum on the short wavelength side is at approximately $\sim 0.61\lambda$, where λ is the wavelength of the principal transmission band. on the long wavelength side the nearest maximum is at approximately 4.1λ. It is clear that, using the lowest order interference, the presence of secondary maxima is not a serious problem. In particular, if the transmission band is at or near the limit of narrowness, the intensity of the short wavelength secondary bands should be very low, since in theory they should be much narrower than the principal band in accordance with (22), and narrowing the transmission band below the limit leads, as we have seen, to a sharp decrease in intensity.

April 11, 1958

References

1. P. G. KARD: IAN ESSR, 6, 344 (1957)
2. P. G. KARD: OIS, 4, 643 (1958)
3. G. V. ROZENBERG: UFN, 47, 173 (1952)
4. A. G. VLASOV et al.: Prosvetlenie Optiki (Optics made clear) Gostekhizdat, Lenin., 1946
5. A. F. TURNER: J. Phys. Rad., 11, 444 (1950)

TOM VI, Vyp. 3 OPTIKA I SPEKTROSKOPIIA Mart, 1959
VOL. VI, No. 3 OPTICS AND SPECTROSCOPY March, 1959

On the Threshold of Sensitivity of an Infrared Absorption Gas Analyzer with Gas Modulation

A. O. SALL'

Abstract: A single flow absorption infrared gas analyzer is described, in which the quantity of the component to be determined of the mixture being analyzed in the flow path, varies periodically. The dependence has been investigated of the threshold sensitivity of such a gas analyzer on the threshold sensitivity of the radiation receiver being used, the length of the working chamber and the absorption coefficient of the component to be determined. A formula has been obtained to calculate the threshold response.

The sensitivity of a two-stream infrared absorption gas analyzer [1-5] is usually limited by the possibility of a random change in one of the radiation flows (or a different change in both radiation flows), which leads to a shift in the zero point of the absorption meter scale. Such random changes cause the appearance of a false signal, which appear as a change in the concentration of the component to be determined in the mixture being analyzed. In order to increase the sensitivity of the gas analyzer (in order to eliminate the influence of different changes in the radiation flows being used for the analysis), it was proposed earlier [6] to use just one radiation flow. This radiation flow is passed through the operating chamber with the mixture being analyzed and is directed to the radiation receiver. The quantity of molecules of the component to be determined, which is in the working chamber in the path of the radiation flow, varies periodically. This can be accomplished, for example, either by periodically changing the length of the working chamber or by changing the pressure of the gas mixture being analyzed or, finally, by alternately admitting the mixture to be analyzed and the comparison mixture, which does not contain the component to be determined, to the working chamber at a definite frequency. The radiation receiver should be constructed so that it can react only to periodic changes in the radiation flux. An alternating signal of the same frequency will occur in the radiation receiver. The concentration of the component to be determined is found according to the signal magnitude.

The method of gas modulation using periodic changes in the pressure of the gas mixture being analyzed in the working chamber was recently described abroad also [7].

All the above mentioned methods of gas modulation have one essential deficiency: namely, as the total quantity of the component to be determined changes in the path of the radiation flux, the quantity of molecules of the components not to be determined which absorb radiation also changes. In many cases, this deficiency limits the sensitivity of the absorption gas analyzer. For example, let the concentration of the interfering component (i.e. other than the component whose analysis is desired) in the mixture being analyzed be within limits up to 1 per cent by volume. For simplicity of reasoning, let us consider that the interfering component and that to be determined absorb infrared radiation approximately with the same intensity and that the absorption bands of these components are not superposed, in practice. Then, as computations and experiments show, the absolute sensitivity of finding the concentration of the component to be determined in the mixture being analyzed by using the optico-acoustic gas analyzer will be of the order of magnitude 10^{-5} - 10^{-6} % (vol,) in the best case. If the absorption bands of the components are superposed, then the sensitivity of the absorption meter will be even less.

In order to increase the sensitivity of an absorption gas analyzer by gas modulation, it is necessary to proceed in such a way that the periodic change in the quantity of molecules of the component to be determined in the path of the radiation flux will not be accompanied by a periodic change in the quantity of molecules of the interfering component. This can be realized if the component to be determined were to be removed from the d a mixture being analyzed (for example, by chemical absorption) without, in practice, removing the interfering components.

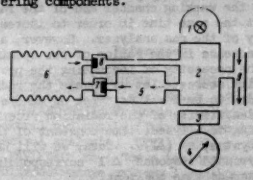

Diagram of the principle of a single-flow absorption gas analyzer with gas modulation

The principle of the absorption meter is presented in the sketch. The radiation flux from the source 1 is directed through the working chamber 2 into the radiation receiver 3. A recording instrument 4 is connected to the output of the radiation receiver. A system, including the apparatus 5 to remove the component to be determined from the mixture being analyzed (for example, by chemical absorption), a periodically changing pulsator volume 6 with two valves 7 and 8 which pass the mixture in just one direction (indicated by arrows on the sketch), is used to change periodically the content of the component to be determined in the working chamber. During the half-cycle when the pulsator volume is increasing, the mixture being analyzed is sucked into the pulsator from the mainline 9, in which the mixture flows continuously, by going through the working chamber, the apparatus to change the content of the component to be determined in the mixture being analyzed and the valve 7. The valve 8 prevents the mixture going from the working chamber into the pulsator and bypassing the apparatus to remove the component to be determined from the mixture. During the other half-cycle, the pulsator volume diminishes and the mixture from which the component to be determined has been eliminated is ejected through the valve 8 into the working chamber.

In those cases when the duration of the process to eliminate the component to be determined from the mixture being analyzed in the apparatus 5 can be made less than the period required to modulate the radiation flux, the system for the periodic replacement of the mixture can consist of just the series-connected pulsator and the apparatus to remove the component to be determined from the mixture. In these cases, the valve 8 and the pipes connecting it to the working chamber and the pulsator and the valve 7 too are absent.

Let us consider the threshold sensitivity of a gas analyzer with gas modulation.

When a selective optico-acoustic receiver is used in infrared gas analyzers, the signal, which occurs because of the fluctuation of the number of quanta in the flux, will not exceed the threshold signal corresponding to the threshold sensitivity of the receiver. The sensitivity of a gas analyzer with a selective receiver and gas modulation is consequently, limited by the fluctuating noise in the radiation receiver. Let us consider that the diameter of the opening of the radiation receiver equals the diameter of the opening of the working chamber. Then it can be shown that it is necessary to increase the radius of the opening of the working chamber and of the radiation receiver at the same time in order to increase the sensitivity of the gas analyzer. However, a significant increase in the radius of the opening leads to the necessity of increasing the power of the radiation source. Let us assume the radius of the window to be $r = 1$ cm. Let us denote the threshold sensitivity of the radiation receiver, corresponding to a 1 sec. time constant of the recording system, by $(\Delta I)_1$. Then, we will have for the threshold response ΔI corresponding to a t seconds time constant:

$$(\Delta I) = \frac{(\Delta I)_1}{\sqrt{t}} \tag{1}$$

As has been shown before [8], in determining the magnitude of the acoustic pressure occurring in the radiation receiving cylinder of a selective optico-acoustic radiation receiver, it is necessary to take into account that the heat being liberated in a layer of gas at the opening to the chamber, is eliminated to the window and does not participate in the excitation of acoustic vibrations. Let us designate this layer as "passive". The quantity of thermal power being used to heat the absorbing gas in the radiation receiver changes, as the concentration of the component to be determined changes by Δc in the mixture being analyzed, by

$$\epsilon\left[\int_0^\infty I_\nu k(e^{-\eta k v} - e^{-k v})d\nu\right] L\Delta c \tag{2}$$

where I_ν is the spectral intensity of the radiation flux; k the absorption coefficient of the component to be determined; L the path length of a ray in the working chamber; v the product of the ray path length in the radiation-receiving cylinder of the radiation receiver by the concentration of the component absorbing the radiation in the mixture filling the receiver chamber; η the ratio of the thickness of the passive layer at the opening of the radiation receiver to the ray path length in the radiation-receiving cylinder; ϵ a numerical coefficient.

The numerical value of the coefficient ϵ is determined by a specific technique of carrying out the method of periodically changing the quantity of molecules of the component to be determined in the path of the radiation flux. If the modulation is accomplished by a periodic change in the length of the working chamber without any change in the mixture pressure, in practice, then ϵ can be considered equal to 1. When a method is used which periodically replaces the mixture being analyzed containing the component to be determined by a mixture without the component to be determined in the working chamber, then also $\epsilon = 1$ (if the gas pressure in the chamber changes insignificantly). If the modulation is performed by a periodic change in the pressure of the gas mixture being analyzed, then ϵ depends on the amplitude of the pressure change. It can be considered that $\epsilon = 1$ when the pressure changes from zero to atmospheric. As the pressure rises periodically from atmospheric, ϵ approximately equals the ratio of the magnitude of the pressure change to atmospheric pressure, if the effect of a change in the absorption spectrum of the component to be determined is not taken into account as the pressure changes.

Analyzing the solution of a generalized heat transmission equation [8], the following can be shown: If the cut-off frequency is so large that the depth of penetration of the temperature vibrations is considerably less than the depth of the radiation-receiving cylinder, then the thickness of the passive layer equals one-half the depth of penetration of the temperature vibrations. If $\eta \ll 1$, then such a concentration of the component to be determined can be selected in the radiation receiving chamber that we will have

$$e^{-\eta k v} - e^{-k v} \simeq 1 - \eta k v \simeq 1$$

within the limits of the fundamental part of the line of the absorption band of the component to be determined.

Then we will obtain in place of (2)

$$\epsilon\left[\int_0^\infty I_\nu k d\nu\right] L\Delta c \tag{3}$$

It can be considered a first approximation that the spectral intensity I_ν is constant within the limits of the absorption band of the component to be determined. Then, equating expressions (1) and (3), we obtain:

$$\Delta c = \frac{(\Delta I)_1}{\epsilon L I_\nu\left(\int_0^\infty k d\nu\right)\sqrt{t}} = \frac{A}{\epsilon L\sqrt{t}}, \tag{4}$$

where A is a constant independent of the effective chamber length and the time constant of the recording apparatus.

If the threshold response Δc is expressed in per cent by volume, the chamber length in mm, and the time in seconds, then the numerical values of A do not usually exceed an order of magnitude of 10^{-4} [for $(\Delta I)_1 = 10^{-8}$ W]. Putting $\epsilon = 1$, $L = 100$ mm, $t = 60$ sec., we obtain $\Delta c \leq 10^{-6}$%. Formula (4) is

also applicable to computations of the threshold response of an optico-acoustic gas analyzer in the case of low enough cut-off frequency (at least to an order of magnitude accuracy).

Now, let us dwell on the case of using a non-selective optico-acoustic radiation receiver in an infrared gas analyzer whose film absorbs almost all the radiation incident thereon. When using sufficiently powerful non-selective sources of radiation, it is necessary to filter out the ballast radiation not being absorbed by the component to be determined. Otherwise, the fluctuations of the number of quanta being absorbed by the receiver film can be higher than the threshold response of the radiation receiver.

As the film absorbs radiation, it and the surrounding gas are heated. Let the radius of the base of the cylindrical chamber be 1 cm and the depth $l = 0.8$ cm. Let us consider that the chamber is filled with air. Then, in order that the temperature drop ϑ_m between the film and the wall of the chamber does not exceed 100°, the radiation flux being absorbed by the film must be not more than

$$G_m \vartheta_m = \left(\frac{8\pi\lambda r^2}{l} + 4\pi\lambda l\right)\vartheta_m \simeq 1W$$

where G_m is the heat conduction referred to maximum temperature; λ is the thermal conductivity of the gas filling the radiation receiving chamber.

In order to diminish overheating of the absorbing film and the gas surrounding it by the radiation flux directed at the film, it is also necessary to filter out the ballast radiation which is not absorbed by the component to be determined.

The sensitivity of a non-selective optico-acoustic radiation receiver at low enough cut-off frequency is somewhat higher than the sensitivity of a selective receiver. Consequently, if the flux of the useful radiation (the radiation absorbed by the component to be determined) is insignificantly diminished during the filtration of the ballast radiation, then the sensitivity of a gas analyzer with gas modulation and with a non-selective radiation receiver can be somewhat greater than the sensitivity of a gas analyzer with a selective optico-acoustic receiver. However, this can only occur in the analysis of mixtures with low content of the interfering component absorbing the radiation. In analyzing mixtures with a high content of the interfering component, the sensitivity of a gas analyzer with a non-selective radiation receiver will be limited not by the sensitivity of the receiver but by the possibility of changing the concentration of the interfering component in the mixture being analyzed, which can lead to a change in the reading of the gas analyzer.

If a gas analyzer with gas modulation and the usual two-stream gas analyzer without gas modulation with a movable mechanical cut-off have the same working chamber lengths, then the sensitivity of the latter, limited by the instability of the zero point of the scale, will be several orders of magnitude lower [9]. Increasing the length of the working chamber and raising the pressure of the mixture being analyzed therein, the sensitivity of the usual two-stream gas analyzer without modulation can be made almost the same as for a gas analyzer with modulation in certain cases. However, this increase in the sensitivity can be achieved only by a costly complication in the construction of the gas analyzer.

May 9, 1958

References

1. M. L. VEINGEROV: DAN USSR, 19, 387 (1938) (In English)
2. M. L. VEINGEROV: Za. Lab., No. 4, 426 (1947)
3. V. M. CHULANOVSKII: Vvedenie v molekuliarnyi spektral'nyi analiz (Introduction to molecular spectral analysis) GTTI, 1950, p. 201
4. V. A. PAVLENKO: Sb.: Novye teploenergeticheskie proizvodstvennye pribory i reguliatory. Edited by Kremlevskii. (New thermal power production instruments and regulators) Mashgiz, 1953
5. V. A. PAVLENKO: Zav. Lab., No. 7, 868 (1954)
6. A. O. SALI': Zaiavka (Claim) MMIP USSR, No. 27226 of Feb. 8, 1955;
   Zaiavka, No. 27233 of Feb. 14, 1955
   Priborostroenie, No. 6, 14 (1956)
7. H. HUMMEL: Chemie-Ingenieur-Technik, No. 12, 776 (1957)
8. A. O. SALI': ZTF, 26, No. 1, 157 (1956) (See Sov. Phys.-Tech. Phys., or RT-4271)
9. A. O. SALI': Priborostroenie, No. 9, 12 (1956)

TOM VI, Vyp. 3 ОПТИКА ИСПЕКТРОСКОПИИ Mart, 1959
VOL. VI, No. 3 OPTICS AND SPECTROSCOPY March, 1959

A High Intensity Atomic Beam Light Source

A. I. ODINTSOV

Abstract: This paper describes the design and construction of an atomic beam light source in which excitation is provided by electron bombardment. This instrument has a light yield considerably greater than devices used hitherto. A calculation is made of the intensity of the luminescence of atomic beams excited by electron bombardment, on the basis of which conclusions are drawn concerning the proper dimensions and location of the slits which shape the beam. Experiment has shown that the present atomic beam light source gives an extremely intense luminescence.

Atomic beam light sources, which allow one to obtain lines of width close to the natural width of spectral lines, solve a great many problems of importance to high resolution spectroscopy. However, because of the low intensity of luminescence given by atomic beams, only the brightest lines of elements could be investigated with them up to now.

The present work was an attempt to create an atomic beam with electron bombardment which would give an intense luminescence over a prolonged period of time.

CALCULATION OF INTENSITY OF LUMINESCENCE OF ATOMIC BEAMS WITH ELECTRON BOMBARDMENT

The theory of atomic beams as light sources was developed by Minkowski and Bruck [1]. They obtained an expression for the distribution of intensity over a spectral line produced by an atomic beam as a function of wavelength. However, in view of the complexity of the calculations, the authors limited themselves to the particular case in which the slits shaping the beam are parallel to the direction of observation.

The logical design and placement of slits has never before been carefully studied. In most atomic beam sources [2-4], including Minkowski and Bruck's, the slits were arranged parallel to the line of observation. However, such an arrangement, as will be shown below, leads to low intensity, especially with highly collimated beams.

The construction of the electron bombardment atomic beam device is depicted schematically in figure 1, where F_1 is the orifice of the oven in which the substance under investigation is evaporated, F_2 is the orifice in the aperture diaphragm forming the atomic beam. We restrict ourselves to the case which is the most important in practice, i.e., that in which F_1 and F_2 are rectangles with parallel sides. The beam of atoms travels along the z-axis, the bombarding electrons flow along the y-axis and the luminescence of the beam is observed along the x-axis at a distance l from the orifice of the oven (at point M on fig.1.).

The dimensions of the apertures s_1 and s_2 along the line of observation and the distance between them, h, define the collimation α of the atomic beam

(1) $$\alpha = \frac{s}{h}$$

where s is the greater of the quantities s_1 and s_2.

Let us recall that the Doppler width of a line emitted by an atomic beam is proportional to the degree of collimation of the beam α.

The integrated intensity of any spectral line emitted by an atomic beam excited by electron bombardment is defined by the expression*

(2) $$I = C\int n(x)\,dx \cdot jq,$$

where $n(x)$ is the density of atoms in the beam along the line of sight ($y = 0$, $x = l$), j is the density of the electron beam, q is the value of the excitation function of the atoms and C is the numerical coefficient including the transition probability and the quantum number of the spectral line under investigation. For simplicity, it is assumed that the density of the electron current is uniform over the entire cross-section of the atomic beam.

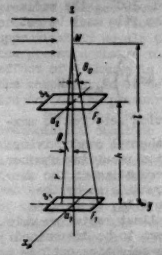

Figure 1. Method of arrangement of the components of the atomic beam. The direction of motion of the electrons is shown by the parallel arrows

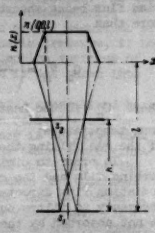

Figure 2. Density distribution of atoms $n(x)$ in the atomic beam

Introducing the notation $f_a = \int n(x)\,dx$, let us write (2) in the form

(3) $$I = C \cdot f_a \cdot jq.$$

The factor jq characterizes the efficiency of excitation of the atoms of the beam by electron bombardment, which is the case investigated by us. f_a defines the intensity of the atomic beam proper as a light source, regardless of the manner in which the atoms are excited.** For a given efficiency of excitation of the beam, the intensity of the beam f_a is proportional to the integrated intensity of the spectral lines emitted by the beam. For beams used in the absorption method, the intensity of the beam is proportional to the integrated absorption coefficient of the line in the beam.

The distribution of the density of atoms along the line of observation, $n(x)$, can be represented to a good degree of approximation by a trapezoid (see fig. 2). It can easily be shown that this gives the equation

(4) $$\int n(x)\,dx = n(0,0,l)\,s_2\,\frac{l}{h},$$

where $n(0,0,l)$ is the density of atoms on the axis

* More precisely, I is the brightness of an atomic beam light source for a given line.

** It is assumed that the bombardment is uniform over the entire depth of the beam along the line of observation.

of the beam at point M $(x = 0,\ y = 0,\ z = l)$.

The density of atoms $n(0,0,l)$ on the axis of the beam may be calculated from the formula (see fig. 1):

$$n(0,0,l) = \frac{n_0}{4\pi} \iint_{F_1} \frac{\cos\theta}{r^2}\, dF. \tag{5}$$

where n_0 is the density of atoms in the oven [5].

If $s_1 \ll l$, then to a good degree of approximation, we can write:

$$n(0,0,l) = \frac{n_0}{2\pi}\frac{s_1}{l}\sin\theta_0 \quad \left(\theta_0 = \operatorname{arctg}\frac{s_1}{2l}\right). \tag{6}$$

Also, if $a_1 \ll l$, then approximately,

$$n(0,0,l) \approx \frac{n_0}{4\pi}\frac{F_1}{l^2} \quad (F_1 = a_1 s_1). \tag{7}$$

Substituting (6) into (4), we obtain an expression for the intensity of the atomic beam

$$i_a = \frac{n_0}{2\pi}\frac{s_1 s_2}{h}\sin\theta_0. \tag{8}$$

If $a_1 \ll l$, we will have

$$i_a = \frac{n_0}{4\pi}\frac{a_1 s_1 s_2}{hl}. \tag{9}$$

For the particular case $s_1 = s_2$, equation (9) agrees with the more precise formula of Minkowski and Bruck [1].

From the theory of atomic beams [5], it follows that at least one of the linear dimensions s_1 and a_1 of the orifice of the oven must not exceed the mean free path of the atoms within the oven; otherwise the operation of the beam is disrupted. This condition is expressed by:

$$n_0 d < \frac{0.7}{\pi\sigma^2}, \tag{10}$$

where d is the smaller of the dimensions s_1 and a_1 and σ is the effective diameter of the atoms.

The density of the atoms in the oven, n_0, may not be increased above the maximum value defined by condition (10). The second dimension of the output orifice of the oven is arbitrary; this opening is therefore usually made in the shape of a long, narrow slit. The slit width, according to (6) and (7), has no influence on beam density; the maximum attainable density of atoms in the beam is determined only by the length of the slit.

The low intensity of luminescence of atomic beams is explained by the fact that the atomic density in these beams is very small. For example, if we take $\sigma = 3\times10^{-8}$ cm and a slit length of 1 cm, then at a distance of 5 cm from the slit the density of the atoms in the beam is only $\sim 7.8\times10^{11}$ cm^{-3}. This density corresponds to a pressure of 2.4×10^{-5} mm Hg (at room temperature).

In order to increase the density of atoms in the region of bombardment of the beam, it is necessary to increase the length of the oven slit, for given values of the distances l and h. If the oven slit is situated in the beam parallel to the line of observation of luminescence (this case was examined by Minkowski and Bruck), then the length s_1 of the oven slit is restricted by the degree of collimation of the beam α, since s_1 must be $\leq \alpha h$. The impossibility of using long slits in this case causes low beam intensity (particularly for highly collimated beams. Inserting $n_0 a_1 = \frac{0.7}{\pi\sigma^2}$ $(a_1' \leq a_1')$ into (9), we obtain

$$i_a' = \frac{0.7}{4\pi\sigma^2}\frac{s_1 s_2}{hl}. \tag{11}$$

for the maximum beam intensity attained in this case.

For a given degree of collimation of the beam α', defined by (1), i_a' will be greatest if $s_1' = s_2' = s'$. Under these conditions, we will have

$$i_a' = \frac{0.7}{4\pi\sigma^2}\alpha'\frac{s'}{l} \tag{12}$$

or

$$i_a' = \frac{0.7}{4\pi\sigma^2}\alpha^2\frac{h'}{l}. \tag{13}$$

From the last formula it is clear that the beam intensity quickly decreases with a decrease in the beam collimation α (proportionally to α^2).

In order to permit the use of long slits, it is necessary to orient the oven slit perpendicularly to the line of observation of luminescence. In this case the slit length a_1 is not tied in with beam collimation and the slit may be made long.

Inserting $n_0 s_1 = \frac{0.7}{\pi\sigma^2}$ $(s_1'' < a_1'')$ into (8), we find that for such a beam, the maximum intensity i_a'' will be

$$i_a'' = \frac{0.7}{2\pi\sigma^2}\frac{s_2}{h''}\sin\theta_0.$$

or

$$i_a'' = \frac{0.7}{2\pi\sigma^2}\alpha''\sin\theta_0. \tag{14}$$

The beam intensity i_a'' decreases as the first power of the degree of collimation α. The quantity $\sin\theta_0 \approx \frac{a_1}{2l}$ may be chosen sufficiently large. Therefore, in the atomic beam apparatus whose construction is described below, the oven slit was situated perpendicularly to the line of observation of luminescence.* The ratio $\frac{a_1}{l}$ was 0.43 and $\sin\theta_0 = 0.21$.

Comparing the beam intensities i_a'' and i_a' with identical collimation $\alpha'' = \alpha'$, (13) and (14) give us

$$\frac{i_a''}{i_a'} = \frac{2\sin\theta_0}{\alpha}\cdot\frac{l'}{h'} \approx \frac{\frac{a_1''}{l''}}{\frac{s_1'}{l'}}. \tag{15}$$

Inserting $\sin\theta_0 = 0.21$ and assuming $\frac{l}{h} = 1.2$, we find that with $\alpha = 0.1$, $\frac{i_a''}{i_a'} \approx 5$; $\frac{i_a''}{i_a'} \approx 10$ for $\alpha = 0.05$, etc. Clearly, it is possible to use even larger values of $\frac{a_1}{l}$ with an even greater increase in beam intensity.

Therefore, it may be concluded that to attain atomic beams with a high intensity of luminescence it is necessary to orient the output aperture of the oven perpendicularly to the line of

---

* The advisability of orienting the slits perpendicularly to the line of observation was indicated to the author by F. A. Korolev.

observation and to take the slit length a_1 sufficiently large so that the ratio a_1/l will be large.* Incidentally, this orientation of slits was not used in any of the electron bombardment atomic beam devices described above, even though it was used in the absorption method [6, 7].

In another series of experiments, a circular oven aperture was used [8]. From the viewpoint of beam-shaping, the circular output aperture really does not differ from the rectangular one, for which formulas (11) - (13) are appropriate.

The formulas derived for the intensity of atomic beams define, in conjunction with (3), the integrated intensity of the emitted spectral lines. Minkowski and Bruck [1] obtained the following expression ($s_1 = s_2 = s$, $a \ll l$) for the intensity of a line at its maximum:

$$I_m d\nu = C_1 \frac{n_0 a_1}{2\pi^{1/2}} \frac{s}{l} \frac{d\nu}{b}, \tag{16}$$

where $C_1 = C\,jq$, $b = \nu_0 \frac{\bar{v}}{c}$, $\bar{v}$ is the most probable velocity of the atoms at the temperature of the oven and c is the velocity of light.

If the oven slit is oriented parallel to the line of observation ($a_1 \leq s_1$), then, inserting in (16) $n_0 a_1 = \frac{0.7}{\pi\sigma^2}$, we obtain

$$I_m d\nu = C_1 \frac{0.35}{\pi^{1/2}\sigma^2} \frac{s}{l} \frac{d\nu}{b}. \tag{17}$$

When the oven slit is oriented perpendicularly to the line of observation ($a_1 > s_1$), formula (16) for large a_1/l may be more accurately specified, as:

$$I_m d\nu = C_1 \frac{n_0 s_1}{2\pi^{1/2}} \cdot 2\theta_0 \cdot \frac{d\nu}{b}. \tag{18}$$

Assuming $n_0 s_1 = \frac{0.7}{\pi\sigma^2}$, we have

$$I_m d\nu = C_1 \frac{0.35}{\pi^{3/2}\sigma^2} 2\theta_0 \frac{d\nu}{b}. \tag{19}$$

The comparison of formulas (17) and (19) may be carried out in the same way as the comparison of formulas (13) and (14) for integrated intensity.

In the above calculation of the intensity of luminescence of beams, as well as in the calculations of Minkowski and Bruck, the following essential approximations were made.

Firstly, to all intents and purposes, collisions of atoms directly above the oven slit were ignored, even though they do occur at the oven vapor densities determined by (10). Secondly, it had been assumed that the oven slit is "ideal", i.e. that it has infinitely thin edges. The starting point for the above derivation for the expression for the density of atoms in the beam, (5), is rigorously correct only for an ideal slit and in the absence of atomic collisions above the slit. The occurrence of atomic collisions above the slit, as well as the deviation of the slit shape from the ideal, causes a change of distribution of path directions of the emerging atoms.[5] This necessarily causes deviations from the theoretical formulas.

2. ATOMIC BEAM APPARATUS

To obtain an intense beam, it is necessary that the ratio of length of the output oven slit to the distance from this slit to the point of observation of luminescence, a_1/l, be maximal. On the other hand, the length of the output slit, a_1, determines the consumption of material, and therefore it is undesirable to make it overly large. Consequently it is necessary to decrease the distance l between the output slit and the point of observation of luminescence. The decreasing of distance l and the related distance h involves great technical difficulties, chief of which is clogging of the aperture slit by the condensation of matter from the beam.

In the apparatus described, the length of the oven slit a_1 is 15 mm and distances h and l are 18 and 35 mm respectively. Therefore, the ratio $\frac{a_1}{l}$ is 0.43.

An outline drawing of the installation is shown in fig. 3. The vacuum chamber 1, with the aid of diaphragm 2, is divided into two parts: the evaporation chamber and the chamber for bombardment of the beam. Each chamber is evacuated by a TsVL-100 diffusion pump. The diaphragm has at its center a 6 x 20 mm^2 window for the passage of the beam.

The oven for the evaporation of the substance consists of a steel crucible 3, (volume approximately 50 cm^3), covered by lid 4. The lid is provided with a tube 5 for the egress of vapor; in the upper portion of this tube there is a 0.3 x 15 mm slit. The oven is heated by molybdenum wire coil covered by a layer of alundum. Tube 5, containing the slit, is heated to a higher temperature than the crucible itself, which prevents the fouling of the slit by the substance. The oven is surrounded by a double shield of sheet nickel to decrease radiation losses (this is not shown in fig. 3). Because of the brass shield 6 the greater portion of the escaping heat is led away to the boss 7, cooled by a coiled pipe. The maximum temperature of the oven is 800 - 900°.

Two systems of interchangeable slits, in drums 8 and 9, serve for the formation of the atomic beam. Most of the atoms escaping from the slit condense on the inner surface of drum 8; the drum has 12 equidistant 4 x 16 mm^2 slits for the passage of the beam. On the second drum 9, there are cut 40 slits, which shape the beam to the desired degree of collimation. All of these slits are 15 mm long; their widths range from 0.5 to 4 mm. In this manner, the beam collimation may be varied from $\alpha = 1:4.5$ to $\alpha = 1:36$.

---

*From formulas (11)-(14) it is clear that the intensity of beams depends only on the ratios of linear dimensions s_1, a_1, s_2, h and l, not on their absolute values. Upon a simultaneous proportional increase (or decrease) of all linear dimensions, the beam intensity remains unchanged. We note that the dimension s_2 of the aperture slit (see fig. 1) does not affect the beam intensity if it is taken sufficiently large (so that the total length a_1 of the oven slit is visible from the point of observation of luminescence.

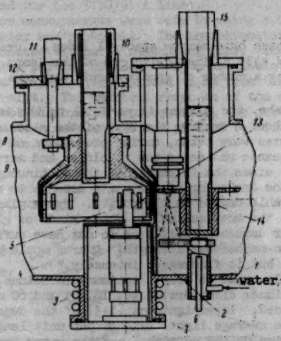

Figure 3. Diagram of Atomic Beam Apparatus The line of observation of luminescence is perpendicular to the plane of the drawing. See text for explanatory material.

The changing of slits while the test is in progress is accomplished by turning the drum by means of shafts 10 and 11. The slits are accurately parallel to the output slit of the oven; by means of a special ratchet, they can be re-set in the same position with a precision of ± 0.1 mm. The inner drum is made of Aluminum, the outer - of Duralumin. Both drums are cooled by liquid nitrogen 12.

An electron gun 13, the construction of which is similar to that described in reference [9], is used to excite the beam to luminescense. The gun produces a comparatively high current density, constituting approximately 4 - 5 A/cm^2 at the focus of the electron beam. The operating voltage is 300 - 400 V.

Obviously, the atomic beam is bombarded more effectively by this arrangement than was the case in other studies involving atomic beams using electron bombardment. The voltage supply to the electrodes of the gun is handled in such a way that there is absolutely no external electric field at the point of bombardment of the atomic beam. In order to avoid scattering of beam atoms by the hot electrodes of the electron gun, the latter is shielded from the beam by the disc 14, which is cooled by liquid nitrogen. The disc has openings for egress of the electron beam, which (openings) may be changed by turning shaft 15. The condensation of the atomic beam occurs on this disc.

While the beam is operating, the pressure in the apparatus is $2 - 5 \times 10^{-6}$ mm Hg in the excitation chamber and from 2×10^{-6} to 2×10^{-5} mm Hg in the evaporation chamber. The luminescence spectrum is completely free of molecular bands.

This apparatus was used for experiments on the generation and excitation of a Cadmium atomic beam. Preliminary results were also obtained on the study of the hyperfine structure of certain Cadmium lines in the atomic beam. The tests indicated that this atomic beam apparatus definitely gives a beam luminescence of great intensity. Thus, the Cd red line was photographed using a Fabry - Perot etalon (with dielectric-coated plates), an ISP - 51 spectrograph, a UF - 84 camera (f=800 mm), and Panchrome film (Sensitivity 180 GOST (State Natl. Std.) units). Good exposures were obtained in a matter of several seconds (for a beam collimation $\alpha = 0.1$). Fig. 4 shows one of the interferograms of the Cadmium red line obtained with a 15 cm. Fabry - Perot etalon. For comparison, Figure 5 shows an interferogram of the same line emitted by a hollow cathode cooled by liquid nitrogen.

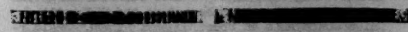

Figure 4. An interferogram of the Cadmium line, $\lambda = 6438$ Å, taken with a 15 cm Fabry-Perot etalon. The beam collimation is $\alpha = 0.1$.

Figure 5. An interferogram of the $\lambda = 6438$ Å Cadmium line emitted by a hollow cathode discharge tube, cooled by liquid nitrogen. The thickness of the Fabry-Perot etalon is 15 cm.

The presence of a great number of interchangeable aperture slits allows one to load a large quantity of a substance into the oven, so that the beam may operate uninterruptedly over a long period of time. In the tests conducted, about 100 grams of Cadmium* were loaded into the oven; this quantity lasted for 15 - 20 hours of beam operation. The metal which condensed on drums 8 and 9 was recovered and used for subsequent evaporations.

The combination of high intensity of luminescence with the opportunity to perform lengthy exposures allows one to use the described installation for the investigation of weak spectral element lines, as well as for metrological purposes.

In conclusion, the author wishes to thank F.A. Korolev for suggesting the topic and supervising the work, and V.A. Gromov for a number of valuable suggestions.

April 7, 1958

References

1. R. MINKOWSKI, H. BRUCK: Z. Phys., 95, 274 (1935)
2. R. MINKOWSKI, H. BRUCK: Z. Phys., 95, 284 (1935)
3. W. PAUL: Z. Phys., 117, 774 (1941)
4. L. G. MUNDIE, K. W. MEISSNER: Phys. Rev., 65, 265 (1944)
5. R. G. J. FRASER: Molecular Rays. N.Y. Macmillan, 1931
6. D. A. JACKSON, H. KUHN: Proc. Roy. Soc., A164, 48 (1938)
7. P. BRIX, A. STEUDEL: Z. Phys., 128, 260 (1950)
8. G. V. DEVERALL, K. W. MEISSNER, G. J. ZISSIS: Phys. Rev., 95, 1463 (1954)
9. E. G. LINDER, K. G. HERNQVIST: J. Appl. Phys., 21, 1088 (1950)

*This construction permits the evaporation at one loading (without dismantling) of remarkably large quantities of a substance; e.g. 25 - 30 cm^3.

TOM VI, Vyp 3 OPTIKA I SPEKTROSKOPIIA Mart, 1959
VOL. VI, No. 3 OPTICS AND SPECTROSCOPY March, 1959

Low Pressure Mercury Arc for the Investigation of Light Scattering

M. L. SOSINSKII

Three types of low pressure mercury lamps are analyzed which have narrow spectral lines, a weak continuous spectrum, and low relative intensities of the 4348 and 4339 Å lines, with one of the lamps having high emission stability. Experiences with the lamps in solving a number of spectroscopic problems gave completely satisfactory results.

High pressure PRK-2 mercury lamps, which are widely used as sources in the investigation of scattered light spectra, have a number of major deficiencies: an intense continuous spectrum, quite broad spectral lines, and the presence of comparatively intense 4348 and 4339 Å lines (10 and 3% of the intensity of the 4358 Å line). The quality of the spectra in low-pressure mercury arcs is considerably higher. The imperative need of constructing such light sources for wide usage was noted in a number of speeches at the VIIth All-Union Conference on Spectroscopy. These considerations impelled us, at the suggestion of G. S. Landsberg, to undertake the development of low-pressure mercury arcs for the study of scattered light and to investigate them in detail [1-3] since their properties are only partially recorded in the literature. We tried to simplify the lamp construction as much as possible and to make them accessible to a wide range of researchers. We also considered it necessary that certain of the lamps should be adaptable for use in the widely used PS-44 illuminator. In addition to the structural work, we also considered the fundamental processes in the discharge in order to produce optimum conditions [3].

On the basis of the work [4-6] on the absorption of the visible triplet lines and the data on the non-monotonic behavior of the curve describing the dependence of the intensity of the 5461 Å line on the mercury vapor pressure, it has been shown that a vapor pressure of 10^{-2} mm is optimum for the 4358 Å line. At high current densities, the appearance of "saturation", which is very essential to emission stability, could be expected on the "intensity vs current" curve. A lower electron concentration than in the PRK-2 lamp should lead to a reduction in the intensities of the 4339 and 4348 Å lines in comparison with the 4358 Å line intensity. Less brilliance of the source than in the PRK-2 lamp is compensated to a considerable extent by the greater volume of illumination.

LINEAR LAMP L-1 WITH TOTAL COOLING

The production of a mercury arc in which a pressure on the order of 10^{-2} mm Hg would be maintained at high current densities is beset with a number of technological and structural difficulties. We used the idea of cooling the lamp, proposed by E. F. Komarov, as well as the experience of I. L. Fabelinskii, in attempting to construct such a lamp.

Figure 1. L-I linear lamp

Shown in Figure 1 is the lamp L - 1 which we constructed [1-3] with a coolant passing through the liquid electrodes and along the whole column of the gas discharge. In the horizontal part of the tube, the coolant is parallel to the lamp axis and about 2 mm from the rear of the glass envelope. Measures were taken, during production of the lamps, to cleanse and degas the envelopes and mercury carefully since the intensity of the continuous spectrum and the darkening of the glass depends to a very considerable degree on the purity. Pyrex glass seems to be the most suitable. Other kinds of glass are either darkened rapidly or do not have sufficient thermo-mechanical strength. Quartz would be the best, but it fluoresces intensely.*

In order to select optimum dimensions, lamps with inner diameters of 14, 18, 25 and 60 mm were produced. Investigations [1-3] of the dependence of the average light flux ϕ per unit length of the lamp on the current I and the water temperature t in the cooling tube, showed that for the 4358 Å line an 18-20 mm diameter is most efficient. Self absorption is considerably larger in lamps of greater cross section. Greater light flux from such lamps can only be obtained at the expense of an increase in the line width and an excessive growth in the current. Moreover, it is doubtful whether the light flux from a source of large cross section can be used effectively under the specific conditions of illuminating the object in scattered light investigations. All the subsequent research was carried out with lamps of 18 mm diameter.

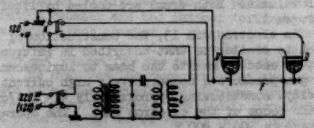

Figure 2. Ignition circuit. Explanation in text.

The introduction of a small quantity of helium does not cause noticeable line broadening nor enhancement of the continuous spectrum but the light flux for the 4358 Å line is enhanced by 20% at 15 amp. The introduction of helium, which facilitates ignition of the lamp, and the use of a special igniter circuit permitted elimination of a third electrode. A Sventitskii generator in a somewhat modified circuit (Fig. 2) was used for ignition. Metal rings D, interconnected by means of the wire F (or by using the frame of the illuminator) and connected as well to the positive electrode, are superposed on the external surfaces of the electrode bulbs about 2 mm from the mercury surface. With the proper electrical polarity, a short high-voltage impulse from the transformer L is sufficient to produce an arc discharge for dc line voltages of 100 V and less. After ignition, the generator is shut off by means of the knife switch K.

Also investigated was the dependence of the average light flux ϕ per unit length of the lamp

* Certain experiments of D. A. Goukhberg show promise of the possibility that non-fluorescing quartz can be produced successfully.

on I, t, and the helium pressure P, for the visible triplet and for the 5770/91 Å lines.

These measurements were made by using a UM-2 monochromator and photocell. The monochromator slit was illuminated without a condensing lens. The lamp, whose center section of about 80 mm was isolated by using a diaphragm, was placed 1 mm from the monochromator slit. The spectral response of the apparatus was not calibrated; consequently, the curves for the various wavelengths are plotted to different scales in our graphs.

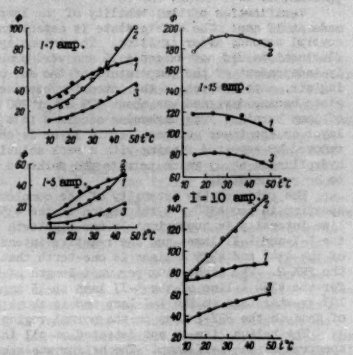

Figure 3. Light flux ϕ as a function of the water temperature t. L-1 lamp 1 - 4358 Å; 2 - 5461 Å; 3 - 5770/91 Å lines

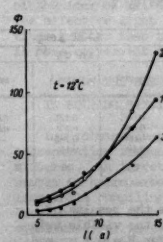

Figure 4. Light flux ϕ as a function of current I. L-I lamp. 1 - 4358 Å; 2 - 5461 Å; 3 - 5770/91 Å lines

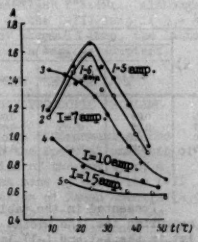

Figure 5. Dependence of the ratio $A = \frac{4358}{5461}$ on the water temperature t, L-I lamp. For different currents (in amps.): 1 - 5; 2 - 6; 3 - 7; 4 - 10; 5 - 15.

Given in Figure 3 is the dependence of ϕ on t (in deflection of the galvanometer in the photoelectric circuit) for different current values I. Given in Figure 4 is the dependence of ϕ on I for $t \sim 12°$, and in Figure 5 is the dependence on t of the ratio of the light fluxes for the 4358 and 5461 Å lines $A = \frac{358}{5461}$ (in arbitrary units). A similar curve with a peak is obtained for the dependence of A on I. The steepness of the curves in Figures 3 and 4 for I = 10 amp is related to the fact that the thickness of the luminous layer is slight at low currents and cooler temperatures because of vapor condensation on the horizontal part of the cooling tube. As I or t increases, the layers closest to the cooling surface start to glow. The difference in behavior of the curves for lines with a common upper level can only be caused by self-absorption. The behavior of the curves for the 5770/91 Å lines in Figure 3 indicates a significant reduction in the electron temperature for I = 10 amp. Using the results of Fabrikant and co-workers [7], it can be shown that a mercury vapor pressure of $0.5 - 1.0 \times 10^{-2}$ mm corresponds to the maximum in Figure 5. Actually, the helium lines in gas filled lamps at 15 amp vanish only for $t \geq 25°$.

ϕ as a function of the helium pressure P for various current intensities and $t = 12°$ is given in Figure 6. The value of ϕ at P = 0 is taken as the unit of light flux for each line. The measurements were made with a lamp disconnected from the vacuum apparatus so that the helium density in the discharge was lower than the average density in the apparatus. However, this has no essential significance for subsequent use. The behavior of the curves indicates the great increase in self-absorption in addition to the reduction in the electron temperature as P increases. Evidently, the fundamental reason for the large growth of ϕ with P for I = 10 amp is not an increase in the electron concentration as a consequence of the drop in the rate of drift electron diffusion, but is an increase in the mercury vapor pressure because of the drop in the rate of vapor diffusion to the cooling surface, which is confirmed by visual observations on the condensation of mercury on the horizontal section of the cooling tube. On the basis of these results, the optimum helium pressure is 0.1 mm.

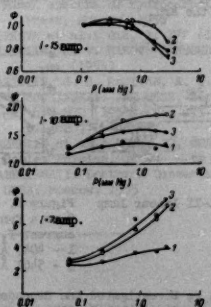

Figure 6. Light flux as a function of helium pressure P. L-1 lamp. 1 - 4358 Å; 2 - 5461 Å; 3 - 5770/91 Å lines

It is impossible to account for the instability of the arc emission by the variations in I and t; it is related to the falling of the mercury droplets from the horizontal part of the cooler to the hot surface of the envelope. During the above mentioned measurements the mercury droplets were removed from the envelope surface by agitation. A rise in stability could be achieved by changing the lamp construction.

LINEAR LAMP L-II WITH PARTIAL COOLING

The lamp L-II [3-4] pictured in Figure 7 was constructed on the basis of an analysis of the results of the L-I lamp investigations. In this lamp, the liquid electrodes and the section of the gas column near the electrodes were cooled by running water. The cooling element was divided in two. Each part consists of a sphere of about 18 mm diameter, submerged in mercury approximately up to the middle and terminating in a flat spiral of 1 1/2 turns. The fundamental cause of the instability was thus eliminated. A small increase in the pressure and, therefore, in the line width as well, are of no consequence for Raman spectra, but some rise in intensity and the appearance of 'saturation' could be expected here, which is no small factor in the emission stability.

Migration of the mercury from the anode to the cathode usually occurs in mercury arcs with liquid electrodes. The insertion of cooling windings in the gas discharge space over the electrode surfaces insures continuous condensation of the mercury vapor since the relative area of the free gaps in the spiral is small. The migration of the mercury is so slow in the L-II lamp that the lamp can operate for 50 and more hours without restarting. Actually, the total evaporation is less at the cathode than at the anode; however, it is concentrated on a small surface in the region of the cathode spot where a high temperature is developed. The evaporation in this region is explosive and depends somewhat on a 10 - 20° change in the mercury temperature. The vapors being ejected at high speed are collected at the spiral cooler more slowly than in the anode region. Hence, it is seen just how essential is the cooler configuration to the build up of the mercury vapor pressure in the arc.

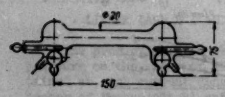

Figure 7. L-II linear lamp

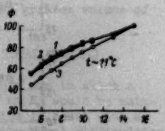

Figure 8. Light flux ϕ as a function of the current I, L-II lamp, 1 - 4047 Å; 2 - 4358 Å 3 - 5461 Å lines

In [4] we investigated the dependence of ϕ on I, t and P. We found that ϕ either increases slightly for I = 7 amp as P changes from 0 to 0.1 mm or it remains unchanged; a further rise in the helium pressure leads to a reduction in the light flux for all lines of the visible triplet and for the 5770/91Å lines. Hence, the optimum helium pressure is 0.1 mm. The intensity of the 4358 Å line is almost independent of t. The curve of the dependence of the ratio A on I is similar to the curve for L-I. Shown in Figure 8 is ϕ as a function of I. It follows from the results obtained that we will be in the pressure range close to the maximum of absorption of the 5461 Å line and in the range of the maximum of the 4358 Å line intensity for I = constant and variable mercury vapor pressure. Hence, the mercury vapor pressure is 10^{-2} mm.

Verification of the stability of the lamp was made at 12 amp. The stable state is established several seconds after ignition. The intensity fluctuations did not exceed ± 1% and were practically independent of the temperature of the surrounding air. Attenuation in the intensity because the glass became darkened was about 30% after 200 hours of lamp burning. The darkening occurred in a thin layer on the inner surface. (This layer is easily removed by repeated rinsing with a weak solution of hydrofluoric acid, which permits the darkened lamp to be regenerated.)

The ratio of the intensity of the complex spectrum in the 4358 - 4916Å region to the 4358 Å line intensity is approximately one-eightieth in the L-I and L-II lamps and the relative intensity of the 4348 and 4339 Å lines is one-tenth that in the PRK-2. The light flux per unit length of lamp for the 4358 Å line of the L-II lamp at 15 amp is 10% greater than in the L-I lamp and is about 40% of than in the PRK-2 lamp in the normal region.

The helium line is not detected at all in the spectrum of the L-II lamp. The helium was subsequently replaced by argon, which facilitates ignition considerably.

Line Width $\Delta\nu$ as a Function of the Current Intensity I

I(in a)	L-I lamp (in cm^{-1})			L-II lamp (in cm^{-1})		
	λ 4047 Å	λ 4358 Å	λ 5461 Å	λ 4047 Å	λ 4358 Å	λ 5461 Å
5	0.08	0.08	0.09	0.085	0.125	0.09
7	0.08	0.085	0.09	0.085	0.13	0.09
10	0.085	0.095	0.09	0.09	0.135	—
15	0.095	0.12	0.115	0.10	0.15	—

Presented in the table are the results of measuring the line widths $\Delta\nu$ of the visible triplet in the L-I and L-II lamps for P = 0.1 mm and t ~ 12°. The measurements were made using a Fabry-Perot etalon in conjunction with an ISP-51 spectrograph. The averaging was made over 10 contours. As is seen from the table, the widths of the 4047 and 5461 Å lines are almost the same in the L-I and L-II lamps, while width of the 4358 Å line is noticeably larger in the L-II lamp. This is related to the specific dependence of the absorption on the vapor pressure for this triplet component [7]. Broadening of the 4358 Å line in the L-I lamp at 5 amp is slight because of self-reversal, and approaches Doppler broadening at 15 amp and is twice the Doppler broadening in the L-II lamp at 15 amp. A comparison with the PRK-2 lamp in the low voltage region [2,4] shows that the minimum value of $\Delta\nu$ of

the 4358 Å line is less than in the PRK-2 and that the light flux of the L-I and L-II lamps is 20 - 30 times greater, for equal width of this line, than in the PRK-2.

SPIRAL LAMP L-III

The construction of Kemp et al. [8] was taken as the basis of the L-III lamp. Our work consisted of simplifying the construction and the ignition conditions. The cooling system of the linear L-II lamps was used for the spiral lamp (Fig. 9). The lamp consists of three turns of 20 - 22 mm tubing. The gap between turns is 4 - 6 mm, the inner diameter of the spiral is 60 mm. The lamps are filled with a mixture of inert gases at a 0.1 mm pressure in the following concentrations: 97% argon, 2.8% krypton and 0.2% xenon. The gas filler and the use of our ignition circuit (Fig. 2) simplified as much as possible the lamp ignition process even in the absence of an additional electrode (see[8]). Ignition is from dc mains at 150 V; the voltage on the lamp is about 80 V . The relative intensity of the complex spectrum is approximately the same as for the L-II lamp. The effective light flux for the 4358 Å line was determined from observations of the intensity of the 992 cm^{-1} Raman line of benzene. It appears that the L-II lamp in a cylindrical illuminator at 10 amp and the PRK-2 lamp in a PS-44 yield approximately the same intensities. Wide application of the spiral lamps is limited as yet because of the lack of cylindrical light filters. Although the effective light flux of the L-III lamp is 3 - 4 times greater than that of the L-II lamp, the latter is more convenient for use in various adapters.

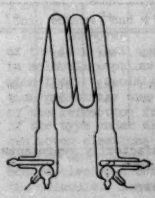

Fig. 9. L-III spiral lamp

ON THE USE OF A LOW PRESSURE LAMP

IN SOLVING SPECIFIC SPECTROSCOPIC PROBLEMS

Low voltage lamps permit enhancement of the concentration response in the spectral analysis of mixtures. An investigation of the purity of a number of hydrocarbons was made by using the L-II lamp while compiling an atlas of Raman spectra [4,9]. Because of the high lamp stability, we had the opportunity of investigating the rotational isomerism of 1,2-dichlorethane in low concentration mixtures [4]. The low relative intensity of the 4348-4339 Å lines is very important here. If a PRK-2 lamp were used, then the superposition of the Raman lines excited by these lines would in a number of cases eliminate the possibility of quantitative measurements. It has also been shown that low pressure lamps simplify the problem of obtaining spectra of glass-like substances and of inhomogeneous crystals as well as of 'low frequency' spectra [4, 10, 11].

Use of a low pressure lamp with narrow spectral lines simplifies the problem of investigating the Raman line width [9, 12, 13]. Replacement of the PRK-2 lamp in the low voltage region by L-I and L-II lamps in interferometer investigations of the line structure of scattered light, would lead to a reduction in the exposure time of 15 - 25 times [4, 14]. It is most expedient to use the L-I lamp, which has the narrowest lines, to investigate the fine structure of Rayleigh scattering lines. The instability in the lamp emission is here inconsequential since all the fine structure elements are photographed at the same time.

The research was performed under the guidance of Academician G. S. Landsberg, to whom I am grateful for its successful completion.

Jan. 10, 1958

References

1. M. L. SOSINSKII: IAN USSR, Ser. fiz., 14, No. 4, 387 (1950)
2. M. L. SOSINSKII: IAN USSR, Ser. fiz., 17, 621-23 (1953)
3. M. L. SOSINSKII: IAN USSR, Ser. fiz., 18, No. 6, 709 (1954) (See CTT Bulletin, p. 389)
4. M. L. SOSINSKII: Cand. dissertation. MFTI, Moscow, 1956
5. V. A. FABRIKANT: IAN USSR, Otd. Est. i Mat. Nauk, 441-461 (1935) (English summary 461-462)
6. V. A. FABRIKANT: Tr. VEI, No. 41, 236 (1940)
7. V. A. FABRIKANT, et al.: ZETF, 7, 733 (1937)
8. J. W. KEMP, J. L. JONES, R. W. DURKEE: JOSA, 42, 811 (1952)
9. G. S. LANDSBERG, P. A. BAZHULIN, M. M. SUSHCHINSKII: Osnovnye parametry spektrov kombinatsionnogo rasseianiia uglevodorodov (Basic parameters of Raman spectra of hydrocarbons) Akad. Nauk Press, Moscow, 1956
10. E. N. LOTKOVA et al.: OIS, 1, 772 (1956)
11. P. A. BAZHULIN, A. V. RAKOV: DANUSSNR, 105, 54 (1955)
12. P. A. BAZHULIN, S. G. RAUTIAN, A. I. SOKOLOVSKAIA, M. M. SUSHCHINSKII: IAN USSR, Ser. fiz., 18 No. 6, 678-679 (1954) (See CTT Bulletin, p. 362)
13. P. A. BAZHULIN et al.: ZETF, 29, 822 (1955) (See Soviet Physics, JETP)
14. I. L. FABELINSKII: Doctoral Dissertation, FIAN USSR, Moscow, 1955

ТОМ VI, Вып. 3 OPTIKA I SPEKTROSKOPIIA Март, 1959
VOL. VI, No. 3 OPTICS AND SPECTROSCOPY March, 1959

BRIEF REPORTS

The Correlation Between Refraction and the Ionization Potentials of Atoms

S. S. BATSANOV

It was established that there is a correlation between the refraction and the ionization potential of atoms in a series of papers [1-4]. However the formulas given in these papers were not of very great accuracy due, in our opinion, to the fact that they tried to establish a strict dependence of the refraction and the energies of atoms on their sizes.

It seemed more rewarding to investigate the connection between refraction and the ionization potentials of atoms from the point of view of their dependence on the magnitudes of their charges. In this case the correlation of the optical and energetic properties may be found without any special assuptions.

Table 1

Relative Change in the Ionization Potentials

Element		Z							
		0	+1	+2	+3	+4	+5	+6	+7
VI gr.	O	0	3.2	11.3	24.0	42.0	68.3	100	—
	S	0	3.8	12.2	24.8	42.0	68.2	100	—
	Se	0	3.8	12.2	24.8	41.6	67.9	100	—
	Te	0	3.9	12.5	25.1	41.8	68.1	100	—
VII gr.	I	0	2.8	7.9	17.4	30.7	48.2	72.0	100
	Cl	0	3.2	9.0	18.7	31.8	48.4	72.0	100
	Br	0	3.2	9.0	18.7	31.7	48.0	71.7	100
	J	0	3.2	9.1	18.9	31.9	48.1	72.0	100

In Table 1 we present the relative changes (in percent) of the atomic ionization potentials of the elements in groups VI and VII of the periodic system, computed according to the relation $\overline{\Delta P} = P + z / P_{ion}$, where P_{ion} is the sum of the successive ionization potentials up to the maximum (group) valence, and P_{+z} is the corresponding sum of ionization potentials up to the valence $+z$. The values for the ionization potentials were taken from [9].

The tabulated data display marked similarities. These suggest the possibility of a common approach to all these atoms. In Table 2 we give the average values $\overline{\Delta P}$ for these elements (first line).

Not long ago we showed [10] that using the method of Sanderson [8] it is possible to compute the ionic radii of these elements in good agreement with experiment, using their covalent radii. Hence it is possible to calculate the size of these atoms corresponding to their ionization. It is characteristic that the relative changes in the volumes of the atoms take place in exactly the same fashion in various groups of the periodic system. If the refraction is proportional to the volume, the electronic polarization of the atoms will depend in the same way on the charges they acquire. In Table 2 (line 2) we give the average values of the relative changes $\overline{\Delta R}$ of the refraction of atoms of the elements in groups VI and VII of the periodic table.

Table 2

Comparison of the Relative Changes in P and R

Element		Z							
		0	+1	+2	+3	+4	+5	+6	+7
VI gr.	$\overline{\Delta P}$	0	3.7	12.0	24.7	41.9	68.1	100	—
	$\overline{\Delta R}$	100	42.0	22.0	12.2	6.3	2.8	0	—
VII gr.	$\overline{\Delta P}$	0	3.1	8.7	18.4	31.5	48.2	71.9	100
	$\overline{\Delta R}$	100	45.7	24.8	15.1	9.0	5.2	2.2	0

An equation which satisfactorily represents the data in this table has the form

$$(\overline{\Delta R} + 5) \times (\overline{\Delta P} + 5) = 500.$$

This formula may be easily verified. Knowing the ionization potentials of the processes $X^- - 1e = X^0$ [11,12], we can determine the percentage change in P_{ion}. Substitution in the above formula then gives immediately the percentage change in refraction $\Delta R = R_{atom} - R_{+z}$, corresponding to the atom's acquisition of a single electron. From this, calculation of the ionic refraction of a given element is straight forward.

In Table 3 we give the ionization potentials P_1 of the halogens and the atoms of oxygen and sulfur for the process $X^- - 1e = X^0$ and the totals P_2 for maximum valence, and the relative values $\overline{\Delta P}$ for the process indicated, and the relative changes in the atomic refraction $\overline{\Delta R_1}$, calculated according to the above formula.

Table 3

Relative Changes in $\overline{\Delta R}$ and $\overline{\Delta P}$ of Ions in Groups VI and VII of the Perodic System

Element	P_1	P_2	$\overline{\Delta P} = \frac{P_1}{P_2}$	$\overline{\Delta R_1}$
F	3.56	657.3	0.54	85.2
Cl	3.75	408.3	0.92	79.5
Br	3.51	367.5	0.96	78.9
J	3.17	321.7	0.99	78.0
O	1.48	431.2	0.34	88.6
S	2.07	275.6	0.75	82.0

The potentials for adding a second electron to the ions of oxygen O^- and sulfur S^- are equal to -9.11 and -4.51 eV respectively [13]. The sum of these values and the ionization potentials for the first electron of the corresponding element gives the least absolute magnitude of the ionization potential common to both electrons, (and hence the value of the refraction), rather than the value for one electron, and is physically meaningless.

In order to get around this difficulty it is possible to proceed as follows. From the first ionization potential we compute the refraction of the ions O^- and S^-, and from the second ionization potential we compute the change of the refraction

(percent) from the given monovalent ions. The relative changes $\overline{\Delta R}_2$ due to the addition of the second electron to oxygen and sulfur are equal, respectively to 168 and 143%.

The values of $\overline{\Delta R}_1$ and $\overline{\Delta R}_2$ were used to calculate the ionic refractions given in Table 4. In order to obtain the refraction due to the outermost electron cloud it is necessary to subtract off the refraction due to the ion core from the atomic refraction. The data following can be calculated with good accuracy from the formula of Kordes [14] $R = 0.603\left(r \cdot Z^{\frac{2}{n-1}}\right)^{4.5}$ where r is the radius, Z the ionic charge, and n is the Born repulsion coefficient. Moreover it is necessary to take account of the fact that the atomic refraction encountered in molecular optics does not correspond to refraction from an isolated atom, for which the ionization potentials are defined, but rather to half of the refraction from a molecule X_2. In an atom of the type under discussion, in addition to its own seven electrons (a halogen) or six electrons (oxygen and sulfur) there are also one or two bonded electrons obtained from the other atom in the molecule. According to Braun and Holemann [15] the refraction due to a halogen atom itself is 7/8 of a half of the molecular refraction (6/8 in the case of a chalcogen).

Table 4

Calculation of the Ionic Refraction

Element	R_D	R_{+Z}	R_{cl}	R_a	ΔR	R_{ion} Calculated value	R_{ion} Literature value	ΔR_{ion} (in %)
F	1.60	0.13	1.47	1.29	1.10	2.52	2.65 2.44 2.27	0
Cl	5.80	0.16	5.64	4.93	3.92	9.01	9.30 9.06 8.17	0
Br	8.67	0.35	8.32	7.08	5.59	13.02	12.14 12.66 12.90	0.9
J	13.95	0.45	13.50	11.81	9.21	20.67	18.07 19.21 20.46	1.0
O	2.00	0.13	1.87	1.47	1.30[1] 4.87[2]	7.77	9.88 6.95 6.84	0
S	8.00	0.20	7.80	5.85	4.80[1] 15.51[2]	26.36	26.0 22.7 19.8	1.4

[1] — ΔR_1.
[2] — ΔR_2.

In Table 4 we give values of the atomic refraction R_D (half of the molecular refraction, except in the case of iodine, where in order to avoid the influence of dispersion it was necessary to use data on organic compounds); we also give the refraction due to the ion core R_z, the refraction due to an eight-electron cloud R_{cl}, the refraction due to the outer electrons belonging to the atom itself R_a, the absolute increase in the refraction due to the addition of one or two electrons, and finally, the ionic refraction $R_{ion.} = R_a + \Delta R + R_z$. In the next to the last column we give, for purposes of comparison, the generally accepted values for the ionic refraction due to Pauling [16], Fajans [17], and Kordes [14], in lines one, two, and three respectively.

The calculated values show that the formula we have given allows one to calculate satisfactorily the ionic refraction --- the mean error is 0.5%.

Thus we have demonstrated the form of the correlation between the ionization potential and atomic refraction to be hyperbolic, in complete correspondence with previous work. Moreover it has been established that it is possible to calculate the refraction of atoms in bonds of intermediate character, using the method of Sanderson to calculate the changes in the atomic volume from the ionization of the atom.

April 5, 1958

References

1. H. A. KRAMERS: Zs. Phys., 13, 312 (1923)
2. G. I. SKANAVI: Fizika dielektrikov (Physics of Dielectrics), GTTI, Moscow 1949, p. 29
3. T. M. REED, III: J. Phys. Chem., 59, 428 (1955)
4. V. SAHINI: Anal. Univ. C. I. Parhon Bucuresti, Ser. stiint nat. 13 (1957) pp. 85 - 92
5. T.-H. LIU: J. Chinese Chem. Soc., 9, 119 (1942) (In English)
6. W. GORDY: J. Chem. Phys., 14, 305 (1946)
7. K. B. IATSIMIRSKII: Zh. Obshch. Khim., 23, 180 (1953) (English translation in Jnl. Gen. Chem. USSR, 23, 185(1953))
8. R. T. SANDERSON: J. Amer. Chem. Soc., 74, 272 (1952)
9. Spravochnik khimika (Chemical handbook) G. Kh. I., vol. 1, Moscow, p. 273 (1951)
10. S. S. BATSANOV: ZFKh., 30, 2640 (1956)
11. T. L. BAILEY: J. Chem. Phys., 28, 792 (1958)
12. L. M. BRANSCOMB, S. J. SMITH: J. Chem. Phys., 25, 598 (1956)
13. H. O. PRITCHARD: Chem. Rev., 52, 529 (1953)
14. E. KORDES: Z. Phys. Chem., 44, 249 (1939)
15. A. BRAUN, P. HOLEMANN: Z. phys. Chem., 34, 357 (1936)
16. L. PAULING: Proc. Roy. Soc., London, 114 (1927) pp. 181-211
17. N. BAUER, K. FAJANS: J. Amer. Chem. Soc., 64, 3023 (1942)

TOM VI, Vyp. 3 OPTIKA I SPEKTROSKOPIIA Mart, 1959
VOL. VI, No. 3 OPTICS AND SPECTROSCOPY March, 1959

A Simple Method of Producing Potassium Bromide Plates for the Infrared Spectroscopy of Solids

A. I. FINKEL'SHTEIN, F. L. MALACHEVSKAIA, A. N. FISHER, B. G. RABOVSKII

In recent years, the method of investigating the infrared spectra of solids in the form of pressed plates of a mixture of the material to be studied with alkali-halide salts, mainly potassium bromide, has received widespread usage. However, the methods, described in the literature [1-3], of producing the pressed plates is much too complicated. Usually the plates are pressed in the form of discs, which requires a considerable total pressure (on the order of 25 - 30 tons). In order to improve the transmission, pressing under a vacuum and with heating is usually used.

A simple method is described herein by which quadrangular plates of mixtures of the material to be investigated with potassium bromide or sodium chloride are obtained which are suitable for the measurement of infrared spectra.*

The potassium bromide or sodium chloride, to be used for these purposes, must not contain potassium chloride, which would give absorption in the 7 and 3μ range. Potassium bromide can be recrystallized from water in order to remove the potassium chloride.

In order to remove the moisture, the salts were subjected to calcining at 200° C for 12-18 hours, where the salt was ground in a porcelain mortar every four hours.

The potassium bromide or sodium chloride thus produced could be stored in an desiccator over calcium chloride for an unlimited time.

Mixtures of potassium bromide or sodium chloride with the material to be investigated were prepared for investigations of the infrared spectra. The mixtures were pulverized in a porcelain mortar for 5 - 7 minutes. Usually the mixtures contained 0.1, 0.33, 1 and 3% of the material to be investigated. The spectra of each mixture were recorded in the range where the clearest spectra were obtained for a given concentration. A so-called "internal standard", i.e., a material having an absorption band which does not overlap the analytic band, is first introduced into the potassium bromide. The content of the material to be investigated is determined by the requirements of sensitivity and accuracy of the analysis.

The compression is done by using the apparatus shown on figure 1. The lower (1) and upper (2) punches and the guide ring (3) are produced from hard stainless steel; the mold (4) and the plate (5) from plastic. In contrast to the methods described in the literature, the mixture of the material being investigated is not spread over the whole matrix in the shape of an elongated quadrangle with the aid of the mold (4) and the plate (5). To do this, the ring (3) is put onto the lower platform (1) and the mold (4) is mounted atop the ring. The prepared mixture of the material to be investigated and potassium bromide or sodium chloride is charged into the quadrangular opening of the mold (4) and is leveled and compressed by the plate (1). Then the mold (4) and the plate (5) are removed and a level and compressed quadrangular layer of the mixture remains on the lower area. After this, the upper stage (2) is mounted on the ring (3) and the whole apparatus is inserted under a press. The magnitude of the pressure and the compression time depend on the area of the quadrangular opening in the mold (4). This area is approximately 1 cm^2 (5x20 mm) in the IKS-11 spectro-photometer. In this case, the compression time is several seconds at a pressure of 10 - 15 tons. It should be noted that such pressures are easily achieved in a laboratory oil press giving an oil pressure of 250 - 500 atm.

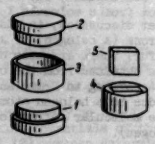

Figure 1. Details of the apparatus to press the plates.
1 - matrix; 2 - punch; 3 - guide rings; 4 - mold; 5 - plate

After release of the pressure, the press-mold is dismounted, the plate is removed and placed in front of the slit of the spectro-photo-meter at the location of the baffle window. It is convenient to place the plate in a factory mandrel by using two gaskets of black paper in which rectangular holes have been made.

The "method of base lines" is used to investigate the spectra of substances when just the set of vibrational frequencies must be determined. To do this, such a concentration of the material to be investigated is selected on the plate that sections with transmission equal to or almost equal to 100% would be in the spectra. Combining such sections, a line is obtained which corresponds to 100% transmission over the whole spectrum. Making marks with zero transmission (closing the light source to do this) and combining them, a line is obtained which corresponds to zero transmission. The presence of such lines permits the percent transmisiion to be determined for the absorption band. Its own concentration must be selected for the individual sections of the spectrum with this method (we usually used concentrations of 1, 0.33 and 0.1%).

When using this method for quantitative analysis, the intensity is measured in arbitrary units at analytic points at the absorption maximum of the "internal standard" and at point where light absorption by the substance being analyzed and by the "internal standard" is lacking (the zero absorption point).

Insertion of the "internal standard" enables changes in the plate thickness to be taken into account and the zero absorption point enables changes in the plate transparency to be taken into account.

* In certain cases, it is possible to use the powder of organic resin (for example, polyethylene).

Let the light intensity be J_0' at the zero-absorption point, J_{st} at the maximum of the standard absorption band, J_a at the analytic point. In the absence of a standard and material to be analyzed, we have for a constant light source temperature and a constant monochromator slit width

$$J_{0st} = J_0' a,$$
$$J_{0a} = J_0' b,$$

where a and b are constant nondimensional quantities.

On the basis of the Lambert -Buger- Beer law, we have (k is the absorption coefficient, c the concentration, d the plate thickness)

$$J_{st} = J_{0st} \cdot 10^{-k_{st} c_{st} d} = J_0' \cdot a \cdot 10^{-k_{st} c_{st} d},$$
$$J_a = J_{0a} \cdot 10^{-k_a c_a d} = J_0' \cdot b \cdot 10^{-k_a c_a d}.$$

Hence, after algebraic manipulation, we have

$$c_a = \frac{c_{st} \cdot k_{st}}{k_a} \cdot \frac{\log \frac{J_0}{J_a} + \log b}{\log \frac{J_0}{J_{st}} + \log a}.$$

Since the quantities c_{st}, k_{st} and k_a are constants,

$$c_a = g \cdot \frac{\log \frac{J_0}{J_a} + \log b}{\log \frac{J_0}{J_{st}} + \log a}.$$

The quantity g is a constant.

The relations mentioned can easily be extended to the case of a multicomponent mixture.

Use of the proposed method in practice has shown the wide possibilities of its application to solve various problems by the method of infrared spectroscopy.

June 24, 1958

References

1. J. L. HALES, W. KYNASTON: Analyst, 79, 702 (1954)
2. E. FAHR, W. P. NEUMANN: Angew. Chem., 67, 277 (1955)
3. S. E. WIBERLEY, J. W. SPRAGUE, J. E. CAMPBELL: Anal. Chem., 29, 210 (1957)

TOM VI, Vyp 3 OPTIKA I SPEKTROSKOPIIA Mart , 1959
VOL VI, No. 3 OPTICS AND SPECTROSCOPY March , 1959

On The Question of The Thermal Quenching of Fluorescence

V. V. ZELINSKII, V. P. KOLOBKOV AND H. D. KRASNITSKAIA

In many substances, the ability to flouresce is strongly temperature dependent. At liguid nitrogen temperature many substances begin to flouresce which at room temperature flouresce only very weakly or not at all. This fact is ascribed either to thermal quenching being eliminated, or to the elimination of mobility between the individual parts of the molecule in a frozen medium. We wish to draw attention to another factor which in some cases has just as great an effect on the fluorescence yield, q_{fl}, as a function of temperature as do the two factors mentioned above. As we have shown in [1], some substances show significant changes in the fluorescence spectrum with changing temperature and state of aggregation. On the other hand it has been shown in [2] that in some organic substances the value of q_{fl} for 20° is related by means of a rule to the positions of the appropriate fluorescence spectra. In general this dependence consists of two parts; an increase in q_{fl} as the maximum of the fluorescence spectrum ν_{fl}^{max} moves to higher frequencies, and then a decrease in q_{fl} proportional to the shift of the fluorescence spectrum to the short wavelength side. Thus we may expect that when q_{fl} increases at low temperature, the accompanying spectral changes in the fluorescence may be related in some way to the change in position of the fluorescence band. We will examine this question using as an example some derived phthalimides and aminomaleimides.

It was shown previously [3] that the fluorescence yields of 4-amino-N-methylphthalimide, and 4-dimethylamino-N-methylphthalimide, which differ markedly at room temperature in ethanol, become equal at -180° and attain the value 0.95-1.0.* 3 -amino, 3 -monomethylamino, and 3 -dimethylamino-N-methlyphthalimide have been observed to behave similarly. At -180° the fluorescence yields of these three substances are very different from the room temperature values, and attain approximate equality with the value 0.60 - 0.68. In previous investigations [2,4], the sharp increase in q_{fl} at low temperature was wholly ascribed to thermal quenching - i.e. to the fact that with changing temperature the positions of the ground and excited state potential curves remain unchanged, but there is a change in the vibrational distribution of excited state molecules. However in these substances there is also a marked change in the position of the fluorescence spectra when the temperature is lowered (Fig. 1) which shows that the relative positions of the excited and ground state potential curves are also changed in these cases. Moreover as may be seen from Fig. 1, the fluorescence spectra at -180° in ethyl alcohol occupy positions of much greater frequency than at room temperature. Thus ν_{fl}^{max} is 18700 cm^{-1} in 4-amino-N-methylphthalimide at 20°

---

* Taking into account the change in refractive index on lowering the temperature from 20 to -180°; in [3] values of q_{fl} were given without taking account of this refractive index change.

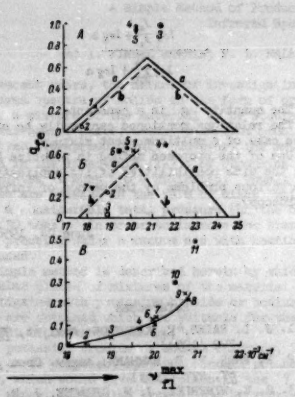

Fig. 1 Dependence of fluorescence yield q_{fl} on the position frequency of the maximum in the fluorescence spectrum, ν_{fl}^{max}.

(A) Dependence of fluorescence yield, q_{fl}, on ν_{fl}^{max} at 20° (schematic): (a) 4-amino-N-methylphthalimide; (b) 4-methylamino-N-methylphthalimide
Solutions in ethanol at 20°: (1) 4-amino-N-methylphthalimide, (2) 4-dimethylamino-N-methylphthalimide
Solutions in ethanol at -180° : (3) 4-amino-N-methylphthalimide; (4) 4-dimethylamino-N-methylphthalimide ; (5) 4-diphenylamino-N-methylphthalimide
(B) Dep. of fluor. yield q_{fl} on ν_{fl}^{max} at 20°:
(a) 3-amino-N-methylphthalimide; (b) 3-monomethylamino-N-methylphthalimide Solutions in ethanol at 20°: (1) 3-amino-N-methylphthalimide, (2) 3-monomethylamino-N-methylphthalimide, (3) 3-dimethylamino-N-methylphthalimide Solutions in ethanol at -180°: (4) 3-amino-N-methylphthalimide; (5) 3-monomethylamino-N-methylphthalimide; (6) 3-dimethylamino-N-methylphthalimide; (7) 3-diphenylamino-N-methylphthalimide.
(C) Curve showing the dependence of q_{fl} on ν_{fl}^{max} for aminochlormaleimide at 20° in various solvents: (1) in methanol; (2) in ethanol; (3) in ethylacetate; (4) in pinacoline; (5) in isoamyl acetate; (6) in acetone; (7) in chloroform; (8) in toluene (9) in benzene (10) is for aminochlormaleimide in ethanol at -180°, and (11) for anilinomaleimide under the same conditions.

but at -180° it is 21,700 cm^{-1}. In 4 dimethylamino-N-methylphthalimide at room temperature ν_{fl}^{max} is 17,650 cm^{-1} and at -180° it is 20,400 cm^{-1}. Marked shifts in the fluorescence spectra for a temperature drop from 20 to -180° in ethanol is also shown in 3-derived phthalimides. In 3-amino-N-methylphthalimide the shift is 1400 cm^{-1}, from 20,200 to

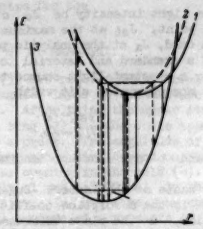

Fig. 2 The change in the relative positions of the ground and excited state potential curves brought about by lowering the temperature.
(1) Excited state at room temperature; (2) Excited state at low temperature (3) Ground state

21,600 cm^{-1}. The fluorescence spectrum of 3-monomethylamino-N-methylphthalimide shifts to the short wavelength side by 800 cm^{-1}, from 19,100 to 19,900 cm^{-1}. In 3-dimethylamino-N-methylphthalimide the shift is 500 cm^{-1} (from 19,000 to 19,500 cm^{-1}).

Thus in the amino derived phthalimides in ethanol the intersection of the ground and excited state potential curves at 20° is significantly closer to the minimum in the excited state curve than is the case at -180° (Fig. 2). Consequently the increased internal conversion at 20° occurs not only because of an increase in the height to which the vibrational levels are populated, but largely because of the movement of the intersection towards the vibrationally populated levels of the excited state as temperature increases. Confirmation of the fact that the fall in quantum yield of fluorescence on increasing temperature comes not only as a result of a redistribution of the vibrational population, but also from a change in the relative position of the ground and excited state potential curves comes from the case of 3-diphenylamino-N-methylphthalimide. The fluorescence spectrum of this substance in ethanol at -180° is shifted farther to long wavelengths than is the case for other derived phthalimides (Fig. 1b). Correspondingly this substance shows a significantly lower value of q_{fl}, of only 0.28, than do the other 3-derived phthalimides, or than that of the analogous 4-diphenylamino-N-methylphthalimide. The latter has a q_{fl} no different from the other 4-derived phthalimides, but the fluorescence spectrum is at considerably shorter wavelengths than that of 3-diphenylamino-N-methylphthalimide.

The marked increase in q_{fl} at low temperature is also observed in substituted maleimides (Fig. 1c). In aminochlormaleimide in ethanol, on lowering the temperature from 20° to -180° q_{fl} rises from 0.01 to 0.30. In the related anilinomaleimide which shows a fluorescence spectrum (at -180°) at shorter wavelength there is also a correspondingly greater value of q_{fl} equal to 0.49.

Thus in several derived phthalmides and maleimides, thermal quenching is very large at room temperature, and in a few cases even at -180°. However the fall in q_{r1} with increasing temperature is due not only to the thermal quenching itself, i.e. to the population of upper state vibrational levels, but also to the change in relative positions of the potential curves for the ground and excited states.

June 28, 1958

References

1. V. V. ZELINSKII, V. P. KOLOBKOV: OiS, 5 423 (1958)
2. V. V. ZELINSKII, V. P. KOLOBKOV, L. G. PIKULIK: OiS, 1, 161 (1956)
3. V. V. ZELINSKII, V. P. KOLOBKOV: DAN USSR, 106, 1042 (1956)
4. V. V. ZELINSKII, V. P. KOLOBKOV, L. G. PIKULIK: OiS, 2, 405 (1957)

TOM VI, Vyp. 3 OPTIKA I SPEKTROSKOPIIA Mart , 1959
VOL.VI, No. 3 OPTICS AND SPECTROSCOPY March , 1959

On Collisions of the Second Kind in a Mixture of N_2 + A

V. P. SYCHEV

Investigations of the intensity of the nitrogen bands in a nitrogen-argon mixture, in both condensed [1] and glow discharges [2 - 4], has shown an increase in the intensity of the nitrogen bands of the second positive system, which could arise from collisions of the second kind between nitrogen molecules and metastable argon atoms in the $^3P_2$ state. The author's investigations [4] have shown, however, that at a total pressure of 1 mm Hg and various nitrogen concentrations, collisions of the second kind occur very rarely, perhaps because of the small effective cross section of these processes. We have, therefore, the problem of determining the relative magnitude of the effective cross section for collisions of the second kind between metastable argon atoms and nitrogen molecules.

We will assume that each collision of the second kind leads to emission of light. Then for the light intensity I arising from these collisions we have

$$I = \beta h\nu \tag{1}$$

where β is the number of collisions of the second kind per unit time per unit volume.

From the kinetic theory of gases we know that

$$\beta = 1.04 \cdot n \cdot n_1 \cdot Q \cdot \bar{v}. \tag{2}$$

Here n is the concentration of metastable atoms, n_1 the concentration of molecules, Q the effective cross section of the processes under consideration, $\bar{v}$ the mean arithmetic relative velocity of the interacting particles, so that

$$\bar{v} = 1.45 \cdot 10^4 \sqrt{\frac{T}{\mu}} \ \frac{cm}{sec}, \tag{3}$$

We know [5] that

$$n = \alpha \tau \tag{4}$$

where τ is the life of the atom in the excited state, and

$$\alpha = 1.48 \cdot 10^8 \, n_e n_2 Q_2 \sqrt{U_o} \, \frac{b-1}{b^3} \left(2 + \frac{3}{2} b \frac{U_a}{U_o}\right) \exp\left[-\frac{3}{2}\frac{U_a}{U_o}\right] \tag{5}$$

where n_2 is the concentration of A atoms, so that

$$n_2 = \frac{9.7 \cdot 10^{18} p}{T} \tag{6}$$

and p_2 is the partial pressure of argon, n_e the concentration of electrons,

$$b = 1 + \frac{2}{3} \frac{U_o}{U_m - U_a}; \ U_o$$

is the mean electron energy developed under the given conditions, U_m the energy of electrons at the maximum of the excitation function for collisions of the first kind, Q_2 the corresponding effective cross section, and U_a the excitation potential of the metastable atoms.

According to the theory of Fabrikant [6], the intensity of emission I_1 due to electron collisions is given by the equation

$$I_1 = 1.48 \cdot 10^8 \cdot h\nu \cdot n_e n_1 Q_1 \sqrt{U_o} \, \frac{b_1 - 1}{b_1^3} \left(2 + \frac{3}{2} b_1 \frac{U_{n2}}{U_o}\right) \exp\left[-\frac{3}{2}\frac{U_{a2}}{U_o}\right] \tag{7}$$

where n_1, Q_1 and $b_1 = 1 + \frac{2}{3} \frac{U_o}{U_{m2} - U_{a2}}$ have the same meaning as the corresponding symbols in equation (5), but refer to nitrogen. In particular, U_{a2} is the energy of the highest vibrational level with the quantum number v = 2 of the second positive system

Taking into account the fact that $U_{m2} - U_{a2} = 4$ ev [8], and that the values of U_a and U_{a2} are close together, we have from equations (1)---(7)

$$(8)\qquad \frac{Q}{Q_1} = \frac{\exp\left[\frac{3}{2U_o}(U_a - U_{a2})\right]}{1.46\cdot 10^{23}\cdot \tau p Q_2}\cdot\sqrt{\mu T}\cdot\frac{I}{I_1}$$

The relative intensity $\frac{I}{I_1}$ can be measured, according to the following line of reasoning.

Let I be the intensity of some nitrogen band of the first positive system in the pure gas with molecular concentration n, and let I_o and n_o be the same constants for a mixture of nitrogen and argon. Then, on the basis of Fabrikant's theory (assuming that collisions of the second kind play no part we have approximately

$$I' \sim n' \exp\left[\frac{3}{2}\frac{U_{a1}}{U'_o}\right] \text{ and } I_o \sim n_o \exp\left[-\frac{3}{2}\frac{U_a}{U_o}\right],$$

so that

$$\frac{I_o\cdot n'}{I'\cdot n_o} = \exp\left[\frac{3}{2}U_{a1}\left(\frac{1}{U'_o} - \frac{1}{U_o}\right)\right]$$

Let

$$(9)\qquad \frac{I_o\, n'}{I' n_o} = C_1$$

then

$$(10)\qquad C_1 = \exp\left[\frac{3}{2}U_{a1}\left(\frac{1}{U'_o} - \frac{1}{U_o}\right)\right]$$

By analogy, for the second positive system we find for the nitrogen bands in the same concentration range as above,

$$(11)\qquad \frac{I_1 n'}{I'_1 n_o} = C_2$$

and

$$(12)\qquad C_2 = \exp\left[\frac{3}{2}U_{a2}\left(\frac{1}{U'_o} - \frac{1}{U_o}\right)\right]$$

From (10) and (12) we derive the relation

$$(13)\qquad \lg C_2 = \frac{U_{a2}}{U_{a1}}\lg C_1$$

Our investigations [4] have shown that the observed value of C_2, obtained from measurements of the relative intensities of the nitrogen bands in the second positive system with v = 2, is larger than the value calculated from equation (13). This indicates that in the excitation of nitrogen bands in nitrogen-argon mixtures there are other processes in addition to electron collision. Such processes might include collisions of the second kind.

In fact, the metastable $^3P_2$ level of argon and the nitrogen vibrational level v = 2 of the second positive system are quite close together. Moreover, the interaction of metastable argon atoms with nitrogen molecules in the ground state satisfies Wigner's rule.

We assume in this connection that the observed emission intensity I_2 of the nitrogen band is composed of the intensity I_1 due to electron collisions and the intensity I due to collisions of the second kind. Then $I_2 = I_1 + I$ denoting the observed value of the increase in intensity by C_3, we have

$$(14)\qquad C_3 = \frac{I_2\cdot n'}{I'_1\, n_o} = \frac{(I_1 + I)\cdot n'}{I'_1\, n_o}$$

It follows from (11) and (14) that

$$\frac{C_3}{C_2} = \frac{I_1 + I}{I_1}$$

whence

$$(15)\qquad \frac{I}{I_1} = \frac{C_3 - C_2}{C_2}$$

It has been shown experimentally that for a total pressure of 1 mm Hg and for a partial pressure of argon equal to 0.88 mm Hg,

$$\frac{I}{I_1} = 0.3$$

We put T = 400° K. Keeping in mind that $\tau = 1.4 \times 10^{-3}$ sec, and $Q_2 = 10^{-17}$ cm^2 [8], and that under the experimental conditions [4] $U_o = 3$ eV, p = 0.88 mm Hg, $I/I_1 = 0.3$, $U_a = 11.66$ ev, $U_{a2} = 11.48$ ev, we obtain from equation (8) the approximate value $Q/Q_1 \approx 10^{-2}$. We should note that with a change in the composition of the gas mixture the mean energy U_o of the electrons changes. Under the conditions of our experiment, a change in the nitrogen content from 0.2% to 99.8% corresponded to a decrease in U_o from 4.4 to 2.9 eV. However, as a simple calculation will show, the expression

$$\sqrt{U_o}\,\frac{b_1 - 1}{b_1^3}\left(2 + \frac{3}{2}b_1\frac{U_{a2}}{U_o}\right)$$

remains practically constant.

If we calculate the concentration of electrons, on Langevin's theory and Townsend's experimental data [9], we find that under our experimental conditions n_e may vary by a factor of about 1.6.

The probability of decay of the metastable state, according to the data of Mitchell and Zemansky [10], will change by a factor of about 2 over the range of variation of the partial pressure of argon, and in our experiment this decay should occur primarily at the walls of the discharge tube.

Therefore, the relationship between electron concentration and the variation in the probability of decay of the metastable states making up the mixture of N_2 + A which are induced by changes in partial pressure, should have nothing to do with the determination of the order of magnitude of the quantity Q/Q_1.

It should be noted that, as applied to our conditions (pressure 1 mm Hg), the assumptions underlying equations (1), (5), and (7) are of a crude nature.

Nevertheless, under conditions similar to ours (i.e at the same pressure) Fabrikant's theory was successfully applied by Panovkin [8]. This is the reason for our use of the same theory.

In summary, there are grounds for supposing that in a mixture of N_2 + A the effective cross section for excitation of nitrogen molecules with v = 2 in the second positive system by collision of the second kind is two orders of magnitude smaller than the cross section for excitation of this level by electron collisions.

The minor role of collisions of the second kind in nitrogen excitation was noted also by Kaplan [11], in his analysis of the work of Ta Jou-wu [12] on excitation processes in the upper atmosphere. There are grounds for assuming [4] that the strengthening of the nitrogen bands in mixtures of argon-nitrogen [1--4] is influenced by electron temperatures rather than by collisions of the second kind.

In conclusion I express my deepest thanks to N. A. Prilezhaeva for her valuable advice and direction in connection with this study.

July 10, 1958

References

1. M. TOUSSAINT: Z. F. Phys., 19, 271 (1923)
2. W. STEUBING, M. TOUSSAINT: Z. F. Phys., 21, 128 (1924)
3. R. BERNARD: Ann. de Phys., 13, 5 (1940)
4. V. P. SYCHEV: Cand. Dissertation, Tomsk, 1954
5. V. FABRIKANT, F. BUTAEVA, I. TSIRG: ZETF, 7, 733 (1937)
6. V. FABRIKANT: Tr. VEI, 41, 236 (1941)
7. P. THIEME: A. f. Phys., 78, 412 (1932)
8. K. PANOVKIN: ZETF, 9, 1007 (1939) (See translation in J. Phys. USSR, 2 (1940), pp. 39-48)
9. J. S. TOWNSEND: J. Franklin Inst., 200, 563 (1925)
10. A. C. G. MITCHELL, M. W. ZEMANSKY: Resonance radiation and excited atoms. N.Y., Macmillan 1934 (ONTI, Moscow, 1937, pp. 205 - 209)
11. J. KAPLAN: Phys. Rev., 73, 530 (1948)
12. TA-YOU WU: Proc. Ind. Acad. Sci., 18A (1943), 40-66

TOM VI, Vyp. 3 OPTIKA I SPEKTROSKOPIIA Mart, 1959
VOL. VI, No. 3 OPTICS AND SPECTROSCOPY March, 1959

Luminescence Yield of CsI(Tl) Crystals Under α And γ Excitation As A Function of Tl Concentration

IU. A. TSIRLIN, S. N. KOMNIK, AND L. M. SOIFER

Recently there have been a number of studies [1--4] of the scintillation properties of single crystals of thallium-activated cesium iodide. These have revealed a number of advantages of CsI(Tl) for scintillation applications -- high luminescence yield under excitation by fast particles, relatively short quenching time (~ 0.5 μsec), appreciable density, and high average atomic weight (this latter property is especially important in the detection of γ-rays). The single crystals also possess noteworthy properties -- mechanical stability, almost total absence of hygroscopy (which is important in the use of scintillators without moisture-proof containers for the detection of charged particles), and the comparative ease with which large clear crystals may be grown. Although useful data are currently available on the quantum output as a function of concentration for KI(Tl)[5] and especially for NaI(Tl) [6-8], there are only a few scattered reports on CsI(Tl) [9].

Since CsI(Tl) is widely used as a scintillator, it is worth while to investigate the relationship between its scintillation properties and the thallium concentration. Single crystals were grown by Stockbarger's process. The length was of the order of 50 mm, diameter 15 mm. The Tl content was in the range from 0.005 to 0.5% by weight. Each of the crystals was cut into disks, which were ground and polished to a thickness of about 2 mm.

The distribution of thallium along the axis of the crystal was determined by chemical analysis [10]. A typical curve showing the concentration of thallium along the crystal is given in Figure 1.

The dependence of the relative yield I_γ of γ-luminescence on the concentration C of thallium in the CsI(Tl) crystals was investigated under bombardment by γ-rays from Cs^{137}. The α-luminescence was investigated under bombardment by α-particles from Po^{210}. The experiments were carried out at room temperature (22-25°).

Observations of the relative yield of luminescence were made with an FEU-29 photomultiplier by two methods: a) measurement of the anode current of the photomultiplier; b) counting pulses and measuring the magnitude of the pulses using an amplifier (with a time constant of 1 μsec) and a pulse analyzer.

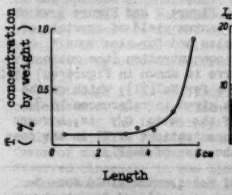

Fig. 1. Distribution of thallium along the crystal of CsI(Tl). Thallium content 0.3% (0.5% TlI).

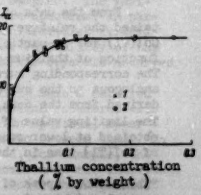

Fig. 2. Dependence of the output of α-luminescence of CsI(Tl) (in arbitrary units) on the thallium concentration.
1 -- pulse method
2 -- current method.

The results of these measurements are given in Figure 2. The abscissa corresponds to the thallium concentration C, in percent by weight. The ordinate is the quantum yield of the α-luminescence, I_α in relative units. From the fact that the results of both series of measurements (pulse count and anode current) fall on the same curve, within the limits of experimental error, it follows that there is no significant dependence of the quenching time of the scintillations on the thallium concentration within the range of concentrations studied in this experiment. This is corroborated by direct observation of the pulses from the scintillator on an oscillograph.

The basic method for work with γ-rays was counting pulses. In view of the small size of the samples (the thickness being comparable to the path-length of secondary electrons from γ-rays of Cs^{137}), irradiation was carried out in both the axial and radial directions. The dependence of the relative yield of γ-scintillations on the concentration of Tl is shown in Figure 3; the data represent the average of these two series of measurements. The current measurements are less exact because of the uncertainty involved in referring the current measurements to a standard mass of scintillator. The curve obtained was, however, not much different from that shown in Figure 3.

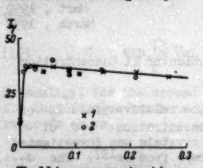

Fig. 3. Dependence of the output of γ-luminescence of CsI(Tl) (in arbitrary units) on the thallium concentration
1-pulse method
2-current method

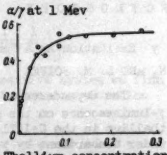

Fig. 4. Dependence of α/γ on thallium concentration in CsI(Tl) crystals.

From the data of Figure 2 and Figure 3 we obtained the relative quantum yield of crystals of CsI(Tl) for α-particles and for electrons * as a function of thallium concentration (the ratio α/γ). The corresponding curve is shown in Figure 4. It is analogous to the curve for NaI(Tl), which can be derived from the data given in references [6-8]. The limiting value of the ratio α/γ is, however obtained at lower concentrations of Tl in the case of CsI(Tl) than in the case of Na(Tl).

*The authors speak of the quantum yield for α-particles (which is consistent) and for electrons which makes no sense since they have been speaking of γ excitation all along. An electron is a β-particle and a γ ray is a high energy photon. Why they have mentioned electrons at all, I don t know. R.D.

CONCLUSIONS

1. The luminescence yield of crystals of CsI(Tl) under α-bombardment has a well-defined limiting value, reached at Tl concentrations of 0.1%. When these crystals are used for counting α-particles, the Tl concentration must not be less than 0.1%.

2. The luminescence yield of CsI(Tl) crystals under γ-bombardment has a maximum in the range 0.01-0.03% Tl concentration. Further increase in the Tl concentration (up to 0.3%) causes the yield to decrease to some extent.

3. The dependence of the ratio α/γ on the Tl concentration (at room temperature) was obtained. This ratio tends to a constant value (the limiting value is approximately 0.55). The limiting value is essentially attained at C~ 0.1%. The low values of the ratio α/γ at lower values of the concentration can be attributed to the high specific energy losses of the α-particles. The dissipation of this energy in the scintillator is possible if there are enough activation centers in the region near the path of the particles.

In conclusion, we express our thanks to a group of our colleagues, directed by A. M. Bulgakova, for making the chemical analyses of the crystals to determine the thallium content.

July 14, 1958

References

1. A. GALONSKY, C. H. JOHNSON, C. D. MOAK: REV. Sci. Instr., 27, 58 (1956)
2. S. BASHKIN, R. R. CARLSON, R. A. DOUGLAS, J. A. JACOBS: Phys. Rev., 109, 454 (1958)
3. H. KNÖPFEL, E. LOEPFE, P. STOLL: Helv. Phys. Acta, 29, 241 (1956)
4. W. BEUSCH, H. KNOEPFEL, E. LOEPFE, D. MAEDER, P. STOLL: Nuovo Cimento, 5, 575 (1957)
5. L. M. BELIAEV, M. D. GALANIN, Z. L. MORGENSHTERN, Z. A. CHIZHIKOVA: DAN USSR, 99, 691 (1954)
6. L. M. BELIAEV, M. D. GALANIN, Z. L. MORGENSHTERN, Z. A. CHIZHIKOVA: DAN USSR, 105, No. 1, 57 (1955) (See CCT-1270TM, 2 pp., for translation)
7. F. S. EBY, W. K. JENTSCHKE: Phys. Rev., 96, 911 (1954)
8. J. A. HARSHAW, H. C. KREMERS, E. C. STEWART, E. C. WARBURTON, J. O. RAY: AEC Report No. NYO - 1577 1952
9. L. M. BELIAEV, M. D. GALANIN, Z. L. MORGENSHTERN, Z. A. CHIZHIKOVA: IAN USSR, Ser. fiz., 21, No. 4, 548 (1957) (See CTT Bulletin, 21, 544 (1957))
10. A. M. BULGAKOVA, A. M. VOLKOVA, G. S. PLOTNIKOVA: Trudy IREA (in press)

Line Luminescence of X-rayed LiF Crystals

A. A. KAPLIANSKII

The absorption spectrum of colored LiF crystals, which have much in common with the spectra of other colored alkali-halide crystals [1], has certain interesting peculiarities. In 1953, Pringsheim and his colleagues [2,3] discovered that there were numerous narrow lines in the visible and near ultraviolet regions of the spectrum in the absorption spectra, at low temperatures, of strongly-colored LiF crystals along with the broad bands characteristic of color centers of alkali-halide crystals. The spectrum of this line absorption is changed substantially as a result of different ways of treating the crystal (pre-heating, ultraviolet irradiation, etc.). The origin of the narrow lines in the absorption spectrum of colored LiF crystals remains completely unclear.

In this connection, it would also be interesting to investigate the luminescence spectrum of these crystals more carefully. According to existing data [4,6], several very broad bands located in the infrared, visible and ultraviolet regions of the spectrum exist in the emission spectrum of colored LiF.

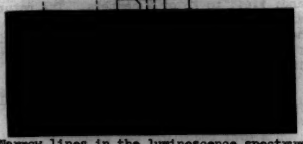

Figure: Narrow lines in the luminescence spectrum of x-rayed LiF crystals. a,b - spectrograms taken at different exposures; c - Fe comparison spectrum

Luminescence spectra of colored LiF crystals in the visible range of the spectrum at T = 77°K have been investigated herein. The light of a SVDSh-1000 mercury lamp through a UFS-1 filter excited the luminescence of samples placed in a low-temperature quartz cell. The emission spectra were photographed by means of a prism spectrograph with ~ 40 A/mm dispersion in the green part of the spectrum. Artificially grown LiF single crystals, subjected to lengthy x-ray treatment for ten hours until the appearance of visible coloration of the crystals, were used as samples.* Samples of LiF with various degrees of coloring were examined; the absorption spectrum of these crystals at T=77°K was analogous to that described by Pringsheim [2], a narrow λ 523.5mμ line with feeble short wavelength satellites, a broad, so-called, M - band, λ 450 mμ, defining the visible coloring of the crystal, and an equidistant group of narrow bands with wavelength λ 391 mμ

It has been discovered that there is a significant number of very narrow "atomic" emission lines located basically in the λ600 - 520 mμ region in the luminescence spectra of x-rayed LiF at T = 77°K as well as the known [4,6] broad red and green bands. Upon heating the crystals to room temperature, the narrow lines in the luminescence spectrum vanish while the broad bands remain. Line luminescence was observed at T=77°K in all the LiF samples investigated which had various degrees of coloring. Hence, the observed difference in the general intensity of the line luminescence in the different samples should be noticed. In addition, while the basic character of the spectra are retained, there exist certain variations in the line emission spectra of the various crystals.

In the line luminescence spectrum of LiF (see figure), there is first of all isolated a long wavelength group inherent in the emission of all crystals and consisting of at least four lines, λ 569.8, 578.0, 586.2 and 595.0 mμ. The difference in the frequencies between all the adjacent terms of this group is the same, within the limits of measurement accuracy. As the wavelength increases, the lines are broadened more and more and their intensity drops. Hence, the equidistant group of lines mentioned has the character of an electronic-vibrational series. It is interesting to note that the frequency difference of this series of emission lines ($\Delta\nu$ = 247 cm^{-1}) is close to the difference $\Delta\nu$ in the equidistant group of lines λ 391 mμ, observed in the absorption spectrum of colored LiF [2,3]. Several narrow lines, of which the most intense are λ 581.0 and 583.0 mμ, are located between the members of the equidistant group. Furthermore, there is a number of lines λ 562.7, 553.5 and 546.0 mμ, on the short wavelength side of the series, where the first is especially powerful in the emission from densely-colored crystals. The line λ 531.6 mμ is also observed in the luminescence spectra of samples subjected to lengthy ultraviolet irradiation after having been x-rayed. Moreover, the additional lines λ 524.0, 444.0 mμ and certain others were observed in the spectra of individual samples. The variability of the LiF luminescence spectrum, in particular, under the effect of ultraviolet irradiation, is in agreement with the variability of the absorption spectra of colored LiF crystals observed in [2,3].

Although it is difficult to make a detailed comparison of the line luminescence spectrum with the lines of the LiF absorption spectrum, apparently a definite relation exists between them. In favor of such an assumption is, for example, the observed closeness in the location of the individual luminescence and absorption lines, which permits the resonance character of the light absorption and emission processes in lines to be spoken of (thus, the luminescence line λ 524 mμ is close to the intense absorption line λ 523.5 mμ). As regards the question of the origin of narrow lines in the luminescence spectrum of x-rayed LiF, it remains open, as does the question of the origin of the

*The author is grateful to I.N. Zimkin and N. IA. Karasik for x-raying the crystals.

absorption lines of crystals. A joint study of luminescence and absorption of LiF crystals, including samples with different pre-history, can contribute to the clarification of the reasons for the interesting phenomenon, the existence of narrow "atomic" lines in the spectra of colored LiF crystals.

The author is grateful to Corr. Member E.F. Gross for interest in the research.

Sept. 19, 1958

References

1. H. F. IVEY: Phys. Rev., 72, 341; 873 (1947)
2. C. J. DELBECQ, P. PRINGSHEIM: J. Chem. Phys., 21, 794 (1953)
3. P. PRINGSHEIM: Zs. Phys., 136, 573 (1954)
4. C. C. KLICK: Phys. Rev., 79, 894 (1950)
5. J. A. GHORMLEY, H. A. LEVY: J. Phys. Chem., 56, 548 (1952)
6. P. P. FEOFILOV: DAN USSR, 92, 743 (1952)

TOM VI, Vyp. 3 OPTIKA I SPEKTROSKOPIIA Mart, 1959
VOL. VI, No. 3 OPTICS AND SPECTROSCOPY March, 1959

Orientation of Centers of Linear Luminescence in X-rayed LiF Crystals

Narrow lines, which appear in the absorption spectra of lithium fluoride crystals subjected to the effect of x-rays, fast electrons or neutrons and then cooled to liquid nitrogen temperatures, were discovered and investigated in the research of Pringsheim and his colleagues [1]. The appearance of narrow lines was also detected recently by Kaplianskii [2] in the luminescence spectra of such crystals excited through a light filter which passed shortwave ultraviolet rays.

In connection with the extremely great interest which, it seems to us, the detection of the narrow "atomic" lines in the spectra of colored crystals represents, we determined the character of the orientation of the centers responsible for the line spectra in the cubic crystalline LiF lattice. This determination was made by the method of studying the azimuthal dependences of the polarization of the luminescence [3]. The degree of polarization was measured by a spectro-photographic method, which we had used earlier to study the character of the orientation of Eu^{+++} ions in the CaF_2 crystal lattice [4].

The degree of polarization, determined at 77°K for two crystal positions (a = 0° and 45°), appeared to be identical for the narrow 5627 and 5698 Å lines within the limits of experimental accuracy, as well as for the broad red band of luminescence with a maximum at around 6900 Å. This means, in correspondence with [3,5], that the centers responsible for the line spectra are oriented along the second order axes of symmetry. This latter circumstance, as well as the fact that the narrow luminescence lines abut directly on the short wavelength edge of the "red" band and are only observed in samples having an intense red glow permits the hypothesis to be expressed that they should be ascribed to the same centers as for the broad "red" band, i.e., to F_2 or M centers. The nature of the narrow lines and the reasons for the exclusivity of the LiF crystals with respect to the possibility of observing line spectra of coloring centers continues to remain unclarified.

December 15, 1958

References

1. C. J. DELBECQ, P. PRINGSHEIM: J. Chem. Phys., 21, 794 (1953)
   P. PRINGSHEIM: Zs. Phys., 136, 573 (1954)
2. A. A. KAPLIANSKII: OiS, 6, 424 (1959) (See preceding article)
3. P. P. FEOFILOV: DAN USSR, 92, 743 (1953) (See translation RT-845, 4 pp.); ZETF, 26, 609 (1954); UFN, 58, 69 (1956)
4. P. P. FEOFILOV: DAN USSR, 92, 731 (1954)
5. A. M. BONCH-BRUEVICH, G. A. TISHCHENKO, P. P. FEOFILOV: OiS, 2, 136 (1957)

TOM VI, Vyp. 3 OPTIKA I SPEKTROSKOPIIA Mart, 1959
VOL. VI, No. 3 OPTICS AND SPECTROSCOPY March, 1959

Determination of the Luminescence Quantum Yield of the Trivalent Terbium Ion in Solution

E. V. KONDRAT'EVA

There is a very limited number of papers in which a measurement is made of the luminescence quantum yield of trivalent ions of the middle rare-earths (Sm, Eu, Gd, Tb, Dy) in crystals [1,2]. Insofar as we know, analogous measurements have not been made for solutions. A measurement of the luminescence quantum yield affords the possibility of determining the probability of deactivation processes of excited ions.

As is known [3], the luminescence spectrum of the trivalent terbium ion in aqueous solutions consists of seven bands 100 - 200 Å in width, with maxima at the wavelengths λ_{max} = 4890, 5450, 5890, 6200, 6480, 6700 and 6810 Å. According to [2], these bands correspond to transitions from the $^5D_4$ upper term to components of the ^7F term. All of the transitions are forbidden for the free ions since they occur between levels of the same parity. The quantum yield of the luminescence of Tb^{+++} in solution has been determined in the present study by the same methods as were used in [1,2]. Knowledge of the following quantities is necessary in order to determine the quantum yield by this method: 1) the relative intensities of all the bands; 2) the probability of a radiative transition for one of the bands, 3) the lifetime of the excited level.

The luminescence spectrum of aqueous solutions of terbium chloride and sulfate was excited by a spark discharge between nickel electrodes at right angles to the direction of observation. The light from the spark discharge was projected into a quartz cell containing the solution to be investigated. The luminescence light was projected onto the slit of an ISP-51 spectrograph by using a three-lens system. The spectra were photographed on 350° GOST sensitivity isopanchromatic film. The relative intensities of the bands were measured by the usual methods of heterochromatic photometry. The contours of the bands being investigated were constructed by plotting intensity against λ; the relative intensities of the seven bands were determined by comparing the areas under these curves. The results of the measurements are presented in the table. The ratios of the intensities of the bands with λ_{max} = 4890, 5450, 5890 and 6200 Å have also been measured photoelectrically. The results of the photoelectric measurements are in agreement with the photographic results within the limits of the error of the latter.

Band Number	Wavelength of band maxima (λ max)	Relative intensity (I)	Root mean square error, determined from 20 measurements (in %)
6	4890	1.00	5
5	5450	3.10	3
4	5890	1.10	5
3	6200	0.76	5
2	6480	0.33	7
1	6700	0.20	12
0	6810	0.05	20

It has been verified that the ratio of band intensities is the same in aqueous terbium chloride and sulfate solutions and does not change substantially over the concentration range 0.2 - 0.02%.

The measurement of the lifetime τ after luminescence was made by using an "electronic shutter" circuit [4]. The method of making the measurement is described in [5].

It has been remarked in [3] that the interval rule is obeyed well by all the luminescence bands except those at very short wave lengths. In this connection it is interesting to see whether τ is the same for the λ_{max} = 4890 Å band as for the others. It has been determined that the τ values are the same for the λ_{max} = 4890, 5450 and 5890 Å bands, equal $(5.5\pm0.2)\times10^{-4}$ sec at 15° C, and decrease identically with temperature.* This result is an additional verification of the hypothesis that all seven luminescence bands of Tb^{+++} represent transitions from the same upper level. According to the data of Hoogschagen and Gorter [6], the oscillator strength of the blue band of Tb^{+++} in aqueous $TbCl_3$ solutions is: $f_{4890} \approx 4\times10^{-9}$. Making use of this value, the probability $A_{4,6}$ of the radiation transition $^5D_4 - {}^7F_6$ can be estimated according to the Ladenburg formula;

$$A_{4,6} = \frac{8\pi^2 e^2}{mc} \frac{g_6}{g_4} \frac{f}{\lambda^2} \approx 2 \text{ sec.}^{-1},$$

where g_6 and g_4 are the statistical weights of the lower and upper levels; λ is the wavelength of the given transition; e and m are the charge and mass of an electron; c is the velocity of light. Using the value of $A_{4,6}$ and the relation $I_0 : I_1 \ldots I_6 = A_{4,0}\nu_0 : A_{4,1}\nu_1 : \ldots A_{4,6}\nu_6$ (I is intensity, ν frequency), let us determine the probabilities of the remaining six radiational transitions: $A_{4,5} \approx 6$ sec.$^{-1}$; $A_{4,4} \approx 3$ sec.$^{-1}$; $A_{4,3} \approx 2$ sec^{-1}; $A_{4,2} \approx 0.8$ sec^{-1}; $A_{4,1} \approx 0.5$ sec.$^{-1}$; $A_{4,0} \approx 0.1$ sec.$^{-1}$; $\sum_{x=6\ldots0} A_{4,x} \approx 14$ sec.$^{-1}$.

According to our measurements

$$\tau = \frac{1}{\sum_{x=6\ldots0} A_{4,x} + \sum_{x=6\ldots0} W_{4,x}} = 5.5\cdot10^{-4} \text{ sec.}$$

$\sum_{x=6\ldots0} W_{4,x}$ is the sum of the probabilities of the radiationless transitions with the $^5D_4$ term in the component of the ^7F term.

The luminescent quantum yield is

$$\eta = \frac{\sum_{x=6\ldots0} A_{4,x}}{\sum_{x=6\ldots0} A_{4,x} + \sum_{x=6\ldots0} W_{4,x}} = \sum_{x=6\ldots0} A_{4,x} \cdot \tau = 0.8\%.$$

* More detailed results are presented in [5].

As mentioned above, Hoogschagen and Gorter present only an estimate of the quantity f_{4890}; consequently, the result of the given computation is only approximate. But even if it is assumed that they had determined only the correct order of magnitude of the oscillator strength $10^{-8} > f > 10^{-9}$ (which leads to values of $2.0\% > \eta > 0.2\%$ for the quantum yield), this does not alter the fundamental conclusion that the probability of radiationless transition for the trivalent terbium ion in aqueous solution is approximately two orders of magnitude greater than for radiational transition. The lifetime of the excited state is determined almost entirely by the probability of the radiationless transitions. The value obtained is of the same order of magnitude as the results obtained by Rinck for europium sulfate crystals [1] and by Geisler and Hellwege for terbium bromate crystals [2].

In conclusion, I am grateful to A. N. Zaidel' for supervising the present work.

September 20, 1958

References

1. B. RINCK: Z. f. Naturforsch., 3a, 406 (1948)
2. H. F. GEISLER, K. H. HELLWEGE: Z. f. Physik, 136, 293 (1953-54)
3. A. N. ZAIDEL', IA. I. LARIONOV, A. N. FILIPPOV: ZETF, 9, 17 (1939)
4. D. W. STEINHAUS, H. M. CROSSWHITE, G. H. DIEKE: Spectr. Acta, 5, 436 (1952-53)
5. E. V. KONDRAT'EVA, V. B. USTINOV: Vestnik, Leningrad Univ., No. 4, 5 (1959)
6. J. HOOGSCHAGEN, C. J. GORTER: Physica, 14, 197 (1948)

ABBREVIATIONS OFTEN ENCOUNTERED AND USED HERKIN

DAN USSR	Doklady Akademii Nauk	(Reports of the Academy of Sciences of the USSR)
DAN UkrSSR	Dopovidi Akademii Nauk UkrSSR	(Reports of the Academy of Sciences of the Ukraine SSR)
DAN ArmSSR	Doklady Akademii Nauk ArmSSR	(Reports of the Academy of Sciences of the Armenia SSR)
IAN USSR	Izvestiia Akademii Nauk USSR	(Bulletin of the Academy of Sciences of the USSR)
	SF Seriia fizika	(Physics series)
	SM Seriia matematika	(Mathematics series)
	OKhN Otdelenie khimicheskikh	(Section of chemical sciences)
OiS	Optika i Spektroskopiia	(Optics and Spectroscopy)
PiTE	Pribory i Tekhnika Eksperimenta	(Instruments and Techniques of Experiment)
AE	Atomnaia Energiia	(Atomic Energy)
AZ	Astronomicheskii Zhurnal	(Astronomy Journal)
FMM	Fizika Metallov i Metallovedenie	(Physics of Metals and Metallography)
Radiotekh.	Radiotekhnika	(Radio Engineering)
RiE	Radiotekhnika i Elektronika	(Radio Engineering and Electronics)
UK	Uspekhi Khimii	(Progress in Chemistry)
UFN	Uspekhi Fizicheskikh Nauk	(Progress in Physical Sciences)
UFZ	Ukrainskii Fizichni Zhurnal	(Ukraine Physical Journal)
ZETF	Zhurnal Eksperimental'noi Teoreticheskoi Fiziki	(Journal of Experimental Theoretical Physics - JETP)
ZTF	Zhurnal Tekhnicheskoi Fiziki	(Journal of Technical Physics)
FTT	Fizika Tverkogo Tel	(Solid State Physics)
ZFKh	Zhurnal Fizicheskoi Khimii	(Journal of Physical Chemistry)
ZOKh	Zhurnal Obshchee Khimii	(Journal of General Chemistry
ZNKh	Zhurnal Neorganicheskoi Khimii	(Journal of Inorganic Chemistry)
ZPKh	Zhurnal Prikladnoi Khimii	(Journal of Applied Chemistry)
Tr.	Trudy	(Transactions, as for instance, Tr. FIAN)
FIAN	Fizicheskii Institut Akademii Nauk USSR	(P.N. Lebedev Physical Institut of the Academy of Sciences USSR)
Sb.	Sbornik	(Collection, as for instance, Fizich. sb. L'vovskogo Universitet)
		Fizich. sb. Fizicheskaia sbornik (Physics Collection)
Uch. Zap.	Uchenye Zapiskii	(Scientific Records)
Vestn.	Vestnik	(Herald or Messenger)
FTIAN	Fiziko-Tekhnicheskii Institut Akademii Nauk	(Physical-Technical Institute of the Academy of Sciences)
GOI	Gosudarstvennyi Opticheskii Institut	(State Optical Institute)
VEI	Vsesoiuznyi Elektrotechnicheskii Institut	(All-Union Electrotechnical Institute)
MFTI	Moskovskaia Fiziko-Tekhnicheskii Institut	(Moscow Institute of Physics and Technology)
NIZMIR	Nauchno-Issledovatel'skii Institut Zemnogo Magnetizma, Ionosfery i Rasprostraneniia	(Research Institute of Terrestrial Magnetism and Ionospheric Propagation)
GIFTI	Gor'kovskii Issledovatel'skii Fiziko-Tekhnicheskii Institut	(Gor'kii Research Institute of Physics and Technology)
NIFI	Nauchno-Issledovatel'skii Fizicheskii Institut	(Scientific Research Institute of Physics, Leningrad Univ.)
NIRFI	Nauchno-Issledovatel'skii Radio-fizicheskii Institut	(Scientific Research Institute of Radiophysics, Gor'kii Univ.)
GITTL	Gostekhizdat - Gosudarstvennoe Izdatel'stvo Tekhniko-Teoreticheskoi Literatury	(State Publishers of Technical-Theoretical Literature)
GIFML	Fizmatgizdat - Gosudarstvennoe Izdatel'stvo Fiziko-Matematicheskoi Literatury	(State Publishers of Physical-Mathematical Literature, formerly Gostekhizdat)
IL or IIL	Izdatel'stvo Inostrannoi Literatury	(Publishers of Foreign Literature)
Izd. AN USSR	Izdatel'stvo Akademiia Nauk USSR	(Academy of Sciences Press)
ZL	Zavodskaia Laboratoriia	(Factory Laboratory)
GOST	Gosudarstvennyi Obshchesoiuznyi Standart	(All - Union State Standard)
LIPAN USSR	Laboratoriia izmeritel'nykh priborov AN USSR	(Laboratory of Measuring Instruments)
IPAN UkrSSR	Institut Fiziki AN UkrSSR, KIEV	(Physics Institute AN Ukr SSR)
SFTI	Sibirskii Fiziko-Tekhnicheskii Institut, Tomsk	(Siberia Physical-Technical Institute)
IPAAN ESSR	Institut Fiziki i Astronomii AN ESSR, Tartu	(Institute of Physics and Astronomy)
IPA AN USSR	Institut fiziki atmosfery AN USSR	(Institute of the Physics of the Atmosphere)

AFFILIATIONS OF AUTHORS FROM ISSUE 3

N. S. SOBOLOV
A. V. POTAPOV
V. F. KITAEVA
F. S. FAIZULLOV
V. N. ALIAMOVSKII
E. T. ANTROPOV
I. L. ISAEV
A. N. NIKITINA
M. D. GALANIN
G. S. TER-SARKISIAN
B. M. MIKHAILOV
V. L. LEVSHIN
V. B. GUTAN
E. N. KARSHAVINA
- FIZICHESKII INSTITUT im. P. N. LEBEDEVA AN USSR (P. N. Lebedev Physics Institute)

R. S. LEBEDEV - KEMEROVSKII PEDAGOGICHESKII INSTITUT (Kemerov Pedagogical Institute)

L. M. SVERDLOV
E. P. KRAINOV
- SARATOVSKII AVTODOROZHNYI INSTITUT (Saratov Auto Highway Institute)

F. I. PEDOROV - BELORUSKII GOSUDARSTEVENNYI UNIVERSITET, MINSK (Belorussian State University, Minsk)
P. G. KARD - TARTUSKII GOSUDARSTVENNYI UNIVERSITET (Tartu State University)
A. O. SALL' - GOSUDARSTVENNOE SOIUZNOE KNOSTRUKTORSKOE BIURO ANALITICHESKOGO PRIBOROSTROENIIA (State Union Construction Bureau of Analytic Instrumentation)

A. I. FINKEL'SHTEIN
F. L. MALACHEVSKAIA
A. M. FISHER
B. G. RABOVSKII
- DZERZHINSKII FILIAL NAUCHNO-ITSLEDOVATEL'SKOGO I PROEKTNOGO INSTITUTA AZOTNOI PROMYSHLENNOSTI (Dzerzhinski Branch of the Scientific Research and Planning Institute of the Nitrogen Industry)

V. V. ZELINSKI
V. P. KOLOBKOV
N. D. KRASNITSKAIA
P. P. FEOFILOV
- GOSUDARSTVENNYI OPTICHESKII INSTITUT

E. V. KONDRAT'EVA - NAUCHNO-ISSLEDOVATEL'SKII FIZICHESKII INSTITUT LENINGRADSKOGO GOSUDARSTVENNOGO UNIVERSITETA (Scientific Research Institute of Physics, Leningrad University)

SYMBOLS FOR SOURCES OF TRANSLATIONS

AIP
American Institute of Physics
335 East 45th Street
New York 17, New York

ATS
Associated Technical Services, Inc.
P.O. Box 271
East Orange, New Jersey

CB
Consultants Bureau, Inc.
227 West 17th Street
New York 11, New York

CCT
Consultants Custom Translations, Inc.
227 West 17th Street
New York 11, New York

CTT
Columbia Technical Translations
5 Vermont Avenue
White Plains, New York

HB
Henry Brutcher
P.O. Box 157
Altadena, California

LC
Photoduplication Service
Publication Board Project
Library of Congress
Washington 25, D. C.

MDF
Morris D. Friedman, Inc.
P.O. Box 35
New Newton 65, Mass.

NRCC
National Research Council, Library
Ottawa 2, Canada

OTS
Office of Technical Services
Department of Commerce
Washington 25, D.C.

PS
Primary Sources
11 Bleecker Street
New York 12, New York

RIS
Research Information Service
40 East 23rd Street
New York 10, New York

SLA
SLA Translation Center
The John Crerar Library
86 East Randolph Street
Chicago 1, Illinois

A. I. ODINTSOV
Istochnik sveta s atomnym puchkom bol'shoi intensivnosti 398 — A High Intensity Atomic Beam Light Source 250

M. L. SOSINSKII
Rtutnaia duga nizkogo davleniia dlia issledovaniia passeianiia sveta 405 — Low Pressure Mercury Arc for the Investigation of Light Scattering 254

KRATKIE SOOBSHCHENIIA — BRIEF REPORTS

S. S. BATSANOV
Vzaimosviaz' refraktsii i potentsialov ionizatsii atomov 412 — The Correlation Between Refraction and the Ionization Potentials of Atoms 258

A. I. FINKEL'SHTEIN, F. L. MALACHEVSKAIA, A. M. FISHER, B. G. RABOVSKII
Prostoi sposob prigotovleniia plastinok iz bromistogo kaliia dlia infrakrasnoi spektroskopii tverdykh tel 415 — A Simple Method of Producing Potassium Bromide Plates for the Infrared Spectroscopy of Solids 260

V. V. ZELINSKII, V. P. KOLOBKOV, N. D. KRASNITSKAIA
K voprosu o temperaturnom tushenii fluorestsentsii 417 — On The Question of The Thermal Quenching of Fluorescence

V. P. SYCHEV
K voprosu ob udarakh vtorogo roda v smesi gazov N_2+Ar 419 — On Collisions of the Second Kind in a Mixture of N_2+Ar 263

IU. A. TSIRLIN, S. N. KOMNIK, L. M. SOIFER
Zavisimosti vykhoda liuminestsentsii pri alfa i gamma bozbuzhdenii kristallov CsI(Tl) ot kontsentratsii Tl 422 — Luminescence Yield of CsI(Tl) Crystals Under α and γ Excitation As A Function of Tl Concentration 265

A. A. KAPLIANSKII
Lineichataia liuminestsentsiia rentgenizovannykh kristallov ftoristogo litiia 424 — Line Luminescence of X-rayed LiF Crystals 267

P. P. FEOFILOV
Orientatsiia tsentrov lineichatoi liuminestsentsii v rentgenizovannykh kristallov LiF 426 — Orientation of Centers of Linear Luminescence in X-rayed LiF Crystals 268

E. V. KONDRAT'EVA
Opredelenie kvantovogo vykhoda liuminestsentsii trekhvalentnogo iona terbiia v rastvorakh 427 — Determination of the Luminescence Quantum Yield of the Trivalent Terbium Ion in Solution 269

Abbreviations Often Encountered and Used Herein 271

Affiliations of Authors from Issue 3 272

Symbols for Sources of Translations 272

RUSSIAN ALPHABET WITH TRANSLITERATION

А а	a		Р р	r	
Б б	b		С с	s	
В в	v		Т т	t	
Г г	g		У у	u	
Д д	d		Ф ф	f	
Е е	e		Х х	kh	
Ж ж	zh		Ц ц	ts	
З з	z		Ч ч	ch	
И и	i		Ш ш	sh	
Й й	i		Щ щ	shch	
К к	k		Ъ ъ	mute hard sign	
Л л	l		Ы ы	y	
М м	m		Ь ь	mute soft sign	
Н н	n		Э э	e	
О о	o		Ю ю	iu	
П п	p		Я я	ia	

Litho Printed by Blackburn Printing Company, West Concord, Mass.

TOM VI, Vyp. 3 OPTIKA I SPEKTROSKOPIIA Mart, 1959
VOL. VI, No. 3 OPTICS AND SPECTROSCOPY March, 1959

SODERZHANIE

L. M. VOLKOVA
Effektivnye secheniia vozbuzhdeniia spektral'nykh linii kaliia 273
E. IA. SENKEVICH
Izmerenie intensivnostei v bal'merovskoi serii i opredelenie kontsentratsii vozbuzhdennykh atomov v razriade 279
N. N. SOBOLEV, A. V. POTAPOV, V. F. KITAEVA, F. S. FAIZULLOV, V. N. ALIAMOVSKII, E.T. ANTROPOV, I.L. ISAEV
Spektroskopicheskoe issledovanie sostoianiia gaza za udarnoi volnoi. I 284
S. P. EKKVICH
O sile ostsilliatora dlia gamma-sistemy polos NO 297
V. A. LOGINOV
Opredelenie molekuliarnykh postoiannykh iz polosatykh spektrov metodom parabolicheskogo interpolirovaniia 304
V. N. SOBENIKOV
Temperaturnaia zavisimost' secheniia pogloshcheniia vidimogo sveta dvuokis'iu azota 315
I. G. FRIEDMAN
Raspredelenie energii v spektrakh poliarnykh siianii v oblasti 3900 - 8700 Å 323
R. S. LEBEDEV
Raschet kolebatel'nogo spektra molekuly metiltsiklopentana 329
L. M. SVERDLOV, E. P. KRAINOV
Kolebatel'nye spektry nepredel'nykh uglevodorodov. VII. Raschet i interpretatsiia kolebatel'nogo spektra 334
I. D. POLIAKOVA, SH. SH. RASKIN
O spektrakh kombinatsionnogo rasseianiia nekotorykh galoido-proizvodnykh uksusnoi kisloty v raznykh fazovykh sostoianiiakh 343
O. V. SVERDLOVA
O vliianii rastvoritelia na elektronnye spektry pogloshcheniia benzola i khlorbenzola 349
A. N. NIKITINA, M. D. GALANIN, G. S. TER-SARKISIAN, B. M. MIKHAILOV
Spektry pogloshcheniia i liuminestsentsiia rastvorov nekotorykh zameshchennykh polienov 354
IU. V. NABOIKIN, E. N. PAVLOVA, B. A. ZADOROZHNYI
Osobennosti liuminestsentsii ortodizameshchennykh aromaticheskikh uglevodorodov. I 366
V. L. LEVSHIN, V. B. GUTAN, E. N. KARZHAVINA
O vozmozhnosti rekombinatsionnykh protsessov svecheniia v vol'frematakh i uranilovykh soedineniiakh 372
F. I. FEDOROV
K teorii opticheskoi aktivnosti kristallov II 377
G. B. BAIS
Formuly Frenelia dlia sluchaia padeniia obyknovennoi volny na ploskost' dvoinikovaniia odnoosnogo prozrachnogo kristalla 384
P. G. KARD
Ob ustranenii dubletnoi struktury polosy propuskaniia svetofil'tra s polnym otrazheniem 389
A. O. SAILI'
O porogo chuvstvitel'nosti infrakrasnogo absorbtsionnogo gazoanalizatora s gazovoi moduliatsiei 394

CONTENTS

Effective Excitation Cross-sections of the Spectral Lines of Potassium 179
Measurements of Intensities in the Balmer Series and Determination of the Concentration of Excited Atoms in the Discharge 182
Spectrographic Investigation of the State of a Gas Behind a Shockwave. I 185
On the Oscillator Strength of the γ-Band System of NO 193
Determination of Molecular Constants from Band Spectra by the Parabolic Interpolation Method 197
Temperature Dependence of the Absorption Cross Section of Nitrogen Dioxide for Visible Light 203
Energy Distribution in the Polar Aurorae in the Region 3900 - 8700 Å 208
Calculation of the Vibrational Spectrum of the Methylcyclopentane Molecule 211
Vibration Spectra of Unsaturated Hydrocarbons VII. Calculation and Interpretation of the Vibration Spectrum of Cyclopentene 214
On the Raman Spectra of Some Halogen Derivatives of Acetic Acid in Various Phases 220
Solvent Effects on the Electronic Absorption Spectra of Benzene and Chlorobenzene 223
The Absorption and Luminescence Spectra of Solutions of some Substituted Polyenes 226
The Luminescence of Ortho-disubstituted Aromatic Hydrocarbons 231
On The Possibility of Recombination Processes in the Luminescence of Tungstate and Uranyl Compounds 234
On the Theory of Optical Activity in Crystals II 237
Fresnel Formulas for an Ordinary Wave Incident on the Twinning Plane of a Transparent Uniaxial Crystal 241
On Elimination of the Doublet Structure of the Transmission Band in a Total-Reflection Light-Filter 244
On the Threshold of Sensitivity of an Infrared Absorption Gas Analyzer with Gas Modulation 247